INFORMATION TO USERS

This manuscript has been reproduced from the microfilm master. UMI films the text directly from the original or copy submitted. Thus, some thesis and dissertation copies are in typewriter face, while others may be from any type of computer printer.

The quality of this reproduction is dependent upon the quality of the copy submitted. Broken or indistinct print, colored or poor quality illustrations and photographs, print bleedthrough, substandard margins, and improper alignment can adversely affect reproduction.

In the unlikely event that the author did not send UMI a complete manuscript and there are missing pages, these will be noted. Also, if unauthorized copyright material had to be removed, a note will indicate the deletion.

Oversize materials (e.g., maps, drawings, charts) are reproduced by sectioning the original, beginning at the upper left-hand corner and continuing from left to right in equal sections with small overlaps. Each original is also photographed in one exposure and is included in reduced form at the back of the book.

Photographs included in the original manuscript have been reproduced xerographically in this copy. Higher quality 6" x 9" black and white photographic prints are available for any photographs or illustrations appearing in this copy for an additional charge. Contact UMI directly to order.

UMI®

Bell & Howell Information and Learning
300 North Zeeb Road, Ann Arbor, MI 48106-1346 USA
800-521-0600

NOTE TO USERS

This reproduction is the best copy available

UMI

DISSERTATION

COLLECTION EFFICIENCIES OF AIR PURIFYING RESPIRATORS CONTAINING ELECTROSTATIC FILTER MEDIA

Submitted by

Diana L. Larson

Department of Environmental Health

In partial fulfillment of the requirements

for the Degree of Doctor of Philosophy

Colorado State University

Fort Collins, Colorado

Spring 1999

COLORADO STATE UNIVERSITY

March 29, 1999

WE HEREBY RECOMMEND THAT THE DISSERTATION PREPARED UNDER OUR SUPERVISION BY DIANA L. LARSON ENTITLED "COLLECTION EFFICIENCIES OF AIR PURIFYING RESPIRATORS CONTAINING ELECTROSTATIC FILTER MEDIA" BE ACCEPTED AS FULFILLING IN PART REQUIREMENTS FOR THE DEGREE OF DOCTORATE OF PHILOSOPHY.

Committee on Graduate Work

Advisor

Department Head

ABSTRACT OF DISSERTATION

COLLECTION EFFICIENCIES OF AIR PURIFYING RESPIRATORS CONTAINING ELECTROSTATIC FILTER MEDIA

Electrostatic media are widely used in particulate air purifying cartridges and filtering facepiece respirators. Such media provides high collection efficiency while affording low breathing resistance to the wearer. The certification method used by National Institute for Occupational Safety and Health (NIOSH) is considered to represent worse case respirator performance. Respirator certification does not consider either the mechanism of particle capture or the type of filter media used in a respirator. The correlation between respirator penetration with particles less than 1 μm for predicting worker exposure to air contaminants greater than 1 μm has not been validated.

This research was undertaken to: 1) evaluate the collection efficiency of particulate air purifying respirators containing electrostatic filter media and 2) determine if the NIOSH method used for respirator certification accurately predicts collection efficiency of these respirators loaded with contaminants representative of the workplace. Two of the three contaminants selected for this project, asphalt fumes and synthetic metal cutting fluid mist, possess chemical and/or physical properties in addition

to a vapor stage that could mask or degrade the charge on the electrostatic fibers. The third workplace aerosol, aluminum oxide dust, was selected to be representative of a solid particulate mineral dust.

Filtering facepiece respirators are often used in environments where they become saturated with the wearer's perspiration. Perspiration contains ions that could interact with the charge on an electrostatic filter. Affect on collection efficiency was determined after a respirator saturated with artificial perspiration was dried with HEPA filtered air.

The findings of this work support the following conclusions: 1) the NIOSH method test for N95 respirators underestimates penetration of respirators loaded with laboratory and field generated workplace contaminants, 2) N95 respirators containing electrostatic filter media did not perform significantly different from an N95 mechanical filter media respirator, 3) penetration of some N95 respirators fully loaded with either asphalt contaminants or synthetic metal cutting fluid mist increased beyond the rating of the respirator, and 4) performance of filtering facepiece respirators saturated in artificial perspiration were not significantly affected after the respirators were dried.

Diana L. Larson
Department of Environmental Health
Colorado State University
Fort Collins, CO 80523
Spring 1999

ACKNOWLEDGMENTS

I wish to express my appreciation to the members of my graduate committee, Dr. Phil Bigelow, Dr. Roy Buchan, Dr. James Jackson, Dr. Paul Mielke, and Dr. Alan Tucker, for their guidance and support through this project. I am deeply grateful to all the individuals who assisted me with this work especially Dr. Art Biermann and Dr. Werner Bergman for their expertise and counsel in aerosol physics; Dr. Dan Moore II for his statistical guidance; Dr. James Johnson for his assistance; to all the respirator manufacturers, 3M Company, Louis M. Gerson Company Inc., Moldex-Metric Inc., Mine Safety Appliance Company, Pro-Tech Respirators, Inc., Tecnol Inc., Uvex Safety Inc., and Willson Safety Products, who donated respirators for this project; and finally to the technicians and mechanical technologists of Lawrence Livermore National Laboratory, Scott Doughty, Bob Rego, Sterling Sawyer, Kirk Staggs, and Kent Wilson, for their support with design, fabrication, assembly, and calibration of equipment, without their assistance this work would not have been possible.

I want to thank individuals who have been my proofreaders, Marie Driskill and Dr. Virginia Lew. I especially want to thank my uncle, Dr. Robert Thompson, for his encouragement to attend graduate school to pursue a career in industrial hygiene and for the many hours he spent proofreading this document.

Special appreciation is given to Dr. Marv Tillery for his thoughtful review of this completed work.

Recognition is extended to NIOSH for providing financial support, and for James Jackson and Lawrence Livermore National Laboratory for providing the resources and funding to complete this research, for which I am very grateful.

Finally, I want to express my deepest thanks my parents and family and dedicate this work to them. Their love, support, and encouragement are the source of my strength and perseverance.

TABLE OF CONTENTS

LIST OF TABLES

LIST OF FIGURES

CHAPTER I

INTRODUCTION

Overview

Particulate air purifying respirators are commonly used in the workplace for protection against nuisance and hazardous materials. Most airborne particles are less than 1 μm in diameter and are difficult to remove [1]. Respirators relying solely upon mechanical filtration mechanisms capture these small particles if the fibers have a small diameter and are closely packed. Filters with this structure impart a high resistance. By contrast, respirators containing fibers carrying a permanent electric charge have the added capability of attracting particles by electrostatic forces. Respirators do not require as many *electret* fibers in order to provide the same filtration efficiency thus offering the respirator wearer additional comfort and reduced breathing resistance. However, collection efficiency may deteriorate when loaded aerosols interact with the fiber charge [2]. Once fiber charge is lost, worker protection can be compromised. Today, most particulate respirators contain electret filter material.

Electrostatic Filter Media

Nicolaij Louis Hansen first developed electrostatic medium for respirator filters in 1930. He found that mixing a powdered resin with wool fibers greatly increased the collection efficiency of respirator filters [3]. In his 1932 patent, it was not clear if Hansen himself was fully aware of the mechanism by which his filter was able to effectively capture sub-micrometer sized particles. The mystery surrounding the high efficiency of the resin-wool filter was not elucidated until 1942 when Walton [4] authored Porton Report No. 2465, "The Electrical Characteristics of Resin Impregnated Filters".

On March 25, 1974, Jan van Turnhout of the Netherlands patented a method for producing an electrically charged fibrous filter from a high molecular weight non-polar resin [5]. Although the art of manufacturing electrostatically charged filament from polymer resin for improved collection efficiency of filters was not new [6], van Turnhout was credited with introducing a process by which it could be efficiently produced. This filter medium was an extruded thermoplastic film, stretched and corona charged. The stretching process realigned the molecular structure causing the film to be strong in the stretched direction and weak in the perpendicular direction. The film was easily split by a variety of methods, a needle roller was one mechanism used for this process termed fibrillation. The non-polar resin used had low electrical conductivity so that the electrical charges could be trapped in the polymer structure and were less likely to decay [1]. The split film resembled ribbons with dimension of about 10 μm thick and widths

varying between 50 and 250 μm. The bipolar charged fibers with positive charge on one side and negative charge on the other attracted both charged and uncharged particles [7]. Since the polymer was hydrophobic and thermally stable, these filters were not affected by high humidity as long as the fibers did not become saturated and the filters could be used up to temperatures of 80 ^{o} C. These patents were later sold to 3M Company in St. Paul, Minnesota. "Filtrete" was used in 3M products and sold to other respirator manufacturers [8].

Two other processes can produce electrostatic filter media: electrostatic spinning and melt blowing. Numerous patents have described the methods in which these filter media were manufactured and charged [9, 10, 11, 12, 13]. A major distinguishing feature of these filter media as compared to the split fiber electret was the shape of the filter fibers and their charge configuration.

The fiber diameters of the filter media ranged from 1 to 10 μm for electrostatically spun and 1 to 20 μm for melt blown [14]. The fiber diameter was determined by the viscosity of the polymer solution and the resin that was used [15]. The fine fibers of the spun bond caused them to behave partially like a mechanical filter with corresponding airflow resistance [16]. Other factors that influenced pressure drop included filter thickness and packing density, aerosol loading, viscosity of the air, and filtration velocity [17]. Melt blown nonwoven filters were recommended to be used at

temperatures below 60 ^{o} C since it was found that temperatures above 80 ^{o} C would rapidly decrease electrostatic charge [18].

Filtration Efficiency

Previous studies conducted at Los Alamos National Laboratory and by Ackley [16, 18] showed a continual decline in collection efficiency of electrostatic media stored at elevated temperature and high relative humidity. Degradation continued until only the mechanical efficiency of the filter remained. The effect on collection efficiency due to filter saturation has not been reported in published literature and has only been hinted at in a study conducted by Moyer and Stevens [18] when preconditioning equipment malfunctioned. Their study observed a 10 percent reduction in the efficiency of saturated filters which was determined with a monodisperse neutralized sodium chloride (NaCl). This was a significant decrease in collection efficiency compared to the 2 to 6 percent reduction in collection efficiency for filters preconditioned at 38 ^{o} C and 85 percent relative humidity which were not saturated. Previous work conducted at Lawrence Livermore National Laboratory [19] found decreased collection efficiency in electrostatic filters submerged in water solutions, rinsed, and dried prior to evaluating filter penetration with a NaCl aerosol. Researchers surmised that when fibers were sufficiently wetted ions from the water solutions neutralized the charge on the filter fiber.

Electrostatic media were desirable to use in respirator filters; however under certain conditions, the electrostatic charge could become unstable.

Captured aerosol particles and vapors reduced filtration effectiveness by three different mechanisms. First the aerosol interacted chemically or physically with the fiber surface and disrupted the surface layer so that it could no longer hold a charge. Second, charged aerosol particles captured by an oppositely charged region of the fiber neutralized the charge on the filter fiber. Lastly, neutral aerosol particles screened filter charge by covering the fiber and weakening its electrostatic attraction. If the deposited aerosol was electrically conductive, filter screening was more pronounced, especially if the aerosol was electrically conductive [2, 19]. Aerosol penetration has been shown to be dependent upon: a) the chemical and physical properties of the test agent, b) aerosol size, c) aerosol charge, d) airflow, e) respirator category, f) filter packing density, g) fiber size, and h) fiber charge [20].

Oily aerosols such as dioctyl phthalate (DOP) do not form structured deposits but spread out smoothly to coat the fibrous surface of a filter fiber effectively screening out the electric charge [21]. Liquid aerosols such as DOP produced structural changes in the filter fibers. A drop of liquid bridging two fibers will bring the fibers closer together and will fill the void space in the filter. As a result, the fibers clump which reduced filtration efficiency and increased airflow resistance. [22]. Recently, 3M patented a fluorochemical additive that enabled melt blown electrostatic media to retain their charge in the presence of oily aerosols and water [23, 24]. Although this process has been known for many years in the non-woven textile industry [25], 3M was the first to adapt its use to filtration.

In a previous study [19], researchers found that sodium chloride particles carry a larger number of charges as compared to DOP. The highly charged sodium chloride aerosol resulted in the filter fiber charge being more rapidly neutralized. Solid particles captured by electrical forces were initially collected over the entire fiber surface that contributed to an increased diameter of the fiber. Once a sufficient number of particles had been collected, a particle chain or dendrite was initiated at any location on the filter fiber [21, 26]. In the absence of electrical forces, dendritic structures projected from the front and sides of the fiber restricting the airflow and increasing pressure drop [27]. Coarse dust did not penetrate into the filter but formed a porous cake that contributed little to either the resistance or the efficiency of the filter. Fine dust was very penetrating and caused both resistance and efficiency to increase; the structure of these deposited aerosols resembled fine fibers [21]. Although a large particle carried a greater charge than a small particle for a given total mass, a fine aerosol carried a greater total charge than a coarse aerosol if the number of the fine aerosol particles was sufficiently large [19]. Filters with very open structures or a low packing density tended to resist clogging since the dendrites had to grow considerably before the filter clogged and an internal cake formed [26]. Penetration of an electrically charged filter material increased over time as the electrostatic effects became neutralized or coated. When sufficient loading occurred and the interstitial spaces were blocked, filter efficiency again increased due to mechanical action of diffusion, interception, impaction, and gravitational settling [28].

The filter's electrostatic charge was generally uncharacterized and because it was difficult to measure, collection efficiency was not easily predicted [28]. Brown [21] described several methods for measuring the magnitude of charge and net charge on an electrostatic filter. The most reliable method was by measuring filter penetration with a standard NaCl aerosol where loss of charge was a function of ionizing radiation dose. The problem with this method was identifying the neutralization endpoint with an acceptable degree of precision. Additionally, effective fiber diameter and packing density of the filter had to be determined before the charge density of the filter was ascertained.

Aerosol charge was found to be a more critical parameter of decreased filter collection efficiency than preconditioning at elevated temperatures and increased relative humidity [18, 30]. Measuring aerosol charge was not easy despite a variety of charge measurement methods available such as first- and second-order mobility spectrometers, aerosol electrometers, and variations of the Millikan oil-droplet apparatus [30, 31]. Many instruments were laboratory-built and were only used by the laboratory in which they had been developed. Most commercially available measurement applications were for monodisperse aerosols and adaptations were required to measure charge on polydisperse aerosols [19]. This was accomplished by fractionating the aerosol according to the electrical mobility of the particle and then determining the particle-size distribution of each mobility fraction. An inordinate amount of data was generated which had to be stored and integrated in a computer [31].

The most penetrating particle size for electrostatic filters was dependent on the filter velocity. Diffusion and/or electrostatic attraction removed small particles; as face velocity increased the most penetrating particle size decreased. At low flow rates, there was more time for particle removal by electrostatic forces [20]. Small particles were collected primarily by charge dependent Coulombic effects. In addition, Brownian diffusion and induction forces were significant for the collection of fine particles by electrostatic media [32]. For larger particles, polarization effects dominated particle collection and particle charge became less important [33]. As face velocity increased, removal by mechanical filtration mechanisms such as interception and impaction dominated for particles larger than 1.7 μm [30]. Collection efficiency increased as the number of elemental charges increased for a fixed particle size. Workplace aerosols had varying levels and distributions of electrical charge depending on the source of aerosol generation. As an aerosol aged, it stabilized to a Boltzman charge distribution due to diffusion charging from ions in the air [34].

Respirator Certification

In 1995, the respirator certification standard was revised and published as 42 CFR Part 84 that gave the National Institute for Occupational Health and Safety (NIOSH) sole responsibility for testing and certifying respirators [35]. NIOSH has estimated that 7 to 10 million American workers rely on respiratory protection to protect against workplace hazards [36].

Respirator certification methods did not distinguish mechanical from electrostatic filter media and manufacturers were not required to disclose the collection mechanisms by which their respirators performed. Respirator manufacturers indicated the materials used in their respirator on the application form; filter medium was usually identified with a part number. The NIOSH certification method used neutralized test aerosols of polydisperse NaCl or DOP [35]. Both tests examined maximum aerosol penetration during steady-state high airflow velocity. The collection efficiency curve during the NaCl test was characteristic for electrostatically charged filter media. Collection efficiency began relatively high and as filter loading increased the charge became depleted and penetration increased. After a sufficient number of particles was collected, a filter cake formed whereby mechanical filtration dominated and collection efficiency again increased. This test was based on how well a filter medium was able to form a dust cake whereby pressure drop and fit were not limiting factors. The DOP test did not display a characteristic curve for electrostatic media. The maximum

penetration for both electrostatic and mechanical filters occurred at the end of the aerosol challenge.

Worker Protection

Electrostatic media were widely used in filtering facepiece respirators due to their economical cost, enhanced filtration efficiency, and reduced breathing resistance [31]. Eighty to 90% of the filtering facepiece respirators submitted for certification under the new regulation displayed collection efficiency curves characteristic of electrostatic media [37].

Workers were taught two indices that determined the end of the service life of a respirator. One was by increased breathing resistance and the second was by detection of contaminant breakthrough [38]. If the charge on electrostatic media was degraded from contaminants, filter clogging with its accompanying increased breathing resistance may not occur. Worker exposure could result when the service life of a respirator was reached without the wearer's knowledge. The second method by which workers determined "end of respirator service life" was contaminant breakthrough. Some solid or liquid aerosols may not have an odor or taste associated with the contaminants and breakthrough may be undetected [35]. Since the type of mechanism by which a respirator performed had not been identified on products, the wearer may not have been aware of differences in detecting end of service life.

The ability of laboratory data to adequately predict workplace performance of respirators with electrostatic media remains unclear. Field

testing examining the performance of respirators containing electrostatic filter media is limited [2]. The correlation between respirator penetration in the laboratory with submicrometer particles for predicting worker exposure to supermicrometer contaminants in the workplace has not been validated [28]. Studies that have attempted to correlate workplace exposure to laboratory tests have been unsuccessful [39]. Previous researchers have questioned the validity of the NIOSH method to predict worker protection [28, 29, 30]. Additional information is needed to elucidate which environmental conditions and contaminants might be detrimental to this type of filter media.

CHAPTER II

LITERATURE REVIEW

Filtering Respirator History

The development of respiratory protection has been ongoing for the past 2000 years. The earliest need for respiratory protection from industrial dusts was recorded by Pliney the Elder, a Roman, who lived from 23-79 A.D. He recommended the use of animal bladders to loosely cover the faces of miners and lead oxide refiners to prevent inhalation of mercuric sulfide dust, referred to as vermilion dust in early writings [40, 41]. The bladders were thin which allowed workers to see through the skin [42, 43]. In the 16th Century, Agricola wrote extensively on mineralogy and geology and discussed mining operations in his book *De Re Metallica*. The environment in the mines was described as being very dry which contributed to the generation of 'corrosive' dust. Mine workers were advised to tie loose veils over their faces to protect both their lungs and eyes. The harsh working conditions in the mines often shortened the lives of miners and some local women were known to have been married as many as seven times [42]. Silicosis was the disease suspected of provoking the high mortality rate among the hard-rock miners [44].

Development of industrial filtering respirators was spurred by the need to protect fire fighters. In 18th and 19th century Europe, a common prerequisite for a person to become a firefighter was that they had a full beard that could be dipped in water and held between the teeth for smoke protection [40]. The first respirator with a filter appeared in 1814. Brisé Fradin developed a box filled with cotton that had a breathing tube going to the mouth while the nostrils were plugged with cotton. The efficiency of this respirator was tested with mercury vapors that were known to be dangerous to gilders [45].

In 1825, the Royal Society of Arts in England presented John Roberts, a coal miner, with a prize of 50 guinea for developing a filtering mask for firemen. The wearer's head was encased with a leather hood and eyepieces were fashioned from either glass or mica. The wearer breathed through a tube that terminated near the ground where there was less smoke during a fire. Attached to the lower end of the tube was a filter of wool with a moist sponge on top [3]. In 1868, John Tyndall collaborated with the Chief Officer of the Metropolitan Fire Brigade and developed a complicated filter used in conjunction with a facepiece known as the 'fireman's respirator' [45]. This particulate filter was made of tightly packed cotton wool in three layers with lime fragments, charcoal, and wool soaked in glycerin. The filters were encased in brass canisters 2 inches in diameter and 4 inches in length [46].

Lewis Haslett [47] patented one of the first respirators in the United States in 1849. The 'Inhaler or Lung Protector' filtered dust or injurious substances from inhaled air. The filter was made from wool fabric or other porous substance that

was to be moistened with water prior to use. The respirator could be fitted to either the nose or mouth; the respirator body was held in place with an elastic band. A 'clapper valve' directed the airflow for inhalation and exhalation [46]. The invention had an optional flexible tube attaching to the respirator extending the air inlet to with in a few inches from the floor; the filter was attached to the end of the hose [47]. This feature was similar to the respirator designed by John Roberts.

The Nealy Smoke Mask, patented on September 18, 1877, supplied air to the mask by two rubber tubes connected to a sponge or porous material filter. The filters were saturated with water supplied by pipes from the water bag carried on the wearer's chest. Breathing air was purified when it passed through the wetted sponges [45]. The collection efficiency of wetted sponge filters was 22% and increased to 55% when loaded with particles. If allowed to dry out, the efficiency of sponges dropped to 9% [48].

By the 19th century, dust respirators were fairly common. Since respirators had not been properly studied, these respirators were of low efficiency with unusually high breathing resistance and a poor face seal; these early masks probably had little useful effect [49, 50]. Tyndall [40], a well known physicist, made the first scientific investigations on the properties and behavior of atmospheric particulate matter. Three years after his development of the fireman's respirator, the coarse fiber from flax or hemp referred to as 'oakum', was used as a filtering medium in respirators; glass wool was developed about the same time [3].

Early respirators for industrial applications in the United States had filters made from a variety of materials whose list was seemingly endless [51]. Respirator filters constructed of felted cotton or wool fabric were either supported on a reusable backing, such as fly screen, or gathered to make a 'bag' or 'pouch' [52]. Neither design contained valves so that both inhalation and exhalation air passed bidirectionally through the filter medium. Bag or pouch-type respirators, so named for their unique shapes, were intended to be reused by dislodging particulate build-up by shaking. Other fabric respirators were intended to be discarded or washed in warm soapy water once soiled. The first respirator using layers of gauze and cotton fabric with an elastic band to secure the device over the wearer's nose and mouth was patented in 1866 [53]. In a unique design, a respirator was constructed from cotton wool quilted between layers of cheesecloth and then gathered to form a nose pouch. Many of these fabric respirators were intended to protect workers from dust and organisms which carried diseases although others were intended to be used for spray paint applications [54]. The usefulness of cotton as an efficient filter was demonstrated in 1854 when perishable foods were shown to have much slower decay rates when ambient air was filtered though cotton [53]. Disposable filters made from cotton fiber paper or tissue paper were generally unacceptable due to their small pores, which easily clogged and resulted in high breathing resistance [54].

The A.W. Dolfini Company of New York City introduced the 'Midget Smoke Protector' in 1897. This device appeared to be made from cloth filtering

material, supported on a backing, and held close to the wearer's face by a single strap [45]. The Pulmosan respirator manufacturer displayed a product in their circa 1917 catalog whose design appeared to be a forerunner of the modern disposable filtering facepiece. The unique cone shape of this product along with the single fastening strap appeared to be similar to the modern disposable filtering facepiece respirator. Although the type of filter medium in this product was unclear it was probably a felted fabric supported on a wire frame giving the respirator rigidity [51].

In 1905, a contest was held in England to develop an acceptable 'dust-arresting respirator', the winner was to be awarded a prize of 20 pounds. Although more than 60 models and drawings were submitted to the technical committee for consideration, none were found to be acceptable. The small filtering area of the respirators was deemed inadequate and the air temperature inside the facepiece was determined to be uncomfortably hot [3].

The need for developing respiratory protection was accelerated by World War I during which time Germany resorted to large scale chemical warfare. Lack of adequate respiratory protection resulted in unconventional devices being used by both civilians and troops. People tied wetted socks and handkerchiefs over their noses and mouths in desperate attempts to protect themselves from the gas attacks. Some even tried breathing through perforated corned beef tins or broken whiskey bottles filled with earth and grass as a filtration medium. A tremendous national undertaking in England produced a simple disposable filtering mask that was sent to France about two weeks after the first attack. The respirator

consisted of a nose and mouth pad of cotton impregnated with washing soda and glycerin enclosed in a strip of black muslin tied at the back of the neck with cloth straps [50]. As a result of Germany's deployment of hazardous gases, activated charcoal was developed by a Russian, N. D. Zelinskiy, in 1915 [55]. Respirators made with these carbon filters effectively adsorbed chlorine and phosgene gases; however, the Germans sought to penetrate this filter with arsenical smokes. Arsine gas was filled into glass bottles and placed inside high-explosive shells. Dispersal was inefficient and particles were too few and too large to cause serious damage. The use of arsenic resulted in a modification of the military gas masks by placement of particulate filters in front of the charcoal granules [3].

In London, a small department was set up shortly after the gas attacks to conduct defense research. A location at Porton Down, Wilshire, England was acquired for trials of gas weapons. Research to improve respirator design continued at this location throughout World War I and ended with the 'Small Box Respirator'. When the American troops entered the war, they had to rely upon the English research as respirator development in the United States had been passive up to this time. The English supplied the Small Box Respirator to many of the allies, the most notable was Italy. The Porton station increased in size and function and soon after World War I was established as the center for all research on chemical defense in England. It became known as the Chemical Defense Experimental Establishment (CDEE) [50].

In 1910, the Bureau of Mines was established in the United States. This agency was created to promote mining and conduct research to improve mining methods. The need for adequate respirator protection was most critical in mining operations when workers would don a self-contained breathing apparatus of unknown quality and risk their lives to assist in rescue operations after a disaster. Initial work at the Bureau was devoted to the development of an army gas mask for use during World War I [56]. The gas mask used by the United States army during World War I was similar to Tyndall's fireman's respirator with the exception that activated charcoal and soda lime were used as adsorbents and had improved filtration properties [49].

Between World Wars I and II, Germany continued to develop more efficient methods of generating arsenical smoke. Particles produced by thermal generation had diameters between 0.2-0.5 μm which easily penetrated the deep lung and resulted in serious damage [3]. From Tyndall's previous work, it was known that smokes penetrated fibrous filters and were not effectively adsorbed by charcoal [57]. The need to develop a more efficient respirator filter escalated. Industrial workers benefited from advances made in respirator protection. In Great Britain, the first industrial dust mask that provided protection against silica dust was developed immediately before World War II [49].

Respirator Certification and Testing

One of the first methods developed to evaluate the collection efficiency of a respirator was described in a 1911 German procedure. A subject donned a respirator and entered a 3-m3 cabinet into which dust-laden spores had been

sprayed. At the end of one minute, the respirator was doffed and the person remained in the chamber, nostrils plugged with cotton. It was assumed that cotton was a perfect filter and respirator efficiency was determined by culturing and comparing bacterial counts [40].

In the United States, the Bureau of Mines promulgated the first performance and quality standards for self-contained breathing apparatus on March 5, 1919, which was known as Schedule 13. Schedule 14 for gas masks was promulgated in May 1919 and was based on the earlier work with military gas masks [48, 56]. Subsequently, the demand for performance requirements relating to other types of respiratory protective devices led to the issuance of Schedule 19 for hose masks in 1927; Schedule 21 for filter-type dust, fume, and mist respirators in August 1934; and Schedule 23 for chemical cartridge organic vapor respirators in November 1944 [56]. The authority for conducting respirator evaluations was given to the Bureau of Mines by an act of Congress on February 25, 1913 (37 Stat. 681) [57]. The Bureau was charged with the responsibility of promulgating procedures and testing respiratory protective devices [40].

The Bureau of Mines, however, did not have regulatory authority. The testing and certification of respirators was strictly voluntary for the respirator manufacturer [58]. The Bureau's purpose was to act as an impartial testing agency and to make available a list of respiratory protective devices that met their performance requirements [59]. However, industry leaders believed that the federal approval on respirators was an additional legal safeguard against

damage suits [43]. This led to the large-scale purchase of approved respirators instead of lower grade ones [40]. By 1966 most state labor and health codes required Bureau-approved respirators when respiratory protection was needed. Often Federal contracts contained clauses making Bureau-approved equipment mandatory [56].

Schedule 21 for 'dispersoid respirators' was divided into three groups. Group A was for respirators that protected from dusts generated mechanically from the disintegration of solid materials such as drilling and blasting. Group B respirators provided protection from metal fumes generated during sublimation or condensation of their vapor, or as a result of a chemical reaction between the vapor and gases. Group C respirators protected workers from mists which were formed during electroplating and paint spraying where the liquid vehicle did not produce harmful gases or vapors [40, 57]. When Schedule 21 was first promulgated there was not a respirator in the country that would pass the certification. Five years later, the Bureau of Mines had certified only 28 respirators [38]. As respirator quality improved and more respirators met the certification requirements, those respirators that did not meet the Bureau of Mine Schedule 21 were referred to as 'second-grade' or 'nuisance dust' respirators. It was claimed that these respirators were adequate to protect workers against nontoxic dust such as zinc oxides in brass foundries and organic dusts such as flour and cocoa [58, 40].

In 1917, an investigation by the Bureau of Mines found that miners would not wear respirators due to skin irritations caused by face contact with the respirator, unless the conditions were unusually severe. As a result, workers either labored in dusty environments without any form of respiratory protection or tied handkerchiefs, rags, and other fabric cloths over their breathing zone placing comfort above efficiency [48]. Some respirator manufacturers supplied 'facelets', a knitted cotton cover that fitted over the edge of the facepiece which prevented contact between the rubber and the wearer's face increasing the comfort of the protective device [60].

Under Schedule 21, respirators were evaluated for design, durability, and practicality. Respirators had to demonstrate that they provided adequate protection for a suitable period of time and had to be reasonably comfortable and convenient to wear. Lastly, the respirators had to be constructed of durable materials [48]. The three main criteria of evaluation included: efficiency, resistance, and fit of the respirator.

The collection efficiency of all dispersoid respirator categories was evaluated at 40-70% relative humidity, temperature at approximately 25 degrees °C, and 32 liters/minute (lpm) steady-state airflow. The maximum allowable pressure drop was 50 mm H_2O for inhalation resistance and 25 mm H_2O for exhalation assessed at 85 lpm continuous airflow. It was felt that respirators that were continuously worn should not exceed a breathing resistance of 2 inches of H_2O (49 mm H_2O), preferably less than 1 inch (24.5 mm H_2O). Respirators with a breathing resistance greater than 4 inches of H_2O (98 mm H_2O) were impractical

to be worn, even for short duration [61]. Previously published values for resistance indicated that physical discomfort to the wearer occurred above 50 mm H_2O resistance at 85 lpm [62].

A total of three respirators were evaluated for collection efficiency against each challenge agent. A coal dust tightness test was performed which evaluated face seal fit of a respirator. Three subjects with different face shapes wore respirators in a chamber with visible coal dust for 30 minutes while various tasks were alternated which simulated moderate work and resting activities. Forced nasal discharge and sputum were examined for coal dust residue along with visual inspections of the nasal cavities of the test subjects to determine the effectiveness of respirator fit [57]. In 1926, some respirators fit the face so poorly that most of the air was inhaled through openings between the face and the respirator without any dust removal [49]. The adjustable portions of the respirator that allowed it to conform to the contours of the wearer's face included: a metal body; a wire at the nose portion; a wire that extended under the respirator and upward toward the nose portion; and a metal brace inside the facepiece. These bendable sections were intended to provide an adequate face seal [60].

Type A respirators were challenged with dust which contained 99+% free silica at both a high and a low concentration of 50 mg/m^3 and 5 mg/m^3 respectively. The duration of the test was three 30-minute intervals for the high concentration and a single 156-minute sampling period for the low concentration. Three respirators were tested at each concentration [57]. The

maximum mean particle size of silica was 0.6 μm with a geometric standard deviation of less than 1.9.

Type B respirators were certified with two different types of fumes, 'low-plugging' and 'high-plugging'. The 'low-plugging' challenge agent was lead oxide fume at a concentration of 15 mg/m^3. The length of sampling was a single 156-minute period. The 'high-plugging fume' was magnesium oxide at a concentration of 100 mg/m^3. This test terminated when approximately 200 mg of material had been pulled through each respirator.

Type C respirators were evaluated using three different test suspensions: chromic acid mist at a concentration of 15 mg/m^3, lead from paint spraying at 300-600 mg/m^3, and silica mist produced by spraying at a concentration of 10 mg/m^3. Three respirators were challenged by each of the test agents for two 156-minute sampling periods.

On April 19, 1955, the Bureau of Mines amended Schedule 21 to Schedule 21A adding additional fit testing requirements to the certification protocol. Negative and positive pressure tests to evaluate fit were made by 15 to 20 subjects who had different facial shapes and sizes. A quantitative fit test employing isoamyl acetate was added to Schedule 21A. Fifteen to 20 subjects were placed in a chamber with 100 ppm of this agent. Either the detection or absence of odor or taste of isoamyl acetate determined fit. Modifications were made to the coal dust fit test. Instead of individuals performing various tasks in a test chamber for 30 minutes, coal dust was blown around the breathing zone of persons wearing respirators for three minutes [63].

The duration of the silica dust test for Type A respirators was changed from three 30-minute periods to a single 90-minute interval for each respirator. The low silica dust concentration was eliminated and replaced by a lead dust test. The concentration of lead dust was 15 mg/m^3 with a geometric mean of 0.6 μm and a geometric standard deviation of 1.9. Environmental conditions and length of the test were the same as in the silica dust test. Magnesium oxide fume, the 'high-plugging' fume, test for Type B respirators was deleted in the schedule revision as was the lead mist test for Type C respirators [63].

The Bureau of Mines' specifications for certification of dispersoid respirators were based on the premise that the dusts, fumes, and mists were not significantly more toxic than lead. As a result of industry generating highly toxic particulates such as beryllium and the use of radioactive materials, Schedule 21B was promulgated on January 19, 1965 [57]. Beryllium was 100 times more toxic than lead and radioactive materials were five million to three billion times more toxic than lead [64]. The Bureau of Mines found a number of filter media capable of providing protection against these highly toxic substances, the problem was to develop a test to evaluate fit [56]. Schedule 21B added two new tests for evaluating fit and filtration efficiency of highly toxic substances, the uranine-chamber test and the DOP Man Test [65].

The uranine-chamber test was developed by Silverman et al [65] at the Harvard School of Public Health. This was the first quantitative method to evaluate respirator efficiency that considered fit [58]. Uranine is a commercial

dye and previously had been used as a tracer for air pollution. A respirator was sealed to a head form and placed in a test chamber with a uranine concentration of 1 to 2 milligrams per cubic meter (mg/m^3). The geometric mean of the aerosol was 0.2 μm and the geometric standard deviation was less than 1.96 [56]. Air was drawn through the facepiece at 32 lpm cyclic flow via a breathing machine. Leakage though the exhalation valve, around grommets, and the seals between the filter or filter cartridge and the facepiece was evaluated [56]. Since this disodium salt of fluorescein readily dissolved in water, filter efficiency was determined by leaching the captured uranine and exposing it to blue light of 440 to 510 nm. The high energy source of the spectrophotometer excited the fluorescein atom that reemitted light in the 510 to 590 nm wavelength range. Intensity of the transmittance determined uranine concentrations in the part per billion range [64].

The DOP test, originally developed by the US Army as Military Standard 282, was designed to provide a meaningful measurement of respirator efficiency and rapidly degrade electrostatic charge on resin-wool filters [66]. The Bureau of Mines used the DOP Man Test System as an indicator of leakage both around the face seal and other points of entry on the mask [56]. For this test, six men with varying facial sizes and shapes wore particulate respirators. The subjects entered a test chamber containing DOP levels 10, 100, or 1000 times the maximum permissible concentration or threshold limit value. Test subjects wore respirators in the chamber while performing activities that included head and face movements while DOP penetration was determined by sampling air from inside

and outside the facepiece. In order to meet the maximum allowable penetration requirement of 0.5%, the Bureau of Mines found it necessary to eliminate certain exercises such as talking and facial movements [65].

Schedule 21B amended the concentrations of the particulate challenge agents: silica dust increased from 50 to 55 mg/m^3, lead dust and lead fume changed from 15 to 17.5 mg/m^3 of lead, and chromic acid mist increased from 15 to 17.5 mg/m^3. Silica mist concentration was raised considerably from 15 to 22.5 mg/m^3. In recognition of the health hazards associated with silica, the maximum allowable penetrations of silica mist and dust were reduced by one-half their former values [56].

In 1970, legislation known as the Occupational Safety and Health Act (OSH Act) was enacted, which created the National Institute for Occupational Safety and Health (NIOSH). NIOSH was assigned joint responsibility with the Bureau of Mines for respirator certification and together the two agencies promulgated Title 30 Code of Federal Regulations, Part 11 [65].

Under the new legislation, respirator certification changed from being voluntary to mandatory. In 1973, the Bureau of Mines was reorganized and the regulatory functions, which included respirator approval and certification, were conveyed to the Mining Enforcement and Safety Administration (MESA). Another reorganization in 1977 transferred MESA's functions to the Mine Safety and Health Administration (MSHA) and respirator approvals were issued jointly by NIOSH and MSHA [67].

Several key changes were made in the respirator approval procedures and testing when 30 CFR 11 was enacted. The addition of the 'single use' category was spurred by a product manufactured by 3M Company, a molded disposable filtering facepiece respirator which was contoured to the face of the wearer. The advent of this product created a new class of respiratory protection. Previously 3M had produced filtering masks from thermoplastic fibers that were used by the health care industry for surgery and whose shape was flat [68]. In 1972, 3M's model 8710 disposable dust mist respirator with split fiber electrostatic filter media received the first approval for this new respirator class by the Bureau of Mines [69]. The technology used to successfully produce the model 8710 was actually a failed attempt by the company to 3-dimensionally mold a bra cup [70]. Today molded respirators are sometimes referred to as 'bra cup' respirators.

Filtering facepiece respirators were composed of three general parts. The outer cover that protected the shell and acted to collect large dust particles prevented overloading of the second layer. The overall contribution to collection efficiency was small but provided support to the filter layer [71]. The inner layer contained the filtration medium that was responsible for removal of submicrometer particles. The filter layer contained at least one type of filtration medium that could be mechanical, electrostatic media, or a blend of the two. When higher filtration efficiency was required, the thickness of this layer was usually increased. In turn, the middle filter layer was responsible for most

airflow resistance [71]. The back cover that functioned to support and protect the inner filter was commonly made from spunbond polyester [70, 72].

Disposable filtering facepiece respirators were produced by cutting desired shapes for each layer from rolls of flat media. Each part of the respirator contained one or more sections that were stacked and thermally fused. Molded respirators acquired their unique shapes by heat application. During processes that elevated the temperature of the fibers, some of the electrostatic charge could be lost [72].

Other key changes in 30 CFR 11 included reclassification of particulate respirators. The new respirator categories included: high efficiency particulate aerosol (HEPA); dust/fume/mist (DMF) respirators; and dust/mist (DM). After March 1972, the DOP Man Test was deleted as a quantitative fit testing requirement in part due to adverse health hazards associated with this agent [65].

Qualitative fit testing with isoamyl acetate was changed from a certification requirement that used a 'test population' to a fit testing procedure for an individual respirator user. Under 30 CFR 11, this fit testing requirement was extended to include HEPA and DMF respirators. Respirator wearers were challenged with 100 ppm of isoamyl acetate for two minutes when they wore respirators that were intended to provide protection against fume concentrations greater than 0.05 mg/m^3. The duration of the test was changed to five minutes with inclusion of alternating physical activities for respirators that protected against radionuclides or when the contamination level was less than 0.05 mg/m

^{3}. The concentration of the challenge agent was increased to 1000 ppm if the respirator was a full facepiece, hood, or helmet [74].

Airflow resistance was evaluated at 85 liters/minute steady-state flow. If filters were to be used in pairs, the flow rate was reduced by half. Inhalation resistance across the respirator was assessed both initially and at the completion of each test, exhalation resistance was only measured initially [74]. The maximum allowable resistances are listed in Table 2.1.

Table 2.1
Maximum Allowable Breathing Resistance (mm H_2O) per 30 CFR 11

Type of Respirator	Initial Inhalation	Final Inhalation	Exhalation
Disposable (single-use)	12	15	15
Dust, fume, and mist with replaceable filter	30	50	20

Single use respirators certified as dust (D) or dust mist (DM) were not required to meet the breathing resistance requirements. The silica dust and the silica mist tests prescribed performance requirements for disposable respirators. Most disposable respirators were certified as DM. The dust test was more stringent and respirators passing this test would also pass the silica mist test [73].

Cyclic airflow was used to evaluate single use respirators during the silica dust test; air was cycled through a breathing machine at a flow rate of 40 lpm. 'Exhaled' air was warmed to 35 °C and 94 % relative humidity that simulated human breathing conditions. Silica dust that passed though the respirator was collected on an absolute filter mounted downstream, mass was determined gravimetrically. The duration of the test was 90 minutes; however, the test length

was increased and the flow rate changed from cyclical to steady state for respirator categories other than single use. The concentration of silica dust was 50 to 60 mg/m ^{3} and the particle size distribution had a geometric mean of 0.4 to 0.6 μm and a geometric standard deviation of less than 2.0 [74].

The lead fume test for air purifying respirators was 321 minutes in duration and utilized steady-state airflow of 32 liters/minute. Concentration of the lead-oxide fume ranged between 15 and 20 mg/m ^{3}, similar to the concentration specified in 21B. Environmental conditions in the respirator chamber were 20 - 80 % relative humidity and 25 °C. For tight fitting facepieces and powered air-purifying respirators (PAPR) the length of the test was decreased to four hours; flow rate was increased to 115 liters/minute for tight-fitting and to 170 liters/minute for PAPR. The total amount of unretained lead was not allowed to exceed 1.5 mg for air purifying respirators; however, more lead was allowed to be unretained for the other respirator categories [74]. There were significant differences between the collection efficiency obtained by the lead fume as compared to the silica dust test, with lead fume collection efficiency being much lower [30].

The silica mist test shared the same environmental temperature and humidity parameters, flow rates, and duration as the lead fume test. The concentration of silica mist in the respirator chamber was 20 to 25 mg/m ^{3}, about half the concentration specified in Schedule 21B. Unretained silica dust on air purifying respirator samples could not exceed 2.5 mg but the total amount of silica was increased for other respirator types [74].

HEPA respirators, intended to provide protection against a combination of more than one type of particulate hazard (dust, mists, and fumes) including radionuclides, were tested with both silica dust and DOP. DOP penetration was tested at dual airflow rates of 32 and 85 liters/minute for a 5 to 10 second duration. These flow rates were reduced by half if filters were used in pairs. At either flow rate, the maximum allowable penetration of DOP was 0.03%. Concentration of DOP was 100 μg/L and had a particle diameter of 0.3 μm [56, 74].

The DOP method used to evaluate HEPA filters was put into question by William Hinds [75] in 1978. Particle size evaluation of DOP had been determined with a polarized-light scattering device known as the 'owl'. Hinds et al [76] reported that DOP aerosol was not as monodisperse as had previously been assumed by demonstrating that the owl was unable to distinguish infinite particle-size distributions. The concern was that different particle-size distributions that had the same owl reading would yield different penetration results.

On June 8, 1995, Title 42 Code of Federal Regulation Part 84 [35] was enacted which superseded 30 CFR Part 11. This revision was prompted by the medical community as there had been an upswing in the number of reported tuberculosis cases. Respiratory devices used in health care settings by workers for protection against communicable diseases had not been regulated [77]. Under 30 CFR 11 the only air purifying respirator that met the Centers for Disease

Control (CDC) performance criteria for protection against tuberculosis was the high efficiency (HEPA) filter [35]. Respirators certified under all categories of the new standard met or exceeded the CDC guidelines and were less expensive than the HEPA filters. Under 42 CFR 84, authority for respirator certification was exclusively given to NIOSH. Only some equipment used for mine emergencies and rescue operations were jointly certified by NIOSH and MSHA. Sales and shipment of respirators certified under 30 CFR 11 were allowed to continue until July 10, 1998.

Particulate non-powered air purifying respirators were reclassified into nine new categories based upon type of respirator and their efficiency. The three new classes of respirators were N, R, and P with minimum collection efficiencies of 95%, 99%, and 99.97% designated as 95, 99, and 100.

Deleted in the new regulation was the isoamyl acetate qualitative fit test. Reasons for eliminating this fit testing requirement were that the isoamyl acetate test lacked both validation and correlation to worker protection. It was claimed that fit-testing individual workers as required by the Occupational Safety and Health Administration's (OSHA) respiratory protection program best served worker health concerns. The new standard was devoid of any fit testing requirements; certification was based on filtration efficiency alone. Only two aerosols were used for respirator certification, and DOP; both were neutralized to the Boltzman charge distribution [35].

Harwell Hounam [3, 54, 65, 79, 80] of the United Kingdom (UK) developed the method in 1962 which was used to determine the overall leak rate

of a respirator. Leakage was ascertained by comparing the concentration of salt aerosol inside and outside the facepiece of the respirator using flame photometry; this detection method had been used in the UK since 1948. Sodium chloride was adopted as the British standard for respirator testing in 1969 [82, 83]. In the United States, was considered to be more representative of a solid, polydisperse particulate contaminant in the size range commonly encountered in mining and industry. Varying the concentration of salt in solution for aerosolization [79] easily changed the size of the aerosol. The Bureau of Mines had experienced difficulty in generating and maintaining stable mass concentrations of lead fume and silica dust aerosols for respirator certification procedures stipulated in 30 CFR 11 [79]. For the first time in the United States, respirator penetration during certification was measured instantaneously using photometry and collection efficiency of the filter media was continuously monitored over the entire test period. This was a big advantage over the time-weighted averages for silica and wet-chemical methods that determined collection efficiency gravimetrically.

Deleted from 42 CFR 84 was the maximum allowable breathing resistance at the end of the loading test. The initial inhalation and exhalation resistance remained unchanged and single use disposable respirators were no longer identified in a separate category. The inhalation and exhalation resistance was recorded for 20 respirators at their designated flow rates of either 85 or 42.5 lpm depending if the respirator had a single filter or had filters which were used in pairs [35]. NIOSH determined that since the physiological limits on breathing

resistance were not the same from person to person, discomfort to the respirator wearer was the index selected to determine end of service life based on filter clogging.

'N' series respirators were intended to provide protection against particulates not containing any oil. Collection efficiency was determined from the maximum penetration measured over the test period for each of the three respirators evaluated. Respirators were required to be preconditioned at 38 °C and 85% relative humidity for 25 hours prior to testing. Preconditioning was intended to degrade the charge on electrostatic filters. Respirators submitted to NIOSH for certification did not designate the mechanism by which the respirator performed, electrostatic or mechanical. Instead, the filter medium was identified as a part number by the manufacturer [37]. The regulation specified the test aerosol concentration could not exceed 200 mg/m^3; however, no minimum concentration was stipulated. The concentrations of test agents used by the Certification and Quality Assurance Branch at NIOSH to challenge respirators were 15 to 20 mg/m^3 for sodium chloride and 100 to 120 mg/m^3 for DOP [84]. The main apparatus used by NIOSH for respirator testing was the Thermo-Systems Inc. (TSI) Model 8130. Disposable filtering facepiece respirators were either secured into a test jig or sealed onto a flat metal plate with beeswax. Determination of an adequate seal was intuitive based on experience. A 2% salt solution was atomized prior to aerosol pretreatment that removed larger particles and reduced the standard deviation. The aerosol had a count median diameter of 0.075 μm with a geometric standard deviation of less than 1.86. The method used to remove large particles was a cyclone but later was replaced with

an impaction plate. The new design was made available by TSI in March 1997 [85]. The duration of the certification procedure for N series respirators was about 180 minutes and terminated when 200 mg of aerosol contacted the respirator.

For aerosol, maximum penetration for mechanical filters occurred at the very beginning of the test or about 1/3 the way through the test if the respirator contained electrostatic media. In electrostatic respirators, the maximum penetration of increased for all particle sizes initially with loading. As aerosol deposition continued, the particle size of maximum penetration shifted to the smaller sizes when capture mechanisms changed from electrical to mechanical [86].

Both 'R' and 'P' series respirators were evaluated for certification with DOP aerosol. DOP was considered to be the most degrading aerosol to which a respirator filter could be challenged. The R series respirators were 'resistant' to oily aerosols whereas the P series respirators were considered 'oil-proof'. DOP aerosol had a count median diameter of 0.185 μm with a geometric standard deviation of less than 1.60. The R series test terminated when 200 mg of DOP contacted the filter. Termination of testing for the P series respirators had an additional requirement; filter penetration could not continue to increase after 200 mg had contacted the filter. Testing continued until penetration was stable. Maximum DOP penetration occurred at the end of the test period [36].

Electrostatic filters loaded with an oily aerosol similar to DOP, dioctyl sebasate (DOS), had increased penetration for all particle sizes. Maximum

penetration shifted to the larger particle sizes when the electrostatic fiber lost its charge [86].

Development of Electrostatic Respirator Filters

The empirical and theoretical relationships between filter efficiency and fiber diameter was established in the late 1930's [87]. This first effort which scientifically studied filtration was made in Germany. Albrecht and Kaufmann [3] made an original approach and developed a theory on the mechanism of aerosol filtration by fibrous pads. From this work, the use of glass fiber and other polymer fibers for high efficiency filtration was developed. Prior to this time, there were no guidelines to improve filtration efficiency and researchers would try anything they could lay their hands on in an attempt to create a more efficient respirator [40]. Materials impregnated with various substances indicated a complete lack of filtration understanding [85]. Different fibers were mixed together. When asbestos fibers were blended with wool they proved to be a very effective filter. Asbestos formed into pleated paper filters yielded the benefits of a large surface area combined with low breathing resistance [3]. High moisture and high temperature environments did not affect the efficiency of this filter. It was soon realized that when a fibrous filter was tested against smoke over a long time, the filtration efficiency increased as the filter was loaded. Various means of creating partially blocked filters were tried by incorporating fine powders into a fibrous mat [87].

In December of 1931, Nicolaij Louis Hansen [21], Director of the Danish Army Research Laboratory, patented the first electrostatic filter made of resin impregnated wool. Particles of resin were carded with wool fibers exchanging electrical charges. Resin was a good electrical insulator; its low electrical conductivity ensured that the charge on the filter material was stable [3, 21]. This discovery increased the collection efficiency of a wool filter from 50% to 99.99% [46]. The process for making this filter carded colophony (resin) powder with a diameter of 1 μm into wool fibers having diameters of 17 to 20 μm. The filter mat was passed through rotating rollers covered with metal hooks; adjacent rollers turned at different speeds [16, 21]. The card wires aligned the fibers into a web that developed a frictional charge. The resin acquired a negative charge while the wool fiber became positively charged [21, 88]. The web was combined into a fleece by either wrapping the web many times around a roller known as a lap drum or by placing the web in a zigzag pattern called cross-lapping. The entire fleece could be punched with barbed needles to form a needled felt. Since the surface of a wool fiber was naturally scaly, fibers were held together and felts could be made from wool without needling [21, 44]. Colophony was superseded by a colophony modified *p*-tetrabutyl phenol formaldehyde resin that impregnated the wool felt with a solution [88]. After the solvent evaporated the felt was subjected to mechanical friction thereby generating the electrostatic charge [87].

In Hansen's British patent number 384,052, the mechanism of action of the resin-wool filter was not referenced. His claim was that colophony together with its salts and esters had an 'exceedingly high affinity for colloid particles suspended in the air' and that it readily adhered to animal or vegetable fibers [88]. It is possible that Hansen himself did not clearly understand the improved collection mechanism of his filter. It has been speculated that he avoided referencing the electrical nature of the mechanism of action to preserve the novelty of his invention [87]. Seven years later, in 1938, Hill [88] who worked at the CDEE first postulated that an electrical mechanism was responsible for the improved collection efficiency of the resin-wool filter but was unable to account for the longevity of the charge. Gatty and Frank in 1940 implied that the surface resistivity of the colophony accounted for the longevity of the filter charge that they calculated to be 10 years. Equipment available to them at the time limited their ability to prove this claim. Walton [4] confirmed their postulations in 1942 who was able to measure the voltage drop over time. This verified the longevity of the filter charge. He also demonstrated maximum strength of the electric field in the immediate vicinity of the resin particle and concluded that electrification was entirely by friction [4]. Further work by Davies [4, 16, 46] allowed for understanding the longevity of the filter charge. The stability of the charge and long life of the filter were attributed to the high resistivity of the resin and the minute contact area between the resin and the fiber. The charge configuration in the resin-wool filter varied around the fiber circumference as well as along the

length of the fiber [21]. Localized areas of charge were created by the resin particles that resulted in local non-uniform electrostatic fields throughout the filter [16]. Walton [4, 46] found that these electrostatic fields would induce a charge on an aerosol that conveyed the particle to the wool or resin surfaces. This collection mechanism was described as being analogous to a magnet. By 1933, Hansen filters [3] were used by the Danish, Dutch, French, and Italian armies in their gas masks. The British first used the Hansen filters in civilian respirators in 1943.

Electrostatic fibers from a polymer were first developed by A.G. Thomas and documented in his 1956 patent. Thomas disclosed a process of charging thermoplastic fibers by softening the fibers with heat and subjecting them to a strong DC electric potential until the web had cooled. Elongated, hollow filaments were extruded from thermoplastic resins containing a pliable material such as carnauba wax that became electrically polarized. Thomas' patent claimed that fibers produced by this method had increased collection efficiency for solid particulates [6].

Split Fiber Electret

The first extruded molten thermoplastic materials proved to be disappointing for respirator applications [89]. This changed in March of 1974 when Jan van Turnhout developed his patented process for 'Filtrete' [90]. While working at TNO, Division of Technology for Society in Delf, Netherlands, van Turnhout discovered a process by which electrostatic fiber could be economically

produced from polypropylene resin. Although the use of electrets in the form of foils for microphones and headphones had been know for many years, the application of this technology to continuously produce a fiber with higher collection efficiency for particles was revolutionary [1]. This patent was later sold to 3M Company who developed numerous product lines from this process including the disposable filtering facepiece respirator model 8710 [8].

Van Turnhout's process for the manufacture of split fiber electret extruded a polypropylene film 40 μm thick and heated it to near melting point. While the film was warm it was stretched and corona charged [91, 92]. A positive charge developed on the front side of the web and a negative charge on the back. Later this process was improved by charging both sides at the same time that allowed for increased production speeds. After the web was cooled, needle rollers easily fibrillated it and repulsion force spread the fibers into a broad web. The individual fibers had the shape of a ribbon that could vary in width between 50 to 250 μm and a thickness between 10 to 25 μm [14]. Combining several web layers by needling or heating [93] formed a filter. One of the claims of this process was that the rectangular shape of the fibers promoted capture of uncharged particles by creating inhomogeneous electrostatic fields; uncharged particles would be attracted by van der Waals forces [14, 90, 94, 95]. References have cited the charge density for Filtrete filters from 2 to 90 nanocoulombs $(nC)/cm^2$ [90, 96, 97, 98, 99].

Nonpolar polymers such as polyethylene, polypropylene, fluorocarbons (Teflon), and polystyrene were preferred resins for split fiber electrets. Plastics with few or no polar groups would be charged more strongly than those resins with polar groups due to homocharging [100]. Fibers polarized by homocharging occurred during corona injection. The air space between the film and the electrode were ionized and charges trapped. Tightly bound charges in the nonpolar groups were not prone to free migration. This improved the stability of the electrostatic charge [94]. A second charging mechanism occurred via internal orientation of dipoles, known as heterocharging. Free charges in heterocharged materials easily migrated resulting in an unstable charge on the fiber. An advantage of non-polar materials was that the heterocharging mechanism was weak and the retained charge was more stable [94, 100]. Electrets made from polar polymers performed badly under harsh temperature and humidity conditions due to degradation of their charge [95]. This will be discussed in more detail in the section entitled *Charge Degradation of Electrostatic Filters*.

The characteristics of polypropylene lent itself as a popular resin for split fiber electret. First, polypropylene was a semi-crystalline material with numerous small crystallites. These areas which were effective sites for charge storage, added to the stability of the fiber charge. Alignment of the crystalline structures during stretching permitted the film to be easily split into fibers [92]. The extremely low electrical conductivity of polypropylene helped to retain the trapped charges [93]. Lastly, this polymer had a natural hydrophobic

characteristic and was not prone to charge degradation when subjected to high humidity environments [101].

Spunbond

Spunbond fabric, known as Reemay, was introduced in 1965 by DuPont [102]. In the mid 1970's, C.H. Dexter introduced electrostatic melt spinning as a unique process based on molten thermoplastic technology developed at the Battelle Institute [9]. The Carl Freudenberg Company of Germany utilized electrostatic spinning to manufacture microfibers for respirator filters [9]. Electrostatic melt spinning was patented in the United States in 1978, but the process of describing its production for use as a filter fiber did not appear in the literature until 1991 [13, 15]. Electrostatically spun fibers were produced from a liquid polymer that was sprayed in a heterogeneous electric field created by the spray and backing electrode. The liquid polymer was atomized on the edge of the spray electrode or spinneret to form a spray horn. These horns or droplets were stretched out to thread-like structures in the direction of the backing electrode and were deposited vertically onto a carrier medium. A second support web sandwiched the layers together and could be made from a variety of materials that possessed different physical characteristics: soft or rigid, heat sealable, pleatable or moldable, or water repellent [8, 15, 93].

Fibers formed by this process were continuous in length with a bilobed cross section [103]. The unique fiber shape occurred when the outer layer solidified first leading to a collapse of the fiber [22]. Fibers had a height to width

ratio of 1:3 and diameter ranged from 1 to 10 μm [8, 14, 15, 104]. The diameter was determined by the conductivity of the polymer melt adjusted by the addition of solvents or organic salts; diameter increased when the conductivity of the polymer was decreased [13]. Spraying more than one solution of a polymer melt each containing a different level of conductivity created layers in a web. The polarities of the spinnerets could also be alternated so that the web would possess partial positive and negative charges [101]. It was claimed that the charge on spunbond fibers could be retained from several months to two years [15, 105].

Electrostatic charging occurred by induction. Theory predicted that the fiber charge would be the same as the charge on the spinneret and be of only one polarity [22]. In actuality, extruded fibers contained charges of both signs that alternated in polarity and density down the length of the fiber [14, 93]. It was not known why charges of both signs existed [22, 106]. Fibers produced by this process had a charge density of about 6.0×10^{-7} nC/m, significantly lower than the charge level of split fiber electrets [96].

The mechanism by which spunbond fibers increased collection efficiency was a combination of both electrostatic and mechanical forces [2]. The fine fibers contributed to increased mechanical collection efficiency for particles ranging in size from 0.5 to 10 μm. A disadvantage of the small diameter fibers was increased pressure drop [14, 15].

Bonding, which was needed to consolidate the electrostatically spun fibers into a web, could be performed by several methods [103].

a) One type of bonding was needling which used barbed pins to push some of the fibers into an orientation perpendicular to the plane of the material. The surface of the material showed a pattern of small dimples where the needles had entered; punch density was about several ten per square centimeter. Needling could be varied by changing the punch density, the depth of needling, and the needle design [21, 102]. This form of bonding compacted and strengthened the web but often diminished the filtration efficiency [22].

b) Thermal bonding consolidated the web by fusing the fibers together. As the extruded fibers emerged from the spinning machines, their sticky nature adhered the new filaments together to form a web. Secondary heating also fused fibers together once they had cooled below their softening point. Heaters, hot air drums, pressurized steam ovens, or hot calendering through rollers were commonly used for thermal bonding [102].

c) Liquid adhesives or resins were applied to the web that accumulated at the filament contact points and caused them to bond. This wet process was not commonly used [102].

d) The addition of chemical or solvent bonding substances formed interfilament bonds that broke hydrogen chains and formed a complex with an amide group. When the solvent was desorbed, hydrogen bonds reformed between different fibers [102].

Polymers commonly used for electrostatic spun fibers were polycarbonate, polysulfone, or polyester [8]. Polyethylene was used for self-bonding newly formed fibers or heat and pressure could thermally bond the fibers. This polymer was also used as a binder with other fibers [102].

Melt Blown

Melt blown method for producing electrostatically charged fibers was developed by the Exxon Corporation who studied a device made available by the U.S. Naval Research Laboratory [107, 108]. This method was the earliest chemical-to-fiber route known [102]. 3M Company was the first to patent a process for producing electrostatically charged melt blown fibers for enhanced filtration [105]. Via this method, fibers were extruded from a polymer melt through fine orifices akin to electrostatic spinning. Whereas electrostatic spinning employed a polymer solution, melt blown was produced from a polymer melt [22, 107]. Two hot converging air streams at subsonic velocity attenuated the fibers. The aerodynamic force imbedded the corona charge into the attenuated polymer fibers [27]. While the polymer was hot, charges migrated into the polymer that had a lowered electrical resistance and were trapped upon cooling of the fiber [109]. Fibers solidified about 1 inch from the tip of the die and were collected on a moving screen. Extruded fibers entangled to form a cohesive web and thermal bonding occurred from the residual heat of extrusion. Other forms of web consolidation were not necessary as with the spunbond fibers [102, 103].

The fibers formed by this method were only several centimeters in length [27, 102]. The cross section of the fiber was circular and each fiber had an associated large sphere of polymer or 'shot'. The elastic 'snap back' of the fiber ends upon breaking [103] formed the 'shot'. The fiber diameter ranged between 1 to 20 μm and the diameter was adjusted by the polymer to air ratio during extrusion; fiber diameter was inversely related to air pressure [8, 102].

The charge configuration for melt blown fibers was the same as electrostatically spun fibers. Theory predicted the charge configuration to be the same as the charge on the electrode that would result in no electrostatic field [106]. It was unknown how fibers with opposite charges were formed. Thermoplastic polymers commonly used to manufacture melt blown fibers were polypropylene and polyester resins [8]. Polar groups added to the alloy helped catch and retain charge and added charge stability to a filter exposed to high temperatures [9].

Man-made fabrics had a propensity to absorb and hold oils. Application of a polymeric finish gave fibers good oil and water repellence [25]. Long chain perfluoralkyl groups were either added directly to the polymer melt or applied as an additive absorbed by the fiber matrix. A tightly packed chain of fluorocarbons, known as a Teflon finish, was formed. Additives in the polymer melt migrated to the fiber surface during extrusion to form a protective barrier

[25]. In 1991, 3M Company [23, 24] patented this method for respirator filter application.

Numerous techniques to electrostatically charge melt blown webs have been patented; fibers can be charged during different steps of the manufacturing process [11]. Air ionized in the area of the die tip embedded the charge into the fibers before they solidified [105, 109, 110]. Fibers could also be charged on the collector while they were still warm [12]. A patent by Wadsworth [110] charged fibers at ambient temperature by sandwiching the web between two layers of semiconductive fabric prior to passing between two electrodes. Corona charging occurred through conductive contact with the web [111]. 3M's 1980 patent for producing melt-blown fibers claimed a half-life of the electrostatically charged web to be at least one week at room temperature with 100% relative humidity [103].

Methods of Web Charging

The ancient Greeks knew electrostatic charging although they did not understand this phenomenon. They found that if amber were rubbed with wool, light objects would be attracted. Amber, called 'electron' by the Greeks, was fossilized resin [87]. At the beginning of the 17th century, William Gilbert termed 'electrical' the attraction exerted by rubbed amber upon light particles. Due to this rubbing, the term 'frictional electricity' was coined [101].

In order for electrostatic charges to be useful in filtration, a high electric field had to be present in the regions between the fibers. This meant that both positively and negatively charged fibers had to be present so that the filter as a whole was electrically neutral [44]. Within the filter there were nonuniform electric fields which were responsible for particle attraction [87]. An electrostatically charged fiber possessed this permanent electric field without an externally applied voltage. Electrostatic filters were made by either a polarized or electrostatically charged dielectric material [11]. There were three basic methods that charged a web used in respirator filters.

a) Tribocharging occurred when dissimilar fibers were rubbed together to impart a charge. The intensity and polarity of the charge depended on the materials [88]. The Hansen resin-wool filter was charged in this manner; however, a combination of natural and synthetic fibers could also be charged effectively [112].

b) Corona charging occurred when a polymer adsorbed ions or particles moving in an electric field. This method was used to charge the split fiber electret and ambient temperature melt blown fibers [88, 111].

c) Polymer fibers developed a surface charge by induction. Droplets developed a charge as a result of atomization or bubbling in an electrical field. Electrostatically spun and melt blown fibers were charged via this method [22, 88].

Filtration Mechanisms

Fiber diameter, particle diameter and density, packing density, and air velocity [22, 113, 114] determined mechanical collection efficiency in a filter. Mechanisms explained by single-fiber filtration theory included impaction, interception, diffusion, and gravimetric settling. Sieving was not considered to be a mechanical collection mechanism. This required the space between the fibers to be much smaller than the size of the particle and collection by this mechanism was remote [115].

Impaction occurred when a particle with sufficient inertia was unable to follow the air stream and was captured when it contacted the fiber. For particles having the same density, this mechanism was significant for particles larger than 0.4 μm diameter and filtration velocities in excess of 100 cm/sec [116]. When filter face velocity was increased, the Reynolds number of the particle also increased. Impaction was likely to occur when the trajectory of the particle ran closer to the fiber [14].

Interception occurred when a particle followed an air stream that happened to come within one radius of the surface of the fiber. This was the only mechanism that was not dependent on velocity of the air stream [76]. In mechanical filters, interception was a predominant collection mechanism [117]. This mechanism was important for particles that had a diameter between 0.2 to 0.3 μm. This particle diameter was considered to be in the range of minimum collection efficiency.

The effects of diffusional deposition increased as the particle size decreased [32]. An exchange in energy between a particle and a gas molecule resulted in the familiar microscopic motion known as Brownian motion which was greater for smaller particle sizes [21]. In diffusion, particles randomly crossed the air stream and contacted the fiber. Enhanced random motion depended on the particle size being less than 0.1 μm, a low flowrate, and elevated environmental temperature [3].

Aerosol particles tended to settle out in still air under the influence of gravity. The effect of gravitational settling during filtration depended on the direction of the airflow such that gravitational settling either augmented or diminished the transport of particles towards the filter [21]. In order for particles to be captured by gravity, the flowrate had to be low and the particle size greater than 2 μm diameter [118].

Electrical collection mechanisms attracted particles toward the filter fibers by an electrical field especially those in the submicrometer range [17, 115]. Electrical effects accounted for as much as 40% of the total collection efficiency of a filter [71]. There were three types of electrical collection mechanisms: Coulombic, induction, and image force.

Coulombic attraction occurred when both the filter fiber and the aerosol were charged. Collection by this mechanism was highly charge dependent [32, 116]. This mechanism was most efficient for very small particles close to 0.01 μm

and weak for particles close to 0.6 μm. The most penetrating particle size was 0.3 μm [119, 120].

Induction, also referred to as dielectrophoretic or polarization, occurred when the filter fiber was charged and the aerosol was neutral [96]. This mechanism was most efficient for particles close to 0.6 μm diameter and was negligible for particles 0.01 μm. The most penetrating size was less than 0.3 μm [120]. As particle size increased, the charge it carried became less important [32, 116, 119]. Larger particles were collected by polarization while smaller particles were collected by Coulombic attraction. Collection efficiency of particles less than 0.5 μm was strongly dependent on particle charge [120].

Image force, the inverse of induction, occurred when the filter fiber was neutral and the aerosol was charged. This mechanism was important for particles close to 0.01 μm in diameter and was quite weak for particles near 0.6 μm; the most penetrating size was 0.3 μm.

Single-fiber theory predicted that as particle size is increased, interception and impaction mechanisms would predominate. As particle size decreases, collection by diffusion would be enhanced. The most penetrating particle size was found to be between 0.1 to 0.4 μm in diameter. In this range both mechanical and electrostatic collection mechanisms were minimal and as a result penetration was bimodal [96]. Most collection mechanisms were affected by the aerosol flow rate, the exception being interception. As flow rate increased, particle size of maximum penetration shifted downward as electrostatic collection forces were

minimized. This was most noticeable at filtration velocities of 100 to 300 cm/sec [114].

Advantages and Disadvantages of Electrostatically Charged Filters

One of the advantages electrostatically charged filter media had over their mechanical counterparts was improved collection efficiency. These filters displayed greater particle loading capacity [21]. Respirators made with electrostatic filter media were produced more economically allowing the price of a respirator to be more competitive [34]. Since fewer electrostatic fibers were required to obtain equivalent filtration efficiency, filters with electrostatic media were less dense and the pressure drop across them was considerably lower [113, 119]. Air resistance in an electrostatically charged filter was nine times less than conventional unpleated high efficiency filters [1]. Lower breathing resistance resulted in less face seal leakage and improved respirator performance due to fit. Respirator users were provided with improved comfort by enhanced breathing ease thereby assuring greater respirator acceptance [7].

A disadvantage of electrostatically charged filters was that electrical enhancement could be lost when the fiber charge degraded [119]. Electrostatic filters relied heavily upon electrical charge for increased filtration efficiency. If the charge was lost the efficiency of the filter was reduced to a low level [1, 121]. Electrostatic discharge could result from a variety of interactions between a contaminant and the filter fiber.

Charge Degradation of Electrostatic Filters

Charge degradation of electrostatic filters was known to be caused by several factors that included: elevated temperature, humidity, and chemical or physical interactions between a contaminant and the fiber. Electrostatic filters preconditioned at an elevated temperature had enhanced aerosol penetration. Augmented penetration was detected for each incremental increase in temperature and was attributed to charge degradation. Since the charges on an electrostatic fiber were held in a range of bound states, shallow charge levels were lost when temperature was elevated while bound charges were retained. Also the chemical nature of the polymers changed with temperature. As temperature increased, polymer molecules moved and this movement was directly proportional to the rate of charge loss. The efficiency of an electrostatic filter stabilized at a given temperature [21]. Polar groups were added to the polymer alloy to help fibers retain a charge under high temperature conditions. Mitsui Petrochemical Industries of Japan [9] developed polar group addition technology. Electret nonwovens were recommended to be used in temperatures below 60 ^{o} C.

Electrostatic filters preconditioned at an elevated temperature and saturated relative humidity had collection efficiency decreased 2-6% [122]. Absorbed moisture lowered the dielectric resistivity of the filter when it formed a conductive path and drained the charge [16]. Since the dielectric constant of water was 80 times greater than air, exposure to moisture was much more degrading than exposure to ambient air. In water, the concentration of ion pairs

was at least 10^{13} compared to air that had 10^{3} [46]. More ions were available to interact and degrade fiber charge when filters were exposed to moisture. Water in equilibrium with the atmosphere contained carbon dioxide plus other impurities. Combined, they provided a conductive film on an electrostatic filter and leaked charge [88]. The degree of charge degradation due to humidity depended on the type of filter. In a 60% relative humidity environment, moisture regain in wool was 14%; however, this regain dropped considerably for synthetic fibers and regain ranged between 4% for nylon and 0.1% for polypropylene [2]. One study found that penetration in electrostatic filters made from synthetic fibers increased only 0.1% after 91 days of pretreatment [16]. Other studies concluded that collection efficiency was decreased by 2-6% due to pretreatment [18, 122]. Materials that were sensitive to elevated humidity were more adversely affected by a combination of elevated temperature and humidity than by either factor alone. Electrostatic filters preconditioned in elevated temperature and saturated relative humidity environments continued to decline in efficiency until only the mechanical filtration mechanisms remained [18].

Collection efficiency of electrostatic filters declined when captured particles interacted chemically or physically with the fiber. Organic solvents chemically interacted with the fiber surface charge and reduced filter efficiency [19]. Previous researchers have rinsed filters with isopropyl alcohol to completely remove electrostatic charge [31]. Submerging filters in benzene and

toluene [26] has also neutralized electrostatic charge. Dioctyl phthalate (DOP) interacted with the resin-wool filter by dissolving the resin [3, 16]. Chemical reactions between an organic solvent and a polymeric finish disrupted the fiber charge [2]. Solvents caused fibers to swell which disrupted the fluorocarbon chains of Teflon coated fibers. Once the protective coating was breached the fiber charge could then be neutralized by continued solvent exposure [25]. Vapors of organic solvent reduced collection efficiency of electrostatic filters from 71 to 49% [86].

Either ionization or charge cancellation can neutralize filter charge. In 1942 Walton [120] found that a dose of 2,000 to 3,000 roentgens increased submicrometer penetration of a resin wool filter from 0.01 to 0.1%. Synthetic filter fibers were more resistant to ionizing radiation and required a dose of 7,000 roentgens to increase penetration 10%. It was for this reason that the fine glass paper HEPA filter in atomic energy and biochemical manufacturing industries superseded the Hansen filter. The glass fiber filter was less likely to be discharged by radiation and was less bulky than the Hansen filter [87]. In 1978, Brown [44] demonstrated that a resin-wool filter with a greater packing density required 7,000 roentgens to increase penetration 10%.

The number of elemental charges carried by a particle affected filter penetration. The greater the number of charges, the more rapidly the electrostatic charge was neutralized when charges were transferred from the aerosol to the

fiber surface [19]. Sodium chloride contained less than 200 electron charges per particle compared to dioctyl sebasate (DOS) which had less than 10 electron charges per particle. Filtration efficiency of split fiber electrets decreased 24 times faster upon exposure to as compared to DOS [19]. Another study [122] found collection efficiency to decrease by 5 to 20% when the number of charges on a particle was increased. The most penetrating particles contained greater than 400 elemental charges [30].

The electrical properties of an aerosol may also be significant in degrading electrostatic filters [2]. Captured particles formed a conductive path that drained charge away from the fiber [19].

Particle Capture

In electrostatic filters, particles were captured on the downwind surface of the fiber by electrical forces. Particles were deposited uniformly about the entire fiber and the radius of the fiber was increased until fiber charge neutralization occurred [22]. Small particles were more efficient in coating the fibers than large particles containing the same mass. Coarse particles actually improved mechanical filtration mechanisms as minimum filtration efficiency existed when fiber size was large compared to particle size [95]. Once fiber charge was neutralized, mechanical collection forces, primarily interception and impaction, were the main collection mechanisms [26]. Captured particles became the preferred site for subsequent particle aggregation leading to the formation of

dendrites. These structures were characterized by a series of particle chains that behaved like newly formed fibers [22]. Long dendrites formed at points near 90 and 270 degrees from the upstream line in electrostatic filters. Although long dendrites were not as populous as the shorter ones, more particles were contained in the few long ones [117]. Without electrical enhancement, particles were deposited on the front side of the fiber by interception and impaction mechanisms impeding airflow past the fiber [27]. By comparison, dendrites in mechanical filters formed at 45 and 315 degrees from the upstream line [117]. Eventually the dendritic structures interconnected and blocked airflow [20].

In electrostatic filters, the outer layers of the filter were more likely to be loosely packed than the inner layers. This outer layer was the preferred site for particle deposition and only after it became heavily loaded with particles did the deposition profile creep through the filter [121]. Filters with fine fibers tended to clog more rapidly than filters made with coarse fibers. Reduced interstitial spaces of the fine fiber filters may have accounted for increased loading [22]. Dust cakes formed in electrostatic filters had a porous structure resulting in lower pressure drop [123]. In mechanical filters, the preferential location for particle deposition was the close spaces of the interior fibers. The dust cake formed in mechanical filters that was compact accelerated the blockage of airflow [27]. The rate that a filter clogged depended upon the aerosol concentration and duration of exposure [21]. The effects of filter loading on the collection efficiency of the respirator

could affect the estimated lifetime of the filter and the ultimate protection of the worker [21]. Factors that affected the formation of the dust cake in a filter included: particle size distribution, particle charge, adhesive and cohesive properties of the aerosol, and the pressure drop across the filter [22].

Blocked airflow in respirators resulted in more difficult breathing [22]. Respirators which had pressure drops in excess of 300 N/m^2 (30.48 mm H_2O) were considered unacceptable for conditions requiring heavy work [122]. Pressure drop was not linear with accumulated particulate loading but instead was characterized by sudden sharp increases with time. This resulted from collapse of the dendritic structures and localized compression of the cake structure [123]. Air resistance in electrostatic filters increased at a slower rate than in mechanical filters due to the way in which loading occurred on electrostatic fibers and the structure of the filter.

Van Turnhout [93] recognized that electrostatically charged filters only improved initial collection efficiency; as a filter was loaded with particulates the collection efficiency of the filter decreased. Increased penetration was attributed to particles shielding or neutralizing the electrostatic charge on the fibers. Electrical forces no longer improved particle capture and filtration occurred solely by mechanical filtration mechanisms. Collection efficiency was minimal at the point of charge depletion and began to improve when mechanical collection forces predominated subsequent particle capture. With additional filter loading, airflow resistance increased [21]. The collection efficiency curve for electrostatic

filter media displayed this characteristic dip during filter loading with solid particulates. For mechanical filters, initial airflow resistance was greater than resistance for the electrostatic filters. Collection efficiency of mechanical filters steadily increased with particulate loading and did not display an upswing in the penetration curve [1]. Spunbond fibers, that collected particles by 'mechanical-electrical' collection mechanisms, exhibited a collection efficiency curve resembling a mechanical filter [93].

Structured deposits did not form within a filter challenged by oily aerosols such as dioctyl phthalate (DOP) and the pattern of penetration was very different for liquids than for solid aerosols [21]. The chemical nature of polymers used in filter manufacturing conferred good water repellent characteristics to filters while oily liquids were encouraged to spread over the fiber surface [16, 19, 21]. The affinity of an oil droplet to the surface of a polymer fiber was even greater if the filter was electrostatically charged [21]. The maximum penetration of DOP occurred at the end of the loading period. Oil aerosols reduced collection efficiency by screening the fiber charge and wetting the fibers while some polymer fibers chemically interacted with the DOP. A liquid droplet collected by a filter bridged two adjacent fibers and brought them closer together which clumped the fibers [22]. When fibers clumped, pressure drop was reduced and filtration efficiency decreased [21].

Electrostatic Filter Charge

Electrostatically charged filters carried charges of both signs in about equal amounts although the configuration of the charges was complicated and varied, as previously discussed. Measuring the charge on a respirator filter was very difficult and its contribution to enhanced collection efficiency was not easily predicted [22, 28]. An early method to measure electrostatic charge on a filter was employed by Walton in 1942 [4]. An isolated resin wool fiber was mounted under a microscope and scanned with a quartz fiber. The strength of the electric field was indicated by the degree of deflection that was most noticeable in the vicinity of the resin particles [44]. Contemporary methods used to evaluate electrostatic charge have included the Faraday ice-pail, fiber scanning, bipolar charge measurement, and ionizing radiation.

The Faraday ice-pail was only capable of measuring excess charge of one polarity via an electrometer [21]. Fiber scanning, like the Faraday ice-pail, measured the total charge on a fiber that had been removed from the filter material. The fiber charge was scanned with a microprobe or pair of electrodes. The act of withdrawing a fiber from the filter material potentially altered the fiber charge that led to erroneous results [88].

The strength of the bipolar charge on a corona charged polymer film could be measured prior to fibrillation. Since the splitting process could alter the charge, this technique was only useful for an intact polymer sheet.

A widely accepted method of measuring electrostatic charge exposed the filter medium to ionizing radiation. As air molecules were ionized, ions of both

polarities were produced [124]. These air ions drifted to regions of opposite electrical signs on the fibers and neutralized the filter charge [21]. One roentgen produced 334 x 10^{-6} Coulombs of charge of each polarity in one cubic meter of air. Penetration was then measured by challenging the filter with aerosol. Radiation dose was increased until the penetration curve no longer increased and became flat. About 5,000 roentgens were commonly used to neutralize filter charge [125]. The difficulty with this method was determination of the endpoint for maximum aerosol penetration with a degree of accuracy. In addition to radiation dose, packing density and fiber diameter must also be known before the filter charge can be computed [21]. The charge configuration on the fiber was not determined by this method [22].

Aerosol Charge

Aerosol neutralization occurred when air ions combined with the charges carried on the particle. The majority of particles considered 'neutralized' were charged either positively or negatively depending on particle diameter, although some particles contained zero elemental charges and were considered charge neutral [21, 22]. As particle diameter increased, the number of elemental charges of a single polarity that a particle carried also increased. The distribution of charges for 'neutralized' particles was symmetrically distributed with a larger percentage of the particles possessing fewer elemental charges, referred to as a Boltzman charge distribution. Gunn [126] found that the distribution of charge was asymmetrical and tended to be slightly negative. Charge neutralization was

accomplished by two different means. The particles could either be exposed to an ionizing radiation source, such as krypton 85, or 'aged' in ambient air. An alternative system that avoided the use of radioactive materials was a bipolar corona device.

A popular type of neutralizing device contained ionizing radiation consisting of a small source, usually a few millicuries (mCi) of a low toxicity isotope. Krypton 85, a beta emitter with a maximum beta energy of 0.695 Mev and a half-life of 10.3 years, was an isotope commonly used in these devices [124]. Radiation ionized air in the vicinity of the aerosol and produced equal numbers of positive and negative ions that recombined with the charges carried on the particles neutralizing the aerosol [21].

'Aged' aerosols were neutralized by diffusion charging with ions present in ambient air. The ion concentration of ambient air was about 10^3 ions per cubic centimeter [3]. An example of an 'aged' aerosol was welding fumes. The process of aerosol generation produced particles with very high charge levels. In actuality the charge level tended to be relatively low due to the high concentration of free ions of both polarities which were produced in the hot plasma surrounding the welding process [33]. The method that generated an aerosol determined the level of charging [30].

Collection efficiency of both electrostatic and mechanical filters can be influenced by the number of charges carried on a particle [31]. Neutralizing and DOP aerosols decreased the collection efficiencies of filters by 5-20% [31, 113,

115]. The collection efficiency of filters challenged by silica dust was unchanged whether it was in a charged or neutralized state. However, lead fumes were collected with a higher efficiency when neutralized [31]. Collection efficiency was influenced more by aerosol charge than by filter preconditioning at elevated temperatures and saturated relative humidity environments [18, 30].

As the number of charges increased on a particle, the most penetrating size became larger. As the number of elemental charges swelled from 0 to 500, the most penetrating particle size shifted from 0.3 to 1.5 μm. The most penetrating particles in the submicrometer range had greater than 400 charges [31]. The most penetrating particle size in an electrostatically charged filter was larger for singly charged aerosol than for uncharged or neutralized particles. For uncharged particles, minimum collection efficiency occurred for particle sizes less than 0.1 μm where diffusion and induction forces had the least effect. Diffusion was the dominant collection mechanism for small uncharged particles while induction was the primary collection mechanism for large uncharged particles. For charged particles, minimum collection occurred between Coulombic and induction forces and the most penetrating particle size was greater than 0.1 μm [32]. When Coulombic and induction forces worked simultaneously, a single charge on an aerosol decreased penetration compared to a charge neutral particle [97].

Aerosol charge was one factor determining the most penetrating particle size in respirator filters. Other factors influencing filter penetration included: the test agent, particle size, particle density, airflow (face velocity), respirator category, filter packing density, fiber diameter, and fiber charge [28, 96].

The charge on an aerosol was measured by several methods. The first was an aerosol electrometer. This device integrated the charge on all particles collected. Data were only obtained for monodisperse aerosols. A second method was an electrical mobility spectrometer where charged particles were deposited on a collection plate based on their electrical mobility. The distance from the entrance slit to the point of deposition was proportional to the inverse number of elementary charges. An application of this technology has been extended to measuring particle size [19]. The Millikan chamber, a version of an 'ultramicroscope', directly measured the electrical charge of the aerosol and size of individual particles. This was a very tedious process requiring a great deal of manual effort [75, 76]. The laser Doppler velocimeter measured both size and charge of a particle. An oscillatory acoustic field and a DC electric field were established and particles were directed through the acoustic field. A lag phase was produced which measured aerodynamic particle size. Drift velocity in the electric field was proportional to the electric charge on a particle [19].

Unknown Effects on Collection Efficiency

Fundamental aerosol characteristics affecting the rate of charge degradation on electrostatic filters included the particle size distribution, charge distribution, and chemical nature of the aerosol [121]. Some aerosol properties

and environmental conditions varied so widely that their effects on respirator collection efficiency were either difficult to predict or not completely understood.

Contaminants generated in the workplace often contained more than one phase or type of contaminant. Gaseous or vapor phase contaminants coexisted in conjunction with solid particulates or liquid droplets. It has been known for some time that organic solvents disrupt the electrostatic charge on the fiber [2]. If one fraction of the workplace contaminant disrupted the electrostatic charge on the filter, subsequent particles challenging the filter could be collected with lower efficiency. Teflon coated fibers had their surface fluorocarbon chains disrupted by organic solvents [25]. Once modified, it was possible for other contaminants to interact with the electrostatic charge on the fiber surface decreasing the collection efficiency of the respirator.

Contaminants generated in the workplace varied in physical composition. This factor was a more important determinant of aerosol capture efficiency than the aerosol's chemical composition [21]. A contaminant's physical composition was potentially very damaging to the collection efficiency of electrostatic media [121].

The number of elemental charges a particle carried fluctuated by method of aerosol generation as well as day of generation [34]. Since the degree of aerosol charging changed from day to day, so did the extent to which it penetrated a filter [21]. Highly charged aerosols were typically found in the workplace. Some industrial processes deliberately generated high particle charge

levels to assist in deposition, such as spraying paint or crop-spraying [30]. The mechanism of aerosol charging resulted from the making and breaking of contacts between particles and surfaces. Electrical enhancement of the particle occurred when aerosols were generated in strong electric fields or when solid particles broke contact with a surface in an electric field [33].

Aerosols generated in the workplace were polydisperse. Since collection efficiency was influenced by particle size, as discussed previously, the performance of a filter medium changed depending upon the size distribution of the challenge aerosol.

The type of contaminant exposed to a respirator could alter its collection efficiency. Brown et al [2] discovered that foundry aerosols were much more degrading to electrostatic filters than either dry dust or coal tar fumes. Although the degrading effects of foundry aerosols were not completely understood, one proposed mechanism was the high electrical conductivity of one of its constituents, graphite, plus the presence of metallic fumes. Another proposed mechanism was that the small particle size of foundry aerosols had the capability to screen the charge on an electrostatic filter [22].

Disposable filtering facepiece respirators worn in hot or humid conditions could become saturated with either perspiration, moisture from inhaled high humidity air, or exhaled breath. Moisture accumulation from exhaled breath tended to be more pronounced in filtering facepiece respirators lacking exhalation valves. Collection efficiency has been studied for respirators preconditioned at elevated temperature and saturated relative humidity

environments; however, respirators used under extreme conditions has not been studied [16, 28]. Saturated relative humidity caused moisture to be collected by the fibers which filled the void spaces in the filter thereby increasing the pressure drop and face velocity across the filter. As the velocity of the airflow increased, there was less time for electrostatic collection forces to remove particulates [80]. There were only two studies that inferred what the effects on collection efficiency may be due to a saturated filter. Moyer et al [18] conducted a study that examined the effects of preconditioning respirator filters. The researchers experienced an equipment failure in the preconditioning chamber resulting in the formation of visible water droplets on the filter fibers. Collection efficiency of saturated respirators was reduced 10% compared to the 2 to 6% decrease for respirators which were preconditioned under controlled conditions. In a study conducted at Lawrence Livermore National Laboratory sections of electrostatic filter media were cut from disposable filtering facepiece respirators and submerged in various water solutions. After dipping, filter samples were rinsed and dried prior to evaluating penetration with aerosol. The researchers surmised that when fibers were sufficiently 'wetted', which in some cases required the use of a surfactant, ions in the water solution neutralized the charge on the filter fiber and filter penetration increased [19].

Worker Protection

Electrostatic media were widely used in filtering facepiece respirators due to their economical cost, enhanced filtration efficiency, and reduced breathing resistance [31]. Eighty to 90% of the filtering facepiece respirators submitted for

certification under the new regulation displayed collection efficiency curves characteristic of electrostatic media [37].

Workers were taught two indices that determined the end of the service life of a respirator. One was by increased breathing resistance and the second was by detection of contaminant breakthrough [38]. If the charge on electrostatic media was degraded from contaminants, filter clogging with its increased breathing resistance may not occur. Worker exposure could result when the service life of a respirator was reached without the wearer's knowledge. The second method with which workers determined end of respirator service life was contaminant breakthrough. Some solid or liquid aerosols may not have an odor or taste associated with the contaminants and breakthrough may be undetected [35]. Since the type of mechanism by which a respirator performed had not been identified on products, the wearer may not have been aware of differences in detecting end of service life.

The ability of laboratory performance data to adequately predict workplace performance of respirators with electrostatic media remains unclear. The correlation between respirator penetration with submicrometer particles for predicting worker exposure to supermicrometer contaminants has not been validated [28]. Studies that have attempted to correlate workplace exposure to laboratory tests have been unsuccessful [39]. Previous researchers have questioned the validity of the NIOSH method to predict worker protection [28, 29, 30].

CHAPTER III

PURPOSE AND SCOPE

Rationale

Electrostatically charged filter media are widely used in filtering facepiece respirators and in disposable cartridges for air purifying respirators. Previous studies have questioned the validity of NIOSH's filter loading and penetration tests for respirator certification in predicting worker protection from common aerosols produced in industry [29, 30, 31]. Workplace contaminants can affect the collection efficiency of electrostatic media since they contain varying particle size distributions, can be composed of different parent materials which possess unique chemical and physical properties, and carry different numbers of electron charges per particle. Respirator performance, as determined by the NIOSH certification tests, has not been correlated to the respirator performance in the workplace. It is unknown how well workers are protected when respirators with electrostatic media are placed in environmental conditions that may deleteriously affect the filter fiber charge. Electrostatic charge may be depleted or masked which reduces the collection efficiency of the respirator prior to being sufficiently loaded with contaminants increasing the breathing resistance. Wearers may not be aware

that the "end of service life" for their respirator containing electrostatic media has been reached if increased breathing resistance is not indicated.

The collection efficiency of respirators with electrostatic media may be overestimated by the NIOSH respirator certification method, which uses a neutralized NaCl or DOP aerosol. Workplace aerosols may have a higher filter penetration than aerosols used for respirator certification. A recent notice issued by NIOSH indicated that the collection efficiency of the P-series respirators might be seriously reduced below the established rating of the respirator during long-term oil exposure in the workplace [127].

Degradation of the fiber charge on the electrostatically charged respirator media is known or suspected to occur during certain use and environmental conditions [2, 26]. When an electrostatic respirator becomes waterlogged, void spaces in the media fill with moisture and ions can interact with the fiber charge reducing their collection efficiency by charge neutralization.

Hypotheses

1. Respirators with electrostatic media will have lower collection efficiency than predicted by the NIOSH certification method when exposed to certain workplace contaminants. Workplace contaminants will neutralize the charge on the filter fibers by charge cancellation, mask fiber charge, or degrade fiber charge by chemical alterations.
2. The collection efficiencies of respirators with electrostatic filter media will be lower than respirators containing mechanical filter media when loaded

with contaminants representative of the workplace. The physical and/or chemical characteristics of workplace contaminants will mask or degrade the fiber charge on electrostatically charged filter media.

3. Filtering facepiece respirators containing electrostatically charged media that are saturated with simulated perspiration will have decreased collection efficiency. Ions from the perspiration will neutralize the electrostatic charge on the fiber.

Research Objectives

This research objective was to determine if the NIOSH particulate air purifying respirator certification method adequately predicts the collection efficiency of respirators with electrostatically charged media exposed to workplace contaminants; some contained a gas or vapor phase. Respirators saturated with simulated perspiration were evaluated for degradation of collection efficiency.

Scope

Electrostatically charged filtering facepiece respirators and cartridges for air purifying respirators were obtained from various respirator manufacturers. All respirators used for this study were NIOSH certified under the current regulation (42 CFR Part 84). Respirator screening tests were conducted using either NaCl or DOP aerosol with Boltzman charge distributions under steady state airflow. Selection of the aerosol was based on the respirator series. The protocol used for the screening tests was equivalent

to the NIOSH respirator certification method specified in 42 CFR Part 84. The purpose of the screening tests was to:

1) evaluate filtration performance of electrostatic media, and

2) identify respirators to be used for testing with workplace contaminants

The criteria for selecting respirators for subsequent testing with workplace contaminants were based on average collection efficiency, standard deviation of the collection efficiency, the respirator category, respirator style, and consideration of the respirator manufacturer. The number of replicates for each test was set at a minimum of five.

Respirators were loaded with aerosols generated both in the laboratory and in the field. One aerosol, metal cutting fluid mist, was duplicated to include both modes of aerosol generation, field and laboratory. Aerosols generated in the laboratory include aluminum oxide dust and metal cutting fluid mist. Field generated aerosols included asphalt fumes and metal cutting fluid mist. These contaminants were used to determine if the performance of respirators with electrostatically charged media was altered from the predicted performance according to the NIOSH method.

In the laboratory, aerosol concentration and particle size distribution were determined with analytical equipment. In the field, aerosol concentration data were collected using industrial hygiene sampling methods and particle size distribution determined with a cascade impactor.

Respirators were preconditioned by loading with varying masses of each of the workplace aerosols. Collection efficiency was determined with the "test" aerosol, a dilute concentration of NaCl aerosol neutralized to Boltzman charge distribution. Under steady-state airflow, penetration the "test" aerosol was determined from upstream and downstream concentration measurements. To ascertain if electrostatically charged respirator media collection efficiency was altered by saturation, respirators were submerged in a solution of simulated perspiration prior to evaluating penetration with a dilute concentration of DOP aerosol.

CHAPTER IV

METHODS AND MATERIALS

Overview of Experimental Design

This research attempted to determine if the National Institute for Occupational Safety and Health's (NIOSH) particulate air purifying respirator certification method, described in 42 CFR 84, accurately predicts collection efficiency of air purifying respirators containing electrostatically charged filter media while exposed to, or following exposure to, air contaminants representative of the workplace. Since the NIOSH certification method does not differentiate the mechanism by which a respirator collects particles, the standard applies equally to respirators containing either electrostatic or mechanical filter media. The collection efficiency of air purifying respirators containing electrostatic and mechanical filter media was evaluated by loading them with aerosols either generated in the laboratory or produced from field operations. Some of the workplace aerosols contained a gas or vapor phase in addition to the particulate fraction. The effect on the collection efficiency of filtering facepiece respirators saturated with artificial perspiration was also evaluated in the laboratory.

Particulate air purifying respirators were evaluated under four different test scenarios. Specifically:

a) The collection efficiency of respirators containing electrostatic media were evaluated using the NIOSH method with a test aerosol of either sodium chloride (NaCl) or dioctyl phthalate (DOP), depending upon the respirator category, N95 or P100;

b) Representative workplace aerosols (aluminum oxide dust and metal cutting fluid mist) were generated under laboratory conditions and were loaded onto each respirator. The collection efficiency was determined at two-hour intervals by challenge with a dilute charge neutralized NaCl, hereafter referred to as the 'test' aerosol. The loading time ended after six hours;

c) Aerosols of metal cutting fluid mist and asphalt fumes represented air contaminants produced in the workplace and were loaded onto each respirator. The collection efficiency was determined at two-hour loading intervals by challenge with the 'test' aerosol. The loading time ended after six hours;

d) The impact on collection efficiency from a filtering facepiece respirator becoming saturated with the wearer's perspiration was determined by submerging respirators in a solution of artificial perspiration. The respirator was allowed sufficient contact time with the solution to permeate void spaces in the filter media. These respirators were dried with HEPA filtered air and the collection efficiency was evaluated with the 'test' aerosol;

e) Using the NIOSH method test, statistical analyses compared predicted collection efficiencies of individual respirators to their actual collection efficiency when loaded with each contaminant representative of the workplace. Performances of N95 respirators containing electrostatic filter media were compared to an N95 respirator with mechanical filter media for each test scenario.

The principal objective of this research was to address the following research questions:

a) Does the NIOSH certification method for air purifying respirators accurately predict the collection efficiency of electrostatically charged filter media respirators that are challenged with contaminants representative of workplace environments?
b) What is the effect upon the collection efficiency of air purifying respirators that have been saturated with artificial perspiration?
c) Is there a difference between the collection efficiency of respirators containing electrostatic media and those containing mechanical filter media?

Study Respirators

Non-powered air purifying respirators were divided into nine categories under 42 CFR 84. The least protective respirator category, N95, was only approved for respirator protection from particulate nonoily aerosols. The most protective respirator category, P100, was equivalent to a HEPA filter and

was considered to be resistant to degradation from oily aerosols. These two categories were selected for this project as they encompassed the range of respirator collection efficiency in this class of respiratory protection. A listing of N95 and P100 series respirators certified according to 42 CFR 84 was obtained from NIOSH. During a telephone survey of respirator manufacturers, approved products containing electrostatically charged filter media were identified. Some respirators approved under 42 CFR 84 were very new and were not available for release from the manufacturer, as production was limited. A total of thirteen N95 and three P100 respirators from nine different manufacturers were either supplied or purchased for testing. Refer to Appendix Table B.1 for a listing of the respirators used in this study by test scenario. Racal Delta N95 was counted twice because two sets of respirators from different lot numbers represented different respirator sizes, small and medium.

One N95 respirator and one P100 respirator selected for this project contained only mechanical filter media. The Racal mechanical N95 respirator was selected for this project because its overall configuration was similar to the Racal Delta. The filter media in the Racal mechanical was a melt blown fiber, a very common filter medium used in air purifying respirators [93]. When melt-blown fibers are not corona-charged, enhanced electrostatic filtration mechanisms are absent. However, it is possible for some particles to be collected by electrostatic filtration mechanisms such as image force where the fiber charge was neutral and the aerosol was charged.

The number of electrostatic P100 respirators approved under the new certification standard, 42 CFR 84, was very limited. Only a few of these new products had been placed into production allowing them to be commercially available. 3M was one of the few respirator manufacturers who produced both electrostatic and mechanical P100 products and was able to provide samples for this research project. The filter medium in the mechanical P100 respirator, 3M 7093, was glass fiber and representative of respirators in this classification [129]. Glass fiber filter medium provided good mechanical filtration efficiency. Its fine fiber diameter can be altered by the manufacturing process [111].

All respirators were evaluated according to the NIOSH certification method based upon their classification, N or P series. The criterion used for selecting respirators for additional testing with workplace contaminants was based upon the classification of the respirator, the style of the filter, and other qualities that uniquely represented the variety of products available to the worker.

Aerosol Selection

Aerosols and the methods used for describing the NIOSH certification method are outlined in 42 CFR 84. NIOSH uses two different aerosols for certifying air purifying respirators: NaCl for N series respirators and DOP for P series respirators. Both aerosols have been used for over 30 years to evaluate respirator filtration efficiency and/or respirator fit [58]. DOP has been used for HEPA filter testing was selected by NIOSH as the test aerosol for R and P series

respirators since it is the most degrading aerosol known. This severity was an integral part of the part 84 testing and addressed the uncertainties of the effects of actual workplace aerosols [31]. Tests duplicating the NIOSH certification method were used for comparing the collection efficiency of respirators loaded with workplace contaminants.

Two of the three workplace aerosols, metal cutting fluid mists and asphalt fumes, were selected for this project because of their current importance in the industrial hygiene community and also because they also contain either a gas or vapor phase in addition to the particulate phase. The third aerosol, aluminum oxide dust, was selected to represent a mineral dust and its collection efficiency was expected to be similar to NaCl that should not degrade respirator performance.

The Threshold Limit Value (TLV) committee of the American Conference of Governmental Industrial Hygienists (ACGIH) is currently reviewing the carcinogen classification of asphalt fumes. The reclassification of this aerosol has been the topic of widespread debate. It contains both particulates and volatile hydrocarbons [130, 131]. Existing epidemiological data for worker asphalt fume exposure are severely confounded with coal tar pitch. NIOSH has identified over 1,000 compounds in characterizing roofing asphalt fumes, yet the hazardous compounds or family of compounds have not been identified [4, 125]. In 1996, NIOSH estimated 500,000 workers were exposed to asphalt fumes from paving roads, roofing, and waterproofing [134].

There has been widespread interest in metalworking fluid mist by NIOSH, labor, industry, academia, and other government agencies. Workers exposed to metalworking fluid aerosols have an increased risk of nonmalignant respiratory disease and skin diseases. Some metalworking fluids have been associated with an increased risk of larynx, rectum, pancreas, skin, scrotum, and bladder cancer. Studies have not been able to identify the specific constituent(s) or contaminant(s) responsible for the increased risk. This is possibly due to the long latency period of the disease or to the diverse nature of the mixtures studied. NIOSH has estimated that over one million workers in the United States are exposed to metalworking fluids [81]. On January 1998, NIOSH instituted a Recommended Exposure Limit (REL) to metalworking fluids at 0.4 mg/m^3 thoracic particulate mass. In light of thoracic samplers not being widely available, a total particulate mass of 0.5 mg/m^3 was established as determined by gravimetric analysis, NIOSH Method 0500 [136]. Many metalworking fluids have significant vapor pressure at room temperature. In an aerosol form, the droplet can evaporate once it is collected upon a filter thus creating an underestimate of exposure [137]. In an air stream, the volatile components of the aerosol can evaporate, potentially exposing workers to the vapor.

Aerosol Concentration and Penetration Measurements

Electronic Detection of Penetration

Aerosol penetration through the respirators was measured in the laboratory by two different methods; one, counted the individual particles

challenging and penetrating the respirator and two, measured total light scatter corresponding to relative concentration. The first method used for determining respirator penetration measured relative aerosol concentrations upstream and downstream with a photometer model (JM 9000). As particulate matter in the air stream was drawn past the focal point of the scattering chamber, light was scattered forward in the cone. Scattered light detected by the phototube, sent a signal to the amplifier and was displayed on a digital readout. Relative aerosol concentration was derived from the total light scatter from many particles at once. This instrument detected particles ranging from 0.1 to 600 μm and had a dynamic operating range of five decades. The flow rate through this equipment was regulated by a 0 to 500 scfh flow meter (Fischer Porter: model FP-1/2-27-G10/55) operating at 22 lpm.

The photometer was selected for measuring penetration as this equipment gives a quick reading and is currently the instrument used for aerosol detection during respirator certification by NIOSH [30]. Since the photometer measures light scatter from a group of particles, concentration in the airstream, aerosol properties such as size, shape, and optical scattering properties influence the total light scatter [138]. If the size distribution of the aerosol changes, instrument response will change. The most dramatic effects occur when the larger particles in the distribution are removed [67]. If the particle size were to change from 1μm to 0.3μm, the photometer signal can decrease by a factor of one million and the results can be misleading [114]. The photometer penetration measurement emphasizes the larger particles;

penetration measurements are more closely associated with particle surface, larger particles result in a higher intensity of light scatter. Since the response of the photometer weights the large particles, penetration measurement with this instrument may provide a better single estimate of actual aerosol mass exposure to a respirator wearer where chemical contaminants are present.

The Condensation Nucleus Counter (CNC) has also been used to measure HEPA filter penetration [138]. This instrument readout spans eight decades yielding a more sensitive measurement of penetration, which is especially helpful in determining low penetration measurements. The CNC placed equal importance on each particle independent of its size. In this instrument, particles pass through a vapor of butyl alcohol which condense on the particle forming a droplet as the aerosol stream is chilled to 10 ^{o}C. The nuclei grow to about 10 μm diameter, irrespective of their initial size, and pass through a beam of white light. The alcohol size enhancement provides a measurement of particles which otherwise would be too small for detection. Light scatter is used to measure concentrations between 10^{-2} to 10^{7} particles/cm^{3}.

The two operating modes (single-particle optical counting, and photometric) of the CNC (model 3020) were brought into agreement by electronically zeroing the photodetector. Below 10^{3} particles/cm^{3}, droplets were individually counted as they passed through the viewing volume. In the photometry mode, 10^{3} to 10^{7} particles/cm^{3}, total light scatter from all the droplets were measured. The sampling flow rate through the CNC was

regulated by a Matheson 602 flow meter. The flow meter was adjusted to operate at 0.3 lpm with a Dry Cal DC-1 Flow Calibrator.

Since the CNC and the photometer use different detection principles, their measurement of respirator filtration may differ. Filtration measurement by the two instruments is in better agreement at very high penetrations where the size distribution of the challenge aerosol remains relatively unchanged as it passes through the filter. At low penetration rates, the larger particles tend to be removed and the two instruments are more likely to differ. Another factor affecting instrument agreement is the diameter of the challenge aerosol. When the test agent has a mean diameter greater than the diameter of the maximum penetration for the filter, the CNC can be expected to indicate higher penetration values than the photometer [138].

Concentration Measurement of Laboratory-Generated Aerosols

Concentrations of laboratory-generated NaCl, DOP, and aluminum oxide aerosols were determined by collecting samples on desiccated 47 mm diameter 0.45 μm pore size Millipore mixed cellulose esters (HA) filters. The mass collected was evaluated gravimetrically following 24 hours of desiccation. Samples were collected at flow rates of 10 lpm; sampling time varied from 10 to 60 minutes. Concentrations of metal cutting fluid mist generated in the laboratory were determined by collecting samples on 47 mm 0.45 μm Nuclepore Filinert (PTFE) membrane filters at 10 lpm and sampling time was approximately 60 minutes. These Teflon filters were selected for

their hydrophobic quality, low weights, and because they did not require desiccation.

Concentration Measurement of Field-Generated Aerosols

Samples of field-generated aerosol were collected by standard industrial hygiene methods. Sampling trains consisted of clear closed face cassettes with 0.8 μm PVC filters and Gillian high flow pumps. The sampling rate of 2 lpm was calibrated with a flow calibrator. This flow rate was determined from NIOSH Method 0500 for total nuisance dust. To account for ambient dust, diesel exhaust, and other environmental contaminants [130], background samples of ambient air were collected adjacent to the field sites. Sampling pumps were turned off when respirators were removed from the apparatus and taken to the laboratory for penetration evaluation with NaCl aerosol. Concentration measurements for the "control" respirators were expected to be quite low and one cassette was used for each six hours of loading. Initially, cassettes for "exposed" respirators were changed after each six hours of loading but later were changed after each two hours to capture the fluctuations in concentration generation throughout the day. Duration of sampling time for the filter cassettes was recorded with the start/stop timer located on the sampling pumps. Mass of asphalt contaminants and metal cutting fluid mist collected by the cassette filters was determined gravimetrically using a Mettler-Toledo scale model MT5 having an accuracy of 0.001 mg. Industrial hygiene laboratory personnel who weighed the filters also computed the aerosol concentration.

Characterization of Particle Size Distributions

Particle size distributions of aerosols were determined using three different methods. Laboratory generated aerosols were measured with either an optical counter or an electrostatic aerosol classifier having a condensation nucleus counter as the particle detector. In the field, aerosol size distributions were determined with a cascade impactor.

Climet

The Climet Particle Analyzer model 208 counted and sized particles of aluminum oxide dust and metal cutting fluid mist generated in the laboratory. As individual particles were detected, an electrical impulse was produced whose amplitude and frequency corresponded to the size and concentration of the particles. The particle detection assembly used a mirror and a high-intensity filament lamp to detect particles drawn into the detection chamber. The forward-scattered light was collected by optics and converted to electrical impulses by the photomultiplier tube. This electrical output was directed into a BNC Portanim model AP-1 log amplifier and transferred to a 126 channel Multichannel Analyzer. Data were downloaded to a laptop computer for analysis. The source of vacuum for the Climet was an internal pump whose flow rate was calibrated at 7 lpm using the flow calibrator. The range of detectable particles (0.3 to 10 μm) was determined by the settings on the log amplifier. Latex spheres and glass beads of known diameter were used to calibrate the channels from which a linear model was constructed and used for computing the size distribution of aerosols. Latex

spheres were visually inspected for spherical shape under a microscope. This instrument was used to determine the size distribution of metal cutting fluid mist and aluminum oxide dust.

Differential Mobility Analyzer

The size distributions of charge neutralized NaCl and DOP aerosols were measured with a TSI Differential Mobility Analyzer (DMA). Aerosols were neutralized to a Boltzman charge distribution as they passed through two TSI 10 mCi krypton sources, model 3054, at a flow rate of 85 lpm. A TSI 2 mCi krypton source, model 3077, was placed on the inlet port of the DMA to ensure complete sample charge neutralization. Neutralized particles flowed through the mobility analyzer as a thin laminar stream between two concentric cylinders; an extraction slit was cut in the center rod. Particles with higher electrical mobility were collected on the upper portion of the rod. Particles with mobility less than the cutoff, as determined by the voltages on the tubes, passed out the exhaust. The remaining particles in the narrow mobility range and correlated to a known diameter, passed through the narrow slit in the center electrode. These collected particles were counted by the CNC (248, 54). The voltage of the collector rod and airflow rate determined particle extraction. Airflow rates, 3 lpm for the sheath air and 0.3 lpm for the aerosol flow, were calibrated with the flow calibrator. The intervals of the voltage settings were established so that the range of particles collected at each setting was contiguous to the next. Correlation of particle size to a voltage setting was confirmed with monodisperse latex spheres. The

detectable size range of particles was from 0.005 to-1 μm. The number of voltage settings evaluating NaCl was 32, mean particle diameter ranged from 0.014 to 0.809 μm. The number of voltage settings evaluating DOP was 29; mean particle diameter ranged from 0.024 to 0.837 μm. The count median diameter (CMD) and geometric standard deviation (GSD) were computed from the raw data using the following equations [76].

$$CMD = \exp\left[\frac{\sum n_i(\ln d_i)}{N}\right] \qquad \text{(equation 4.1)}$$

$$GSD = \exp\left[\frac{\left(\sum n_i(\ln d_i - \ln d_g)^2\right)}{N-1}\right]^{1/2} \qquad \text{(equation 4.2)}$$

Where: d_i is the midpoint diameter of the *i*th group, d_g is the geometric mean diameter, n_i is the number of particles in the *i*th group, N is the total number of particles in the sample,

The voltage settings collected particles for a discrete size range from an aerosol sample, not the entire particle population, as voltage settings were incrementally increased. By sequencing the voltage intervals and estimating particle counts with the CNC, some particles may not have been counted. To compensate for this effect, the fitted size distribution was computed which minimized the total residual variability or the sum of the overall distances between the observed and the estimated lognormal distributions. Using an Excel™ spreadsheet, the total number of particles counted, the CMD, and the GSD were varied to compute a fitted distribution of the sample. Using these variables, iterations of the computations were made until the sum of squares

error was at its lowest value. This indicated that the fitted distribution was as close as possible to the observed particle counts for each particle diameter.

Andersen Cascade Impactor

The Andersen Cascade Impactor Mark I was used in the field to measure the aerodynamic size distribution of particulate mater. Particulate matter was fractionated size wise into increments by inertial impaction on collection surfaces. Each collection plate on the seven stage impactor, was covered with either a Millipore or Nuclepore filter. Asphalt contaminants were collected on either 0.2 μm Millipore hydrophobic polyvinlyidene fluoride GV filter or a 0.45 μm mixed cellulose esters Nuclepore Membra-Fil filter (Separation Division of Corning Inc., Acton, MA). The back up filter following the seventh stage for collection of particles smaller than 0.2 μm was either an 8.0 μm Millipore mixed cellulose esters SC filter or a 5.0 μm Millipore mixed cellulose esters SM filter. The detectable aerodynamic particle size range was from 0.001 to 9 μm. All filters used for evaluating asphalt contaminant size distribution were pre- and post-desiccated for a minimum of 24 hours. Metal cutting fluid mist was collected on 0.45 μm Nuclepore Filinert (PTFE) membrane filters. This hydrophobic filter was used for covering each of the seven collection plates and the back up filter. Desiccation was not necessary since their inherent qualities repelled moisture. Post-desiccating filters used for collecting metal cutting fluid mists was avoided as some cutting fluid mass may possibly have been lost. Mass collected was determined gravimetrically using an Ohaus scale model AP110S

having an accuracy to 0.0001 grams. The cascade impactor operated at a flow rate of 28 lpm as per the instruction manual for this instrument. The mass median diameter (MMD) and GSD were computed from the raw data collected on the eight filters. Since mass collected on each stage of the Andersen Cascade Impactor was dependent on the aerodynamic properties of the particles, the equation for MMD computes the mass median aerodynamic diameter (MMAD). The size distributions from the cascade impactor were reported as MMAD using the computational formula for MMD [76]:

$$MMD = \exp\left[\frac{\sum n_i d_i^3 \ln d_i}{\sum n_i d_i^3}\right] \qquad \text{(equation 4.3)}$$

Where n_i is the number of particles in the ith group and d_I is the midpoint diameter of the ith group

Each filter stage collected a wide range of particle diameters based upon the flow rate through the cascade impactor. To refine calculations of MMAD and GSD, a fitted size distribution was computed. Similar to the calculations for fitted size distributions with the DMA, the fitted size distribution of the cascade impactor minimized the total residual variability or the sum of the overall distances between the observed distribution and the estimated distribution. Using an Excel spreadsheet, the total number of mass concentration (mg/L) per log width, the MMAD, and the GSD were varied to compute a fitted distribution of the sample. Using these variables, iterations of the computations were made until the sum of squares error was at its

lowest value. This indicated the fitted lognormal distribution, with 47 data points, was as close as possible to the observed mass concentration per log width for each of the eight particle size bins.

After each two hour asphalt contaminant loading, respirators were removed from their holders and were returned to the laboratory to evaluate penetration. During this interim of approximately one hour, the pump operating the cascade impactor was turned off. The cascade impactor was covered with a clean plastic bag and remained at the field location. Covering the opening of the cascade impactor prevented ambient air particles from being blown into or settling on the first filter layer. Metal cutting fluid aerosol generated in the field was also collected on the cascade impactor in a machine shop where no other operations were occurring. During intervals between aerosol loading on the respirators, airflow to the cascade impactor was turned off and it remained uncovered.

Test Apparatus Assembly and Test Conditions

Replicating the certification method tests used by NIOSH for N and P series non-powered air purifying respirators required equipment to be assembled into an apparatus to duplicate the function of TSI model 8130, the standard equipment used for respirator certification. Schematic drawings of the NaCl test apparatus can be found in figure 4.1; the dioctyl phthalate schematic is detailed in figure 4.2. The testing setup was designed to operate under negative pressure to prevent aerosols from escaping to ambient surroundings and causing potential worker exposure. The source of vacuum

for both the system flow and operation of the detection equipment was supplied by a carbon vane pump. One photometer and one CNC recorded respirator penetration; upstream and downstream measurements were alternated and instrument readings were recorded simultaneously. Sodium chloride aerosol was considered well mixed with the HEPA filtered air at the point of upstream aerosol sampling. HEPA filtered air passed through the NaCl generator and transported the aerosol through a thirty-six inch section of two inch diameter ducting, two neutralizers, and a sharp edge orifice meter before reaching the sampling probe. Location of the sampling probe was located ten duct diameters downstream from the sharp edge orifice. An unobstructed zone without bends five to ten duct diameters downstream is the preferable location of sampling in a duct [76].

The Reynolds number (Re) is a dimensionless number that characterizes fluid flow through a pipe as being either laminar or turbulent as is computed using equation 4.4.

$$\mathrm{Re}=6.6Vd \qquad \text{(equation 4.4)}$$

Where V is the flow velocity in the duct and d is the diameter of the duct.

In a turbulent system, aerosol is well mixed insuring that the samples collected for determining aerosol concentration, both gravimetrically and electronically, were representative of the concentration being loaded on to the respirator.

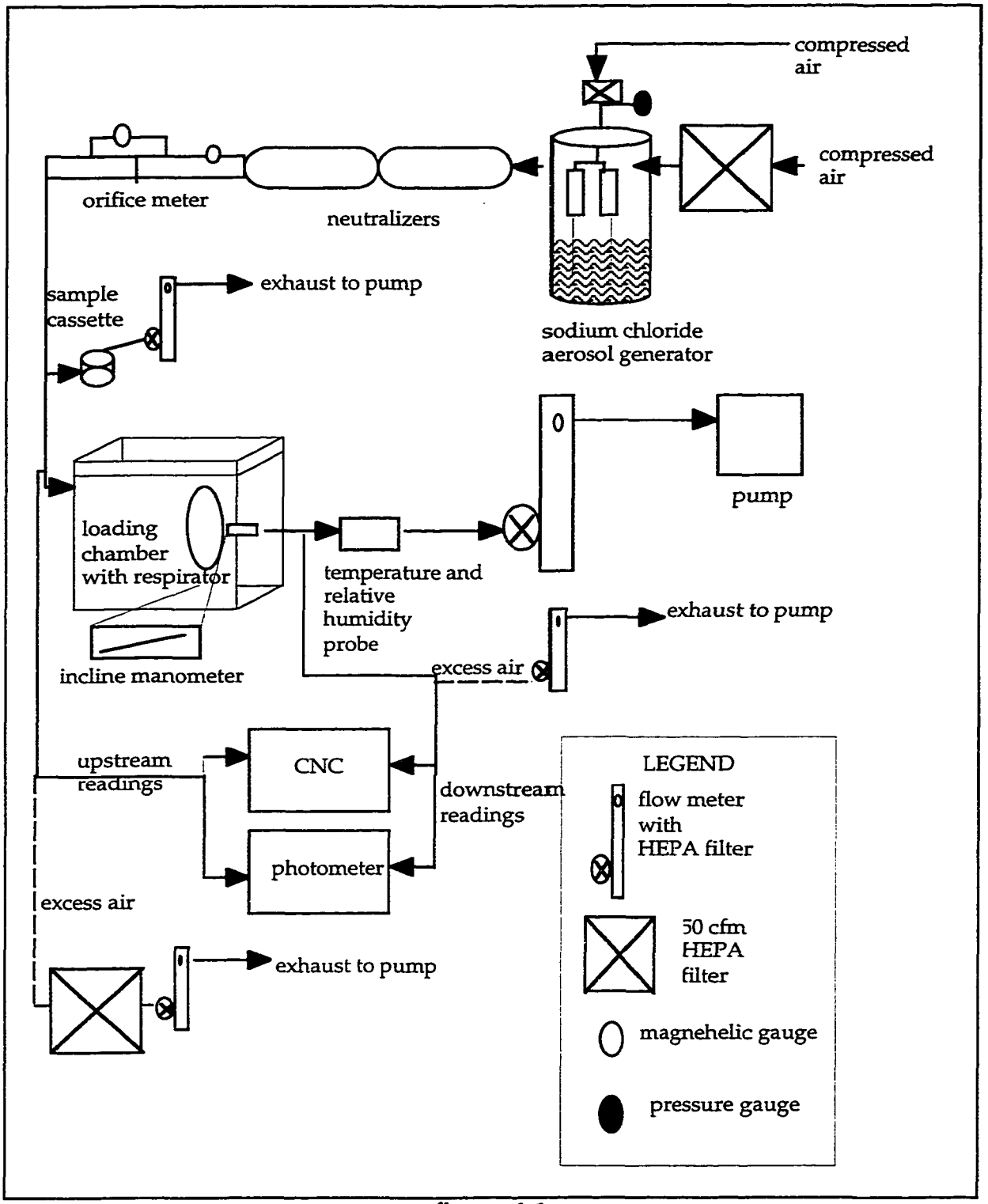

figure 4.1
Schematic View of Sodium Chloride Test Apparatus

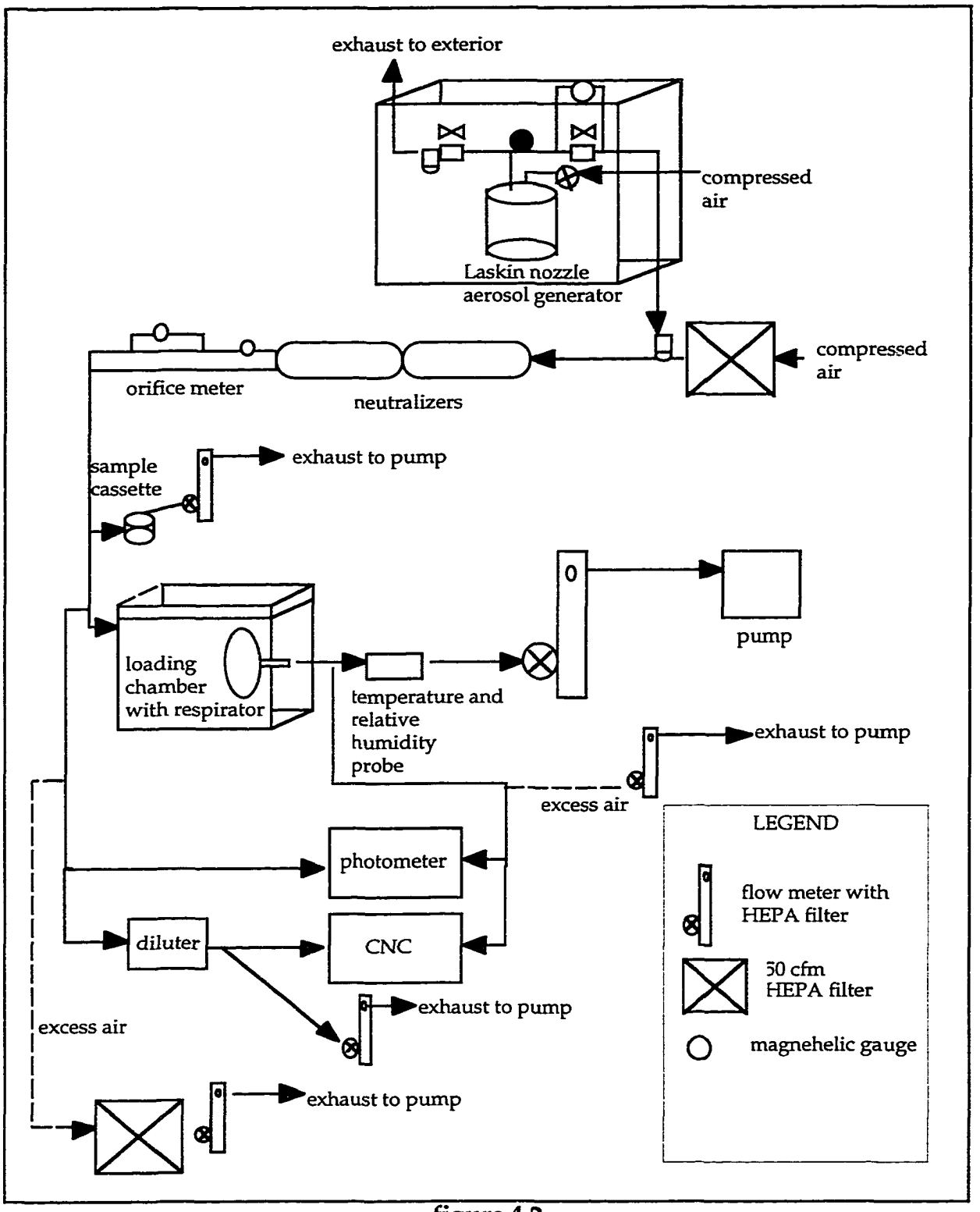

figure 4.2
Schematic View of Dioctyl Phthalate Test Apparatus

When respirator testing was at 43 lpm, airflow through the two inch diameter duct at the upstream sampling probe was computed to be turbulent with a Reynolds number of 2067; the Reynolds number increased to 3225 when respirator testing was 85 lpm.

DOP aerosol was considered well mixed with the HEPA filtered air. Once the aerosol left the Laskin nozzle generator, it traveled through tygon tubing where some particles coagulated. A condensate trap, located at the point of aerosol introduction into the two inch duct containing HEPA filtered air, removed these particles. This location was upstream from the neutralizers, sharp edge orifice meter, and a three foot section of ducting. Airflow through the two inch diameter duct was computed to be turbulent, at the location of the sampling probe, with a Reynolds number of 2205.

The diameter of the upstream sampling probe used for NaCl tests was 1.0 cm through which flowed the sample air to the CNC, photometer, and 47 mm sampling cassette. The probe's diameter was too small for isokinetic sampling to occur at either the 43 or 85 lpm respirator flow rate; velocity in the probe was much greater than velocity in the duct which may have accounted for sampling loss. The diameter of the NaCl aerosol was very small, 0.085 μm, resulting in a computed Stokes numbers of less than 0.00001 at both flow rates. The Stokes number indicates how well a particle is able to follow an airstream. As the Stokes number decreases and approaches zero, a particle will follow an airstream perfectly and not resist changing its direction from the duct to the inlet of the sample probe. For NaCl, the effects from

anisokinetic sampling were computed to be less than 0.01% using equation 4.5 [76].

$$C/C_o=1+[(U_o/U)-1][1-(1/(1+(2+0.62(U/U_o)Stk))]$$

C is probe concentration, C_o is concentration in the airstream, U is air velocity in the probe, U_o is air velocity in the airstream, and Stk is the Stokes number

(equation 4.5)

The diameter of the upstream sampling probe used for the DOP tests was 1.0 cm through which flowed the air sample to the photometer, diluter and CNC, and 47 mm cassette. The diameter of the probe was too small for isokinetic sampling to occur, velocity in the probe was much greater than the velocity in the duct. This may have resulted in sampling loss. However, since the diameter of the DOP aerosol was small, 0.20 μm, and the computed Stokes number was less than 0.00002. In this region, the effect from anisokinetic sampling was computed to be less than 0.01%.

The air temperature of the test apparatus was controlled by the heating and air conditioning system of the room. An external heat lamp placed directly over the copper orifice meter provided additional heat. A Relative Humidity and Temperature Transmitter (model 850) placed downstream from the respirator monitored both relative humidity and temperature of the air. The accuracy of this probe was $\pm$ 2.0% relative humidity and $\pm$ 0.5 ^{o}C. This location was selected to protect the probe from particle deposition which could potentially alter the calibration of the device. Direct current input voltage was supplied to the transmitter by a regulated power supply (model

LH 124 FM). Input voltage was displayed on a digital multimeter (model 6100). The output voltage was displayed on a digital multimeter (model 3466A). The temperature calibration curve supplied by the manufacturer was confirmed using a mercury thermometer. The relative humidity calibration curve was confirmed using saturated salt solutions.

42 CFR 84 stipulated that the relative humidity of air for NaCl testing N series respirators range between 20 to 40%. Since the relative humidity of ambient room air was greater than 40%, dried compressed air was supplied to the inlet of the AstroCel HEPA filter via an air plenum constructed from a plastic bag. The compressed air supplying the plenum was adjusted with a regulator. The system pressure was monitored with a magnehelic gauge having a range of 0 to 0.5 inches water column to insure that it remain negative.

Pressure drop, the difference between chamber pressure and the pressure inside the mask, was measured with incline manometers having a maximum range of 1, 2, or 10-inch water column. Pressure drop in excess of 10 inches water was measured with magnehelic gauges having ranges of either 0 to 30 or 0 to 50-inch water column. The 0 to 30-inch water column magnehelic gauge was calibrated against an incline manometer filled with gauge oil while the 0 to 50 inch water column magnehelic gauge was calibrated against a manometer filled with mercury. The difference between the magnehelic gauge and the incline manometer readings was ±7%.

Respirator Preconditioning

N series respirators were preconditioned for 25 ± 1 hour in a flow-through chamber with 38 °C (±2.5 °C) air at 85% relative humidity (±5%) following 42 CFR 84 [35]. The source of the warm humid air was from a Flow-Temperature-Humidity Control System (model HCS-301), hereafter referred to as a Miller-Nelson box. The Miller-Nelson box was unable to fully heat the air in the preconditioning chamber to the required temperature. An additional source of heat was needed and was supplied by wrapping heat tape around the discharge line of the Miller-Nelson box; temperature of the heat tape was controlled by a variable autotransformer. Temperature and humidity of the preconditioning chamber was continuously monitored with a temperature-relative humidity probe (HMP 23UT) connected to the Miller-Nelson box. The probe temperature was calibrated against a mercury thermometer. Relative humidity calibration was performed with saturated solutions of potassium chloride and magnesium nitrate. At specific temperatures, the relative humidity of the headspace in the container of salt solution at equilibrium is a primary standard [141].

Respirator Holders

Holders for cartridges and filters were custom fabricated from the cartridge receptacles off their designated elastomeric respirators. Mounting plates for filtering facepiece respirators were constructed from polycarbonate lenses of Survivair full-face elastomeric respirators. At the conclusion of each test, the mounting plates for the filtering facepiece respirators were wiped

clean with isopropyl alcohol removing any residual glue and aerosol residue. Holders for cartridges and filters were washed with soap, rinsed with deionized water, and allowed to air dry before being reused.

Face Seal Integrity of Filtering Facepiece Respirators

3M Company of St. Paul Minnesota developed the Large Particle Quantitative Fit Test (LPQFT) to measure the integrity of the face-seal for filtering facepiece respirators [142]. The 3M method used a monodisperse corn oil aerosol with an aerodynamic diameter of 2.5 μm at a flow rate of 32 lpm for evaluating face-seal leaks of single use dust-mist respirators. They found that face-seal leakage was independent of particle size over the range of 0.8 to 3 μm. This method was intended to be used for filtering facepiece and elastomeric respirators but was not valid for HEPA filters due to higher pressure drop [143]. Researchers determined the penetration rate for dust-mist respirators adequately sealed to a mounting plate with hot melt adhesive averaged 0.1% [144, 145]. Other researchers have demonstrated that particles with 2.0 to 2.5 μm diameters have an 80 to 90% penetration rate though face-seal leaks in filtering facepiece respirators even at low-pressure drop [146].

For this research project, the face-seal integrity of filtering facepiece respirators sealed to the holder with hot melt adhesive and filters placed in holders from elastomeric respirators were evaluated with 2.01± 0.054 μm diameter latex spheres at a steady state airflow rate of 35 lpm. The geometric standard deviation (GSD) of the latex spheres was computed to be less than 1.09 and meets Fuch's criteria for a monodisperse aerosol [147]. A solution of

latex spheres and deionized water was atomized with a custom built nebulizer made at Lawrence Livermore National Laboratory. A capillary tube was submerged into a 500 ml plastic bottle contained the solution of latex spheres. Filtered compressed air at 20 psi was supplied to the nebulizer creating a venturi effect that aspirated liquid into the small orifice. The solution was atomized and large droplets were impacted and dripped back into the reservoir. Fit was determined by evaluating the penetration of the 2 μm particles at a single channel output on the Climet and was expressed as percent penetration.

Sodium Chloride Aerosol

The NaCl aerosol used for both the NIOSH method tests and for challenging respirators loaded with workplace contaminants was generated from four nebulizer blocks from Thermo-Systems Inc. (TSI) Constant Output Atomizers model 3076. The nebulizers were mounted inside a flow through 512 in^3 polycarbonate cylinder having two openings. The inlet side of the cylinder supplied HEPA filtered air into the aerosol generator chamber. The outlet on the cylinder discharged the NaCl aerosols mixed with HEPA filtered air to the krypton neutralizers and the respirator loading chamber. Compressed dry air to the nebulizers was filtered through an Ultra Filter Type H cartridge. Air pressure was adjusted to 35 psi as measured by a 0 to 60-psi pressure gauge mounted on top of the generator. Pneumatic suction drew a solution of 0.95% sodium chloride in deionized water from the bottom of the cylinder into the atomizers. Excess solution from the overflow drains on the

nebulizer blocks dripped back into the reservoir. Every other day of testing, any remaining sodium chloride solution was discarded and replaced with two to four liters of fresh solution. Flushing with warm deionized water every other day of testing cleaned the nebulizers. Solid particles of NaCl were obtained upon evaporation of the droplet. The particle size distribution was adjusted to the desired count median diameter (CMD) by varying the concentration of salt in solution using the equation 4.6 [76].

$$d_s=d_d(F_v)^{1/3} \qquad \text{(equation 4.6)}$$

Where d_s is the size of the final aerosol particle, d_d is the droplet diameter, and F_v if the volume fraction of the solid material

In these tests, a 0.95% concentration of sodium chloride resulted in the optimum size distribution for NaCl aerosol. This concentration was much less than the 2% reported by TSI and NIOSH for use in the TSI model 8160 [85, 148] but is comparable to the 1% solution used by the United Kingdom in the British Standard 4400 [83].

The sodium chloride generator supplied 10 to 24 mg of NaCl per m^3 of air at a flow rate of 75 to 117 lpm. Airflow through the respirator was either 43 or 85 lpm, depending upon the configuration of the respirator. During the NIOSH method tests, all four nebulizers were used. The aerosol concentration was reduced by utilizing only one of the nebulizers when respirators were evaluated for penetration during the loading tests with workplace contaminants to minimize the effect of salt loading. Two aerosol

neutralizers connected in series neutralized NaCl aerosol to the Boltzman charge distribution. The half-life of the sealed krypton sources had been reached which limited the ability of a single sealed source to adequately neutralize the aerosol at the maximum airflow [124].

During the sodium chloride tests, instrument readings were recorded at each one minute interval beginning with the downstream reading. After 15 to 20 minutes, sampling lines were switched for recording upstream readings at the inlet to the respirator loading chamber. Instruments were allowed to purge and were rezeroed prior to sampling downstream. After 45 to 50 minutes more of downstream sampling, the instruments were taken off line and placed on HEPA filters for 5 minutes. Downstream sampling was resumed for six minute intervals with ten minute breaks. This was done to prevent aerosol accumulation inside the detection equipment. The photometer was rezeroed after each ten minute purge. During the last five minutes of the test, upstream readings were again recorded. Balanced flow through the system was maintained when detection equipment was alternated or taken off line by the addition of exhaust lines. Hemostats were used for transitioning airflow between the sample line and the dump line. Percent penetration of NaCl aerosol through the respirators, measured with both the photometer and CNC, was computed by dividing the downstream reading by the upstream reading and multiplying by 100. Percent penetration was carried out for four decimal places. Respirator penetration during the initial 15 to 20 minute sampling interval was computed using the first set of

upstream readings. The remaining penetration measurements were computed from the average upstream readings recorded at the beginning and the end of the test. This method of computing penetration was selected due to the variability in the upstream aerosol readings. Irrespective of the flow rate through the respirators, overall CNC and photometer reading for NaCl were significantly different between the beginning and the ending readings using a paired-t test, $p<0.05$. The results of the paired-t tests can be found in Appendix Tables B.2 and B.3.

Dioctyl Phthalate (DOP) Aerosol

DOP aerosol was generated with a Laskin nozzle (model SG 20). Refer back to Figure 4.2 for a schematic of the DOP test apparatus. The single nebulizer, submerged in liquid contained in the generation pot, was supplied with dried, compressed air filtered with an Ultra Filter Type H cartridge. The compressed air pressure to the nozzle was 12 psi. For added safety from over pressurization, the Laskin nozzle generation pot was retrofitted with a 15 psi pressure relief valve. Agitation by the air jet created a dense foam of microscopic bubbles in the liquid. Droplets were created when these bubbles burst at the liquid surface [76]. The aerosol concentration generated was much higher than desired and was reduced by diverting aerosol flow though a 'T' fitting on the discharge line of the generator. One leg from the 'T' fitting directed the aerosol to the respirator chamber while the other side was connected to an exhaust. Aerosol flows through each leg of the 'T' fitting was regulated with ball valves. The pressure drop across the ball valve for the line

leading to the test apparatus was measured with a 0 to 150 inch water column magnehelic gauge. The aerosol generator was placed inside a 27 ft^3 polycarbonate container connected to the house ventilation exhausting to the exterior of the building. In the event of aerosol leakage, engineering controls prevented worker exposure to this aerosol. The DOP aerosol was neutralized to the Boltzman charge distribution with two aerosol neutralizers as previously described.

The upstream DOP aerosol number concentration exceeded the maximum operating range of the CNC. In order to obtain readings from the CNC, DOP aerosol concentration was diluted. The custom diluter was fabricated from by inserting a 1/8 inch stainless steel capillary tube with knife edge through a 25 cfm HEPA filter; the edges around the tube were sealed with silicon sealant. The diluter operated at a flow rate of 5 lpm, equivalent to the TSI diluter (model 3302). Excess was exhausted through the dump line venting to the building exterior. Pressure drop, the difference in pressure across the filter, was measured with a manometer having a range of 0 to 0.5 inch water column. The diluter was calibrated with DOP at approximately $4x10^6$ particles/cc. Calibration of the diluter was performed on five different days, a total of ten different times. The dilution ratio average was 1403:1 with a standard deviation of 221. Pressure drop across the HEPA filter in the diluter did not change over the course of these tests. This indicated that the filter did not clog and change the dilution ratio. The stainless steel capillary tube was

visually inspected once all testing was completed, there was no evidence of clogging.

Loading a P100 filter or cartridge with DOP did not commence until upstream background readings were less than 2.0 particles/cc. Often, background levels were below 1.0 particles/cc, indicating the system was clean and free from leaks. Loading began when compressed air to the Laskin nozzle was turned on. The system was allowed to equilibrate for one minute prior to recording initial downstream readings. After recording downstream readings for ten to twelve minutes, sample lines were then changed to record upstream readings. Once initial upstream readings were recorded, the photometer was purged for at least five minutes with HEPA filtered air and was electronically rezeroed before additional downstream readings were recorded. Immediately following the purge and rezero of the photometer, downstream readings were initially comparable to the last downstream readings recorded, but then began to climb at an increasing rate. The photometer was taken off line, purged with more HEPA filtered air, and rezeroed for a second time. If the photometer remained downstream only, this phenomenon was not observed. Procedures were changed to increase purge time and the photometer was zeroed several times during the purge cycle in an effort to eliminate these artificial readings. Despite increasing the purge cycle, this anomaly continued to occur. Downstream readings finally stabilized after the instrument was purged and rezeroed for a third time during each test. Downstream readings occurring during these intervals were

later discarded as they were considered an artifact of instrument response and not an accurate reflection of true respirator penetration with DOP. Additional downstream measurements were recorded for approximately the next 30 minutes. A second upstream reading was recorded during the last five minutes of the test. During the first 10 to 12 minutes downstream sampling interval, penetration was computed using the first set of upstream readings. The remaining penetration measurements were computed from the average upstream readings recorded at the beginning and the end of each test. This method of computing penetration was selected for consistency with the method used to compute NaCl penetration. Upstream CNC and photometer readings for DOP aerosol were not significantly different between the beginning and the ending readings using a paired-t test, $p>0.05$. The results of the paired-t tests can be found in Appendix Table B. 4.

The CNC and photometer measurements during the DOP tests were recorded at each 30-second interval. Due to the short duration of these tests, additional data points were needed for constructing the penetration curves. Sampling began downstream and after 10 to 12 minutes was switched to upstream; readings were recorded for 3 to 4 minutes. After sampling upstream, the optics in the photometer required a long cycle time of 10 to 15 minutes to clear and rezero the instrument. Downstream monitoring was resumed and remained fairly continuous for the next 30 to 50 minutes with only two short breaks for purging and rezeroing the photometer. During the last five minutes of the test, upstream readings were again recorded.

The airflow rates of the system used for both the NaCl and DOP tests were measured with a custom orifice meter. A copper pipe with an internal diameter of 4.980 cm had a copper sharp-edge circular orifice with a diameter of 1.885 cm. Pressure drop across the sharp-edged orifice was measured with a magnehelic having a range of 0 to 1 inch water column. The orifice meter and magnehelic gauge were calibrated against an oil-filled five ft^3 capacity spirometer, a primary standard. Airflow through the orifice meter was regulated with an 8 cfm Fischer flow meter.

The termination of each NaCl and DOP test was determined by the aerosol mass contacting the respirator. Once the target of 200±5 mg had contacted the respirator, testing stopped. This mass accounted for aerosol collected on the respirator as well as that fraction of aerosol penetrating the respirator. Determining the endpoint of 200 mg was estimated from upstream aerosol concentration. Samples were collected on 47 mm diameter 0.45 μm pore size Millipore mixed cellulose (HA) filters that were pre- and post-desiccated 24 hours. The sampling rate of 10 lpm was calibrated using the flow calibrator. Airflow through the Millipore filter was regulated using a Matheson 605 flow meter.

Loading Tests With Contaminants Representative of Workplace Aerosols

The collection efficiency of electrostatic and mechanical respirators loaded with aerosols representative of workplace contaminants was evaluated using three different aerosols with four different test scenarios. Two of the contaminants, aluminum oxide dust and metal cutting fluid mist,

were generated under laboratory conditions. The two contaminants generated in the field were asphalt fumes and a metal cutting fluid mist during a lathe turning operation.

None of the respirators for tests with the workplace contaminants were preconditioned. Filtering facepiece respirators had their straps removed prior to being weighed on an Ohaus scale. Respirators from Racal also had the nose tabs clipped and removed for easier sealing to the mounting plate. Once the filtering facepiece respirators were sealed with hot melt adhesive, the total mass was determined with a PM 4800 Delta Range scale having accuracy to 0.01 grams. The holder for the N95 filters had much less mass and weights were determined with the Ohaus scale. 3M 2091 filters were weighed individually as their bayonet mountings allowed these respirators to be easily removed and resealed to their holders. Face-seal integrity of N95 filtering facepiece respirators sealed to their mounting plates and filters placed in their customized holders was evaluated with 2 μm latex spheres using the 3M Large Particle Quantitative Fit Test method at 35 lpm. Face seal leakage was determined using penetration measurement with the Climet. Respirators loaded with contaminants in the field, asphalt and metal cutting fluid mist, were evaluated for face seal leakage the day preceding the test. Respirators, secured to their holders, were stored overnight in clean plastic bags at room temperature. Initial respirator penetration was measured with both the CNC and photometer using a dilute concentration of NaCl aerosol the morning of the loading test. Pressure drop across the respirator was recorded with either

an incline manometer or magnehelic gauge. Airflow rate through the respirator was either 43 or 85 lpm depending upon the respirator configuration. Temperature and humidity of the system for NaCl aerosol was maintained according to 42 CFR 84. Respirators secured to their holders were weighed after fit evaluation, after each penetration evaluation with the dilute NaCl aerosol, and after each two hours of loading with workplace aerosol. Pressure drop and penetration of NaCl aerosol were measured initially and after every two hours of loading. Respirators loaded with asphalt contaminants were placed in plastic bags during transportation to and from the workplace site. Respirators loaded in the field with cutting fluid mist were not placed in bags during transportation as the machine shop was adjacent to the laboratory used for evaluating respirator penetration. Respirators were loaded with workplace aerosol usually for six hours.

Respirator Loading Apparatus in the Laboratory

A separate apparatus was constructed for loading respirators with aluminum oxide dust and metal cutting fluid mist generated under laboratory conditions. Refer to figures 4.3 and 4.4 for schematic details. Ambient room air passed though a 50 cfm MSA HEPA filter and traveled through two inch ducting to the polycarbonate respirator testing chamber measuring 11 x 12 x 17 inches. Aerosols used to load respirators were introduced into the 2 inch duct 44 inches upstream from the respirator chamber and 37 inches upstream from the sampling probe.

Sample probes, placed upstream and downstream from the respirator, were constructed from 0.66 cm diameter stainless steel tubing with a 30 degree bevel. The upstream sampling probe was located in the two inch duct prior to the loading chamber. Upstream concentration of aerosol was continuously sampled from the upstream probe over the duration of the loading test. Samples were collected for 60 minutes at a flow rate of 10 lpm. Flow rates were calibrated with the flow calibrator and regulated with a Matheson 605 flow meter. Aluminum oxide samples were collected on 47 mm diameter 0.45 μm pore size Millipore mixed cellulose esters (HA) filters that were pre- and post-desiccated 24 hours. Cutting fluid mist samples were collected on 47 mm diameter 0.45 μm pore size Nuclepore PTFE filters. These hydrophobic filters were not desiccated as some of the collected mass might have been reduced by desiccation.

The diameter of the probe was too small for isokinetic sampling to occur, velocity in the probe was much greater than velocity in the duct, which may have resulted in sampling loss. However, since the diameter of the aerosols were small, 1.39 μm for the aluminum oxide and 1.00 μm for the metal cutting fluid mist, the computed Stokes number at both 43 and 85 lpm respirator flow rates were also very small. The Stokes numbers were less than 0.003 for aluminum oxide and less than 0.0005 for metal cutting fluid mist. In this region, the effects from anisokinetic sampling was computed to be less than 0.3% for aluminum oxide and less than 0.2% for the metal cutting fluid mist.

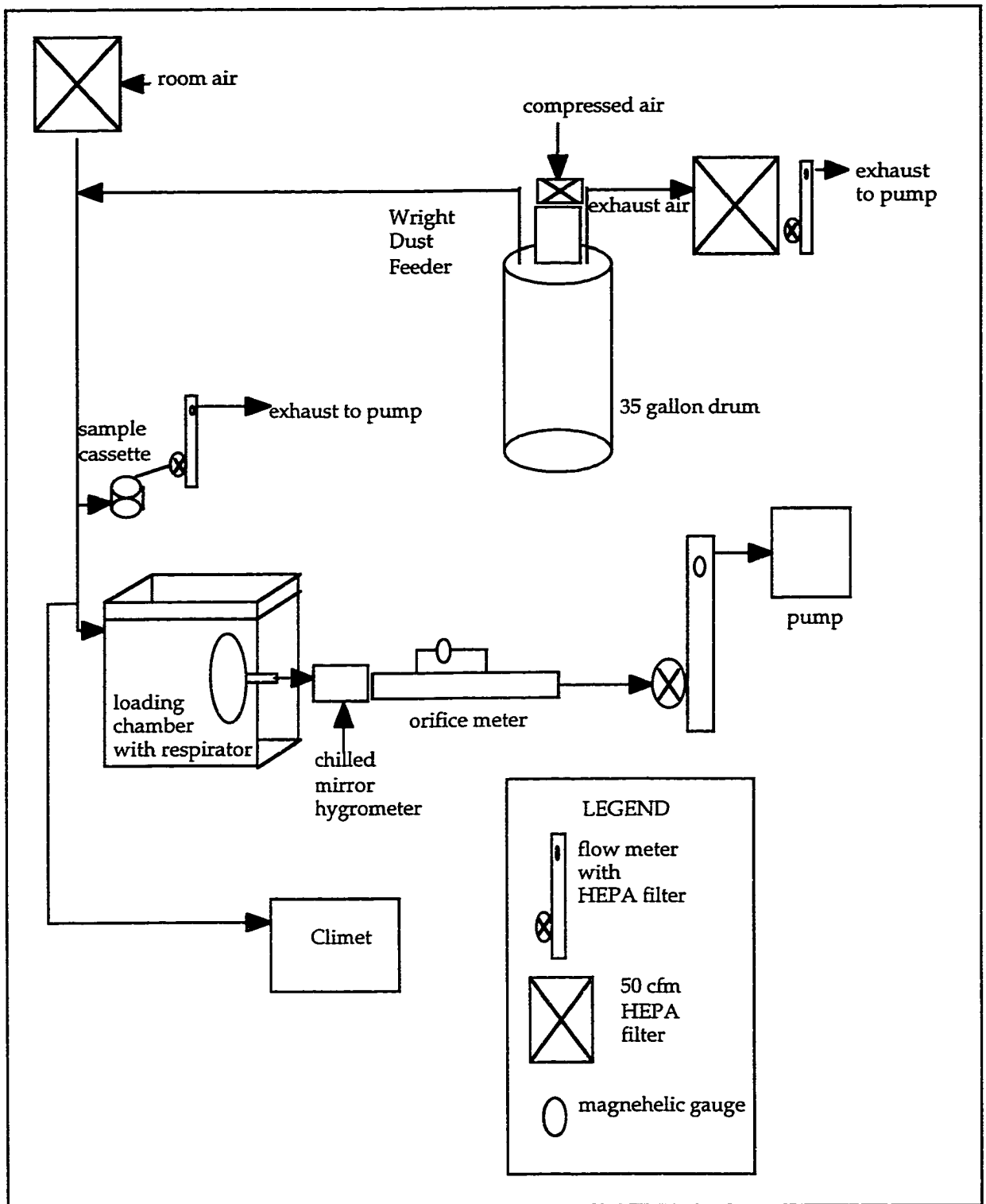

figure 4.3
Schematic View of Aluminum Oxide Loading Apparatus

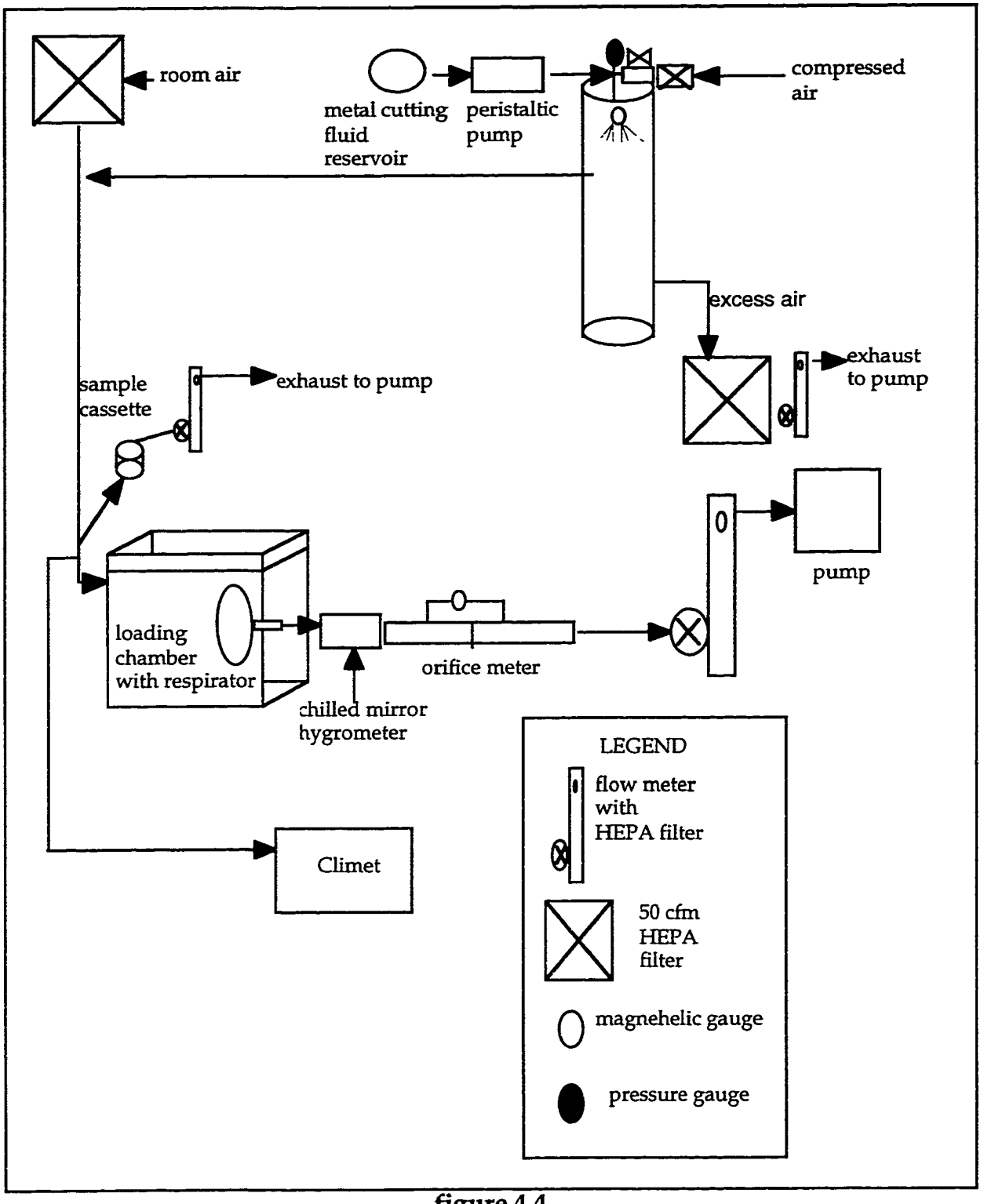

figure 4.4
Schematic View of Metal Cutting Fluid Mist-Laboratory-Generated Loading Apparatus

Sampling for measuring the aerosol size distribution (aluminum oxide dust and metal cutting fluid mist) with the Climet was also drawn from the upstream probe during which time the airflow rate changed from 10 lpm to 17 lpm. Sampling periods were once every two hours and duration was less than five minutes. Air velocity rate through the probe was allowed to fluctuate unlike the NaCl or DOP system where a dump line affixed to the probe maintained airflow balance when detection equipment was not being used. The reason for allowing the fluctuation was that respirators were only being loaded with contaminants and penetration was not being evaluated concurrently. Penetration of the respirators with NaCl was evaluated in a separate test apparatus after each two hour loading interval with aluminum oxide dust. For the NaCl and DOP tests, penetration was being measured in conjunction with loading and a change in the dynamics of the system could affect recorded penetration measurements.

Airflow through the respirator was measured with a custom orifice meter custom placed downstream from the loading chamber. The stainless steel orifice meter had an internal diameter of 2.195 cm and the opening in the orifice was 0.620 cm.; the overall length was 63.2 cm.

Temperature and relative humidity of the air in aluminum oxide and metal cutting fluid mist loading chamber were evaluated with a chilled mirror hygrometer (model 911) Dew All Digital Humidity Analyzer. The accuracy of this instrument was $\pm$ 0.5% relative humidity and $\pm$ 0.1 ^{o}C. Sample air passed through a hydrophobic 47 mm 0.45µm Nuclepore PTFE

filter. This prevented particles from depositing on the mirror and plates of the hygrometer and possibly altering the instrument calibration. Air was sampled from the downstream probe at a flow rate of 2 cfh. Readings were recorded every hour of testing. The manufacturer calibrated this instrument during a reconditioning. Temperature calibration was confirmed with a mercury-glass thermometer.

Pressure drop across the sharp-edged circular orifice was measured with a magnehelic gauge having a range of either 0 to 4 or 0 to 25 inches water column. The orifice meter and magnehelic gauge were calibrated using the spirometer. Airflow through the orifice meter was regulated with a 7 cfm Fischer flow meter.

Laboratory Aerosol Generation

Aluminum oxide dust was generated with a Wright Dust Feeder (refer to Figure 4.5). A plug of aluminum oxide, 99.1% Al_2O_3, was formed by compressing powder into the large stainless steel dust thimble of the Wright Dust Feeder using a custom fabricated packing mandrel. An alignment bushing centered the mandrel and the dust cup during packing with a 0 to 40,000 pound force hydraulic press. Aluminum oxide powder was added to the dust thimble in layers, each layer was compressed using a pressure of approximately 17,000 psi. A gear driven motor rotated the packed powder plug into a fixed scraper blade of the dust feeder. The gearing ratio on the electric motor regulated the speed of the cutting blade. The following gear configuration was used for these tests: 18 tooth gear on the motor, 54 tooth

gear on the intermediate driven, 36 tooth gear on the intermediate driver, and a 36 tooth gear on the cross shaft.

Compressed, dry, air, filtered through an Ultra Filter Type H cartridge, was blown into the lower portion of the packed powder plug passing through the air channel under the scraper blade. Particles were swept into the hollow shaft supporting the blade. The airflow rate through the dust generator was approximately 24 lpm. An impactor and outlet jet nozzle removed large particles and broke up agglomerates. Operating pressure of the compressed air was 10 psi. The target concentration of aluminum oxide dust was 10 mg/m^3, representative of the Threshold Limit Value for an eight hour exposure for Particulates Not Otherwise Classified (PNOC) according to the ACGIH. Concentration of aluminum oxide dust generated by the Wright Dust Feeder exceeded these guidelines and the aerosol flow was divided so that only a portion was directed to the loading chamber housing the respirator.

The outlet of the Dust Feeder was secured to the top of a sealed 32 gallon metal barrel; all particles generated by the dust feeder were directed into the barrel allowing very large particles not dispersed by the impactor to be removed by gravitational settling. Two 1 1/2 inch fittings were also attached to the lid. To the first fitting, a line connected the barrel to ducting with HEPA filtered air and supplied aluminum oxide dust to the respirator chamber. The second fitting was attached to an exhaust line. Excess air was filtered through a 50 cfm HEPA filter with airflow regulated by a Fischer flow meter.

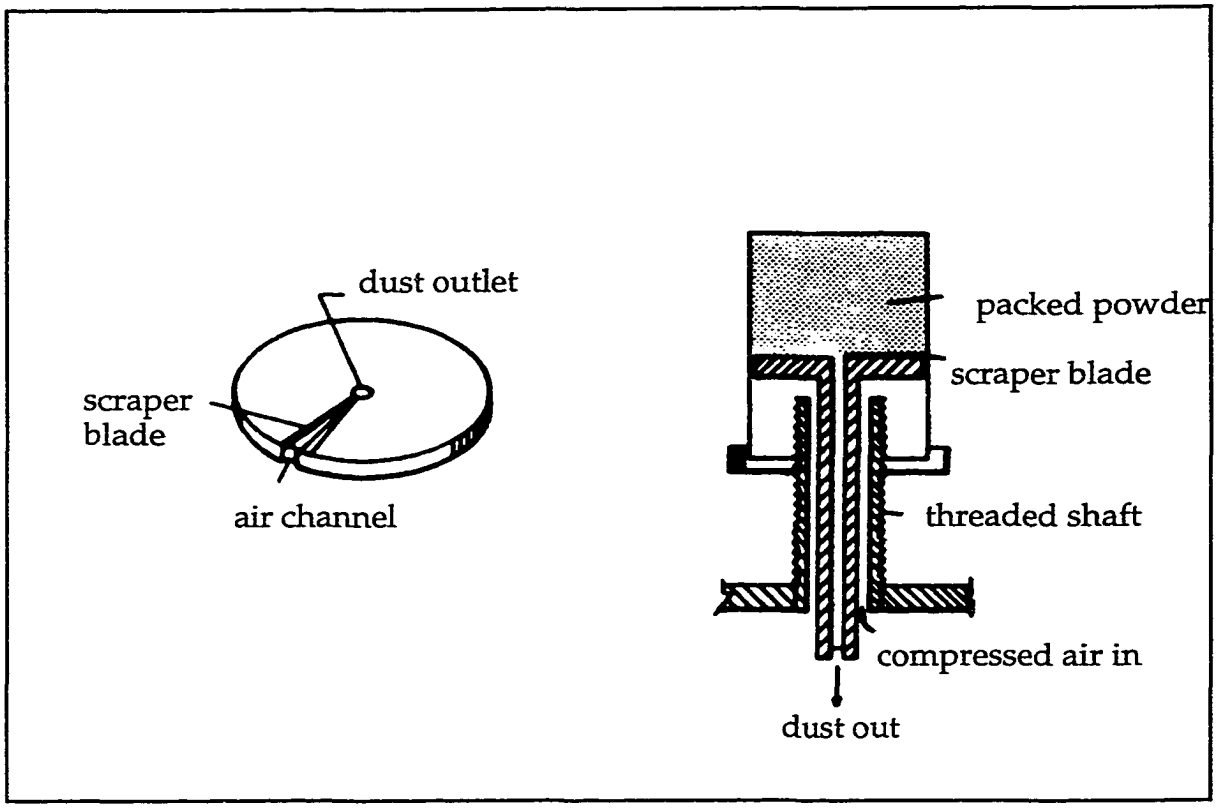

figure 4.5
Schematic View of Wright Dust Feeder

The point of aluminum oxide dust and metal cutting fluid mist introduction was three feet upstream from the sampling probe, 18 duct diameters apart. Airflow rates through the respirators were determined with a sharp edge orifice meter located downstream from the respirator. The aerosol was considered well mixed at respirator flow rate of 85 lpm and airflow was determined to be turbulent with a Reynolds number of 2619. However, at the respirator flow rate of 43 lpm, airflow was computed to be laminar with a Reynolds number of 1461. Laminar flow may have accounted for some of the variability in aerosol concentration and size distribution at

the lower flow rate as aerosol may not have been adequately mixed with HEPA air prior to sampling.

Metal cutting fluid mist, in the laboratory, was generated with TapFree 2 cutting fluid. The mist of synthetic metal cutting fluid (non-oil) was generated from an air atomizing pressure spray nozzle (figure 4.6). Compressed, dried, air filtered with an MSA Ultra Filter Type H cartridge, was supplied to the spray nozzle at 10.5 psi; pressure was measured with a 0 to 60 psi gauge. Cutting fluid was metered to the spray nozzle through the capillary siphon line by a peristaltic pump. Cutting fluid mist was generated in a 2,100 cubic inch plastic cylinder; circumference 8.3 inches and length 42 inches. The target concentration of cutting fluid mist loading respirators was 1.0 mg/m^3.

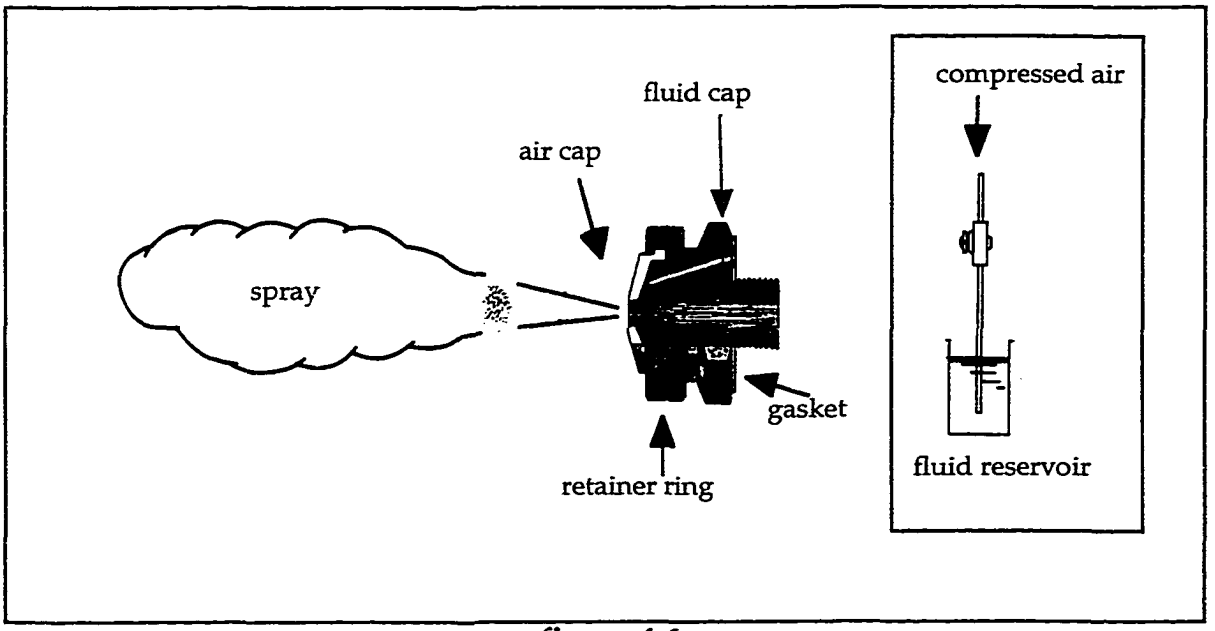

figure 4.6
Schematic View of Air Atomizing Spray Nozzle Used for Generating A Mist of Metal Cutting Fluid in the Laboratory

This concentration was based upon observed occupational exposure averages documented in NIOSH's Criteria for A Recommended Standard: Occupational Exposures to Metalworking Fluid [149]. The concentration of aerosol produced by the spray nozzle exceeded the desired target concentration. Airflow from the mist generator was diverted though two 7/8 inch openings, one at the top and the bottom of the cylinder. Through the opening at the top of the cylinder, cutting fluid mist was supplied to the respirator test chamber. The bottom outlet was directed through a 50 cfm HEPA filter and exhausted. Airflow through the HEPA filter was regulated by an 8 cfm rotometer.

Field Respirator Loading Apparatus

A custom built apparatus was made for field testing respirators exposed to asphalt contaminants and metal cutting fluid mists in the field. A maximum of three respirators could be exposed to environmental contaminants in addition to mounting a cascade impactor for evaluating the aerosol size distribution. The source of vacuum was a carbon vane pump, having a capacity of 31 cfm. Exhaust from the pump was plumbed to an MSA HEPA filter via one inch diameter tygon tubing. From the suction side of the pump, 3/4 inch nylon braided tubing attached to the two inch manifold piping on the five foot tall unistrut frame. On the manifold, three 1/2 inch pipes were placed 18 inches apart each attaching a needle valve to a 10 cfm Dwyer flow meter, and terminating with quick disconnect fittings for respirator holder attachment. The suction line for the cascade impactor

originated with a 1/8 inch pipe from the manifold and mounted a rotometer with a top mounted regulator valve. The 1/8 inch suction line from the rotometer was fitted with a quick disconnect fitting for attaching the Andersen cascade impactor. Casters were placed on the bottom of the unistrut frame for easy movement of the stand. Airflow through the respirators and cascade impactor was measured with either a Kruz hot wire anemometer or a sharp edge orifice. Airflow through the cascade impactor was 28 lpm while each respirator was either 43 or 85 lpm depending upon the respirator design.

A second custom built stand was designed for mounting a single "control" respirator. These respirators were subjected to the same environmental conditions and handling as the "exposed". Their field locations were selected to minimize respirator loading with the environment aerosols/contaminants being studied. This stand was capable of holding a single respirator and the chilled mirror hygrometer. Suction for the system was supplied by a carbon vane pump. The exhaust from the pump was plumbed to a 135 cfm capacity AstroCel I HEPA filter via 1/2 inch diameter nylon braided tubing. The suction side of the pump was connected to the manifold by 1/2 inch nylon braided tubing. Half inch piping from the manifold on the five foot tall unistrut stand connected a needle valve to a 10 cfm Dwyer flow meter. From the flow meter the 1/2 suction line terminated with a quick disconnect fitting for respirator holder attachment. A 1/8 inch pipe from the manifold was plumbed to a 10 cfh Brooks flow meter with a bottom control valve. A hose barb on the suction side of the flow meter

connected tygon tubing to the chilled mirror hygrometer, model 911 Dew-All. An 8.0 μm Millipore mixed cellulose esters (SC) filter was placed at the inlet of the digital temperature-humidity analyzer to protect the sensors from particle deposition.

Asphalt contaminants in the field were generated from a 540 gallon asphalt kettle, 'Fireking' model. Type 3 Steep ASTM D312-89 asphalt was melted by two direct-fired tubes supplied with propane. The holding temperature of melted asphalt in the kettle was 485 to 500 ^{O}F. The kettle was located on ground level and molten asphalt was pumped by an eight horsepower motor to an open-top holding pot located on the roof of the construction site, Building 151 at Lawrence Livermore National Laboratory. From the roof-top, workers obtained molten asphalt for mopping by opening a valve on the bottom of the kettle. The aerosol concentration to which respirators were exposed depended upon several environmental conditions such as the operating parameters of the melting kettle, the volume of asphalt being melted, and ambient wind speed and direction. ACGIH has a TLV of 5 mg/m^3 for an eight hour time weighted average and NIOSH has a 15 minute ceiling limit of 5 mg/m^3 [150].

In addition to generating metal cutting fluid mist in the laboratory, it was also generated in a machine shop with a Metal Cutting Mist Coolant Generator using TapFree 2 metal cutting fluid. House compressed air was supplied to the generator at 20 psi and filtered thought an MSA Ultra Filter Type H cartridge located on the inlet of the mist generator. A knurled nut on

top of the generator regulated the compressed air siphoning cutting fluid into the spray nozzle. There were no graduations on the generator to indicate the amount of cutting fluid being atomized. Visual observations of the aerosol stream and misting quantity on the cutting tool were used to adjust the flow. Compressed air pressure of the misting system remained constant at 20 psi. The atomized coolant was directed onto the carbide tip left hand turning tool mounted on a lathe. A stainless steel 304 rod with a diameter of 4 inches and length of 14 3/4 inches was turned at speeds of either 898 or 585 rpm. The travel speed of the cutting tool was either 0.007 or 0.0013 inches per revolution with a cutting depth of 0.02 inches.

Saturation with Perspiration

This series of tests evaluated the performance of filtering facepiece respirators saturated with artificial perspiration and subsequently dried before being tested. Filtering facepiece respirators can adsorb moisture from several sources: perspiration, humidity from exhaled breath, and moisture from ambient inhaled air. Perspiration was selected because it contains ions in solution that could potentially interact with the electrostatic charge on the filter media and reduce collection efficiency. The formula and formulation instructions can be found in Appendix A and have been used by previous researchers at Lawrence Livermore National Laboratory.

None of the respirators used for these tests were preconditioned. All respirators had their elastic head straps removed prior to recording initial weights. The Racal (mechanical) respirators also had the metal nose tabs

remove for ease of sealing the respirator to the holder. Small portions of the elastic straps and ends of the metal tabs remaining on the respirators were included in the initial weights. Once filtering facepiece respirators were attached with hot melt adhesive to the holders, total mass for the respirator and holder was measured. The integrity of the hot melt adhesive face-seal was determined using the LPQFT method as previously described. Initial respirator penetration of dilute charge neutralized NaCl aerosol was measured with both the CNC and photometer.

Pressure drop across the respirator was recorded with a manometer. Airflow rate through the filtering facepiece respirator was 85 lpm. Temperature and relative humidity of the air for the NaCl aerosol challenge was in agreement with 42 CFR 84.

After face seal integrity and pre-saturation penetration measurements with NaCl aerosol were recorded, respirators were placed in a hermetically sealed container and held at room temperature until their saturation test commenced. Respirators, sealed to their holders, were submerged into a container of artificial perspiration. The solution was poured into the exhaust line on the back side of the respirator holder so that the void space between the inside of the respirator and the holder was filled. Both front and back sides of the respirator remained in contact with the solution for 40 minutes. At the end of the saturation cycle, excess solution was poured out of the void space and the respirator was shaken vigorously to remove any excess liquid. Fluid remaining inside the respirator was removed by absorption with soft

disposable towels before the respirator was weighed. The wet respirator was placed inside the sodium chloride loading chamber; residual aerosol had been purged from the system. The compressed air line at the inlet of the HEPA filter was used to adjust the relative humidity of the dry HEPA filter air to approximately 22%. Drying was terminated when downstream humidity reached 25%.

Respirator-holder weights were determined following: the fit evaluation with latex spheres, after the initial sodium chloride test, post saturation, after drying, and after the final sodium chloride test. It is realized that a respirator wearer would not wear a respirator saturated to this degree. The objective of these tests was to demonstrate the maximum adverse effect of perspiration on the collection efficiency of filtering facepiece respirators.

Data Analysis

Statistical analyses were conducted using DataDesk™ and Excel. A total of 263 respirators were tested across seven different matrices: two representative of the NIOSH method certification tests, four using contaminants representative of the workplace, and one with artificial perspiration. The initial set of tests using the NIOSH certification method with NaCl or DOP aerosol used five replicates of each respirator. This number of replicates was larger than previous studies which used either three [151] or four replicates [152] and comparable to tests using five replicates [113, 146]. Field measurements of respirator penetration were anticipated to contain

more variability, six replicates were evaluated. Additional replicates increased the ability to detect differences between respirator types.

Analysis of Variance (ANOVA) has been used in previous studies [151, 115] to compare filter penetration and was also used for these studies. The General Linear Model (GLM) was chosen for its ability to perform analysis of covariance. Photometer and CNC measured penetration from each set of loading tests with workplace contaminants (asphalt, metal cutting fluid mist, and aluminum oxide dust) were modeled independently. Variables defining mass of contaminant loaded on the respirator, respirator manufacturer and model, initial fit, relative humidity and temperature of the test environment, airflow rate through the filter, and minutes loaded were correlated and added to the model. Only terms that had a probability value (p value) <0.05 remained in the model. Exponential terms for mass loaded were added incrementally to the model and remained if found to be significant. All two-way interactions were added to the model and then removed in a backward-elimination based upon their p values. Interaction terms with the largest p value exceeding 0.05 were deleted first and the sum of squares recalculated. This process was repeated until only interaction terms with p values less than 0.05 remained in the final model which was tested for the assumptions of homogeneity of variance, linearity, and normality. For data that did not meet the assumption of homogeneity of variance or normality, a transformation of the penetration data was indicated so that p values correctly reflected the statistical significance of the factors tested in the model. Transformations

from Box-Cox [153] were sought to make residuals normally distributed. Transformations were characterized by the equation:

$$y(p)=(y^p-1)/p \qquad \text{for } p\neq 0, \qquad \text{(equation 4.7)}$$

$$\log(y) \qquad \text{for } p=0; \qquad \text{(equation 4.8)}$$

where p is the transformation parameter and y is the response or respirator penetration. Usually p is decremented in steps of 1/2 starting with p=1 (untransformed, since subtraction of the constant 1 does not change the shape of the distribution), then p=1/2 (square root transformation), p=0 (log transformation), etc., until a value is found which makes the residuals normally distributed. It was sometimes necessary to transform penetration data containing zeros. In order to preserve penetration measurement of zero value in the analyses, some number had to be added to the original penetration measurement prior to transforming the data. The value selected was done with the aid of a slider in DataDesk. An adjustable value was added to the penetration measurements prior to transforming the data. The slider was adjusted so that the graphed data of the modified penetration measurements against its normal score, values that would be expected from a standard normal distribution of the data, was a straight line and the correlation value was as large as possible. The intercept of the GLM represented initial respirator penetration and the slope represented change in respirator performance. Coefficients generated in the ANOVA were used to compare intercepts and slopes between the mechanical and electrostatic respirators using the Wald test. The significance level of this test was 0.05.

This tested the hypothesis: do electrostatic respirators perform differently from mechanical respirators loaded with the same workplace contaminant. If no difference was found between the slopes of mechanical and electrostatic respirators, respirator performance could not be attributed to change in electrostatic collection mechanisms.

For the field tests with asphalt and metal cutting fluid mist, if performance of the exposed respirator changed with loading, this difference could be attributed to either loading the respirator with workplace contaminants or as a result from exposure to field conditions and laboratory testing. In order to assess the impact of the testing method upon the change in measured respirator penetration, "control" respirators were compared to their "exposed". Each respirator model was evaluated independently using an ANOVA. The only covariates added to the model were "minutes of exposure" and "control/treatment". It was assumed that all other parameters were the same and differences between the slopes would be attributed to aerosol loading. The initial respirator penetrations and slopes of the penetration curves were compared using the p value generated in the ANOVA table. There were two objectives of this comparison. The first was to see no difference between the intercepts, indicating respirator performance between the "control" and the "exposed" was the same prior to loading. The second objective was to observe a difference between the slopes of the "control" and the "exposed" respirators. Any differences in respirator performance were attributed to aerosol loading and not due to the test

protocol. The effect from drawing ambient air of varied temperature and relative humidity through a respirator for a total of six hours and testing penetration with NaCl in the laboratory during four intervals of respirator loading was quantified.

To answer the question of how well the NIOSH method predicted collection efficiency of respirators loaded with workplace contaminants, comparisons were made globally between observed and predicted penetration. All respirators used for each test matrix were included in the analysis and were divided according to the type of instrument used for measuring penetration, CNC and photometer. The observed penetration of respirators loaded with workplace contaminants was measured by challenge with NaCl aerosol. Predicted penetration measurements modeled penetration of respirators from the NIOSH method tests using either NaCl or DOP, depending upon the respirator category. Respirators were grouped according to the workplace aerosol being evaluated and their category, either N95 or P100. There were a total of six N95 and one P100 respirators loaded with asphalt contaminants and four N95 and one P100 respirators loaded with either metal cutting fluid mist or aluminum oxide dust. The NaCl and DOP data from these respirator groupings were modeled independently for penetration by photometer and CNC measurements. The NaCl models were kept as simple as possible and with only one interaction term describing the slope of the penetration curve. Only terms that helped explain penetration, as measured by R^2, were added to the model even though other terms were

found to be significant ($p<0.05$). The DOP model, containing only one respirator, was allowed to contain more variables and interaction terms to help explain the very scattered respirator penetration data. The final models were tested for the assumptions of homogeneity of variance, linearity, and normality. Penetration data not meeting the assumption of homogeneity of variance or normality were transformed according to Box-Cox. The predicted (transformed) penetration values were generated in DataDesk by applying coefficients generated from the NaCl or DOP ANOVA models to the workplace contaminant data. The observed values were the (transformed) penetration measurements with NaCl aerosol recorded during intervals of respirator loading with a workplace contaminant. Comparisons between predicted and observed values were made with an F test. If the null hypothesis was accepted then the collection efficiency of respirators loaded with a workplace contaminant could be predicted using the NIOSH method. Conversely, if the alternate hypothesis was accepted, then collection efficiency of respirators loaded with workplace contaminants could *not* be predicted using the NIOSH method. To refine the answer to the question if the NIOSH method accurately predicts penetration of *electrostatic* N95 respirators, the NaCl and workplace contaminant models were refined into two subsets. The first subset contained the grouping of respirators with electrostatic filter media and the second contained the single mechanical respirator. Terms included in the models remained unchanged from the combined overall; however, the ANOVA computed slightly different coefficients for each terms

resulting in different predicted values. The predicted values were again compared to the observed penetration values using the F test to determine if the NIOSH method predicted penetration of respirators loaded with workplace contaminants. The null and alternate hypotheses tested remained the same with the added distinction of differentiating predicted penetration for respirators containing electrostatic or mechanical filter media.

To examine the effect of saturating respirators with artificial perspiration, changes in penetration measurements were compared using a paired-t test. Photometer and CNC measured penetration, using NaCl aerosol, were evaluated after the respirators were sealed to their holders and again after being submerged in artificial perspiration followed by drying with HEPA air. The paired-t test examined differences between the pre- and post-saturation penetration measurements. Changes in penetration measurements were attributed to the effects of saturation.

CHAPTER V

RESULTS AND DISCUSSION

This study was designed to evaluate the collection efficiency of air purifying respirators containing electrostatic filter media. Respirators were placed in either occupational settings or environments generated under laboratory conditions representative of the workplace which might lead to the degradation or shielding of electrostatic charge on the filter media thereby reducing collection efficiency. The hypothesis tested was that collection efficiency of respirators with electrostatic filter media could be altered by environmental factors. Respirators containing only mechanical filter media would not have their collection efficiency changed when exposed to these same conditions. Collection efficiency of electrostatic respirators loaded with workplace contaminants could be different than that predicted from the NIOSH certification method for N95 respirators that uses NaCl particles of very small diameter which are considered to be extremely penetrating. The first null hypothesis tested was that the predicted collection efficiency of electrostatic respirators, as determined by the NIOSH method, would determine collection efficiency of the same respirators loaded with aerosol representative of the workplace. The second null hypothesis tested was that the collection efficiency of a mechanical respirator would be equal to an electrostatic respirator loaded with asphalt contaminants, aluminum oxide dust, and metal cutting fluid mist.

Sodium Chloride

The purpose of the NaCl tests was to duplicate the NIOSH certification method for constructing a model to compare N95 respirators loaded with workplace contaminants. Since the certification tests use particles having a diameter that were the most penetrating size, certified respirators can be used in environments against other particulates without regard to size and density [56]. The model used to predict penetration of each N95 respirator was constructed using the criterion in 42 CFR 84. Collection efficiencies of respirators loaded with aerosols other than NaCl were compared to these predicted values. A total of 13 different N95 respirators were evaluated with NaCl. Only one respirator, Racal (mechanical), did not contain electrostatic filter media. Five replicates of each respirator type were used for these tests.

Prior to commencing the NIOSH method tests with NaCl aerosol, the aerosol size distribution was characterized with the DMA to ensure that the requirements of 42 CFR Part 84 were met. The NaCl aerosol generated for these tests was within the acceptable range for diameter and size distribution, refer to Table 5.1. The aerosol concentration average of 14 to 19 mg/m^3 was below the maximum allowable concentration of 200 mg/m^3 permitted by 42 CFR 84 and was similar to concentration of less than 20 mg/m^3 reported by NIOSH [18] during actual certification testing. NIOSH does not specify a minimum concentration level of acceptability.

Table 5.1
Comparison of N95 Requirements and Test Conditions for Sodium Chloride Aerosol

	42 CFR 84 Criteria	Actual Testing Conditions
CMD	0.075 ± 0.02 μm	0.085 μm
GSD	<1.86	1.84
Concentration	≤ 200 mg/m^3	43 lpm: 19.5 ± 1.4 mg/m^3 85 lpm: 14.3 ± 1.6 mg/m^3
Temperature	25 ± 5 °C	23 ± 1.1°C
Relative Humidity	30 ± 10 %	26 ±3.9%

Size distribution of sodium chloride aerosol measured with DMA and CNC
Relative Humidity and Temperature Transmitter probe by General Eastern
Number of respirator tests for concentration, temperature and relative humidity =65

Environmental Conditions

Table 5.1 also compares NIOSH requirements for environmental conditions to actual testing conditions. A solution of sodium chloride and distilled water was nebulized to generate the aerosol. The relative humidity of the air rapidly increased when moisture from the nebulized droplets evaporated leaving behind the solid particulate. To compensate for this effect, initial relative humidity of the system was 'set' at the low end of the range specified by 42 CFR 84. Once an N95 respirator was placed in the test chamber, NaCl testing did not commence until the upstream background reading was less than 5.00 particles/cc, indicating the system was clean and free from leaks. The time elapsed confirming background levels resulted in ambient relative humidity in the test apparatus to drift downward and fall below the target value.

Eighty-nine percent of the tests experienced excursions below the target range for relative humidity. All but nine of these respirators had their low readings confined to the first five minutes of the test. Three respirators had excursions for the entire duration of their tests, relative humidity ranged

between 12.6 to 19.3%; after the first five minutes of loading, relative humidity increased above 18%. However, relative humidity below 20% was not expected to decrease particle diameter less than 0.085 μm. Without a change in diameter, penetration of NaCl was expected to remain the same [76]. CNC- and photometer-measured penetration measurements for respirators with excursions lasting more than the first five minutes were compared to their replicates. Observations indicated that low relative humidity excursions may have slightly increased respirator penetration but were not beyond the range of penetration for the respirator type.

The compressed, dried air supply, secured to the inlet of the HEPA filter with duct seal, loosened during two tests, allowing ambient room air to enter the HEPA filter. Without the compressed air supply, relative humidity of the system rapidly increased. The diameter of the NaCl aerosol will increase when in contact with high humidity environments as a result of NaCl absorbing water vapor and swelling. Above 55% relative humidity, hygroscopic materials, such as NaCl, have substantial weight gains [147]. Relative humidity during two tests increased to 47% and 44% after 2 and 5 minutes respectively. Brief excursions up to 47% were not expected to alter the effective diameter of the NaCl particles or to alter the penetration results.

Temperature readings below 20 ^{o}C were limited to three respirator tests and occurred during the winter when the ambient temperature in the laboratory was colder than usual. An infrared lamp was subsequently added to the test apparatus to maintain the target temperature. The lowest temperatures, 18 to 19 ^{o}C, lasted for the entire duration of the test, approximately 3 to 4 hours. Duration

of temperatures below target for the other two tests lasted between 49 to 62% of the testing cycle. Literature [3] reports that penetration of a mechanical filter with NaCl aerosol would increase with decreasing temperature. When viscosity of the air decreases, sedimentation and inertial deposition of particles increase. Theory predicts maximum penetration at a temperature of -37 ^{O} C. For this test matrix, deviations below target temperature might result in penetration readings to be slightly higher than expected. Only one respirator, Tecnol PFR95, exhibited increased CNC-measured penetration for the first 20 mg loading as compared to the other replicates. Inclusion of the data for this respirator may have slightly increased the initial predicted penetration measurements.

Velocities and Face Seal Evaluation

Face velocity measurements of filters, the velocity of air at the face of the filter, allows the results of filtration efficiency to be compared to other studies. Unfortunately, this measurement often goes unreported in filtering facepiece respirator studies making comparisons to previous work more difficult. In this study, face velocity of N95 respirators was determined by measuring the surface area of the respirator and dividing by its airflow rate. Molded filtering facepiece respirators were assumed to have the surface area of one-half of a sphere. Circumference of the sphere was estimated by averaging twice the width across the curvature of the respirator with the perimeter of the face seal. Face velocities by respirator type, size , and lot number are listed in Appendix Table B.6.

Integrity of the face seal of filtering facepiece respirators and the placement of filters in respirator receptacles were evaluated by measuring penetration of monodisperse 2 μm latex spheres at 35 lpm, the 3M Large Particle

Quantitative Fit Test (LPQFT) Method. Penetration of this particle diameter was measured with the Climet yielding count-measured penetration using the following formula [76].

% Penetration=(particle count upstream/particle count downstream) x 100%
(equation 5.1)

In a previous study [144], the face seal integrity for dust-mist (DM) respirators sealed to mounting plates was found to be 0.1%. These researchers used a monodisperse corn oil having a diameter of 2.5 μm. The summary of initial penetration by respirator type with 2 μm monodisperse latex spheres for evaluating face seal fit for the NaCl loading tests conducted by this research is listed in Appendix Table B.6. Collectively the average penetration of N95 respirators and filters was 0.26%. Two respirators, Gerson 2735S and Moldex 2200, had penetration greater than 1.2%, biasing this average. The construction of these respirators had elastic head straps stapled to the body of the respirator. Upon visual inspection, small holes in the respirator body were observed around the staples. These respirators were closely examined for gaps or holes around the face seal that might have accounted for the increased penetration, none were found. Higher than anticipated penetration was attributed to the construction of the respirator and not the integrity of the face seal. The 3M 1860 respirator had a similar construction with the elastic head straps stapled to the molded body. Unlike Gerson 2735S and Moldex 2200, no visible gaps around the staples were observed; initial penetration was 0.17%. Leak rate was also higher than expected

for 3M 8210 which had elastic straps welded to the respirator body; initial penetration was 0.17%. Some areas of attachment had scoring creating an 'x' shaped pattern appearing like an indentation in the welded area. The remaining nine respirators averaged an initial penetration of less than 0.02%. Four of the respirator types tested in this study had average penetration reading above 0.1% which was indicative of possible leak(s) at the face seal. Since visual inspections of the face seal did not reveal any weak areas or gaps, increased penetration was attributed to the construction methods of the respirators and not the integrity of the face seal.

Tests were terminated once the target mass of 200±5 mg NaCl contacted the respirator. The actual mass contacting respirators tested at 43 lpm averaged 203±8 mg NaCl with a range of 189 to 217 mg. Respirators tested at 85 lpm averaged 200±10 mg NaCl with a range of 154 to 214 mg. During respirator loading, aerosol mass was estimated from the upstream mass collected on pre-desiccated Millipore filters and was used for deciding the termination time of the test. Mass reported as contacting the respirator was computed after the Millipore filters had been post-desiccated for 24 hours. Divergence from the target mass was possibly due to computation error, variability in aerosol concentration, or early termination of the tests. Three of the five Tecnol PFR95 respirators, tested at 85 lpm, had their tests terminated early when the respirators collapsed from aerosol loading. The flattened respirators effectively sealed the exhaust outlet on the holder through which sufficient airflow could no longer be drawn. Tests with Tecnol PFR95 were terminated after 155 to 190 mg NaCl contacted the respirator. Four of the five Moldex 2200 respirators, tested at 85 lpm, exhibited some degree of respirator separation ranging from minor to severe; however, the structural

separation of the back layer did not result in complete respirator collapse or early termination of the tests. The tests that were terminated prematurely were at the end of their loading cycle after peak penetration readings were measured. The duration of the NaCl tests for respirator flow rates of 43 lpm averaged 243±18 minutes with a range of 209 to 266 minutes, respirators tested at 85 lpm averaged 167±16 minutes with a range of 135 to 244 minutes.

Respirator Penetration Evaluation

Respirator loading commenced when NaCl generators were turned on. The system was allowed to equilibrate for one full minute prior to recording initial downstream readings. Maximum NaCl penetration occurred during the first 3 to 4 mg of loading for all N95 respirators tested. The photometer-measured penetration curve for most N95 respirators decreased and then reached a short plateau before penetration exponentially declined and in some cases reached zero. The shoulder of the penetration curve occurred between 10 and 60 mg loading. Figure 5.1 illustrates this phenomenon; data are plotted from five replicate NaCl loading tests.

The overall shape of the CNC- and photometer-measured penetration curves declined exponentially after reaching maximum penetration. Plots of photometer-measured penetration plots are shown in figures 5.2 through 5.4, CNC-measured penetration are shown in figures 5.5 through 5.7.

Individual data points were too numerous to clearly identify the trend in penetration by respirator type. An exponential trend line appeared to provide the best visual fit of the data. For ease of interpretation, trend lines of penetration are presented. These plots masked the plateau effect described above for

photometer-measured penetration. This plateau effect was not observed in the CNC-measured penetration curves.

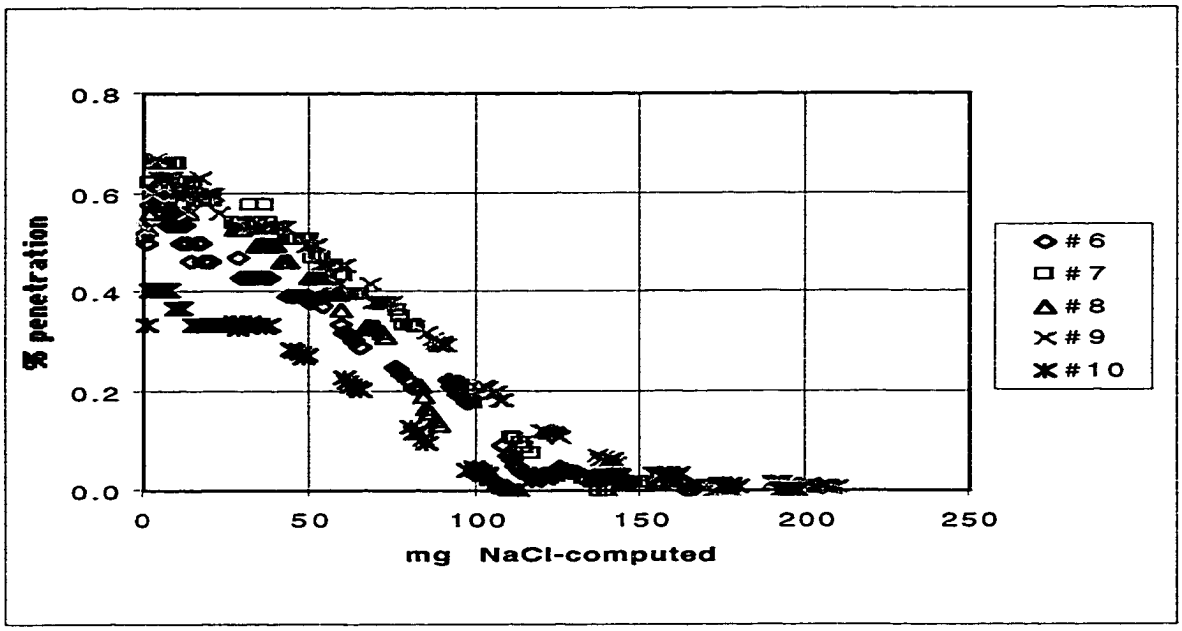

figure 5.1
Sodium Chloride Loading of Tecnol PFR95 Filtering Facepiece Respirators
Photometer-Measured Penetration

The shape of the NaCl penetration curves in figures 5.1 was different than expected for filters made with electrostatic filter media. Sources [92, 21, 129] indicated that penetration through respirators or filters with electrostatic filter media would increase until 15 to 40 mg of NaCl had been loaded.
Once electrostatic mechanisms were shielded or masked, mechanical forces would become predominant and penetration would decrease. The shapes of the photometer-measured penetration curves for this study did not exhibit a delayed peak.

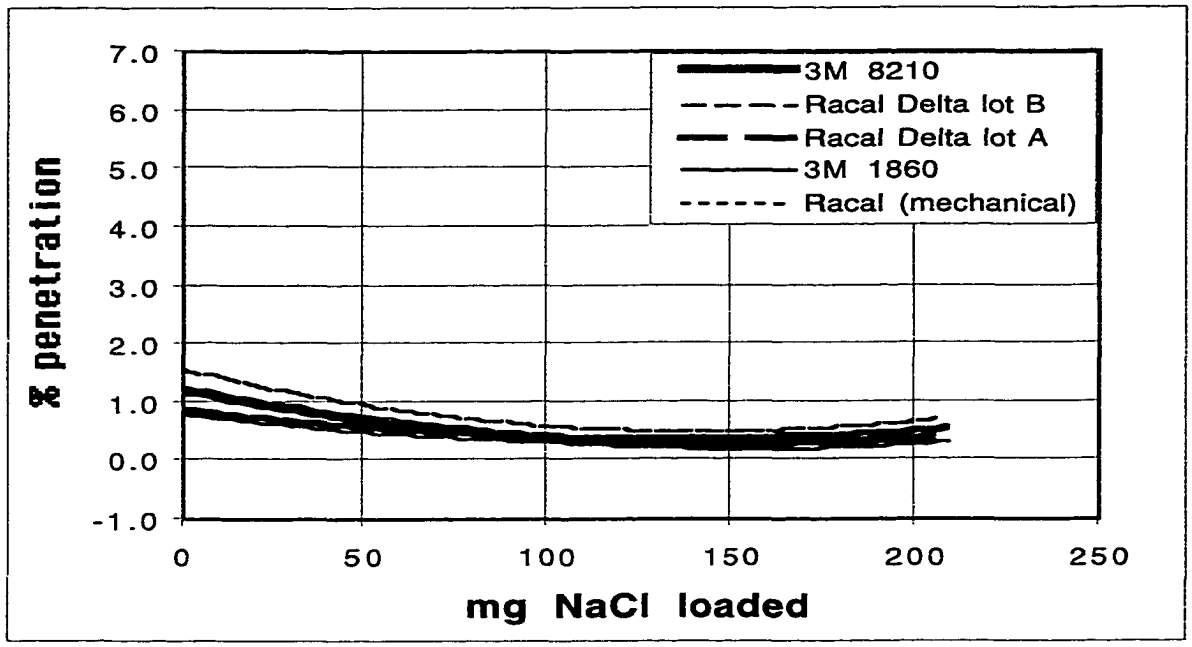

figure 5.2
Photometer-Measured Penetration
N95 Respirators Loaded with Sodium Chloride
Final Pressure Drop Less Than Two Inches of Water
Number of replicates tested= 5 for each respirator type

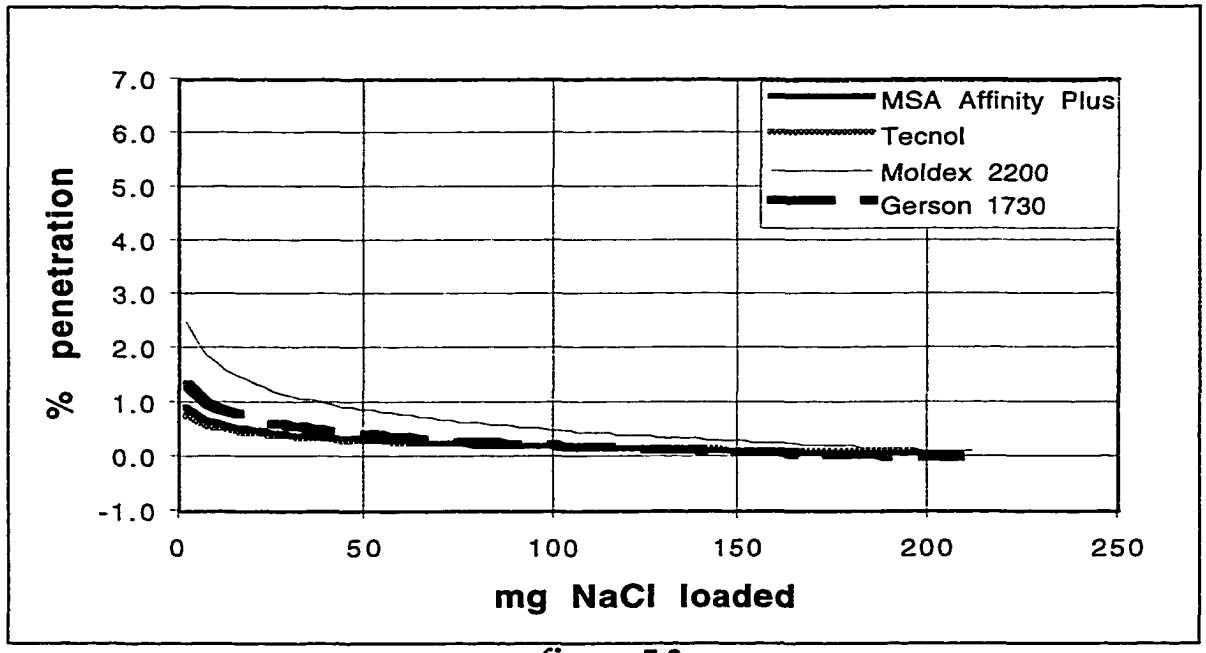

figure 5.3
Photometer-Measured Penetration
N95 Respirators Loaded with Sodium Chloride
Final Pressure Drop Two to Three Inches of Water
Number of replicates tested= 5 for each respirator type

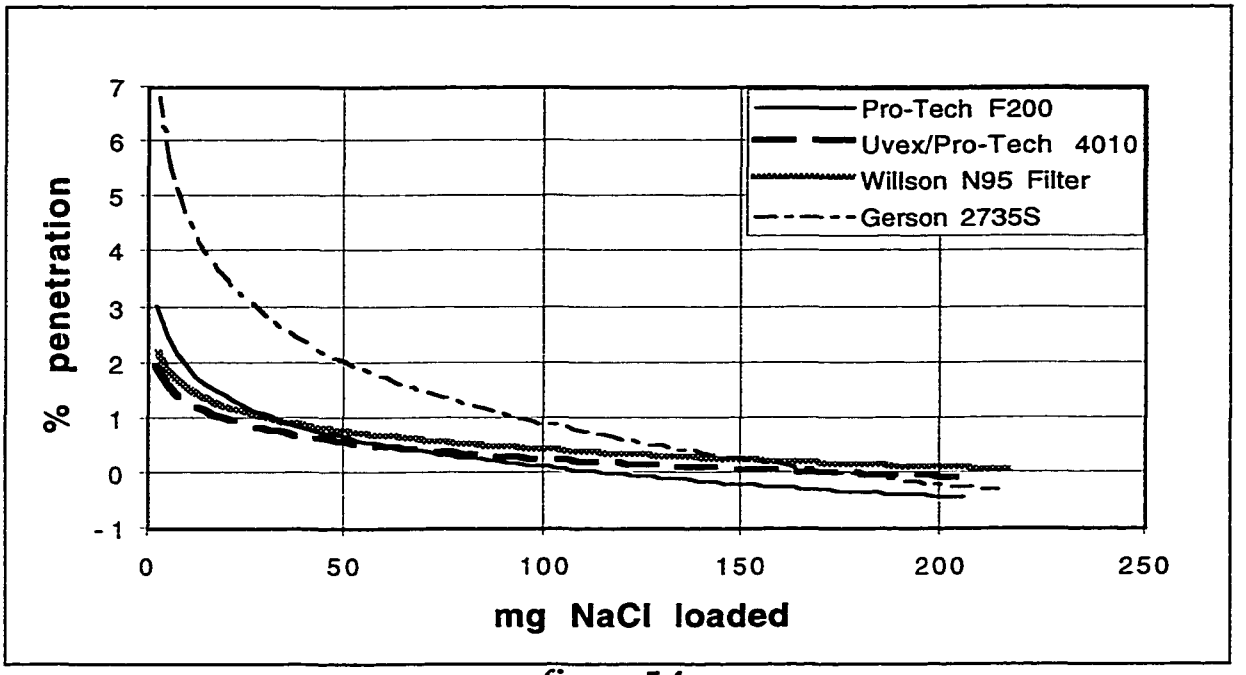

figure 5.4
Photometer-Measured Penetration
N95 Respirators Loaded with Sodium Chloride
Final Pressure Drop Greater Than Four Inches of Water
Number of replicates tested= 5 for each respirator type

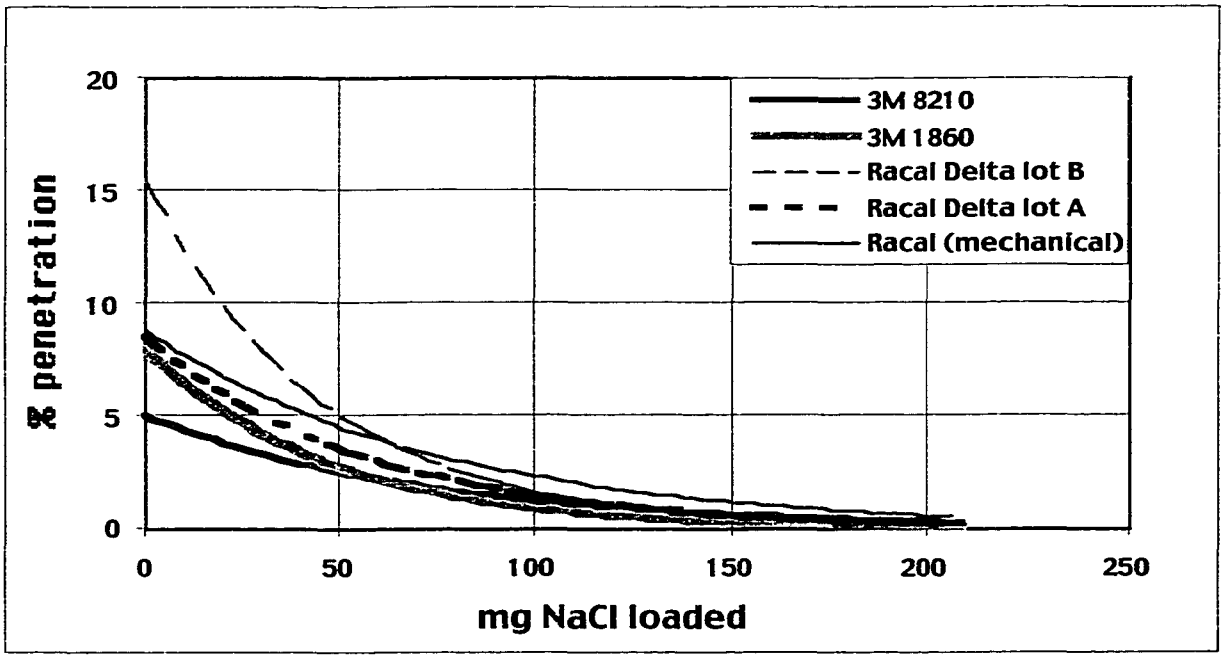

figure 5.5
CNC-Measured Penetration
N95 Respirators Loaded with Sodium Chloride
Final Pressure Drop Less Than Two Inches of Water
Number of replicates tested= 5 for each respirator type

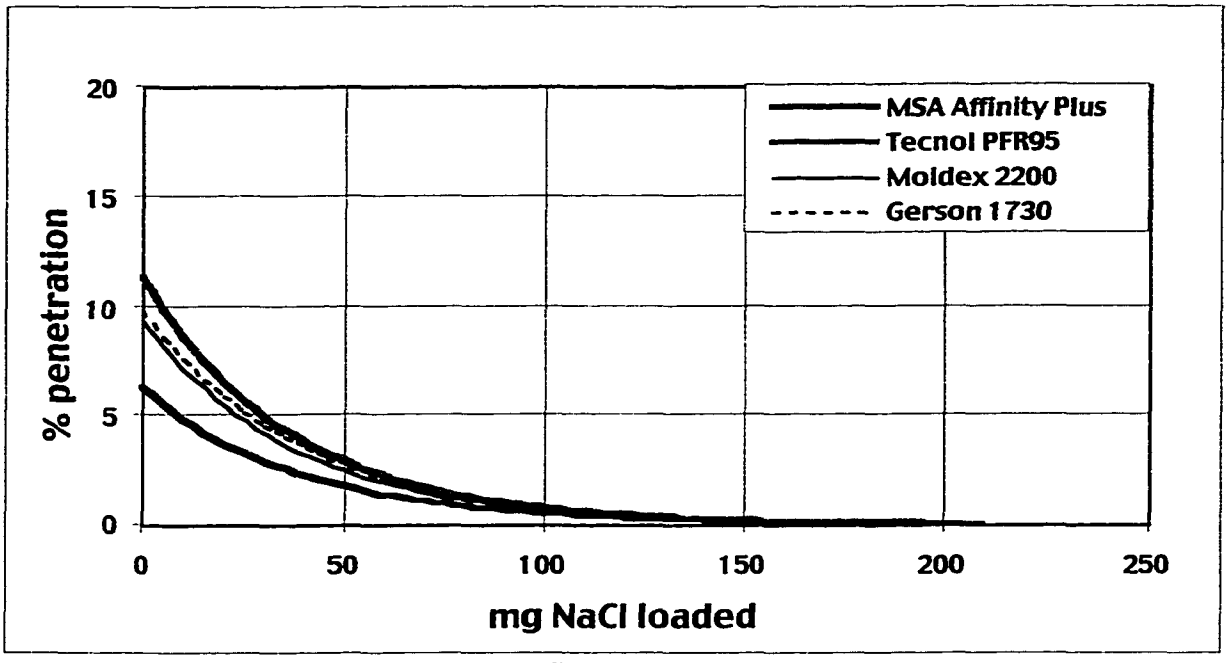

figure 5.6
CNC-Measured Penetration
N95 Respirators Loaded with Sodium Chloride
Final Pressure Drop Two to Three Inches of Water
Number of replicates tested= 5 for each respirator type

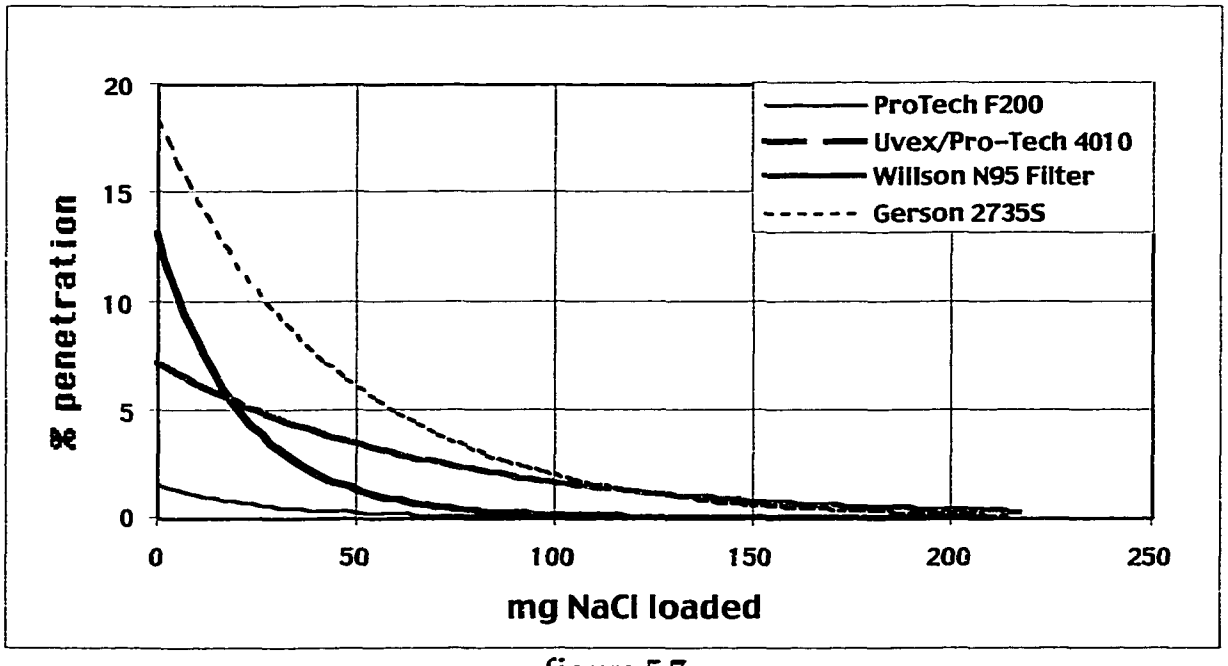

figure 5.7
CNC-Measured Penetration
N95 Respirators Loaded with Sodium Chloride
Final Pressure Drop Greater Than Four Inches of Water
Number of replicates tested=5 for each respirator type

One possible theory that might explain the shoulder in the penetration curve for these tests could be attributed to competition between electrostatic and mechanical collection forces at the beginning of the loading cycle. Both properties are inherent with the fine diameter melt blown fibers. A typical penetration pattern for purely electrostatic filter medium has a peak in penetration curve during the first part of the loading cycle. A typical penetration pattern for purely mechanical filter medium is to have an initial penetration higher than electrostatic and then decrease with loading and possible merge with the purely electrostatic penetration curve. The actual penetration of a respirator having these two collection forces at the beginning of the loading cycle would lie somewhere in between and could be one possible explanation for this shoulder.

More recently, Moyer and Bergman [154] reported maximum photometer-measured penetration of N95 respirators with NaCl aerosol occurring after the first few mg of loading followed by decreased penetration. Some of their data indicated a plateau in the penetration curve during the first approximate 30 mg of loading. It was unknown if the N95 respirators tested in their study contained electrostatic filter media. During a telephone conversation, it was indicated that the shape of their penetration curve was very typical for N95 respirators although it was dependent upon the composition of the filter media [155]. The shapes of the NaCl penetration curves in this study were similar to their findings. Only one of the respirators they tested had a significant rise in penetration later in the loading cycle, similar to the findings of referenced sources.

The penetration measurements by the photometer were very different from the CNC. The differences in the operating characteristics of these two instruments has been studied by Tillery et al. [139] and Biermann and Bergman [138] and is discussed in Chapter IV. These works examined the variation in instrument response by particle size. To obtain a better understanding of how the CNC-measured penetration obtained by this study was so much greater than the photometer-measured penetration, additional work would be necessary. The particle size distribution upstream and downstream from the respirator during the loading cycle would need to be characterized for each respirator type studied. This additional research was beyond the scope of this project.

Sodium Chloride Results

Simplified ANOVA models from NaCl penetration, CNC- and photometer-measured, were constructed to predict penetration of respirators loaded with asphalt, aluminum oxide, and metal cutting fluid. Respirators included in these models were grouped according to the selection of workplace contaminants. The two groupings of N95 respirators modeled for NaCl penetration were:

a) Respirators loaded with asphalt contaminants;

   MSA Affinity Plus, Pro-Tech F200 filter, Racal (mechanical), Racal lot A, Racal lot B, and Tecnol PFR95,

b) Respirators loaded with aluminum oxide dust and metal cutting fluid, both laboratory and field;

   MSA Affinity Plus, Pro-Tech F200 filter, Racal (mechanical), and 3M 8210.

ANOVA models of CNC- and photometer-measured penetration with NaCl aerosol can be found in Appendix Tables B.6 through B.9. "Mass of sodium chloride", "respirator type", and their interaction term were always included in the models as independent variables. Terms for "initial fit", "temperature" and "relative humidity" were correlated and added to the model if they were found to be significant ($p<0.05$). An additional criterion used was that the terms included in the final models had to explain at least one percent of the variability in penetration. Percent penetration, the dependent variable, was transformed, as necessary, using the Box Cox analysis. An example of the effect of the transformation attempting to normalize penetration data is presented in figures 5.8 and figure 5.9.

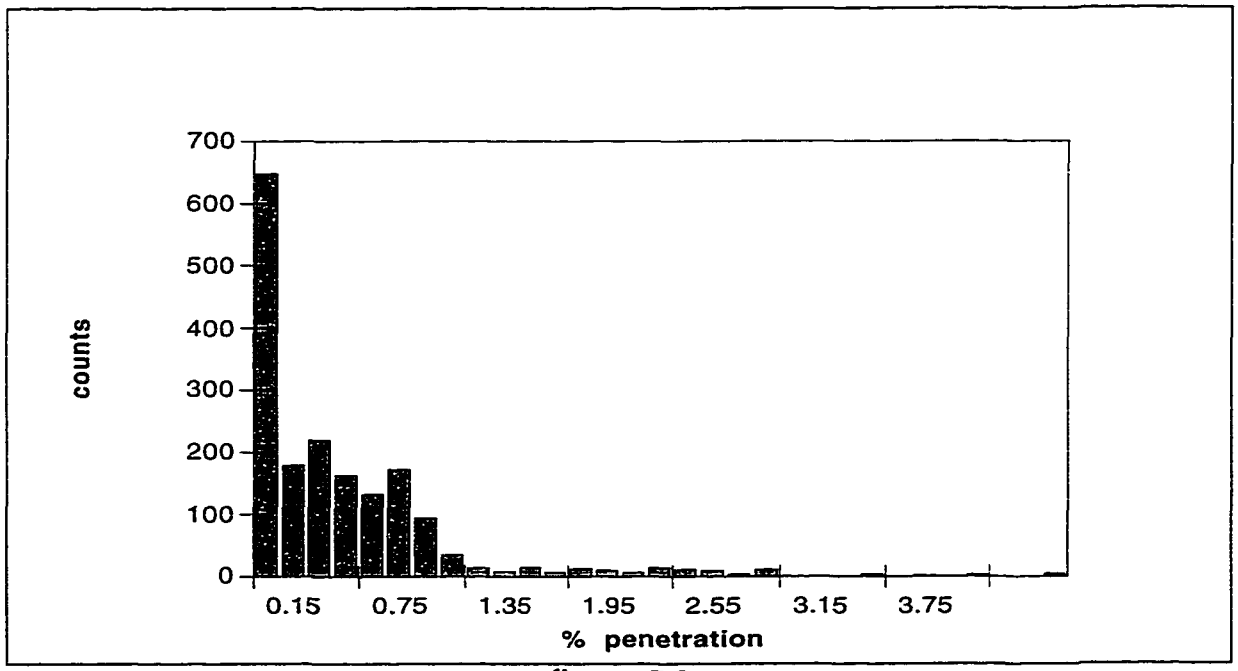

figure 5.8
Distribution of Penetration Measured by the Photometer Untransformed Data N95 Respirators From The Aluminum Oxide Dust-Metal Cutting Fluid Mist Group Loaded With Sodium Chloride Aerosol

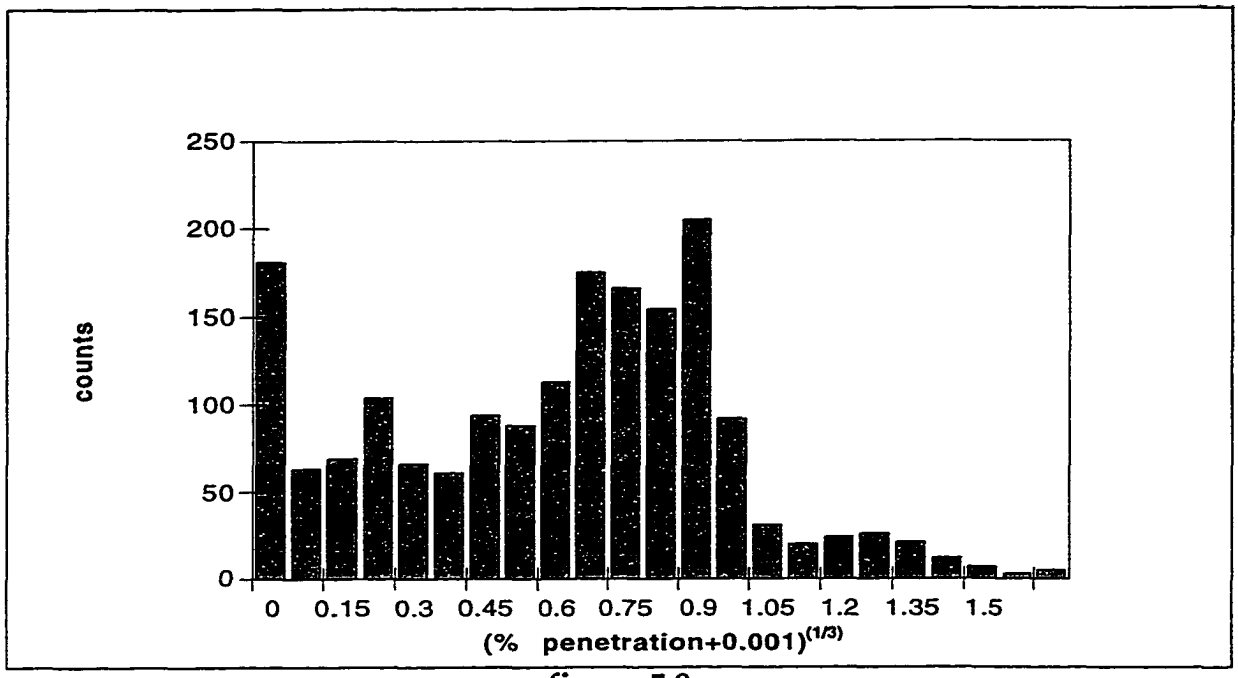

figure 5.9
Distribution of Penetration Measured by the Photometer, Data Transformed N95 Respirators From the Aluminum Oxide Dust-Metal Cutting Fluid Mist Group Loaded with Sodium Chloride Aerosol

These histograms display photometer-measured penetration for the aluminum oxide-metal cutting fluid mist respirator grouping loaded with NaCl aerosol using the NIOSH method tests. The R^2 values of the ANOVA models ranged from 0.767 to 0.847. Coefficients generated from these models were subsequently applied to data from respirator loading with workplace contaminants to compute predicted (transformed) penetration values. Measured penetration measurements from respirators loaded with aerosol other than NaCl could then be compared to their predicted values using an F test.

The reliability of the NaCl ANOVA models for N95 respirators, was confirmed by applying the coefficients from the ANOVA models to the NaCl data from which they were generated. Plots comparing observed and predicted NaCl penetration for each respirator in the asphalt contaminant test matrix are

located in Appendix Graphs C.1 through C.12. These plots are a visual indication of how well the models predicted penetration. Graphs of predicted NaCl penetration indicated that the NIOSH models for Pro-Tech F200 was a poor fit of the actual data. Penetration of the Pro-Tech F200 filter decreased linearly until 50 mg of NaCl had been loaded, with the dependent variable retaining its unique transformation. Observed penetration measurements beyond 50 mg were relatively flat and near zero. The predicted values attempted to make a linear fit across the entire range of loading. Creating separate ANOVA models for this one respirator would have resulted in improved accuracy for comparing observed penetration of this respirator loaded with workplace contaminants to its predicted penetration values based upon the NIOSH certification method. Creating separate models for each respirator type would have prohibited any comparisons between the electrostatic respirators and the mechanical N95 respirator.

Global comparisons with the N95 respirator groupings described above were made between predicted and observed penetration using an F test. The F test values for CNC- and photometer-measured NaCl penetration were 1.00 with a p value of 0.500. The null hypothesis was accepted and the difference between the observed and predicted CNC- and photometer-measured NaCl penetration values were not significantly different, $p>0.05$, indicating the ANOVA models adequately predicted penetration.

Dioctyl Phthalate (DOP)

The purpose of the DOP tests was to duplicate the NIOSH certification method for constructing a model for comparing an electrostatic P100 filter, 3M 2091, loaded with workplace contaminants. In addition to the 3M 2091 filters,

two other P100 cartridges were included for testing, 3M 7093 (with mechanical filter media) and Pro-Tech G108 (with electrostatic filter media). Predicted penetration of the 3M 2091 filters was constructed using the criteria in 42 CFR 84 specifying the testing method for NIOSH certification of P100 air purifying respirators. Collection efficiencies of this respirator loaded with aerosols other than DOP could be compared to their predicted values. Five to six replicates were used for these tests.

Before the NIOSH method tests with DOP aerosol could begin, the aerosol size distribution was characterized to ensure that the requirements of Title 42 CFR Part 84 were met. Table 5.2 compares the criteria for this aerosol to the actual aerosol used for these tests. The DOP aerosol generated for these tests was within the acceptable range for particle diameter. The actual size distribution was at the maximum specified bounds of the requirement. The aerosol concentration for these tests averaged 65±3 mg/m^3 and was below the maximum allowed by 42 CFR 84, which does not specify a minimum concentration level of acceptability.

Table 5.2
Dioctyl Phthalate Aerosol and P100 Respirator Testing Requirements Compared to Actual Conditions

	42 CFR 84 Criteria	Actual Testing Conditions
CMD	0.185 ± 0.02μm	0.20μm
GSD	<1.60	1.60
Concentration	≤200 mg/m^3	65.6±3.5 mg/m^3
Temperature	25 ± 5 ^{o}C	24±0.9 ^{o}C
Relative Humidity	not specified	23±5.7%

Size distribution of sodium chloride aerosol measured with DMA and CNC
Relative Humidity and Temperature Transmitter probe by General Eastern
Number of respirator tests for concentration, temperature and relative humidity =15

This concentration was also less than 100 mg/m^3 used for actual certification testing, as described by NIOSH [84]. Aerosol concentration was intentionally lowered for two reasons. First, lower concentration increased the duration of the test allowing additional penetration measurements to be recorded. Second, fluctuation in concentration above 100 mg/m^3 exceeded the capabilities of the photometer. The DOP aerosol used in this study for evaluating the collection efficiency of P100 air purifying respirators met the 42 CFR 84 requirements.

Environmental Conditions

Table 5.2 also compares the actual environmental conditions to the requirements of 42 CFR 84. There were no excursions in air temperature during these tests and overall this requirement was satisfied. A target range for relative humidity is not stipulated in 42 CFR 84 as the size distribution of an oily aerosol is not influenced by acquiring moisture and swelling, as in the case of NaCl. The large standard deviation for relative humidity during actual testing conditions was primarily due to house compressed air being supplied to the inlet of the HEPA filter at the air intake for the system during some tests and not for others. Overall this variability did not influence penetration measurements.

Face velocities through the respirators were computed by dividing the flow rate by the surface area of the respirator. Respirator cartridges were opened and filter media unpleated prior to measuring the surface area. Face velocities by respirator type and lot number are located in Appendix Table B.8.

Respirator Penetration Evaluation

Tests were terminated once the target mass of 200±5 mg of DOP had contacted the respirator. The actual average mass contacting respirators was

199±5 mg DOP with a range of 188 to 207 mg. During respirator loading, aerosol mass was estimated from the upstream mass collected on pre-desiccated Millipore filters. Mass reported as contacting the respirator was computed after the filters had been post-desiccated for 24 hours. Divergence from the target was due to possible computation error and early termination of the testing.

Penetration measurements of P100 cartridges and filters contained a high degree of variability, making it difficult to construct a penetration curve. As loading increased, overall photometer- and CNC-measured penetration was either flat or increased slightly for the electrostatic respirators and decreased for the mechanical respirator. The shape of the penetration curve was expected to increase with loading as DOP is the most degrading aerosol known [35, 78]. Penetrations of P100 respirators loaded with DOP for these tests are displayed in figures 5.10 and 5.11.

Dioctyl Phthalate Results

Simplified ANOVA models for CNC- and photometer-measured DOP penetration were constructed for 3M 2091 respirator. The independent variable "mg DOP" loaded onto the respirator as computed from upstream sampling was always included in the model. Other terms were correlated and added if found to be significant ($p<0.05$) and were able to explain at least one percent of the variability in penetration. Penetration, the dependent variable, was transformed as necessary based upon the Box Cox test. The R^2 value for the CNC-measured penetration model was 0.70 and the final model did not contain any interaction terms. Photometer-measured penetration contained a high degree of variability resulting in a poor fitting model. Interaction terms added to the model increased

the R^2 from 0.136 to 0.428. This increase was considered to be an artifact adding variability as the model as it attempted to fit the data; therefore, these interaction terms were not included. The photometer-measured penetration model was unable to explain 86% of the variability in penetration and any comparison to it was deemed suspect. These ANOVA models can be found in Appendix Tables B.12 and B.13. Predicted penetration values were generated and used to test the reliability of the model by applying coefficients from the ANOVA model back to the original data. Comparisons between observed (transformed) CNC-measured penetration and predicted (transformed) penetration were made using an F test.

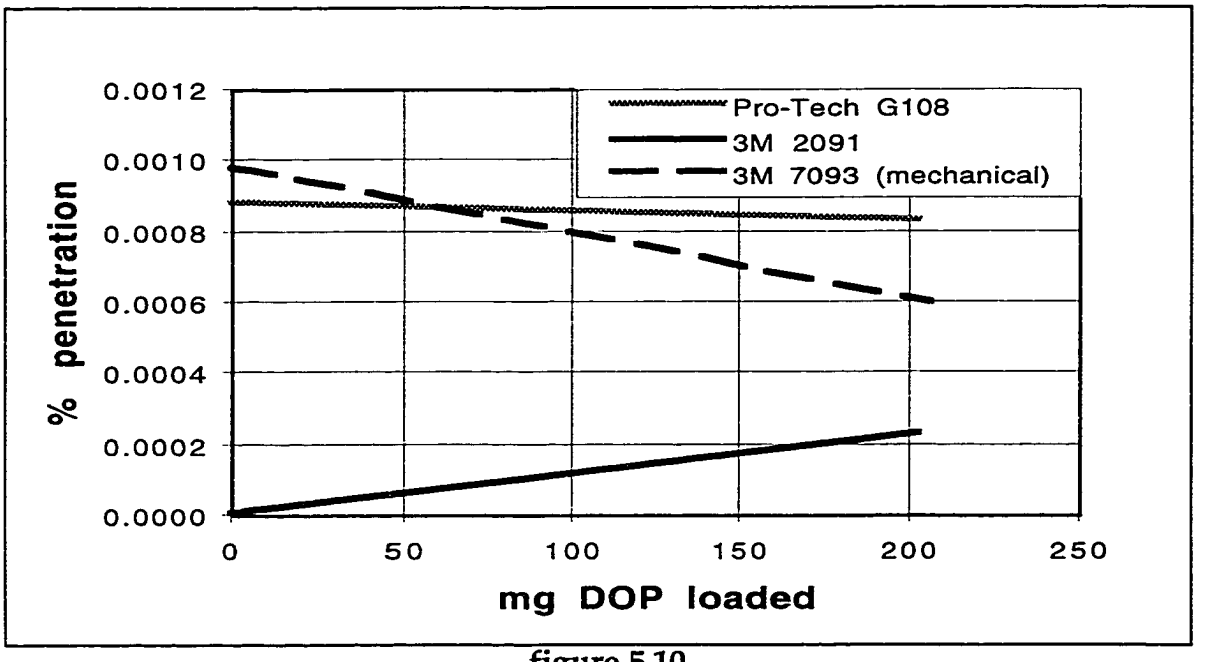

figure 5.10
CNC-Measured Penetration
P100 Respirators Loaded with DOP
Number of replicates tested= 5 for 3M 7093 and Pro-Tech G108; Number of replicates tested=6 for 3M 2091

The F value was 1.00 with a p value <0.998 indicating that there was not any difference between observed and predicted penetration. Measured penetration

measurements from the 3M 2091 respirator loaded with aerosol other than DOP could then be compared to its predicted values.

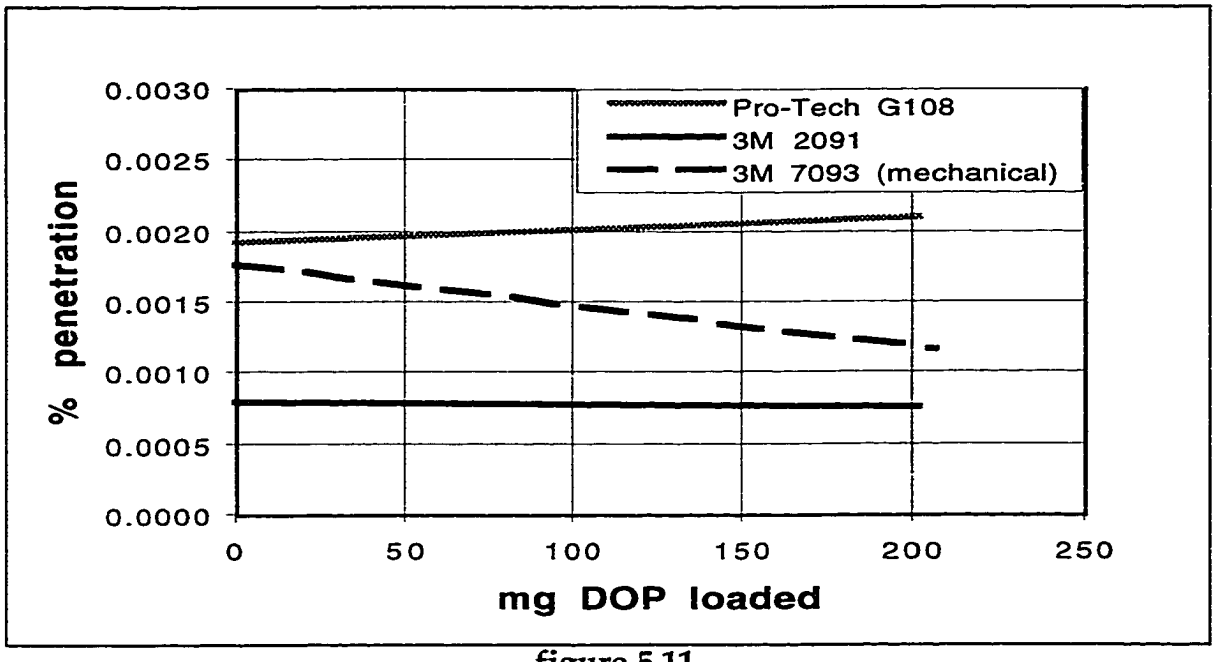

figure 5.11
Photometer-Measured Penetration
P100 Respirators Loaded with Sodium Chloride
Number of replicates tested= 5 for 3M 7093 and Pro-Tech G108; Number of replicates tested=6 for 3M 2091

Asphalt Contaminants

Loading air purifying respirators with contaminants emitted around an asphalt melting kettle was the first field test with workplace contaminants. Testing began on September 9,1997 and continued through the end of October 1997. Due to a building contamination problem at the roofing site, roofing operations were suspended until mid December at which time respirator testing was completed. The day before N95 respirators were loaded with asphalt contaminants in the field, initial fit was evaluated using the 3M LPQFT method. Refer to Appendix Table B.14 for a summary of the average initial fits by

respirator type. Respirators, secured to their holders, were stored overnight in clean plastic bags. Cumulative, initial penetration averaged 0.17%. MSA Affinity Plus had one respirator with an initial leak rate of 4.07% causing the average initial penetration to increase to 0.74%. Including this respirator in the analysis may have resulted in slightly higher penetration readings as face seal leakage was likely. Disregarding this one outlier, the average leak rate for this respirator was 0.26%, with an overall initial penetration of N95 respirators of 0.09%. Face seal leakage for Tecnol PFR95 and MSA Affinity Plus were slightly higher for these tests compared to the NaCl loading tests.

The temperature of the melting kettle was maintained in the range of 485 to 500 ^{O}F. In the morning, the kettle burners operated about 30 to 60 minutes before this temperature was reached. Respirator loading did not begin until a visible white plume was discharged from the melting kettle. The visual and gravimetric amounts of contaminants emitted seemed to be dependent upon the operation of the kettle and the amount of asphalt being melted. Asphalt for melting was added to the kettle in 100 lb plugs. If demand for melted asphalt was high, the kettle burners operated at a higher temperature to quickly melt the additional plugs. The measured concentration of asphalt contaminants started out low in the morning during the first two hours of loading, then increased to the highest levels during the second two hours of loading before tapering off during the last loading period. The wind direction changed throughout the day. In the mornings wind was usually from the southwest and by midmorning to noon, it was from the north to northwest. The "exposed" respirators were on a mobile stand that was repositioned around the asphalt kettle so that the

respirators were downwind from the asphalt aerosol. For maximum loading, the respirator stand was located approximately five feet from the edge of the melting kettle. The "control" respirator was located approximately 60 feet southwest from the asphalt kettle near the duct of a positive pressure building exhausting ambient indoor quality air to the exterior. The exhausted air was directed toward the "control" respirator. This airflow provided additional protection to the "control" respirators from asphalt loading. On a few occasions, the roofing crew finished early and the kettle burners were turned off prior to removing respirators from their stands. Kettle temperature remained in the target operating range but the visible plume was minimal.

Temperature and relative humidity of the ambient air at the roofing site were recorded with a chilled mirror hygrometer. An MSA Ultra filter was connected to the inlet of the sample line to prevent particle deposition on the mirrors from altering the calibration of the instrument. The filter housing and connections attached to the sample line were originally metal that could potentially retain heat and alter the readings. On October 2, a 47 mm 0.45μm Nuclepore filter in a plastic holder replaced the MSA Ultra filter and all connections were changed to plastic. A reflective panel made from a cardboard box covered with aluminum foil was placed over the unit to prevent warming the sensor from the sun's radiant heat. Ambient air temperature next to the "exposed" respirators was compared to the "control" respirator using a mercury-glass thermometer. The mid-day air temperature next to the "exposed" respirators averaged about 2 to 3 ^{O}C higher than the "control" respirator due to the close proximity of the melting kettle.

Halfway through this testing matrix, a yellow residue was observed inside the flow meter regulating airflow for the cascade impactor. The flow meter was disassembled and cleaned and the residue did not reappear. It was suspected that volatiles from the asphalt contaminants had either passed through or were stripped off the backup filter on the cascade impactor and condensed on the glass wall of the flow meter to form this buildup. This residue was not observed inside the flow meters regulating airflow for the respirators. One possible explanation for the yellow residue not forming inside the flow meters for the respirators was that the pressure drop across the respirators was much less than the pressure drop across the cascade impactor. The greater the pressure drop, the more likely volatiles will be removed from the filter by the airflow and condense on the walls of the flow meter.

From September 11, 1997 to October 16, 1997, flow rates through the respirators and the cascade impactor were established with a hot wire anemometer calibrated against the spirometer. After a month of testing, a residue was observed coating the wire. During the cleaning process, the wire was damaged resulting in significant changes to the measured flow readings when the anemometer was rechecked with the spirometer. Flow readings for the last portion of the tests were established with the sharp edge orifice and magnehelic gauges that had been calibrated against the spirometer.

Size Distribution

The Andersen Cascade Impactor was used to determine the size distribution of the contaminants. The target volume of air to be collected by the cascade impactor was 10,000 L. The computed and fitted size distributions of asphalt contaminants collected by the cascade impactor are contained in Table

5.3. Overall, the fitted MMAD was larger than the actual MMAD as reflected in the increased average diameter and standard deviation. On the first stage that captured the largest particles, the mass collected was low but then reached a maximum on the second stage. The mass collected tapered off on subsequent stages collecting smaller particles. The cascade impactor tends to give a bimodal distribution.

Table 5.3
Size Distribution of Asphalt Contaminants

Size Distribution	MMAD ($\bar{x} \pm \sigma$) µm	GSD (range)
Computed	3.9 ± 0.52 µm	1.31 to 2.22
Fitted	4.5 ± 1.04 µm	1.33 to 2.85

Data collected with Andersen Cascade Impactor
Sampling dates 9/11/97 to 12/12/97
Number of testing days=17

The fitted data normalized the aerosol into a lognormal size distribution and indicates that particles were missing in the larger size bins, shifting the distribution slightly to the right. The lognormal probability plot of the fitted asphalt size distribution is presented in figure 5.12.

The low vapor pressure for the volatile fraction of asphalt fumes can result in them being easily removed once they are collected on a filter. This can result in some of the collected mass being lost [156]. It is unknown if the mass lost would vary by particle size and possibly shift the size distribution as reported by the cascade impactor. Quantifying weight loss by particle size would require additional study and was beyond the scope of this project.

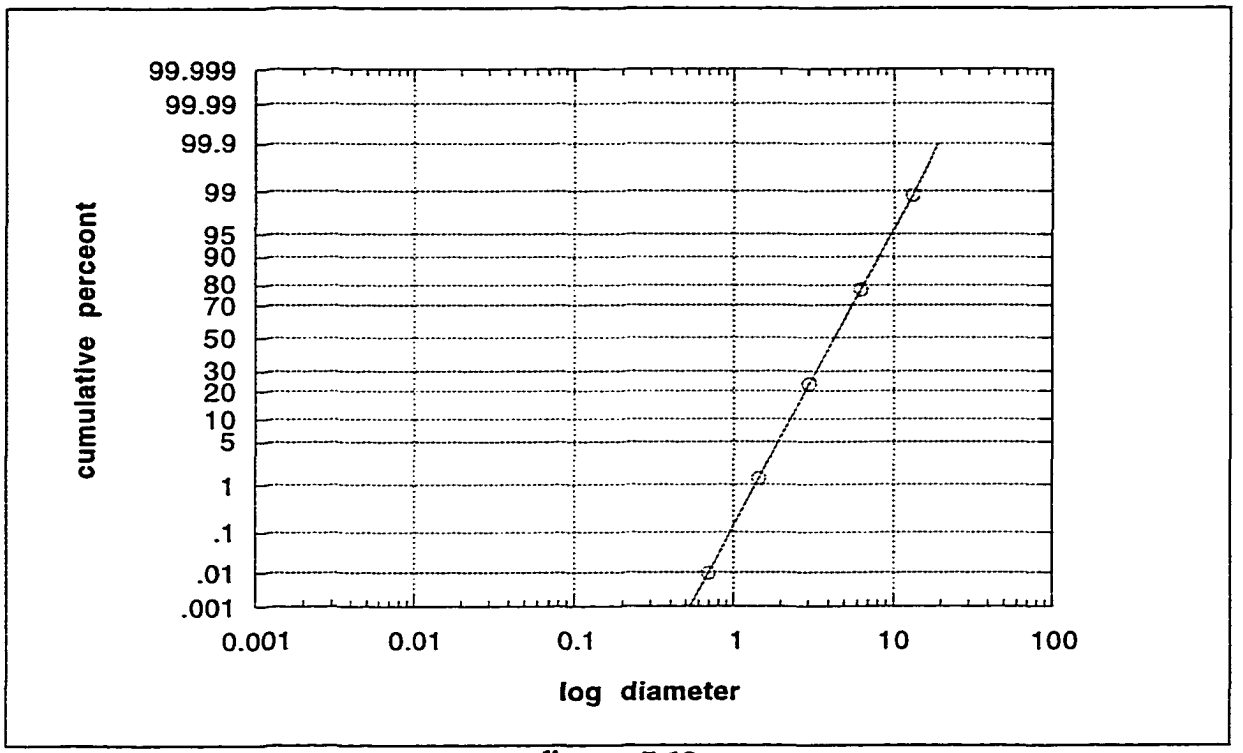

figure 5.12
Fitted Size Distribution of Asphalt Contaminants
Data collected with Cascade Impactor on 9/25/97
Fitted: MMAD 4.74 μm, GSD 1.64

Asphalt Concentration

The concentration of contaminants generated next to the asphalt kettle and ambient background levels next to the "control" respirators were determined using a sampling train consisting of a high volume pump and a closed face filter cassette. Closed face filter cassettes next to the asphalt kettle initially sampled for the entire six hour duration of exposure but later were changed after each two hours of exposure to capture fluctuations in the aerosol concentration throughout the day. The "control" cassettes collected ambient background for the entire six hours. Concentration measurements from the cassette samples were used for computing mass loaded onto the respirators. On October 15, 1997, the lid on the asphalt melting kettle was replaced. The old lid

was cracked, allowing increased emissions from the kettle. Once the new lid was installed, average concentration measurements next to the kettle were severely reduced from 2.25 mg/m^3 to 0.64 mg/m^3. Asphalt contaminant levels were increased slightly by opening two flaps on the kettle lid to allow more of the white vapor and aerosol to escape. Tests with respirators having low loading levels were repeated in an effort to obtain higher loading levels. This resulted in some respirators having a greater number of replicates than others. All respirators were in at least six "exposed" tests with asphalt contaminants and two "control" tests. Racal (mechanical) had a sample size of twelve "exposed" and four "control" tests, Racal lot B had a sample size of nine "exposed" and three "control" tests.

Due to the lid replacement, operating conditions of the kettle, and meteorological conditions, concentration measurements and subsequent asphalt loading varied from day to day. Concentration averages comparing "exposed" and "control" respirators are located in Table 5.4.

Table 5.4
Concentration Comparisons of "Exposed" and "Control" Respirators Loaded with Asphalt Contaminants

	Average Concentration (mg/m^3)	Range (mg/m^3)
"Exposed"	1.7 ± 1.6	0.1 to 7.3
"Control"	0.2 ± 0.1	0.0 to 0.2

According to the NIOSH method 500, the maximum air volume for sampling is 133 L at 15 mg/m^3. Sampling background contaminants for 360 minutes resulted in 720 L being collected exceeding the NIOSH recommended maximum volume; however, the mass collected, 0.14 mg, was far below the 2 mg allowed by the

method. In this study, sorbent backup tubes were not used in the sampling trains that would have captured the volatile fraction. The asphalt contaminant concentrations reported may have resulted in an underestimation of the true mass contacting the respirators.

Asphalt Results

The effects of the sampling protocol on respirator performance were evaluated by comparing "exposed" respirators to their "controls". This determined what effect, if any, resulted from placing a respirator upwind from the asphalt kettle for six hours, drawing through a high volume of air, and evaluating penetration four times with NaCl aerosol. Differences between "exposed" and "control" respirators reflect the effects of asphalt contaminant loading. Comparisons were made using an ANOVA specific to each respirator. These models were kept very simple with the dependent variable, percent penetration, remaining untransformed. "Minutes loaded" and "exposed/control" were the only independent variables added to the models along with their interaction term defining slope of the loading curve. It was assumed that all other terms describing field conditions were equal. A summary of the p values from the ANOVA tests by respirator type and penetration measurement are shown in Table 5.5. The null hypothesis, no difference between "exposed" and "control" respirators, was accepted when p values were greater than 0.05. Conversely, the alternate hypothesis, a difference exists between "exposed" and "control" respirators, was accepted when the p value was less than 0.05. Graphs of the data are shown in Appendix Graphs C.13 through C.26. Intercepts for all respirators were not significantly different. This leads to the conclusion that irrespective of the treatment given the respirators, penetration

measurements were not significantly different prior to loading ($p>0.05$). Slopes of CNC- and photometer-measured penetration for N95 respirators were significantly different for MSA Affinity Plus, Racal lot A, and Tecnol PFR95 respirators. The slopes for photometer-measured penetration were significantly different ($p<0.05$) for Racal (mechanical) and Racal lot B respirators.

Table 5.5
Respirators Loaded with Asphalt Contaminants
ANOVA Summary: p Values For Intercepts and Slopes of Loading Curves Comparing "Control" to "Exposed" Respirators

	CNC-measured		Photometer-measured	
Respirator Type	intercept	slope	intercept	slope
3M 2091 P100	0.9374	0.1483	0.6357	0.1405
MSA Affinity Plus	0.9570	0.0463*	0.6950	0.0041*
Pro-Tech F200 Filter	0.4315	0.7234	0.6466	0.0113*
Racal (mechanical)	0.8546	0.0642	0.8946	0.0004*
Racal Delta lot A	0.2863	0.0153*	0.2259	0.0004*
Racal Delta lot B	0.9890	0.0715	0.7070	0.0031*
Tecnol PFR95	0.6780	0.0067*	0.6454	0.0045*

*denotes a p value < 0.05
Testing dates 9/11/97 to 12/12/97
Number of replicate "exposed" samples: 3M 2091=6, MSA Affinity Plus=6, Pro-Tech F200=6, Racal (mechanical)=12, Racal lot A=6, Racal lot B=9, Tecnol PFR95=6
Number of replicate "control" samples: 3M 2091=2, MSA Affinity Plus=2, Pro-Tech F200=2, Racal (mechanical)=4, Racal lot A=2, Racal lot B=3, Tecnol PFR95=2

All N95 respirators had some differences between the "exposed" and "control" with duration of exposure as evident in Appendix Graphs C.13 through C.26. These differences were attributed to asphalt contaminant loading and not the protocol itself. Data from loading N95 respirators with asphalt were applied to the NaCl model to generate predicted penetration. Any differences between the predicted and observed values were attributed to the effects of asphalt loading and were not considered to be associated with the test protocol.

Differences in slopes for 3M 2091 respirators were not found to be significantly different with duration of exposure, even though the plot of these data indicated that penetration for the "exposed" respirators increased compared to the "controls". This P100 series filter has a much higher efficiency than the N95s and penetration was less likely to degrade from exposure to asphalt contaminants.

In order to answer the question, "Is there a difference between the collection efficiency of respirators containing electrostatic media and those containing mechanical filter media?" the slope of each electrostatic N95 respirator was compared to the mechanical N95 respirator using the Wald test. ANOVAs were constructed for both CNC- and photometer-measured penetration. Data used in these models were restricted to "exposed" respirators. The CNC model found both temperature and relative humidity for field conditions to be significant terms. Data for these variables were not collected nor were they relevant at zero loading when initial penetration measurements were recorded. Later these terms were removed since including them in the model deleted initial penetration data. All interaction terms found to be significant ($p < 0.05$) were included in these models. Refer to Appendix Tables B.15 and B.16. Respirator performance was defined by change in respirator penetration during loading or the slope of the loading curve. Coefficient from the ANOVA model for "mg asphalt" was added to the coefficient for the individual respirator from the "mg asphalt by respirator type" variable to derive individual slopes. The Z test statistic for the Wald test was computed by taking the difference between the slopes for the electrostatic respirator and the mechanical respirator and dividing by the pooled standard error. If the p value of the Z statistic was greater than

0.05, the null hypothesis was accepted and performance of the electrostatic respirator was determined to be comparable to the mechanical respirator. Conversely if the p value of the test was less than 0.05 then the alternate hypothesis was accepted and electrostatic respirator performances were determined to be significantly different from those of the mechanical respirator. ANOVA analyses are located in Appendix Tables B.17. and B.18.

The results of the Wald test found only one electrostatic respirator, Pro-Tech F200, to be significantly different ($p<0.05$) from the mechanical respirator for CNC-measured penetration. This was the only respirator to have a negative slope, penetration decreased with loading, suggesting that it had the best performance of all respirators tested. These findings suggest that the overall filtration efficiency of the electrostatic respirators was comparable to, or slightly better than, the mechanical respirator.

The predicted penetration values derived from the ANOVA models were plotted against mass loaded onto the respirators. Had the transformed penetration values been plotted, it would have been very difficult to visualize the differences between respirator performances. By plotting the backtransformed penetration values from the ANOVA models, the relationships identified by the models can easily be seen. Individual data points were too numerous to clearly identify these relationships. For ease of interpretation, the trend lines for each respirator type are presented in the remaining graphs in this chapter. Figure 5.13 depicts the backtransformed CNC-measured penetration with respect to respirator loading. Figure 5.14 depicts the same group of respirators loaded with asphalt contaminants and the backtransformed photometer-measured

penetration. The length of the lines depicting photometer-measured penetration corresponds to the maximum mass loaded on each respirator type.

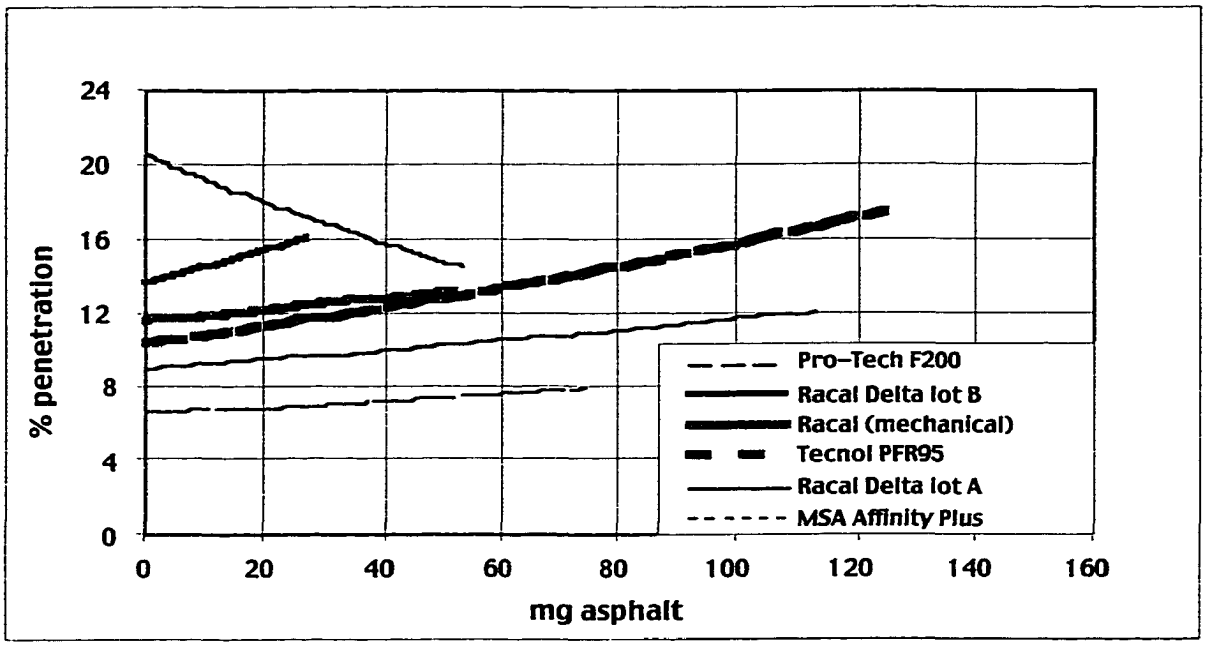

figure 5.13
CNC-Measured Penetration
N95 Respirators Loaded With Asphalt Contaminants
Fitted MMAD 4.5 ± 1.04 μm
Fitted GSD range 1.33 to 2.85
Number of replicate samples: MSA Affinity Plus=6, Pro-Tech F200=6, Racal (mechanical)=12, Racal lot A=6, Racal lot B=9, Tecnol PFR95=6

The results of the Wald test for photometer-measured penetration found two respirators, Racal lot A and Tecnol, to be the comparable to the Racal mechanical, all others were significantly different ($p<0.05$). A closer examination of these data revealed that the Wald approximation was not an accurate reflection of the graphed data for comparison of the mechanical respirator to the Racal lot A and the Tecnol. To correctly determine if these two electrostatic respirators were indeed different from the mechanical respirator, data were recoded and reanalyzed. The data from Racal lot A respirators were coded to

match the Racal mechanical respirators and inserted back into the ANOVA model. The sum of squares error from the new ANOVA model was averaged with the sum of squares error from the old ANOVA model and this value was divided by the mean square error of the original model to compute an F-ratio.

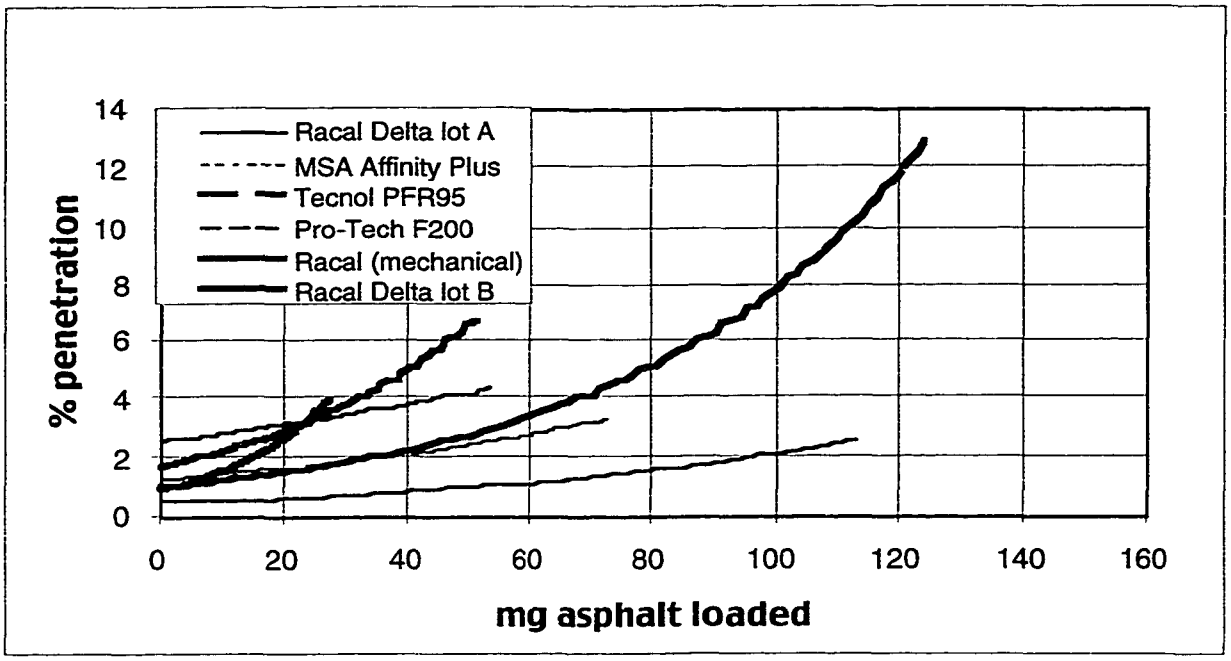

figure 5.14
Photometer-Measured Penetration
N95 Respirators Loaded With Asphalt Contaminants
Fitted MMAD: 4.5 ± 1.04 μm
Fitted GSD: range 1.33 to 2.85
Number of replicate samples: MSA Affinity Plus=6, Pro-Tech F200=6, Racal (mechanical)=12, Racal lot A=6, Racal lot B=9, Tecnol PFR95=6

The p values from the F test for the Racal lot A combined with the Racal mechanical was <0.0001. The p values from the F test for the Tecnol combined with the Racal mechanical was also <0.0001. These tests determined that all electrostatic respirators were different from the Racal mechanical. The Racal Delta lot B respirator had a steeper slope than the mechanical, all other electrostatic respirators had flatter slopes than the mechanical respirator.

These findings suggest that the electrostatic respirators had performances comparable to the mechanical when slope from the CNC-measured penetration was analyzed. However, when comparing the slopes from photometer-measured penetrations, the electrostatic respirators had improved performance when loaded with asphalt contaminants. Since this measure is more closely related to a 'dose' a respirator wearer may experience from exposure to asphalt contaminants, more importance would be placed on the photometer results as compared to the CNC results. Overall the electrostatic respirators had slightly improved filtration efficiency as compared to the mechanical respirator when loaded with asphalt contaminants. This conclusion refuted the hypothesis that the electrostatic charge on fibers in respirators containing electrostatic filter media would be masked or degraded by the volatile fraction or vapors in asphalt contaminants thereby decreasing their collection efficiency as compared to respirators containing mechanical filter media.

Referring to figure 5.14, once 50 to 70 mg of asphalt contaminants were loaded onto Racal (mechanical) and Tecnol PFR95 respirators, collection efficiency decreased below 95%. Extrapolating the slope for Racal lot B, the collection efficiency of this respirator would be expected to decrease below 95% when loaded with approximately 50 mg. These findings suggest that the N95 class of respirators may provide less protection than their rating when loaded with asphalt contaminants. Note that the data points for the Pro-Tech F200 filter reflected a maximum asphalt contaminant loading of about 25 mg, far less than the 60 to 120 mg loaded on the other respirators. The difference in loading was primarily attributed to the flow rate of 43 lpm for a filter compared to 85 lpm for

the filtering facepiece respirators. The configuration of the Pro-Tech F200 had the least filter area and highest face velocity of all respirators tested in this matrix.

Overall, the shapes of the asphalt loading curves were positive, increasing with loading, opposite from expected by the NIOSH method tests. The shape of the NaCl loading curve was negative with increased loading and was used for predicting respirator performance. Applying the asphalt field data to the simplified ANOVA models for N95 respirators from the NIOSH certification method generated predicted penetration values that were compared to the observed values using an F test. The results of this test found that the ANOVA model did not accurately predict the observed respirator penetration, $p<0.05$. Table 5.6 is a summary of the F test values and the corresponding p values for the N95 respirators.

Table 5.6
N95 Respirators Loaded with Asphalt Contaminants
F test Comparing Predicted to Observed Penetration Measurements

	CNC-Measured	Photometer-Measured
F test value	13.83	22.49
p value	<0.0001*	0.0000*

* denotes p value < 0.05

Plots of the predicted and observed penetration measurements can be found in Appendix Graphs C.27 through C.38. Predicted values underestimated true penetration of N95 respirators loaded with asphalt contaminants. Penetrations of N95 respirators loaded with asphalt contaminants were not accurately predicted by the NIOSH certification test method. The penetration characteristic of respirators loaded with asphalt contaminants tended to behave more like a liquid rather than a solid aerosol. Most droplets collected on a filter tend to increase

penetration with loading [21]. Asphalt fumes contain approximately 65 to 75% long chain alkanes which makes the aerosol very sticky with a wax-like consistency [140]. This characteristic is the possible cause for the fluid-like behavior on the respirators.

The global comparison in Table 5.6 included *both* electrostatic and mechanical respirators. In order to answer the question, 'Does the NIOSH certification method accurately predict penetration of respirators containing *electrostatic* filter media loaded with asphalt contaminants?', further refinement of the models was needed to make a statistical evaluation. N95 respirators in the asphalt comparison grouping were divided into two subsets, electrostatic and mechanical. ANOVA models for both the NIOSH method Sodium chloride loading and the sodium chloride penetration of respirators loaded with asphalt contaminants were recalculated using the same independent variables from the overall models. If the dependent variable, percent penetration, had been transformed in the original model, it retained its same unique transformation in the refined models. Once the NaCl NIOSH method models were recalculated, the reliability of these models to accurately predict penetration was again checked using the F test and graphs. The F test values from all tests were 1.00 with corresponding p values of 0.500. These results indicted that the NIOSH method models accurately predicted ($p>0.05$) NaCl penetration independently for N95 respirators containing either electrostatic or mechanical filter media. These findings were unchanged from the overall models combining respirator types. Coefficients generated in the refined ANOVA models for the NIOSH method NaCl loading tests varied slightly from the overall model. Applying the asphalt

field data to these coefficients resulted in slightly different predicted penetration values being generated. Predicted penetration measurements of respirators loaded with asphalt contaminants were compared to their observed values using an F test. The results of the F test, located in Table 5.7, indicates that penetration of respirators loaded with asphalt contaminants is not accurately predicted by the NIOSH method NaCl loading tests for either N95 electrostatic or N95 mechanical respirators. Results from refining the respirator groupings to distinguish between respirators with electrostatic and mechanical filter media remained unchanged from the overall tests where these two respirator types were grouped. The NIOSH method did not accurately predict penetration of N95 respirators loaded with asphalt contaminants regardless of the type of filter media, electrostatic or mechanical.

Table 5.7
Electrostatic and Mechanical N95 Respirators Loaded with Asphalt Contaminants
F test Comparing Predicted to Observed Penetration Measurements

Penetration Measurements	F test	p value
electrostatic respirators: CNC-measured	17.72	<0.0001*
mechanical respirator: CNC-measured	21.09	<0.0001*
electrostatic respirators: photometer-measured	36.49	0.0000*
mechanical respirators: photometer-measured	16.73	<0.0001*

* denotes p value < 0.05

Penetration of 3M 2091 respirators loaded with workplace contaminants was determined using NaCl aerosol. The CNC-measured penetration model to predict penetration was constructed using DOP aerosol. Differences between penetration of a P100 respirator with two different aerosols might create uncertainties in comparing respirator performance. DOP would be expected to

have slightly higher penetration through a HEPA filter than a solid particulate [157, 113] as this liquid aerosol is highly degrading [35] with loading. Other research [78] has indicated that initial NaCl and DOP penetration of HEPA quality filters may be comparable. P100 series respirators were equivalent to HEPA quality. Initial NaCl penetration, CNC-measured, for all 3M 2091 filters used for this study (N=26) was 0.002% compared to DOP penetration of less than 0.00002% (N=6). Sodium chloride had greater penetration than DOP by two orders of magnitude, clearly opposite from what would have been expected. The other P100 series cartridges, 3M 7093 and Pro-Tech G108, tested with DOP loading had initial CNC-measured penetrations that were in agreement with each other and had an order of magnitude greater penetration than 3M 2091. Initial photometer-measured penetration for 3M 7093 and the Pro-Tech G108 was compared to their initial CNC-measured penetration. This comparison found that the average photometer-measured penetration was 1.5 times the CNC-measured penetration. This same comparison for the 3M 2091 respirator found the average photometer-measured penetration to be 25 times the CNC penetration. An order of magnitude discrepancy cast considerable doubt on the reliability of the CNC-measured penetration data for 3M 2091. Any comparisons using these data to generate predicted penetration values for comparison with observed CNC-measured penetration of aerosols other than DOP were suspect and the validity of these analyses were questionable. No obvious cause for the disparity in CNC-measured penetration with DOP for the 3M 2091 filter, and not the other P100 cartridges, could be identified since the order of respirator testing was randomly determined. It was possible that use of the diluter, or the DOP

concentration used to calibrate the diluter, in measuring upstream concentration with the CNC may have played a role. The unreliable model for CNC-measured penetration values precluded the comparison of the predicted penetration to observed penetration of 3M 2091 filters loaded with workplace contaminants.

Aluminum Oxide

Aluminum oxide dust was the only solid workplace aerosol loaded onto respirators in this study. This test matrix evaluated a total of four different N95 respirators/filter and one P100 filter. Only one respirator, Racal (mechanical), did not contain electrostatic filter media. Five replicate tests for each respirator type were conducted.

The integrity of the face seal for filtering facepiece respirators and the placement of filters in the respirator receptacle for N95 respirators were performed using the 3M LPQFT method the morning of the test. A summary of initial fit by respirator type can be found in Appendix Table B.19. Collectively, initial penetration of N95 respirators averaged 0.1%. Face seal leakage for 3M 8210 averaged 0.275%, which was slightly higher when compared to the NaCl loading tests. Respirators and filters were considered adequately sealed to their holders prior to loading.

Air temperature and relative humidity were allowed to fluctuate with ambient room conditions. In the mornings, air temperature was coolest and relative humidity was highest. As the day progressed, air temperature usually warmed and relative humidity declined. Temperature averaged 24±1.5^{o}C, with a range of 13 to 26 ^{o}C. Relative humidity averaged 24±3.1% with a range of 20 to 38%.

Concentration was independently recorded six times during each test, once for every 60 minutes of loading. The concentration of aluminum oxide for all tests averaged 9.6±1.9 mg/m^3, range 4.4 to 18.5 mg/m^3. Overall, the concentration was relatively stable at respirator flow rates of 85 lpm, but tended to be a little higher at the lower respirator flow rate of 43 lpm with the standard deviation being slightly broader. At the lower flow rate, more of the aluminum oxide dust had to be exhausted to the dump to maintain the target concentration of 10 mg/m^3. Also, since airflow through the duct was laminar, greater fluctuations in concentration readings occurred. Refer to Appendix Table B.20 for concentration averages by respirator flow rates.

Size Distribution

The size distribution of the aerosol was recorded three times during each test using the Climet and represented the aerosol loaded for each 2-hour interval. Size distributions were recorded at the beginning of the test, at the start of the fourth hour of loading, and during the last 30 minutes of the test. The size distribution of the aerosol tended to be correlated with concentration readings. As concentration was reduced, the CMD and the GSD decreased. At the higher concentrations, agglomerates were more likely to form increasing particle diameter. For all tests, the average CMD was 1.36 μm, average MMD was 2.05, with the GSD ranging from 1.38 to 1.61. The size distribution for aluminum oxide by respirator flow rate can be found in Appendix Table B.21. An example of the aluminum oxide dust size distribution from 6/11/98 is represented in figure 5.15. Figure 5.15 depicts the overall stable nature of the aerosol size distribution of aluminum oxide dust for most tests.

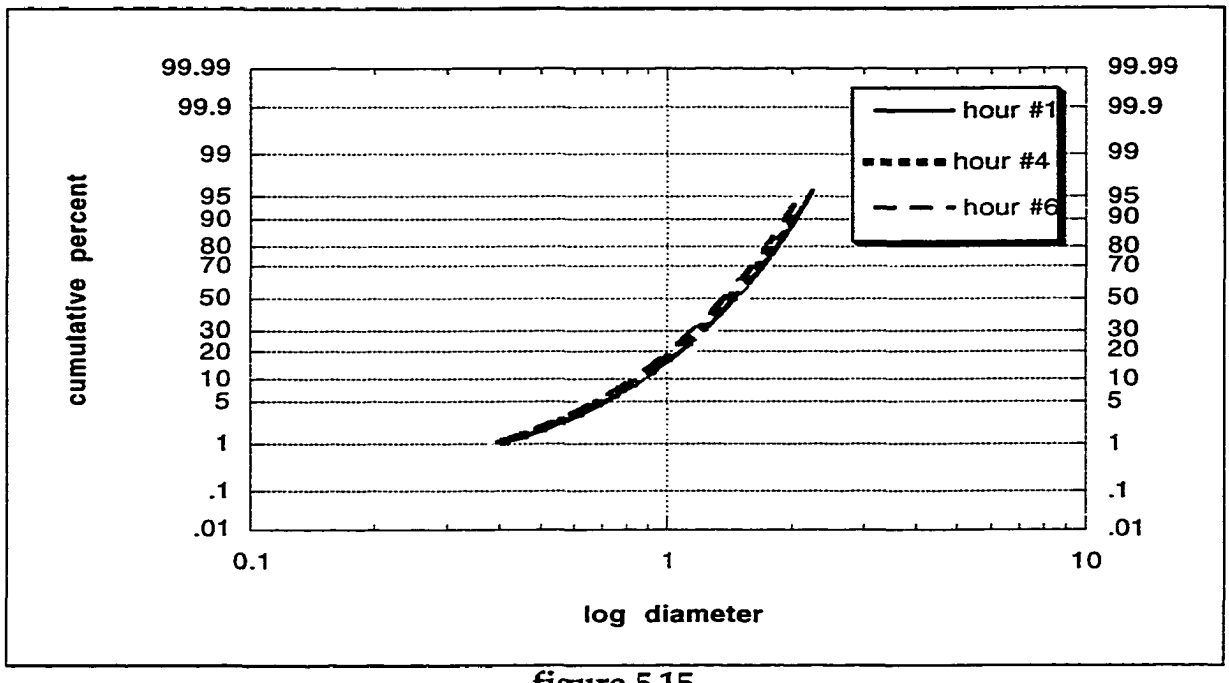

figure 5.15
Aluminum Oxide Dust Particle Size Distribution
a) Test date 6/11/98, size distribution recorded with Climet
b)

	hour #1	hour #4	hour #6
CMD	1.40 µm	1.36 µm	1.44 µm
GSD	1.39	1.40	1.41

Aluminum Oxide Results

In order to answer the question, "Is there a difference between the collection efficiency of respirators containing electrostatic media and those containing mechanical filter media?" the slope of each electrostatic N95 respirator was compared to the mechanical N95 respirator using the Wald test. ANOVA models were constructed for N95 respirators loaded with aluminum oxide dust and contained all terms and interactions found to be significant ($p < 0.05$). These models are located in Appendix Tables B.22 and B.23. Slopes of the penetration curves for each respirator were computed by adding the coefficient from "mg Al_2O_3" to the coefficient for the individual respirator from the interaction term "mg Al_2O_3 by respirator type". The difference between the

slopes for the electrostatic respirator and the mechanical was divided by their pooled standard error to obtain the Z test value. If the p value of the Z test statistic was greater than 0.05, the null hypothesis was accepted and performance of the electrostatic respirator was determined to be comparable to the mechanical respirator. Conversely if the p value of the test was less than 0.05 the alternate hypothesis was accepted and electrostatic respirator performance was determined to be significantly different from the mechanical respirator. These analyses are located in Appendix Tables B.24 and B.25. Figure 5.16 depicts the trend lines of the backtransformed CNC-measured penetration with respect to respirator loading.

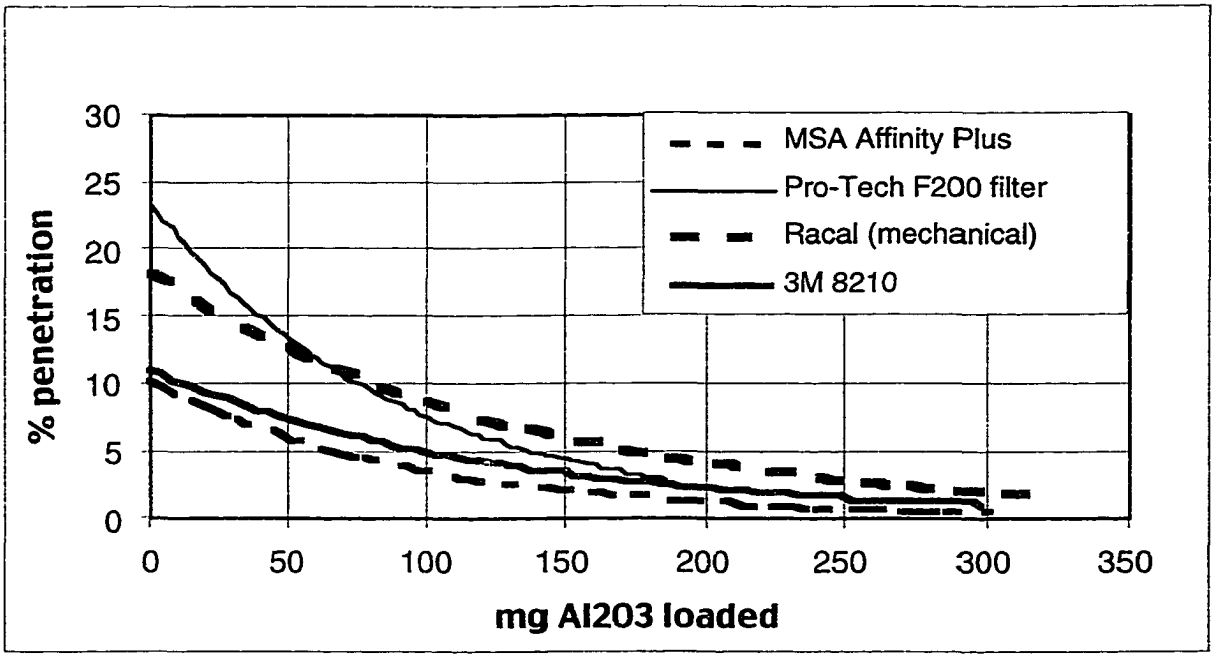

figure 5.16
CNC-Measured Penetration
N95 Respirators Loaded With Aluminum Oxide Dust
CMD: 1.4 ± 0.11 μm; MMD: 1.19 ± 0.11 μm
GSD: range 1.45 to 3.56
Number of replicates tested=5

Performance of all N95 respirators increased with loading. The slope of the mechanical respirator was the shallowest indicating that performance was changed the least with loading.

Results of the Wald test found MSA Affinity Plus and Pro-Tech F200 to be significantly different ($p<0.05$) from Racal (mechanical) respirator. As loading of these respirators increased, penetration of the Pro-Tech F200 decreased at a more rapid rate than the mechanical respirator, an indication of better performance. A closer examination of the data suggested that the Wald approximation may not have accurately reflected the difference between the graphed data for MSA Affinity Plus and Racal mechanical respirator. To correctly determine if this electrostatic respirator was indeed different from the mechanical respirator, data were recoded and reanalyzed. The data from MSA Affinity Plus respirators were coded to match the Racal mechanical respirators and inserted back into the ANOVA model. The sum of squares error from the new ANOVA model was averaged with the sum of squares error from the old ANOVA model and this value and divided by the mean square error of the original model to compute an F-ratio. The p values from the F test for the MSA Affinity Plus combined with the Racal mechanical was <0.0001. This test confirmed that there was a real difference between these two respirators. Penetration of all respirators decreased with loading; the Pro-Tech F200 filter decreased the quickest suggesting that this respirator had the best performance. The Racal mechanical respirator had the next best performance with loading. Overall, the electrostatic respirators performed comparably to the mechanical respirator when loaded with aluminum oxide dust as measured by the CNC. Figure 5.17 depicts the same group of respirators loaded with aluminum oxide dust and the backtransformed

photometer-measured penetration. All N95 respirators had increased performance with aluminum oxide dust loading, as determined by photometer-measured penetration. Results of the Wald test found Pro-Tech F200 and MSA Affinity Plus to be significantly different from the mechanical respirator. The 3M 8210 respirator was comparable to the mechanical respirator. As loading increased, penetration of the Pro-Tech F200 filter decreased the quickest. A closer examination of the data suggested that the Wald approximation may not have accurately reflected the difference between the Racal mechanical respirator and the MSA Affinity Plus respirator.

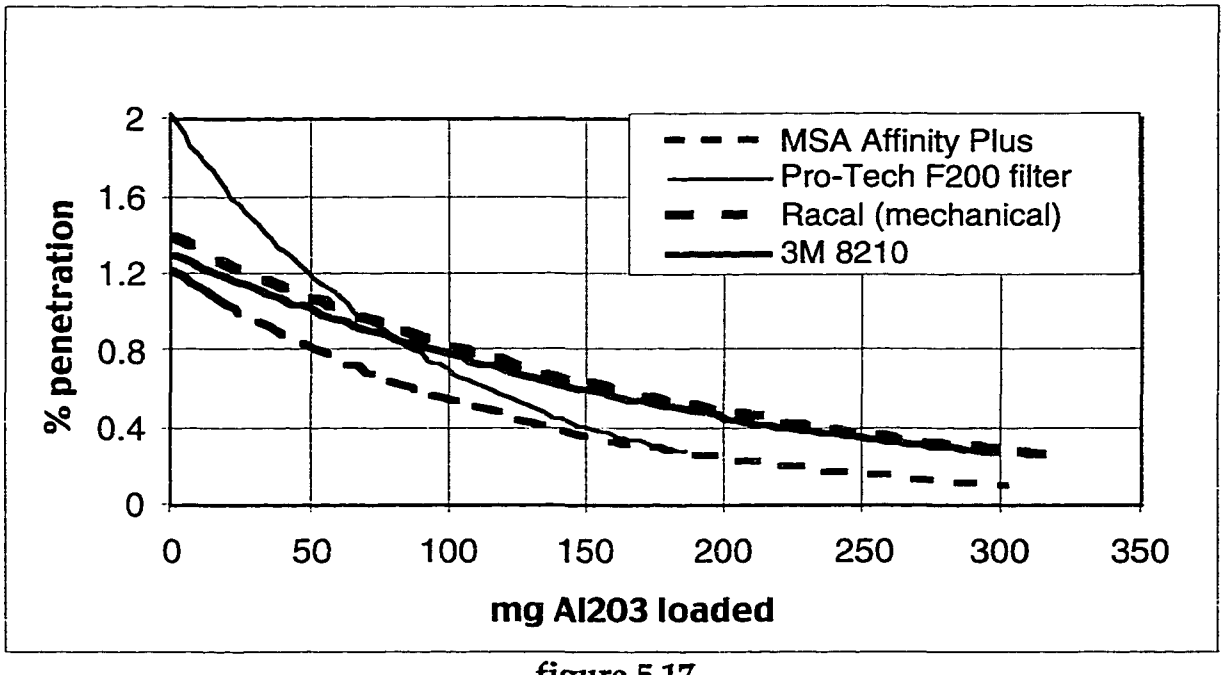

figure 5.17
Photometer-Measured Penetration
N95 Respirators Loaded With Aluminum Oxide Dust
CMD: 1.4 ± 0.11 μm; MMD: average 1.19 ± 0.11 μm
GSD: range 1.45 to 3.56
Number of replicates tested=5

To correctly determine if there was a real difference between the MSA Affinity respirator and the mechanical respirator, data were recoded and reanalyzed. The p values from the F test for the MSA Affinity Plus combined with the Racal mechanical was <0.0001. This test confirmed that there was a significant difference between these two respirators. Initial penetration of the Pro-Tech F200 was the highest and significantly different from the mechanical respirator. Plots of the remaining electrostatic respirators appeared to be comparable to the mechanical respirator. Both the Wald approximation and the F test indicated that a difference exists between the MSA Affinity Plus and the Racal mechanical respirator. The performance of electrostatic respirators loaded with aluminum oxide dust was comparable or slightly improved compared to the mechanical as determined by photometer-measured penetration.

Overall, performances of electrostatic respirators were comparable to the mechanical respirator for this test scenario. Only the Pro-Tech F200 filters had significantly improved performance compared to the mechanical respirator; penetration of this respirator decreased the fastest with loading. The surface area of this respirator was 57 cm^2 and when used in pairs the total surface area increased to 114 cm^2. It is possible that the Pro-Tech F200 with smaller filtration area clogs more rapidly. The filtering facepiece respirators used in this study had an average surface area of about 200 cm^2. The overall shapes of the CNC- and photometer-measured penetration curves of N95 respirators loaded with aluminum oxide dust agreed with the NIOSH method tests; respirator efficiency improved with loading. Coefficients generated with the NaCl ANOVA models for aluminum oxide dust and metal cutting fluid mist were applied to data from

N95 respirator loading with aluminum oxide to generate predicted penetration values. Predicted penetration was compared to measured penetration with a global F test; the results are presented in Table 5.8. The p values from these analyses were less than 0.0001 indicating that NaCl penetration of N95 respirators loaded with aluminum oxide dust was not accurately predicted by the NIOSH method certification tests.

Table 5.8
N95 Respirators Loaded with Aluminum Oxide Dust
F test Comparing Predicted to Observed Penetration Measurements

	CNC-Measured	Photometer-Measured
F test value	38.66	10.29
p value	<0.0001*	0.0000*

* denotes p value < 0.05

Graphs comparing predicted penetration and measured penetration for each respirator tested can be found in Appendix Graphs C. 39 to C.46. Over the first 200 mg of aluminum oxide loading, predicted penetrations, both CNC- and photometer-measured, were less than observed values. Beyond 200 mg, predicted respirator penetration measurements varied uniquely with the respirator type and the instrument used to measure penetration. These findings were different from expected. Penetration of N95 respirators loaded with aluminum oxide dust, a solid particulate, was expected to be predicted by the NIOSH method certification test since the preamble of 42 CFR 84 claimed particle diameter to be independent of maximum penetration. The NIOSH method tests did not accurately predict penetration of N95 respirators loaded with aluminum oxide. The predicted penetration would have been expected to be higher than the observed measurements, indicating that the NIOSH method tests were a more

stringent indicator of respirator performance. The results of these tests indicated that predicted penetration was *lower* than the observed values, underestimating true penetration. These findings indicated that particle size and particle density might have a more significant role in the loading mechanisms and resulting respirator penetration than assumed by NIOSH.

The global comparison in Table 5.8 included *both* electrostatic and mechanical respirators. In order to answer the question, 'Does the NIOSH certification method accurately predict penetration of respirators containing *electrostatic* filter media loaded with aluminum oxide dust?', further refinement of the models was needed to make a statistical evaluation. N95 respirators in the aluminum oxide dust grouping were divided into two subsets, electrostatic and mechanical. ANOVA models for both the NIOSH method NaCl loading and the NaCl penetration of respirators loaded with aluminum oxide dust were recalculated using the same independent variables from the overall models. If the dependent variable, percent penetration, had been transformed in the original model, it retained its same unique transformation in the refined models. Once the NaCl NIOSH method models were recalculated, the reliability of these models to accurately predict penetration was again checked using the F test and graphs. All F test values were 1.00 with corresponding p values of 0.500. These results indicted that the NIOSH method models accurately predicted ($p<0.05$) NaCl penetration independently for N95 respirators containing either electrostatic or mechanical filter media. These findings were unchanged from the overall models combining respirator types. Coefficients generated in the refined ANOVA models for the NIOSH method NaCl loading tests varied slightly from the overall model. Applying data from the aluminum oxide dust tests to these

coefficients resulted in slightly different predicted penetration values. Table 5.9 contains the results of the F tests comparing predicted penetration measurements of respirators loaded with aluminum oxide dust to their observed values.

Table 5.9
Electrostatic and Mechanical N95 Respirators Loaded with Aluminum Oxide Dust
F test Comparing Predicted to Observed Penetration Measurements

Penetration Measurements	F test	p value
electrostatic respirators: CNC-measured	37.06	<0.0001*
mechanical respirator: CNC-measured	126.73	<0.0001*
electrostatic respirators: photometer-measured	12.78	<0.0001*
mechanical respirators: photometer-measured	24.18	<0.0001*

* denotes p value < 0.05

All p values from the F tests in Table 5.9 were less than 0.0001 and the alternate hypothesis was accepted. These analyses determined that real differences existed between observed and predicted penetration as measured by both CNC and photometer. These results support the findings that respirator penetration was not accurately predicted by the NIOSH NaCl loading test method for either N95 electrostatic or the N95 mechanical respirators loaded with aluminum oxide dust. Results from refining the respirator groupings to distinguish between respirators with electrostatic and mechanical filter media remained unchanged from the overall tests where these two respirator types were grouped.

Laboratory-Generated Metal Cutting Fluid Mist

A mist of metal cutting fluid was generated through a spray nozzle using compressed air to nebulize the cutting fluid. The spray generated in a large cylindrical tube was divided between the respirator loading chamber and the

exhaust to the exterior of the building. Penetration of the respirators with NaCl was evaluated in the separate test apparatus after each 2-hour loading interval with metal cutting fluid mist. This test matrix evaluated a total of four different N95 respirators/filter and one P100 filter. Only one respirator, Racal (mechanical), did not contain electrostatic filter media. Five replicates of each respirator type were used for these tests.

Integrity of the face seal was evaluated with latex spheres the morning of the test using the 3M LPQFT method. A summary of N95 respirator penetration is listed in Appendix Table B.26. Overall, initial penetration averaged 0.07% with 3M 8210 again having the highest leak rate of 0.13%. Face seal leakage for these respirators was comparable to the NaCl loading tests. Respirators and filters were considered to be securely fastened to their holders prior to loading with metal cutting fluid mist.

Air temperature and relative humidity were allowed to fluctuate with ambient room conditions. In the mornings, temperature was coolest and relative humidity was highest. As the day progressed, air temperature usually warmed and relative humidity declined. Temperature averaged $24 \pm 1.3^{o}C$, range 20 ^{o}C to 26 ^{o}C. Relative humidity averaged $45 \pm 4.0\%$ with a range of 35% to 55%.

Sampling for measuring aerosol concentration was done at the upstream probe at a flow rate of 10 lpm. The target concentration for respirator loading was 1.0 mg/m^3. The actual concentration of metal cutting fluid mist for all tests averaged 1.7 ± 0.44 mg/m^3, range 0.7 to 3.4 mg/m^3. The average concentration was comparable at both respirator flow rates; however, the standard deviation was a little broader at the lower flow rates. At the lower flow rates, a stable

concentration was more difficult to maintain. This variability may have been attributed to the laminar flow at the lower respirator flow rate. Refer to Appendix Table B.27 for concentration averages by respirator flow rates.

Size Distribution

The size distribution of the aerosol was recorded three times during each test using the Climet and represented the aerosol loaded for each two hour interval. Count size distribution was recorded at the beginning of the test, at the start of the fourth hour of loading, and during the last 30 minutes of the test. The CMD and GSD of the aerosol tended to increase as concentration readings increased. For all tests, the average CMD was 1.00 μm, average MMD 1.54 with the GSD ranging from 1.40 to 1.47. The size distribution of metal cutting fluid mist by respirator flow rate can be found in Appendix Table B.28. An example of the size distribution for metal cutting fluid mist is presented in figure 5.18.

Laboratory-Generated Metal Cutting Fluid Mist Results

In order to answer the question, "Is there a difference between the collection efficiency of respirators containing electrostatic media and those containing mechanical filter media?" the slope of each electrostatic N95 respirator was compared to the mechanical N95 respirator using the Wald test. ANOVA models constructed for N95 respirators loaded with metal cutting fluid mist contained all terms and interactions found to be significant ($p < 0.05$). Field temperature during respirator loading was found to be a significant term in both the CNC- and photometer-penetration models but was not included. Prior to loading with metal cutting fluid, initial respirator penetration measurements were measured by challenge with NaCl aerosol.

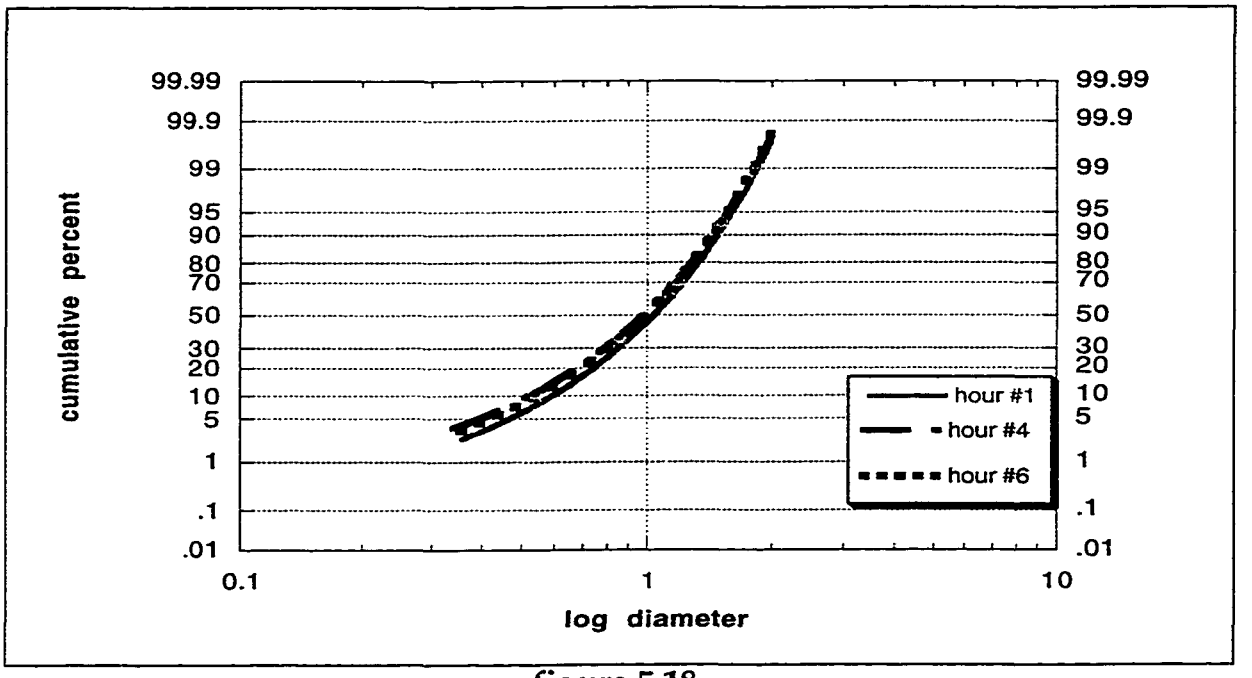

figure 5.18
Particle Size Distribution
Laboratory-Generated Metal Cutting Fluid Mist
a) Test date 7/23/98, respirator flow rate 85 lpm
b) size distribution recorded with Climet
c)

	hour #1	hour #4	hour #6
CMD	1.02 µm	0.96 µm	0.97µm
GSD	1.42	1.45	1.44

Field temperature in the metal cutting fluid mist loading chamber was unrelated to initial penetration measurements and was not recorded.

Since data were missing for this variable, if this term had been including this term in the model it would have resulted in the initial penetration predicted values being removed. These models are located in Appendix Tables B.29 and B.30. Slopes of the penetration curves for each respirator were computed by adding the coefficient from "mg metal cutting fluid" to the coefficient for the individual respirator from the interaction term "mg metal cutting fluid by respirator type". The difference between the slopes for the electrostatic respirator and the mechanical respirators was divided by their pooled standard error to

obtain a Z test value. If the p value of the Z test statistic was greater than 0.05, the null hypothesis was accepted and performances of electrostatic respirators were determined to be comparable to the mechanical respirator. Conversely if the p value of the test was less than 0.05 the alternate hypothesis was accepted and electrostatic respirator performances were determined to be significantly different from the mechanical respirator. These analyses are presented in Appendix Tables B.31. and B.32. Figure 5.19 depicts the trend for backtransformed CNC-measured penetration with respect to respirator loading. The CNC-measured penetration curves decreased with increasing loading for all respirators.

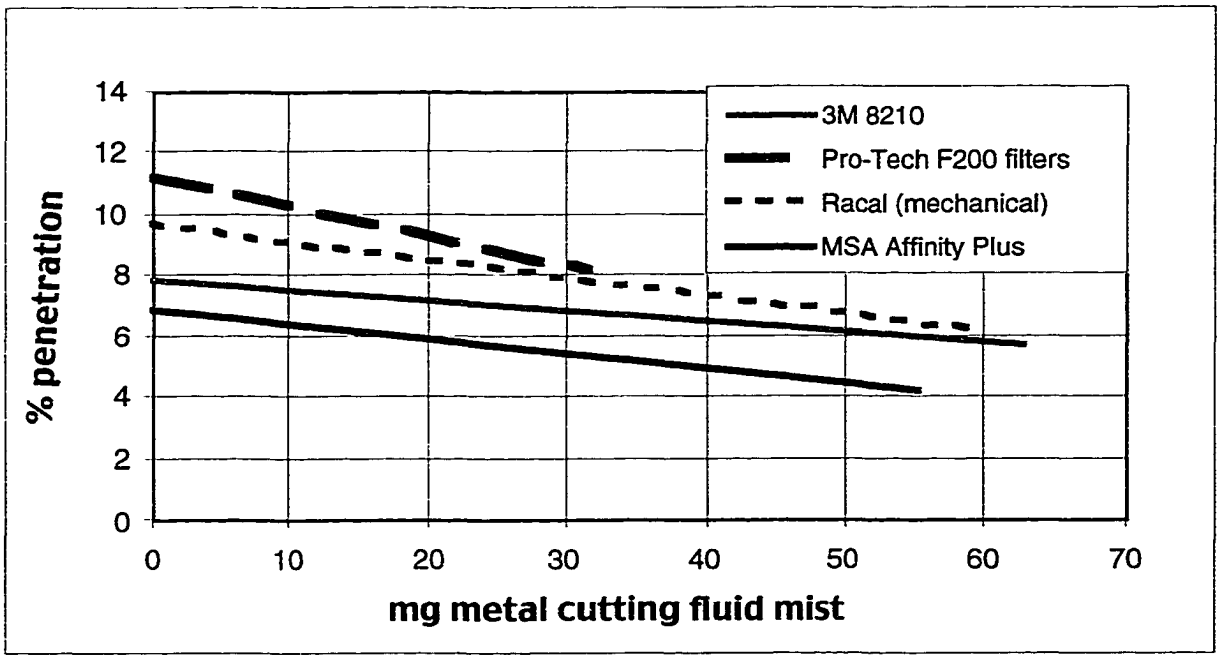

figure 5.19
CNC-Measured Penetration
N95 Respirators Loaded With Laboratory-Generated Metal Cutting Fluid Mist
CMD: 1.0 ± 0.05 μm; MMD: 0.45 ± 0.04 μm
GSD: range 1.40 to 1.49
Number of replicates tested= 5 for each respirator type

Results of the Wald test found that slopes for all electrostatic respirators were comparable to the Racal (mechanical) respirator ($p>0.05$); none were found to be significantly different. As loading increased, slope of the penetration curve decreased the quickest for the Pro-Tech F200 filter, similar to the results of aluminum oxide dust loading.

Figure 5.20 depicts the same group of respirators loaded with metal cutting fluid mist in the laboratory and the trend for backtransformed photometer-measured penetration. Overall photometer-measured penetration curves increased with metal cutting fluid mist loading, opposite of the CNC-measured penetration curves.

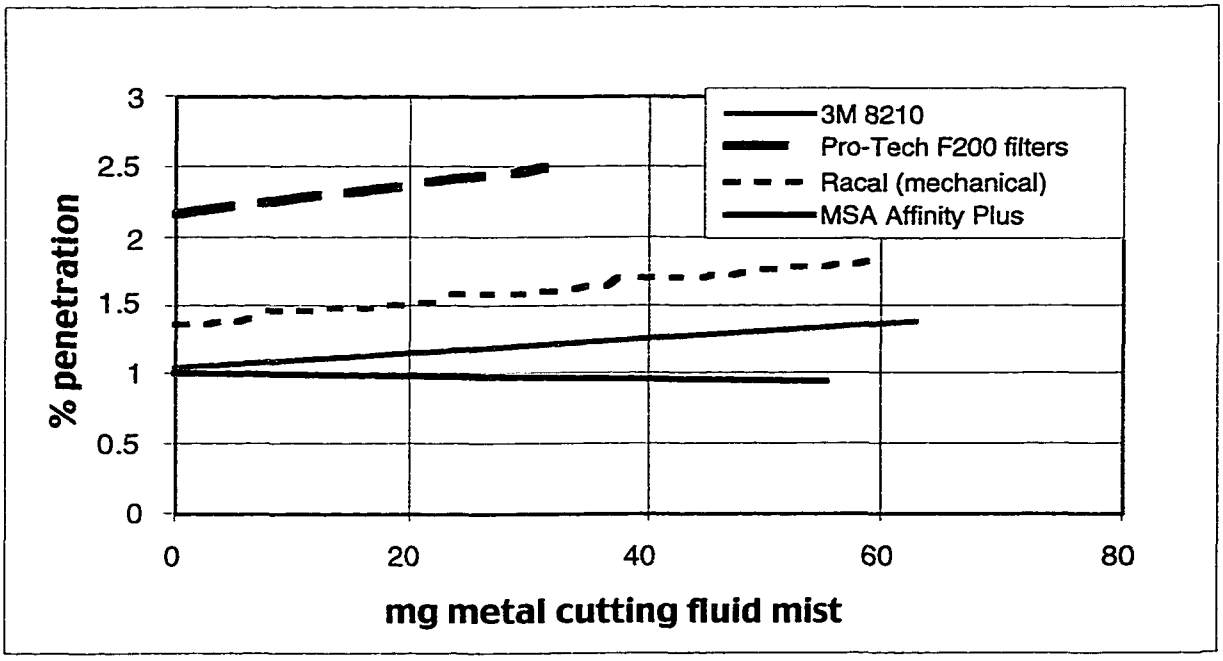

figure 5.20
Photometer-Measured Penetration
N95 Respirators Loaded With Laboratory-Generated Metal Cutting Fluid Mist
CMD: 1.0 ±0.05 µm; MMD: 0.45 ± 0.04 µm
GSD: range 1.40 to 1.49
Number of replicates tested= 5 for each respirator type

The results of the Wald test determined that the performances of all electrostatic respirators were comparable to the Racal (mechanical) respirator ($p>0.05$). A closer examination of these data suggested that the Wald approximation may not have been an accurate reflection of the difference between the Racal mechanical and the MSA Affinity Plus respirator. The slope for MSA Affinity appeared to be decreasing with loading, opposite from all other respirators whose penetration increased with loading. To correctly determine if there was a real difference between the MSA Affinity Plus and Racal mechanical respirator, data were recoded and reanalyzed. The data from these two respirators were matched and inserted back into the ANOVA model. The sum of squares error from the new ANOVA model was averaged with the sum of squares error from the old ANOVA model, this value and divided by the mean square error of the original model to compute an F-ratio. The p values from the F test for the MSA Affinity Plus combined with the Racal mechanical was <0.001 indicating that a real difference existed between the these two respirators. The slope for MSA Affinity Plus was negative with loading suggesting that the performance of this respirator improved with loading.

For this testing scenario, electrostatic respirators were found to be comparable to the mechanical respirator loaded with metal cutting fluid mist. Only the MSA Affinity Plus was significantly better than the mechanical respirator with loading for photometer-measured penetration. The Pro-Tech F200 filter had the highest initial penetration measurements of all respirators tested in this matrix. This difference was significant for the photometer-measured penetration.

The shape of the CNC-measured penetration curve decreased with metal cutting fluid mist loading as would be predicted by the NIOSH method tests with NaCl. The penetration curve for photometer-measured penetration increased with loading, opposite from that predicted by the NIOSH method tests. Coefficients from the simplified NaCl ANOVA models were applied to metal cutting fluid data to generate predicted penetration values of N95 respirators. Predicted penetration was compared to measured penetration globally with an F test, see Table 5.10.

Table 5.10
N95 Respirators Loaded with Laboratory-Generated Metal Cutting Fluid Mist
F test Comparing Predicted to Observed Penetration Measurements

Penetration Measurements	F test	p value
CNC-measured penetration	14.50	<0.0001*
photometer-measured penetration	3.90	<0.0001*

* denotes p value < 0.05

These analyses had p values less than 0.0001 indicating NaCl penetration of the N95 respirator loaded with metal cutting fluid is not accurately predicted ($p<0.05$) by the NIOSH method certification tests. Graphs comparing predicted penetration to measured penetration for each N95 respirator tested can be found in Appendix Graphs C.47 through C.54. Measured penetration was higher than the predicted values for all N95 respirators. Graphs and the global F test indicate that penetration of respirators loaded with approximately 60 mg of laboratory-generated metal cutting fluid mist was not accurately predicted by the NIOSH method tests, penetration was underestimated.

The global comparison in Table 5.10 included *both* electrostatic and mechanical respirators. In order to answer the question, 'Does the NIOSH

certification method accurately predict penetration of respirators containing *electrostatic* filter media loaded with metal cutting fluid mist?', further refinement to the models was needed to make this statistical evaluation. N95 respirators in the metal cutting fluid mist grouping were divided into two subsets, electrostatic and mechanical. ANOVA models for both the NIOSH method sodium chloride loading and the sodium chloride penetration of respirators loaded with metal cutting fluid mist were recalculated using the same independent variables from the overall models. If the dependent variable, percent penetration, had been transformed in the original model, it retained its same unique transformation in the refined models. Once the NaCl NIOSH method models were recalculated, the reliability of these models to accurately predict penetration was again checked using the F test and graphs. All F test values were 1.00 with corresponding p values of 0.500. These results indicted that the NIOSH method models accurately predicted NaCl penetration independently for N95 respirators containing either electrostatic or mechanical filter media, $p>0.05$. These findings were unchanged from the overall models that combined respirator types. Coefficients generated from the refined ANOVA models using the NIOSH method NaCl loading tests varied slightly from the overall model combining respirator types. Applying data from the metal cutting fluid mist tests to these coefficients resulted in slightly different predicted penetration values being computed. Predicted penetration measurements of respirators loaded with metal cutting fluid mist were compared to their observed values using an F test, see Table 5.11. The p values generated from the F tests were less than 0.0001 indicating that there was a real difference between observed and predicted penetration values. Table 5.11 indicated that penetration of respirators loaded with metal cutting fluid, using the refined

models to distinguish between electrostatic and mechanical respirators, could not be predicted and remained unchanged from the overall model. The NIOSH method did not accurately predict penetration of N95 respirators loaded with laboratory-generated metal cutting fluid mist regardless of the type of filter media, electrostatic or mechanical.

Table 5.11
Electrostatic and Mechanical N95 Respirators Loaded with Laboratory-Generated Metal Cutting Fluid Mist
F test Comparing Predicted to Observed Penetration Measurements

Penetration Measurements	F test	p value
electrostatic respirators: CNC-measured	17.16	<0.0001*
mechanical respirator: CNC-measured	35.71	<0.0001*
electrostatic respirators: photometer-measured	4.14	<0.0001*
mechanical respirators: photometer-measured	8.76	<0.0001*

* denotes p value < 0.05

Field-Generated Metal Cutting Fluid Mist

Metal cutting fluid mist was loaded onto respirators generated at a lathe turning operation in a machine shop. Testing began on August 8, 1998 and ended August 25, 1998. This test matrix evaluated a total of four different N95 respirators/filter and one P100 filter. Only one respirator, Racal (mechanical), did not contain electrostatic filter media. All respirators had six replicate tests for "exposed" and two for "control".

Evaluation of face seal for filtering facepiece respirators and placement of filters in respirator receptacles were performed using the 3M LPQFT method the night before the loading tests. Respirators were stored overnight in clean plastic bags at room temperature. Initial penetration averaged 0.06 % and a summary by respirator type can be found in Appendix Table B.33. Again, 3M had the highest

initial penetration of 0.14%. Respirators were considered to be adequately sealed to their holders.

An enclosure around the lathe was constructed to contain aerosols generated by the lathe turning operation. "Exposed" respirators were located inside the enclosure about two feet from the stainless steel rod being turned. A Kool Mist generator created a mist of cutting fluid. The lathe and misting system were allowed to operate for a few minutes before the carbon vane pump supplying suction to the respirators was turned on. After every two hours of loading, the lathe and misting system were turned off and respirators were returned to the laboratory for challenge with NaCl. The "control" respirator was located outside the lathe enclosure in the same machine shop against the wall opposing the enclosure. Distance between the lathe enclosure and the control respirator was approximately 10 feet.

The machine shop did not have an air conditioning system. Doors leading to adjacent rooms remained open and air supplied to these areas by their local air conditioning systems cooled the warm air temperature in the machine shop. Temperature and relative humidity of the ambient air were recorded with a chilled mirror hygrometer. Ambient conditions were recorded at the "control" respirator location. The average temperature was 24±2.2 ^{o}C, range 13 to 28 ^{o}C. Relative humidity averaged 26±2.9%, range 21% to 52 %.

Aerosol Concentration

The sampling train with closed face filter cassettes determined concentration of contaminants generated inside the lathe enclosure. The filter cassettes for monitoring concentration around "exposed" respirators were

changed after each two hours of loading thereby capturing the fluctuation in aerosol concentration throughout the day. Cassettes for "control" respirators collected samples for the entire 6-hour duration. Concentration averages comparing "exposed" and "control" respirators are located in Table 5.12.

Table 5.12
Concentration Comparisons of "Exposed" and "Control" Respirators Loaded with Metal Cutting Fluid Mist-Field

	Average Concentration (mg/m^3)	Range (mg/m^3)
"Exposed"	37.2 ± 15.0	5.4 to 76.7
"Control"	0.6 ±0.3	0.3 to 1.2

According to NIOSH method 500, the maximum air volume for sampling is 133 L at 15 mg/m^3. Sampling background contaminants for 360 minutes resulted in 720 L being collected exceeding NIOSH's recommended maximum volume; however, the mass collected, 0.86 mg, was far below the 2 mg allowed by the method. These concentration measurements were used to compute the amount of metal cutting fluid mist loaded onto the respirators. Respirators with flow rates of 85 lpm were loaded with a maximum of 1800 mg cutting fluid, respirators with flow rates of 43 lpm were loaded with about 650 mg metal cutting fluid. The concentration of metal cutting fluid mist averaged 43 mg/m^3 for this study. The ACGIH exposure limit for metal cutting fluid mist is 5 mg/m^3. The hazard ratio, the concentration of a contaminant divided by its exposure limit, was about seven. The maximum allowable hazard ratio of 10 for a half-face N series respirator selection was approached in this study [158].

Size Distribution

Flow rates through the respirators and the cascade impactor were established using a sharp edge orifice and calibrated magnehelic gauges. The Andersen Cascade Impactor was used to measure the size distribution of the metal cutting fluid mist. It was intended that the cascade impactor operate over the entire duration of the respirator loading to describe the aerosol being loaded onto the respirators. Due to the high contaminant concentration, the backup filter on the cascade impactor clogged and restricted airflow after 10 to 40 minutes of sampling. In order to obtain representative particle size distribution, the backup filter was replaced and sampling continued. Weights from the back-up filters were accumulated. There were five to seven sampling intervals over the coarse of each test and sampling occurred about every hour. Total volume of air collected averaged 2,962±849 L. The computed and fitted size distributions of field-generated metal cutting fluid mist collected by the Andersen Cascade Impactor for this study are presented in Table 5.13.

Table 5.13
Size Distribution of Field-Generated Metal Cutting Fluid

Size Distribution	MMAD ($\bar{x} \pm \sigma$) µm	GSD
Computed	3.43 ± 0.38	1.77-2.13
Fitted	3.85 ± 0.57	1.65-2.45

Data collected with Andersen Cascade Impactor
Sampling dates 8/8/98 to 8/25/98
Number of testing days=10

Overall, the fitted MMAD was larger than the computed MMAD as reflected in the average diameter and standard deviation. The mass collected on the first stage capturing the largest particles was low. The mass collected on the second stage increased and then tapered off on subsequent stages that collected the smaller particles. The cascade impactor tends to give a bimodal distribution. The

fitted data normalized the aerosol into a lognormal size distribution and indicated that particles were missing in the larger size bins, shifting the distribution slightly to the right. The lognormal probability plot of the fitted asphalt size distribution is presented in figure 5.21.

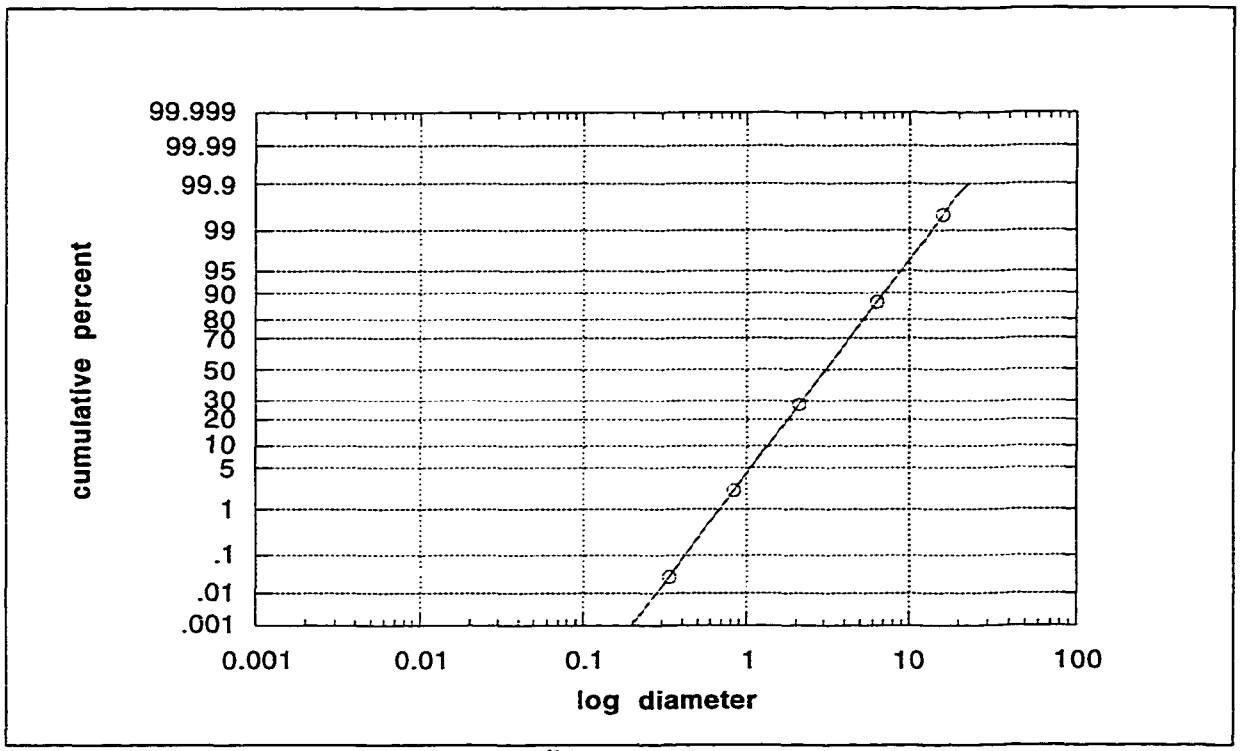

figure 5.21
Size Distribution of Field-Generated Metal Cutting Fluid Mist
Data collected with Cascade Impactor on 8/11/98
Fitted: MMAD 3.34 µm, GSD 1.91

Field-Generated Metal Cutting Fluid Mist Results

The effects of the sampling protocol on respirator performance was evaluated by comparing "exposed" respirators to their "control". This determined what effect, if any, there would be from placing a respirator in a machine shop for six hours, drawing through a high volume of air, and evaluating penetration four times with NaCl aerosol. Differences between

"exposed" and "control" respirators reflected the effects of metal cutting fluid mist loading. Comparisons were made using an ANOVA specific to each respirator. These models were kept very simple with the dependent variable, percent penetration, remaining untransformed. "Minutes loaded" and "exposed/control" were the only independent variables added to the models along with their interaction term defining slope of the loading curve. It was assumed that all other terms describing field conditions were equal.

A summary of the p values from the ANOVA tests by respirator type and penetration measurement are shown in Table 5.14. The null hypothesis, no difference between "exposed" and "control" respirators, was accepted when p values were greater than 0.05. Conversely, the alternate hypothesis, a difference exists between "exposed" and "control" respirators, was accepted when the p value was less than 0.05. Graphs of the data are shown in Appendix Graphs C.55 through C. 64.

Table 5.14
Respirators Loaded with Field-Generated Metal Cutting Fluid Mist
ANOVA Summary: p Values for Intercepts and Slopes of Loading Curves Comparing "Control" to "Exposed" Respirators

Respirator Type	CNC		Photometer	
	intercept	slope	intercept	slope
3M 2091	0.8445	0.2891	0.3708	0.5817
ProTech F200	0.9071	0.2294	0.8537	0.0106
Racal (mechanical)	0.9307	0.0061	0.7170	≤ 0.0001
MSA Affinity Plus	0.7973	0.1183	0.5860	0.0067
3M 8210	0.3900	0.0117	0.7168	≤ 0.0001

N "controls"=2 for each respirator type
N "exposed"=6 for each respirator type

Results of the ANOVAs found intercepts not to be significantly different for all respirators tested. This conclusion indicated that irregardless of the treatment

given the respirators, penetration measurements were not significantly different ($p>0.05$) prior to loading. All N95 respirators showed some differences between the "exposed" and "control" with duration of exposure. Slopes of CNC- and photometer-measured penetration were significantly different for Racal (mechanical) and 3M 8210 respirators. The slope for photometer-measured penetration was significantly different ($p<0.05$) for MSA Affinity Plus and Pro-Tech F200. Only the slopes for 3M 2091 remained unchanged with loading. Overall, all N95 respirators had increased photometer-penetration with loading compared to their controls and half also experienced increased CNC-measured penetration. Analyses comparing penetration of N95 respirators loaded with metal cutting fluid would be attributed to the aerosol loading and not the test protocol. Differences in slopes for 3M 2091 were not found to be significantly different with duration of exposure. Plots of these data indicated that penetration for the "exposed" respirators either increased slightly or remained about the same as compared to the "controls". This P100 series filter had a much higher efficiency than the N95s and penetration was less likely to be affected by exposure to metal cutting fluid mist.

In order to answer the question, "Is there a difference between the collection efficiency of respirators containing electrostatic media and those containing mechanical filter media?" the slope of each electrostatic N95 respirator was compared to the mechanical N95 respirator using the Wald test. ANOVA models were constructed for N95 respirators loaded with metal cutting fluid containing all terms and interactions found to be significant ($p<0.05$). Field temperature was found to be a significant term in the model for CNC-measured penetration but was later removed. Including this term resulted in initial

penetration being dropped from the model. The cubic term for mg loaded along with several interaction terms were found to be significant in the photometer-penetration models. Later these terms were removed as including them resulted in the slopes for the predicted penetration curves being skewed. The final models are located in Appendix Tables B.34 and B.35. Slopes of the penetration curves for each respirator were computed by adding the coefficient from "mg metal cutting fluid" to the coefficient for the individual respirator from the interaction term "mg metal cutting fluid by respirator type". The difference between the slopes for the electrostatic respirator and the mechanical was divided by their pooled standard error to obtain a Z test value. If the p value of the test was greater than 0.05, the null hypothesis was accepted and performances of electrostatic respirators were determined to be comparable to the mechanical respirator. Conversely if the p value of the test was less than 0.05 the alternate hypothesis was accepted and electrostatic respirator performances were determined to be significantly different from the mechanical respirator. These analyses are located in Appendix Tables B.36. and B.37. Figure 5.22 depicts the trend lines of the backtransformed CNC-measured penetration with respect to respirator loading. Overall, slopes for CNC-measured penetration increased with increasing loading of field-generated metal cutting fluid mist for both electrostatic and mechanical respirators.

Results of the Wald test indicated that the slopes for all electrostatic respirators were comparable to the Racal (mechanical) for CNC-measured penetration, $p>0.05$. A closer examination of these data revealed that the Wald approximation might not be an accurate reflection of the graphed data in

detecting differences between the and Racal mechanical respirator and two of the electrostatic respirators, MSA Affinity Plus and 3M 8210

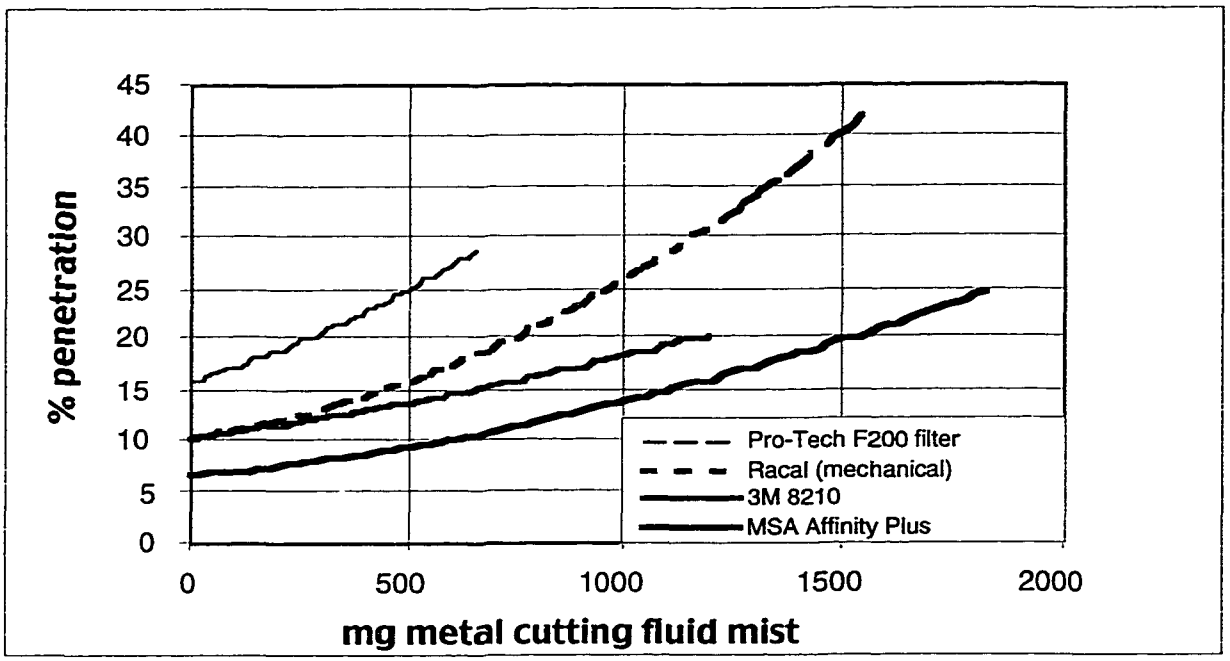

figure 5.22
CNC-Measured Penetration
N95 Respirators Loaded With Field-Generated Metal Cutting Fluid Mist
Fitted MMAD: 3.9 ±0.28 μm
Fitted GSD: range 1.65 to 2.45
Number of replicates tested=6

Data were recoded and reanalyzed to compute an F-ratio. The p values from the F test for the MSA Affinity Plus respirators combined with the Racal mechanical was <0.0001. The p values from the F test for the Pro-Tech F200 filter combined with the Racal mechanical was <0.002. These findings indicated that there was a real difference between these two electrostatic respirators and the mechanical. The p values from the F test for the 3M 8210 respirators combined with the Racal mechanical was greater than 0.4. This test confirmed that the 3M 8210 respirator was significantly different from the mechanical. Slope for the Pro-Tech F200 filter

was the steepest of all respirators tested in this matrix; penetration increased the fastest with loading. All other electrostatic respirators loaded with metal cutting fluid had slopes flatter than the mechanical respirator for CNC-measured penetration. Overall the performances of the electrostatic respirators were comparable or slightly better than the mechanical respirator, as measured by the CNC.

Figure 5.23 depicts the same group of respirators loaded with field-generated metal cutting fluid and the backtransformed photometer-measured penetration. Overall the slopes for photometer-measured penetration increased with metal cutting fluid mist loading.

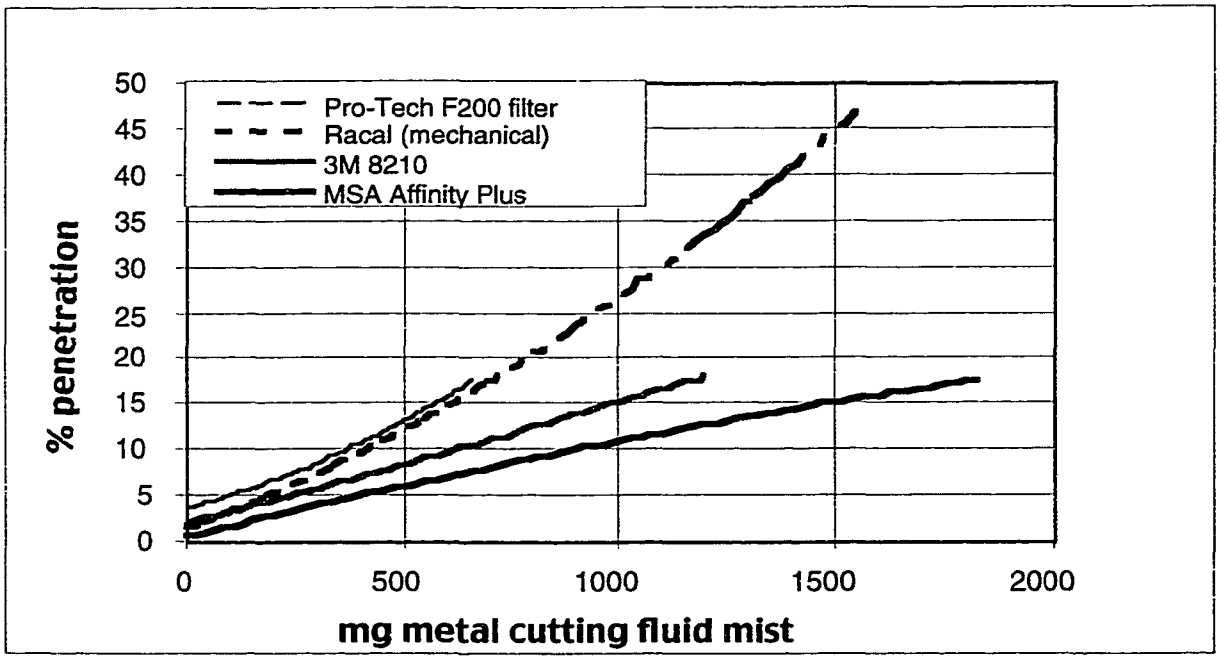

figure 5.23
Photometer-Measured Penetration
N95 Respirators Loaded With Field-Generated Metal Cutting Fluid Mist
Fitted MMAD: 3.9 ± 0.28 μm; Fitted GSD: range 1.65 to 2.45
Number of replicates tested=6

The results of the Wald test found MSA Affinity Plus to be the only electrostatic respirator comparable to the Racal (mechanical) respirator for photometer-measured penetration, $p>0.05$. A closer examination of these data revealed that the Wald approximation might not be an accurate reflection of the difference between the Racal mechanical respirator and the MSA Affinity Plus respirator. To correctly determine if the MSA Affinity Plus respirator was indeed different from the mechanical respirator, data from MSA Affinity Plus respirators were coded to match the Racal mechanical respirators and inserted back into the ANOVA model. The sum of squares error from the new ANOVA model was averaged with the sum of squares error from the old ANOVA model and this value and divided by the mean square error of the original model to compute an F-ratio. The p values from the F test for the MSA Affinity Plus respirators combined with the Racal mechanical was <0.0001. This test indicated that there was a real difference between these two respirators. The slope for the Racal mechanical was the steepest for all N95 respirators tested in this matrix. This result indicated that the electrostatic respirators performed better than the mechanical respirator loaded with metal cutting fluid as measured by the photometer.

For this testing matrix, the slope for the mechanical respirator was either the steepest, as with the photometer data, or the second steepest, as with the CNC data. Only the Pro-Tech F200 filter had a significantly steeper slope than the mechanical, as measured by the CNC. The slopes for all other electrostatic respirators were flatter. More weight was given to the photometer-measured penetration data as this was more closely related to a 'dose' that a respirator wearer might receive. Overall, these findings indicated that the electrostatic

respirators would be expected to have slightly improved performance as compared to the mechanical respirator. Also note that after about 500 mg of metal cutting fluid were loaded on the respirators, photometer-measured penetration increased above 5% for all respirators. This finding suggests that N95 respirators heavily loaded with metal cutting fluid may provide less protection than their N95 rating.

The overall slope of the penetration curves for N95 respirators loaded with field-generated metal cutting fluid mist was positive. These curves were opposite of the NIOSH method NaCl loading curve used to predict respirator performance; the NIOSH penetration curves were negative with loading. The loading curve for field-generated metal cutting fluid mist was computed over a maximum of 1800 mg metal cutting fluid mist loaded and was much greater than the 200 mg loading used for the NIOSH method tests.

Coefficients from the simplified ANOVA models with NaCl were applied to metal cutting fluid data to generate predicted penetration values of N95 respirators. Predicted penetration was compared to measured penetration globally with an F test, see Table 5.15. These analyses had p values <0.0001, indicating that NaCl penetration of N95 respirator loaded with metal cutting fluid was not accurately predicted by the NIOSH method certification tests.

Table 5.15
Electrostatic and Mechanical N95 Respirators Loaded with
Field-Generated Metal Cutting Fluid Mist
F test Comparing Predicted to Observed Penetration Measurements

Penetration Measurements	F test	p value
CNC-measured	2.142E11	0.0000*
photometer-measured	1.046E4	0.0000*

* denotes p value < 0.05

Graphs of the observed penetration for each N95 respirator loaded with field-generated metal cutting fluid mist can be found in Appendix Graphs C. 65 to C.72. After loading approximately 400 mg of cutting fluid mist onto the respirators, the predicted penetration values became erratic. This indicated that the models used for deriving the predicted penetration values appeared to have other variables coming into play when applied to the field-generated metal cutting fluid mist data that were not included in the sodium chloride data. This variability could possibly be related to the amount loading. The sodium chloride models were based on 200 mg NaCl loading and respirators in this test scenario were loaded with 1200 to 1800 mg metal cutting fluid mist. A comparison of the plotted penetration values was made for each respirator type between the data from the sodium chloride tests and the field-generated metal cutting fluid mist. These observations found the penetration of respirators using the NaCl NIOSH method tests to be much less than the observed penetration of respirators loaded with cutting fluid mist. This indicated that the NIOSH method test was a less stringent predictor of penetration. Comparisons of the graphed data and the results of F tests indicate that penetration of respirators loaded with field-generated metal cutting fluid mist were not accurately predicted by the NIOSH method tests.

The global comparison in Table 5.15 included *both* electrostatic and mechanical respirators. In order to answer the question, 'Does the NIOSH certification method accurately predict penetration of respirators containing *electrostatic* filter media loaded with metal cutting fluid mist?', further refinement to the models was needed to make this statistical evaluation. N95 respirators in the metal cutting fluid mist comparison grouping were divided into two subsets,

electrostatic and mechanical. ANOVA models for both the NIOSH method NaCl loading and the NaCl penetration of respirators loaded with metal cutting fluid mist were recalculated using the same independent variables from the overall models. If the dependent variable, percent penetration, had been transformed in the original model, it retained its same unique transformation in the refined models. Once the NaCl NIOSH method models were recalculated, the reliability of these models to accurately predict penetration was again checked using the F test and graphs. All F test values were 1.00 with corresponding p values of 0.500. These results indicted that the NIOSH method models accurately predicted NaCl penetration independently for N95 respirators containing either electrostatic or mechanical filter media. These findings were unchanged from the overall models combining respirator types. Coefficients generated in the refined ANOVA models for the NIOSH method NaCl loading tests varied slightly from the overall model. Applying data from the aluminum oxide dust tests to these coefficients resulted in slightly different predicted penetration values. The results of the F test comparing predicted penetration measurements of respirators loaded with metal cutting fluid mist to their observed values is presented in Table 5.16.

Table 5.16
Electrostatic and Mechanical N95 Respirators Loaded with Field-Generated Metal Cutting Fluid Mist
F test Comparing Predicted to Observed Penetration Measurements

Penetration Measurements	F test	p value
electrostatic respirators: CNC-measured	11368997	<0.0000*
mechanical respirator: CNC-measured	10689279	<0.0000*
electrostatic respirators: photometer-measured	22734	<0.0000*
mechanical respirators: photometer-measured	21346	<0.0000*

*denotes p value < 0.05

The p values generated from the F tests were <0.0000 indicating that there was a real difference between observed and predicted penetration values. The test results in Table 5.16 indicated that the NIOSH method certification test did not accurately predict penetration of respirators loaded with metal cutting fluid mist. Results from refining the respirator groupings to distinguish between respirators with electrostatic and mechanical filter media remained unchanged from the overall tests where respirators with both types of filter media were grouped together.

Saturation

Hot environmental conditions in which filtering facepiece respirators are worn can sometimes result in the respirators becoming damp from the wearer's perspiration. The effect of saturation on the respirator's performance was evaluated by comparing initial penetration of respirators to penetration values of the same respirators after they were submerged in a solution of artificial perspiration and dried with HEPA filtered air. This testing matrix evaluated changes in respirator penetration. Five replicates of each respirator type were tested.

Testing began on 4/1/98 and ended 4/17/98. Three to four respirators were evaluated on a single day. Respirators were sealed to their holders and were evaluated for initial fit the morning of the saturation test using the 3M LPQFT method preceding initial penetration measurement with dilute charge neutralized NaCl aerosol. A summary of initial face seal integrity can be found in Appendix Table B.38. Overall, initial penetration with 2.0 μm latex spheres averaged 0.39%; Gerson averaged 1.61% and 3M 8210 averaged 0.23%. Fit values

for the 3M 8210 and Racal (mechanical) respirator were slightly higher than previously found for the NaCl loading tests.

The target duration a respirator was to remain in contact with the artificial perspiration solution was 40 minutes. Miscalculations in the saturation time for the MSA Affinity Plus respirators resulted in two respirators having saturation times of 31 minutes, reducing the average saturation time for this respirator to 36 minutes. All other respirators averaged saturation times of 40 to 41 minutes. Initial relative humidity readings were adjusted and recorded prior to placing respirators in the chamber and averaged 22±0.9%.

Final relative humidity readings were recorded at the end of the drying cycle and averaged 23±1.5%. The average difference between initial relative humidity and the final downstream relative humidity was 1.3%. Duration of the drying cycle was proportional to the mass of the respirator; respirators with more mass absorbed more solution and required longer drying times. The average drying time was 69±26 minutes. Average drying times and respirator masses are presented in Table 5.17. The average weight changes for saturated and dry respirators are located in Appendix Table B.39.

Table 5.17
Dry Mass and Drying Times of N95 Respirators Saturated with Artificial Perspiration

Respirator Type	Initial Respirator Mass (g)	Drying Time (min)
3M 8210	7.66	92
Gerson 2735S	8.16	61
MSA Affinity Plus	10.03	91
Racal (mechanical)	6.69	423
Tecnol PFR95	6.65	59

Number of replicate samples of each respirator=5

At the end of the drying cycle, only 1 to 3% of the artificial perspiration solution initially absorbed onto the respirators remained. The difference in pressure drop ranged from a loss of 0.6% to a gain of 1% except for Tecnol PFR95 respirators that increased 7%; refer to Appendix Table B.40. Change in resistance may have been attributed to the residual moisture remaining on the respirator indicating that this respirator was not completely dried.

Results

In order to answer the question, "What is the effect upon the collection efficiency of air purifying respirators that have been saturated with artificial perspiration?", differences between initial and final penetration measurements were compared using a paired-t test. The results of the paired t-test for CNC-measured penetration can be found in Appendix Table B.41. Only two respirators had significant ($p<0.05$) changes in CNC-measured penetration, 3M 8210 and MSA Affinity Plus, these data are presented in figure 5.24. The direction of this difference is negative, suggesting that performance improved after respirators were saturated and dried.

A paired t-test was again used to determine if there were any differences between initial and final photometer-measured penetration. The results of the paired t-tests are located in Appendix Table B.42. Only two respirators were found to have significant ($p<0.05$) changes in their photometer-measured penetration, Racal (mechanical) and MSA Affinity Plus. Plots of initial and final photometer-measured penetration are presented in figure 5.25. The direction of this difference is positive for the Racal (mechanical) and negative for the MSA.

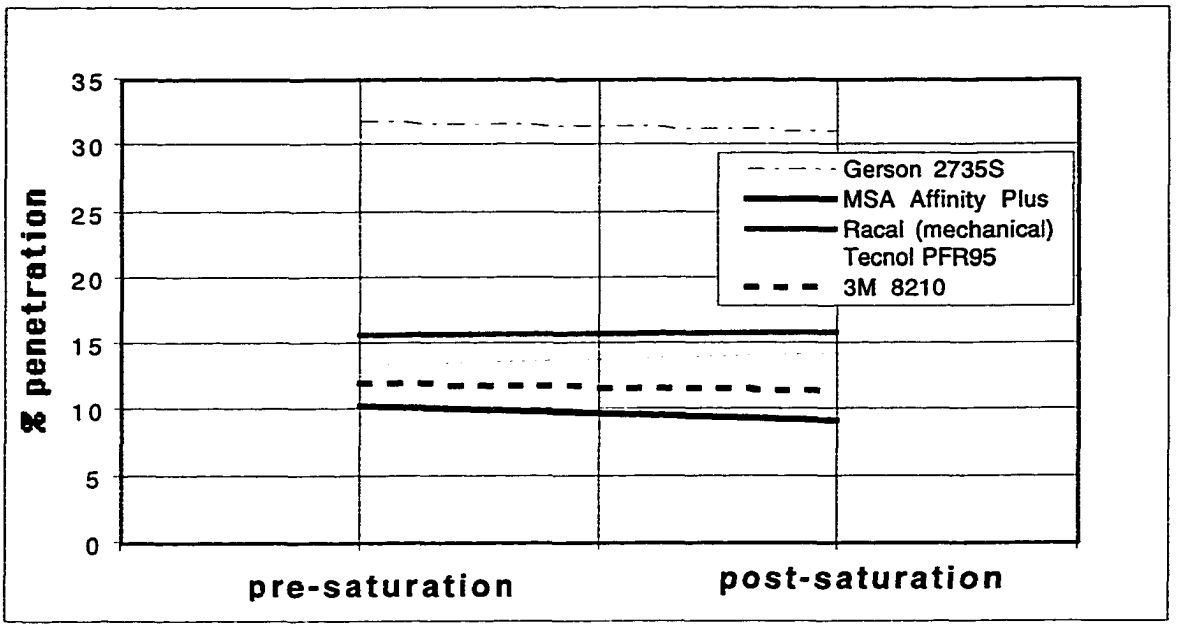

figure 5.24
CNC-Measured Penetration
N95 Respirators Saturated with Artificial Perspiration
% Penetration Pre- and Post-Saturation
Number of replicate samples of each respirator=5

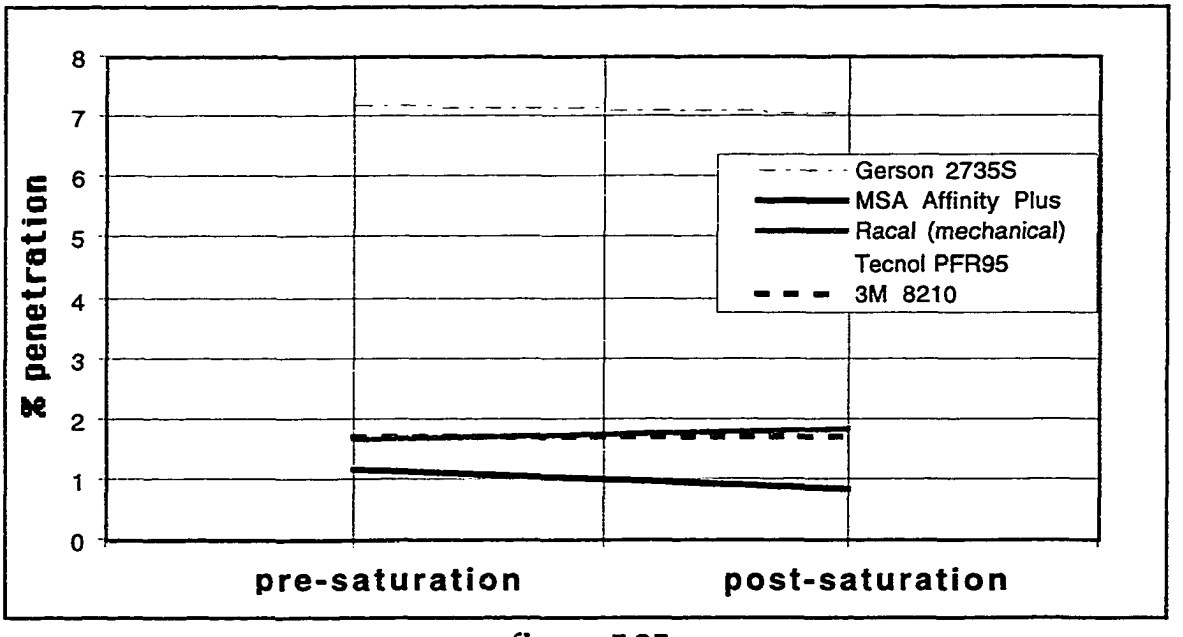

figure 5.25
Photometer-Measured Penetration
N95 Respirators Saturated with Artificial Perspiration
% Penetration Pre- and Post-Saturation
Number of replicate samples of each respirator=5

These findings indicate that performance of the electrostatic respirators remained the same or slightly improved while performance of the mechanical respirator degraded from saturation in artificial perspiration and drying with HEPA filtered air.

Overall respirator performance of all N95 with electrostatic filter media remained unchanged or improved slightly when saturated in artificial perspiration and dried with HEPA filtered air. Performance of MSA Affinity Plus improved for both CNC and photometer-measured penetration. Residual moisture remaining on the Tecnol PFR95 respirators did not alter final penetration measurements. This suggests that the collection efficiency of filtering facepiece respirators containing electrostatic filter media saturated with perspiration would remain unchanged once the respirator was completely dried. The collection efficiency of the Racal (mechanical) respirator was the only respirator whose performance was negatively impacted by this test matrix.

SUMMARY

The objective of this research was to answer the following questions:

a) Does the NIOSH certification method for air purifying respirators accurately predict the collection efficiency of electrostatically charged filter media respirators that are challenged with contaminants representative of workplace environments?
b) Is there a difference between the collection efficiency of respirators containing electrostatic media and those containing mechanical filter media?
c) What is the effect of filter saturation with artificial perspiration on the collection efficiency of filtering facepiece respirators?

A summary of the answers to these research questions is listed by test scenario.

Asphalt Contaminants

a) The NIOSH method did not accurately predict the collection efficiency of electrostatic and mechanical respirators loaded with asphalt contaminants. The predicted penetration values were significantly less than the observed values as measured by both CNC and photometer.

b) The performances of electrostatic respirators were comparable to the mechanical as measured by the CNC. However, electrostatic respirators had improved performance over the mechanical as measured by the photometer.

Aluminum Oxide

a) The NIOSH method did not accurately predict collection efficiency of respirators loaded with aluminum oxide as measured by either the CNC or the photometer. The predicted CNC-measured penetration was underestimated whereas the predicted photometer-measured penetration was sometimes underestimated and other times overestimated depending upon respirator type and mass loaded.

b) Electrostatic respirators were comparable to the mechanical respirator as measured by the CNC. Performances of electrostatic respirators were slightly better than the mechanical as measured by the photometer.

Laboratory-Generated Metal Cutting Fluid Mist

a) The NIOSH method did not accurately predict the collection efficiency of electrostatic and mechanical respirators loaded with laboratory-generated metal cutting fluid mist. The predicted penetration values were significantly less than the observed values as measured by both CNC and photometer.

b) Performances of electrostatic respirators were comparable to the mechanical respirator as measured by both the CNC and the photometer.

Field-Generated Metal Cutting Fluid Mist

a) The NIOSH method did not accurately predict the collection efficiency of electrostatic and mechanical respirators loaded with field-generated metal cutting fluid mist. The predicted penetration values were significantly less than the observed values for the CNC, underestimating penetration. Predicted photometer-measured penetration was a more stringent predictor of penetration than the observed values. This was the only test matrix that found this result.

b) Performances of electrostatic respirators were slightly better than the mechanical respirator as measured by the CNC. This difference was more pronounced for the photometer-measured penetration, performances of electrostatic respirators were much better than the mechanical respirator.

Saturation

a) The overall effect upon the collection efficiencies of filtering facepiece respirators that were saturated with artificial perspiration was unchanged. CNC-measured penetration for two electrostatic respirators improved by as a result of saturation and drying. When penetration was measured by the photometer, the performance of mechanical respirator had significantly decreased whereas the performance of one electrostatic respirator had improved.

CHAPTER VI

CONCLUSION

Summary

This research was undertaken to determine if the NIOSH method used for certifying air purifying respirators accurately predicted collection efficiency of respirators containing electrostatic filter media loaded with contaminants representative of the workplace. Two workplace contaminants, asphalt contaminants and metal cutting fluid mist, selected for this project possessed chemical and/or physical properties that may mask or degrade the charge on the electrostatic fibers, thereby reducing the collection efficiencies of these respirators. Mechanical filter media do not possess this enhanced particle collection mechanism. It was anticipated that respirators having only mechanical filter media would not have their collection efficiencies degraded when loaded with these contaminants. The third contaminant representative of a workplace aerosol, aluminum oxide dust, was selected to represent a solid particulate. The collection efficiency of N95 respirators loaded with this aerosol was expected to be similar to sodium chloride (NaCl) used for certifying N95 respirators.

The basis for comparing collection efficiencies of N95 respirators was the NIOSH method test that uses a charge neutralized NaCl aerosol to

determine respirator penetration. Penetration was measured with two different instruments, a forward light scattering photometer and a condensation nucleus counter (CNC). A total of five replicates from each respirator type was used for the NIOSH method test. These tests terminated after 200 mg of aerosol contacted each respirator. N95 series respirators were divided into two groups according to the workplace contaminants to which they were exposed: asphalt contaminants and metal cutting fluid mist/aluminum oxide dust. Simple ANVOA models from the NIOSH method NaCl data were constructed for each respirator grouping and for both types of penetration measurements. These models were refined to distinguish between respirators containing electrostatic and mechanical filter media. Coefficients from the ANOVA models were then applied to the workplace contaminant data to generate predicted penetration values.

Respirators were loaded with contaminants representative of the workplace for about six hours. After each 2-hour loading interval, penetration was determined using a dilute concentration of charge neutralized NaCl aerosol. To determine if the NaCl loading tests using the NIOSH method accurately predicted penetration of respirators loaded with workplace contaminants, coefficients from the NaCl ANOVA models were applied to workplace test data. The generated predicted penetration values in each respirator grouping were globally compared to the observed penetration values using an F test.

Penetrations of N95 respirators loaded with workplace contaminants were modeled with ANOVAs containing all terms and interactions found to be significant ($p<0.05$). The slope of the penetration curves indicated respirator performance. To determine if there were any differences between the performance of a respirator containing electrostatic filter media and a mechanical respirator, a pair-wise comparison of the slopes was made using the Wald test.

To ensure that any differences in penetration of respirators loaded in the field were attributed to the aerosol of interest and not the testing protocol, penetration of respirators 'exposed' to the contaminants were compared to their 'control'. Control respirators were placed away from point of aerosol generation and subjected to the same environmental conditions and testing methods as the 'exposed'. Comparisons between the penetration of 'exposed' and 'control' respirators were made with the help of an ANOVA. Terms in the models only contained nontransformed penetration, minutes loaded, and control/exposed variables to describe the intercept and slope of the penetration curve. The correlation coefficients ranged from 0.759 to 0.932 indicating that these models were able to explain most of the variability in penetration. The p values from the ANOVA models determined if significant differences ($p<0.05$) existed between the intercepts and slopes of 'exposed' and 'control' respirators

Filtering facepiece respirators are often used in environments where they become saturated with the wearer's perspiration. Perspiration contains

ions that could interact with the charge on an electrostatic filter. Initial penetration of filtering facepiece respirators was compared to final penetration after respirators were saturated and dried with HEPA filtered air. Comparisons in performance was made with a paired-t test.

Results and Conclusions

The results summarized below support the conclusions that: a) the NIOSH method test for N95 respirators underestimates penetration of respirators loaded with workplace contaminants, b) N95 respirators containing electrostatic filter media do not perform significantly different from an N95 respirator with mechanical filter media, c) collection efficiency of respirators saturated in artificial perspiration did not significantly change once the respirators were dried.

1. The NIOSH method test used for certifying N95 respirators did not accurately predict either CNC- or photometer-measured penetration of N95 respirators loaded with asphalt contaminants, metal cutting fluid mist, or aluminum oxide dust. Penetration measurements were underestimated for all workplace contaminants with the exception of photometer-measured penetration of respirators loaded with field generated metal cutting fluid. This was the only matrix that predicted higher penetration than the NIOSH method test. These results suggest that the NIOSH method for certifying respirators may not indicate worst case performance of N95 respirators. When selecting respiratory protection, field hygienists need to be aware that the

NIOSH method may not be the most stringent indicator of respirator performance in the workplace.

2. At the end of the NIOSH method tests, final pressure drop for 8 of the 13 N95 respirators was in excess of two inches of water column, exceeding the physiological resistance for human breathing. Overall, final breathing resistances from the NIOSH method tests were much greater than for loading with aerosols representative of the workplace. Although 42 CFR 84 states that final breathing resistance experienced at the worksite is not represented by the NIOSH method NaCl test, one respirator, Pro-Tech F200 filter, had an average final pressure drop of 18 inches of water column. Approximately 650 mg of field generated metal cutting fluid had been loaded onto this respirator. Workers may find it necessary to replace respirators more frequently than expected in order to maintain adequate comfort when working in environments with high concentrations of metal cutting fluid mist.

3. The collection efficiencies of respirators containing electrostatic filter media were comparable to mechanical respirators when loaded with workplace contaminants. Asphalt contaminants and synthetic metal cutting fluid mist degraded the performance of electrostatic and mechanical respirators equally and penetration increased with increased loading. This finding refutes the hypothesis that charge on electrostatic fibers would be masked or degraded by workplace aerosols resulting in decreased performance compared to mechanical respirators. Collection efficiency of electrostatic and mechanical respirators were not significantly different for most matrices. The

electrostatic respirators tended to have slightly improved performance when loaded with aluminum oxide dust. These findings indicate that field hygienists do not need to be concerned about the type of filter media, electrostatic or mechanical, in non-powered air purifying respirators, both types would be expected to perform comparably when loaded with asphalt, metal cutting fluid mist, and aluminum oxide dust.

4. The collection efficiencies of some N95 respirators, both mechanical and electrostatic, decreased below their expected 95% efficiency rating after loading with asphalt contaminants and synthetic metal cutting fluid mist. This finding suggests that this class of respirator may not provide adequate worker protection in these environments. The collection efficiency of a P100 respirator did not degrade when loaded with these workplace contaminants. This finding indicates that this respirator class would be expected to provide worker protection relative to its certification rating in these workplace settings. These results indicate that field hygienists need to be aware of the loading effect when selecting the respirator class for protection against asphalt and metal cutting fluid mist hazards.

5. Penetration of filtering facepiece respirators saturated in a solution of artificial perspiration did not significantly change, once the wetted respirators were adequately dried. These results refuted the hypothesis that the ions contained in perspiration would interact with the electrostatic charge and reduce collection efficiency of these respirators. Respirator wearers are encouraged to replace a soiled respirator. However, if their filtering facepiece

respirator does become damp from perspiration, its performance would be expected to remain the same once it has been allowed to dry out.

This research focused on the evaluation of N95 particulate air purifying respirators. Instrumentation response and the protocol used for comparing the collection efficiencies of P100 series respirators loaded with contaminants representative of the workplace cast doubt on the accuracy of these analyses. Modifying the protocol used in this project by changing the challenge aerosol from NaCl to DOP for P100 series respirators loaded with workplace contaminants would help clarify the accuracy of the NIOSH certification method test for this respirator category.

REFERCNES CITED

1 van Turnhout, J.; Hoeneveld, J W.J.; Adamse, W.C.; et al.: "Electret Filters for High Efficiency and High Flow Air Cleaning". *Conference Record, Industry Applications Society: IEEE-IAS-1979 Annual Meeting: Papers Presented at the Fourteenth Annual Meeting.* Cleveland, OH (1979).

2 Brown, R.C.; Wake, D.; Gray, R.; Blackford, D.B.; et al.: Effect of Industrial Aerosols on the Performance of Electrically Charged Filter Material. *Annals of Occupational Hygiene.* 32(3): 271-294 (1988).

3 Davies, C.N.: *Air Filtration.* Academic Press New York (1973).

4 Walton, W.H.: *The Electrical Characteristics of Resin Impregnated Filters.* (CDE Porton Report No. 2465) England (1942).

5 van Turnhout, Jan. Method for the Manufacture of an Electret Fibrous Filter, U.S. Patent 3,998,916. (December 21, 1976).

6 Thomas, G.: Electrically Charged Material. U.S. Patent 2,470,184. (April 3, 1956).

7 van Turnhout J.; Albers, J.H.M.; Adamse, J.W.C.; et al.: "Electret Filters for High-Efficiency Air Cleaning". *The Second World Filtration Congress.* London, England (1979).

8 Bergmann, L.: Electret nonwovens - A Fast Growing Breed Of Filtration Fabrics. *Chemiefasern/Textil-Industrie* 40/92(9):E95-E97 (1990).

9 Mitsui Petrochemical Industries Ltd.: Melt-Blown Electret Filter Media Developed In Japan. *Nonwovens Report International* 271:6-7 (1993).

10 Nakao, Etsuro. Method of Manufacturing an Electret Filter, U.S. Patent 4,592,815. (June 3, 1986).

11 Tsai, Peter Ping-Yi and Wadsworth, Larry C.: "Mechanism of Corona Electrostatic Charging of Nonwoven Webs". *Proceedings form the 1994 Nonwovens Conference.* Orlando, Florida. pp 9-11 (1994).

12 Shiga, Ryoichi Togashi and Ando, Katsutoshi: Non-Woven Fiber Sheet and Process and Apparatus for its Production, U.S. Patent 5,051,159. (September 24, 1991).

13 Simm, Walter, Claus Göeling; Bonart, Richard; Falkai, Bélavon: Filter Made of Electrostatically Spun Fibers, U.S. Patent 4,069,026. (January 17, 1978).

14 Baumgartner, Hanspeter and Loffler, Friedrich: "Improved Particle Collection in Deep Bed Filters by Using Electret Fibers". *3rd International Conference on Electrostatic Precipitation.* Abano/Venice, Italy. 601-616 (1987).

15 Sievert, Joerg: "Electrostatically Spun Microfiber Nonwovens as Filter Media in Air Filtration". *Proceedings from INDA's Filtration Conference.* Philadelphia, PA . 87-96 (1991).

16 Ackley, Mark W.: "Degradation of Electrostatic Filters at Elevated Temperature and Humidity". *World Filtration Congress III.* Croydon, England. pp. 169-176. (1982).

17 Chen, C.C.; Lehtimaki, M.; Willeke, K.: Loading and Filtration Characteristics of Filtering Facepieces. *American Industrial Hygiene Association Journal.* 54(2): 51-60 (1993).

18 Moyer, Ernest S. and Stevens, Gregory A.: "Worst Case" Aerosol Testing Parameters: II. Efficiency Dependence of Commercial Respirator Filters on Humidity Pretreatment. *American Industrial Hygiene Association Journal.* 50(5):265-270 (1989).

19 Biermann, Arthur and Bergman, Werner: Measurement of Aerosol Concentration as a Function of Size and Charge. *Aerosol Science and Technology.* 3:293-304 (1984).

20 Bergman W. and Jaeger, R.: Electric Air Filtration Movie. Lawrence Livermore National Laboratory. UCRL 91149. (July 1984).

21 Brown, R.C.: *Air Filtration and Integrated Approach to the Theory and Applications of Fibrous Filters.* Pergamon Press. Tarrytown, NY (1993).

22 Brown, R.C.: Review Modern Concepts of Air Filtration Applied to Dust Respirators. *Annals of Occupational Hygiene.* 33(4): 615-644 (1989)

23 Crater, Davis H.; Howells, Richard D.; Stern, Richard M.; et al.: Fluorochemical Oxazolidinones, U.S. Patent 5,025,052. (June 18, 1991).

24 Jones, Marvin E. and Rosseau, Alan D.: Oily Mist Resistant Electret Filter Media, U.S. Patent 5,472,481. (December 5, 1995).

25 Mares, F. and Oxenrider, B.C.: Modification of Fiber Surfaces by Monomeric Additives. Part I: Extrusion Techniques. *Textile Research Journal* 47(8):551-561 (1977).

26 Biermann, A.H.; Lum, B.Y.; Bergman, W.: Evaluation of Permanently Charged Electrofibrous Filters. *17th DOE Nuclear Air Cleaning Conference.* Denver, CO. (August 1982).

27 Bergman, W.; Biermann, A.; Kuhl, W.; et al.: Electric Air Filtration: Theory, Laboratory Studies, Hardware Development, and Field Evaluations. (UCID 19952). Lawrence Livermore National Laboratory. Livermore, CA. (September 1983).

28 Chen, C.C.; Lehtimaki, M.; Willeke, K.: Aerosol Penetration Through Filtering Facepieces and Respirator Cartridges. *American Industrial Hygiene Association Journal.* 59(9): 566-574 (1992).

29 Brosseau, L.M.; Evans, J.S.; Ellenbecker, J.J.; et al.: *Collection Efficiency of Respirator Filters Challenged with Monodisperse Latex Aerosols.* Prepared for: National Institute for Occupational Safety and Health, Cincinnati, OH (1990).

30 Moyer, Ernest S. and Stevens, Gregory A.: "Worst Case" Aerosol Testing Parameters: III. Initial Penetration of Charged and Neutralized Lead Fume and Silica Dust Aerosols through Clean, Unloaded Respirator Filters. *American Industrial Hygiene Association Journal.* 50(5):271-274 (1989).

31 Chen, Chih-Chieh and Huang, Sheng-Hsiu: "The Effects of Particle Charge on the Performance of an Electret Filtering Facepiece". Presented at the American Industrial Hygiene Conference and Exposition. Washington DC. (May 1996).

32 Kanaoka, Chikao; Emi, Hitoshi; Otani, Yoshio; et al.: Effect of Charging State of Particles on Electret Filtration. *Aerosol Science and Technology.* 7:1-13 (1987).

33 Nelson, Gary O.; Bergman, Werner; Miller, Holly H.; et al.: Enhancement of air filtration using electric fields. *American Industrial Hygiene Association Journal.* 39(6): 472-479 (1978).

34 Johnston, A.M.; Vincent, J.H.; Jones, A.D.: Measurement of Electric Charge for Workplace Aerosols. *Annals of Occupational Hygiene* 29(2):271-284 (1985).

35 *Title 42 Code of Federal Regulation Part 84.* "Respiratory Protective Devices; Final Rules and Notice" as printed in Federal Register 60(110):30336-30404. (June 8, 1995).

36 National Institute for Occupational Safety and Health, "Changes in Occupational Safety Regs Will Permit Better Respirator to Protect Against Dust and Disease" (June 2, 1996) *New NIOSH Respirator Certification Standards.* hhtp://ftp.cdc.gov.niosh/pres1.html [5/29/96].

37 Personal telephone conversation with Jeff Peterson of the National Institute for Occupational Safety and Health (NIOSH) on 9/27/96.

38 Schrenk, H.H.: *Testing and Design of Respiratory Protective Devices* U.S. Bureau of Mines (Information Circular 7086) Government Printing Office (1939).

39 Johnson, Arthur T.; Grove, Corey M.; Weiss, Ronald A.: Mask Performance Rating Table for Specific Military Tasks. *Military Medicine.* 158(10):665-670 (1993).

40 Drinker, Philip and Hatch, Theodore: *Industrial Dust: Hygienic Significance, Measurement and Control* 1st edition New York and London, McGraw-Hill Book Co. Inc. (1936).

41 Dorman, R.G.; Dyment, J.; Poynting, R.; et al.: High Efficiency Air Filter Testing in Factory or Laboratory. *Filtration and Separation* 15:410-416 (1978).

42 Dibner, Bern: *Agicola on Metals* Burndy Library, Norwalk, Conn. Publication No. 15 (1958).

43 Adley, Frank E.; Berry, Clyde M.; Gilliland, E.W.; et al.: *Respiratory Protective Devices Manual.* Joint American Industrial Hygiene Association and the American Conference of Governmental Industrial Hygienists Respirator Protective Devices Committee. Braun and Brumfield Inc. Ann Arbor, MI. (1963)

44 Feltham , F.J.: The Hansen Filter. *Filtration & Separation.* 16:370-372 (1979)

45 Held, Bruce J.: *History of Respiratory Protective Devices in the U.S. Pre World War I.* (UCRL 79973) University of California, Lawrence Livermore National Laboratory, Livermore, CA (1977).

46 Davies, C.N.: Filtration of Aerosols. *Journal of Aerosol Science.* 14(2): 147-161 (1983).

47 Haslett, Lewis P: Inhaler or Lung-Protector. U.S. Patent 6,529. (June 12, 1849).

48 Katz, S.H.; Smith, G.W.; Meiter, E.G.: *Dust Respirator, Their Construction and Filtering Efficiency.* U.S. Bureau of Mines (Technical Paper 394) Government Printing Office (1926).

49 Hounam, R.F.; Morgan, D.J.; O'Connor, D.T.; et al.: The evaluation of protection provided by respirators. *Annals of Occupational Hygiene* 7:353-363 (1964).

50 Trotman, C.G.: *Design and Use of Respirators.* Ed. C.N. Davies Proceedings of a Joint Meeting of the Ergonomics Research Society and the British Occupational Hygiene Society. Porton, England. Pergamon Press Ltd., N.Y. (July 1961).

51 Personal telephone conversation with Jay Parker of E.D. Bullard Company on 3/17/97.

52 Yant, W.P.: *List of Devices for Respiratory Protection Approved by the Bureau of Mines* REPORT Bureau of Mines (Information Circular 6845) Government Printing Office (1935).

53 Hoffmann, Theodore.A.: Improvement in Respirators. U.S. Patent 58,255. (September 25, 1866).

54 Katz, S.H.; Meiter, E.G.; Gibson, F.H.: *Efficiencies of Painters' Respirators Filtering Lead Paint, Benzol and Vitreous Enamel Sprays* U.S. Public Health Service (Public Health Bulletin 177) Government Printing Office (1928).

55 Dubini, M.M.: N.D. Zelinskiy, Creator of the Charcoal Gas Mask. *Bulletin De L'Academies Des Sciences De L'USSR, Classe des Sciences Chimiques* 345-350 (1946). (Russian)

56 Ferber, B.I.: Bureau of Mines Respirator Approval Schedules: New and Revised. *American Industrial Hygiene Association Journal* 27(2):110-114 (1966).

57 *U.S. Bureau of Mines Schedule 21* "Procedure for Testing Filter-Type Dust, Fume, and Mist Respirators for Permissibility" Government Printing Office (1934).

58 American Industrial Hygiene Association. *Monograph Series: Respiratory Protection.* Akron, OH (1985).

59 Pierce, S.J.: *Bureau of Mines Approval System for Respiratory Protective Devices* U.S. Bureau of Mines (Information Circular 7792) Government Printing Office (1957).

60 Pierce, S.J.: *The Use of Dust Respirators in Coal Mines* U.S. Bureau of Mines (Information Circular 7561) Government Printing Office (1950).

61 Katz, S.K.; Smith, G.W.; Meiter, E.G.: *Tests and Characteristics of Dust Respirators* U.S. Bureau of Mines (Report of Investigations 2745) Government Printing Office (1926).

62 Hinds, William C. and Kadrichu, Nani P.: Effect of Dust Loading on the Performance of Half-Mask Respirators. *Applied Occupational and Environmental Hygiene* 9(10):700-706 (1994).

63 *U.S. Bureau of Mines Schedule 21A* "Part 14-Filter Type Dust, Fume, and Mist Respirators" as printed in Federal Register 20(76):2571-75 (April 19, 1955).

64 Burgess, William A.; Silverman, Leslie; Stien, Felix: A New Technique for Evaluating Respirator Performance. *American Industrial Hygiene Association Journal* 22(6):422-429 (1961).

65 Hyatt, E.C.; Pritchard, J.A.; Richards, C.P.: Respirator Efficiency Measurement Using Quantitative DOP Man Tests. *American Industrial Hygiene Association Journal* 33(10):635-643 (1972).

66 Wiswesser, W.J.: Protection against industrial dusts. *Safety Maintenance and Production* 103:64-67 (1952).

67 Lundin, Allen M. revised by Craig E. Colton: "Respiratory Protective Equipment". *Fundamentals of Industrial Hygiene 3rd Edition.* Ed. Barbara A. Plog. National Safety Council. (1988).

68 Mayhew, Delbert J.: Filtration Masks, U.S. Patent 3,613,678. (October 19, 1971).

69 Personal telephone conversation with Chris Coffee of the National Institute for Occupational Safety and Health (NIOSH) on 6/13/96.

70 Personal telephone conversation with Eric Johnson of 3M Co. 5/96.

71 Schurmann G. and Fissan, H.J: "Fractional Efficiencies of an Electrostatically Spun Polymer Fiber Filter". *The Eleventh Annual Conference of the Association for Aerosol Research.* 317-320 (1983).

72 Personal telephone conversation with Mike Rupert of Mine Safety Appliance (MSA) on 6/10/96.

73 Personal telephone conversation with Wayde Miller of Mine Safety Appliance (MSA) on 8/10/96.

74 *Title 30 Code of Federal Regulation Chapter 1, Part 11* "Respiratory Protective Devices; Tests for Permissibility; Fees" (July 1, 1991).

75 Bergman, W. and Biermann, A.: "Effect of Heterodispersion on HEPA Filter-Penetration Measurements" contained in *Recent Investigations in Air Filtration* (UCID-21777) Special Projects Division, Hazards Control Department, Lawrence Livermore National Laboratory. Livermore, CA. (1990).

76 Hinds, William C.: *Aerosol Technology Properties, Behavior, and Measurements of Airborne Particles.* John Wiley & Sons. New York, NY. (1982).

77 Rosenstock, Linda: 42 CFR Part 84: Respiratory Protective Devices Implications for Tuberculosis Protection. *Infection Control and Hospital Epidemiology.* 16(0): 529-531 (1995).

78 Mitchell, R.N.; Bevis, D.A.; Hyatt, E.C.: Comparison of Respirator Filter Penetration by Dioctyl Phthalate and Sodium Chloride. *American Industrial Hygiene Association Journal* 32(6):357-364 (1971).

79 Ferber, B.I.; Brenenborg, F.J.; Rhode, A.: *Respirator Filter Penetration Using Sodium Chloride Aerosol.* U.S. Bureau of Mines (Report of Investigations 7403) Government Printing Office (1970).

80 Burgess, William A. and Reist, Parker C.: Supply Rates for Powered Air-Purifying Respirators. *American Industrial Hygiene Association Journal* 30(1):1-6 (1969).

81 White, J.M. and Beal, R.J.: The Measurement of Leakage of Respirators. *American Industrial Hygiene Association Journal* 27(3):239-242 (1966).

82 Dorman, R.G.; Dyment, J.; Poynting, R.; et al.: High Efficiency Air Filter Testing in Factory or Laboratory. *Filtration & Separation.* 15:410-416 (1978).

83 *Method for Sodium Chloride Particulate Test for Respirator Filters* (British Standard 4400:1969). British Standards Institution. (1969).

84 Personal telephone conversation with Jeff Peterson of the National Institute for Occupational Safety and Health (NIOSH) on 1/13/97.

85 Personal telephone conversation with Tim Johnson of Thermo-Systems Inc. (TSI) on 1/9/97.

86 Bergman, W.; Biermann, A.H.; Lum, B.Y.: "Evaluation of Permanently Charged Electric Air Filters". contained in *Recent Investigations in Air Filtration* (UCID-21777). Special Projects Division, Hazards Control Department, Lawrence Livermore National Laboratory. Livermore, CA. (1990).

87 Feltham, F.J.: Second Thought on the Hansen Electrostatic Filter. *Filtration and Separation* 13(5):467-469 (1976)

88 Smith, P.A.; East, G.C.; Brown, R.C.; et al.: Generation of Triboelectric Charge in Textile Fibre Mixtures, and Their Use as Air Filters. *Journal of Electrostatics* . 21:81-98 (1988).

89 Green, H.L.: Respiratory Protection against Particulates- Problems Solved and Unsolved. *American Industrial Hygiene Association Journal* 26(3):203-211 (1965).

90 Adamse, J.W.C.: "Specialty Nonwovens with Enhanced Filtration Performance". *Proceedings from INDA's Filtration Conference.* Philadelphia, PA . pp 125-137 (1991).

91 van Turnhout J.; Droppert, P.J.; Wubbenhorst , M.: "PP-based blends for electret filters - an appraisal." *Proceedings of the Eighth International Symposium on Electrets.* Paris, France (1994).

92 van Turnhout, J.; van Bochove, C.; van Veldhuizen ,G.J.: Electret Fibers for High-Efficiency Filtration of Polluted Gases. *Staub-Reinhalt. Luft* . 36:36-39 (1976).

93 van Turnhout, J.; Nederveen, P.J.; Roozendaal, G.: "The Filtration of Aerosols by Fibrous Electret Filters" (Report No. CL 69/164, Order No. 1526) Centraal Laboratorium TNO, Deflt, Netherlands. (October 30, 1969).

94 Baumgartner, H.P. and Loffler, F.: The Collection Performance of Electret Filters in the Particle Size Range 10 nm - 10 μm. *Journal of Aerosol Science* 17(3):438-445 (1986).

95 Lathrache, R.; Fissan, H.J.; Neumann, S.: Deposition of Submicron Particles on Electrically Charged Fibers. *Journal of Aerosol Science.* 17(3): 446-449 (1986).

96 Emi, Hitoshi; Kanaoka, Chikao; Otani, Yoshio; et al.: Collection Mechanisms of Electret Filter *Particulate Science and Technology* 5:161-171 (1987).

97 Pich, Josef; Emi, Hitoshi; Kanaoka, Chikao: Coulombic Deposition Mechanism in Electret Filters. *Journal of Aerosol Science.* 18(1): 29-35 (1987).

98 Blackford, D.B. and Brown, R.C.: An Air Filter Made from an electret and a Conductor. *IEEE Transactions on Electrical Insulation.* EI-21(3):471-476 (1986).

99 Teege, Gernot: Electrostatic Charging as a Cause of Dust Deposition on Plastic Surfaces. *Staub-Reinhalt, Luft.* 28(11):73-78 (1968).

100 van Turnhout, J.: The Use of Polymers for Electrets. *Journal of Electrostatics.* 1:147-163 (1975).

101 "Non-Woven Textile Fabrics" *Encyclopedia of Textiles, Fibers and Non-Woven Fabrics.* Ed. Martin Grayson. John Wiley and Sons Inc. New York pp. 252-284. (1984)

102 Buntin, Robert R. and Lohkamp, Dwight T.: Melt Blowing - A One-Step Web Process for New Nonwoven Products. *TAPPI* 56(4):74-77 (1973).

103 Kubik, Donald A. and Davis, Charles I.: Melt-Blown Fibrous Electrets. U.S. Patent 4,215,682. (August 5, 1980).

104 Baumgartner, H.; Loffler, F.; Umhauer, H.: Deep-Bed Electret Filters: The Determination of Single Fiber Charge and Collection Efficiency. *IEEE Transactions on Electrical Insulation.* EI-21(3):477-486 (1986).

105 Smith, Philip: Electrically charged fibers in air filtration. *Textile Horizons* 9(12):38-40 (1989).

106 Wente, Van A.: Superfine Thermoplastic Fibers. *Industrial and Chemical Engineering* 48(8):1342-1346 (1956).

107 Olivieri, P.: Nonwovens: productive technologies and main applications. *Tinctoria* (Italian) 91(6):59-63 (1994).

108 Moosmayer, Peter; Budliger, Jean-Pierre; Zurcher, Erwin; et al.: Apparatus for Electrically Charging Meltblown Webs, U.S. Patent 4,904,174. (February 27, 1990).

109 Deeds, William E.: Charging Apparatus for Meltblown Webs, U.S. Patent 5,122,048. (June 16, 1992).

110 Wadsworth, Larry C. and Hersh, Solomon P.: Method of Making Fibrous Electrets, U.S. Patent 4,375,718. (August 3, 1983).

111 Tsai, Peter P. and Wadsworth, Larry C.: "Electrostatic Charging of Meltblown Webs for High-Efficiency Air Filters". *Advances in Filtration and Separation Technology "Shape Up the Future"* Ed. Kyung-Ju Choi. American Filtration & Separation Society. Northport, AL (1995).

112 Silverman, Leslie; Conners, Edward W. Jr.; Anderson, David M.: Mechanical Electrostatic Charging of Fabrics for Air Filters. *Industrial & Engineering Chemistry* . 47(8):952-960 (1955).

113 Stevens, Gregory A. and Moyer, Ernest S.: 'Worst Case' Aerosol Testing Parameters: I. Sodium Chloride and Dioctyl Phthalate Aerosol Filter Efficiency as a Function of Particle Size and Flow Rate. *American Industrial Hygiene Association Journal* 50(5):257-264 (1989).

114 Barrett, L. and Rousseau, A.: "Not All Respirator Filter Media Are Created Equal" Presented at the American Industrial Hygiene Conference and Exposition. Washington DC. (May 1996).

115 Moyer, E.S. and Stevens, G.A.: *Particulate Air Purifying Respirator Filter Efficiency: Separation of Aerosol Charge and Relative Humidity Effects.* Prepared for: National Institute for Occupational Safety and Health. Morgantown, WV (1989).

116 Hochrainer D.: Measurement Methods for Electric Charges on Aerosols. *Annals of Occupational Hygiene.* 29(2): 241-249 (1985).

117 Trottier R.A. and Brown, R.C.: The Effects of Aerosol Charge and Filter Charge on the Filtration of Submicrometer Aerosols. *Journal of Aerosol Science.* 21(Suppl. 1): S689-S692 (1990).

118 Blackford, D.B.; Bostock, G.J.; Brown, R.C.; et al.: "Alteration in the Performance of Electrostatic Filters Caused by Exposure to Aerosols" *Proceedings from the 4th World Filtration Congress.* Ostende, Belgium 7.27-7.33 (1986).

119 Rossano, A.T. Jr. and Silverman, Leslie: Electrostatic Effects in Fiber Filters for Aerosols. *Heating and Ventilating's Reference Section* May (1954).

120 Oak, Myoung Joon; Saville, D.A.; Lamb, G.E.R.: Particle Capture of Fibers in Strong Electric Fields. I. Experimental Studies of the Effects of Fiber Charge, Fiber Configuration, and Dendrite Structure. *Journal of Colloid and Interface Science* 106(2):490-501 (1985).

121 Ariman, Teoman; Ojalvo, Morris S.; Drehmel, Dennis C.: Novel Concepts, Methods and Advanced Technology in Particulate/Gas Separation. *Journal of the Air Pollution Control Association.* 29(8):818-822 (1979).

122 Fahrbach, Jorg: The Life Span of High Quality Particulate Filters for Respiratory Protection Equipment - A Possibility for their Rapid Evaluation. *Staub-Reinhalt Luft* 33:146-149 (1973).

123 Schmidt, E.: Experimental Investigations into the Compression of Dust Cakes Deposited on Filter Media. *Filtration and Separation* 32(8):789-793 (1995).

124 Liu, Benjamin Y.H. and Pui, David Y.H.: Electrical Neutralization of Aerosols. *Aerosol Science* 5:465-472 (1974).

125 Walker A.J. and Brown, R.C.: Application of Cavity Theory to the Discharge of Electrostatic Dust Filters by X-Rays. *Applied Radiation Isot.* 39(7):677-684 International Journal of Radiation Applied Instrumentation Part A. (1988).

126 Knutson, Earl O.: "Extended Electric Mobility method for Measuring Aerosol Particle size and Concentration". *Fine Particles Aerosol Generation, Measurement, Sampling, and Analysis* Ed. Benjamin Y. H. Liu, Academic Press, Inc. New York (1976).

127 NIOSH Respirator User Notice from Donald L. Campbell, Acting Branch Chief, Certification and Quality Assurance Branch, Division of Respiratory Disease Studies of Department of Health and Human Services, NIOSH to distribution. May 2, 1997.

128 Personal email from Mary Jo Abler of the 3M Company on 9/24/98.

129 Personal telephone conversation with Andy Viner of the 3M Company on 3/17/98.

130 Hicks, Jeffrey: Asphalt Industry Cross Sectional Exposure Assessment Study. *Applied Occupational and Environmental Hygiene* 10(10):840-848. (1995).

131 Dunzik, D.E.; Gilman, R.D.; Haigney, B.C.; et al.: "Evaluation and Enhancement of the Performance of Benzene Soluble Methods for Asphalt Fume Assessment". Scheduled for submittal for publication to American Occupational and Environmental Hygiene Journal. (April 1995).

132 Sivak, Andrew; Menies, Kenneth; Beltis, Kevin; et al. Arthur D. Little, Inc. Cambridge, MA: *Assessment of the Cocarcinogenic/Promoting Activity of Asphalt Fumes* Prepared for: National Institute for Occupational Safety and Health, Cincinnati, OH (contract 200-83-2612) (1989).

133 Niemeier, R.W.; Thayer, P.S.; Menzies, K.T.; et al.: "A Comparison of the Skin Carcinogenicity of Condensed Roofing Asphalt and Coal Tar Pitch Fumes". *Polynuclear Aromatic Hydrocarbons: A Decade of Progress* Tenth International Symposium. pp. 609-647. (1988).

134 National Institute for Occupational Safety and Health, "NIOSH FACTS" (August 12, 1998) *Construction Safety and Health.* http//ftp.cdc.gov.niosh/constfc.html [10/23/98].

135 Woskie, Susan R.; Smith, Thomas J.; Hallock, Marilyn F.; et al.: Size-selective pulmonary dose indices for metal-working fluid aerosols in machining and grinding operations in the automobile manufacturing industry. *American Industrial Hygiene Association Journal* 55(1):20-29 (1994).

136 National Institute for Occupational Safety and Health, *Criteria for a Recommended Standard: Occupational Exposure to Metalworking Fluid* (DHHS Publication No. 98-102) U.S. Department of Health and Human Services, Public Health Services, Centers for Disease Control and Prevention, National Institute for Occupational Safety and Health, Cincinnati, OH. (January 1998).

137 Personal telephone conversation with David Leith of the University of North Carolina on 9/27/96.

138 Biermann, A.H. and Bergman, W.: Filter Penetration Measurements Using a condensation Nuclei Counter And An Aerosol Photometer. *Journal of Aerosol Science* 19(4):471-483 (1988).

139 Tillery, M.I.; Salzman, G.C.; Ettinger, H.J.: "The Effect of Particle Size Variation on Filtration Efficiency Measured by HEPA Filter Quality Assurance Test". *17th DOP Nuclear Air Cleaning Conference.* Denver, CO. 895-908 (1982).

140 Personal telephone conversation with Marv Tillery of Los Alamos National Laboratory on 2/16/99.

141 Nelson, Gary O.: *Gas Mixtures Preparation and Control* Lewis Publishers. Ann Arbor, MI (1992).

142 Han, Don-Hee; Willeke, Klaus; Colton, Craig E.: Quantitative Fit Testing Techniques and Regulations for Tight -Fitting Respirators: Current Methods Measuring Aerosol or Air Lakage, and New Developments. *American Industrial Hygiene Association Journal* 58:219-228 (1997).

143 Myojo, Toshihiko; Willeke, Klaus; Chen, Chih-Chieh: Fit Test for Filtering Facepieces: Search for a Low-Cost, Quantitative Method. *American Industrial Hygiene Association Journal.* 55(9): 797-805 (1994).

144 Iverson, Sandra G.; Danisch, Susan G.; Mullins, Haskell E.; et al.: Validation of a Quantitative Fit Test for Dust/Fume/Mist Respirators: Part 1. *Applied Occupational and Environmental Hygiene* 7(3):161-167 (1992).

145 Danisch, Susan G.; Mullins, Haskell E.; Rhoe, Carol R.: A Quantitative Fit Test for Dust/Mist Respirators: Part II. *Applied Occupational and Environmental Hygiene* 7(4):241-245 (1992).

146 Hinds, William C. and Kraske, Gerhard: Performance of Dust Respirators with Facial Seal Leaks: I. Experimental. *American Industrial Hygiene Association Journal.* 48(10): 836-841 (1987).

147 Willeke, Klaus and Baron, Paul A.: *Aerosol Measurement Principles, Techniques, and Application.* Van Nostrand Reinhold. New York, NY. (1993).

148 Personal telephone conversation with Michael Bergman of the National Institute for Occupational Safety and Health (NIOSH) on 12/26/96.

149 National Institute for Occupational Safety and Health,"Criteria for a Recommended Standard: Occupational Exposure to Metalworking Fluid" (April 1, 1996) http//www.cdc.gov/niosh/mwfcd.html [8.27/96].

150 National Institute for Occupational Safety and Health, "Benzene-Soluble Fraction and Total Particulate (Asphalt Fumes)" (November 2, 1998) *PFP#982365983.* http://www.cdc.gov/niosh/pdfs/5042.pdf [3/3/99].

151 Brosseau, Lisa M.; McCullough, Nicole Vars; Vesley, Donald: Mycobacterial Aerosol Collection Efficiency of Respirator and Surgical Mask Filters Under Varying Conditions of Flow and Humidity. *Applied Occupational and Environmental Hygiene* 12(6):435-445 (1997).

152 Myojo, Toshihiko and Sugimoto, Mitsumasa. Comparative Study of Challenge Aerosol for Performance Test for Dust Respirators. *Industrial Health* 35(4):502-507 (1998).

153 Moore II, Dan H.; Tucker, James D., Jones, Irene M.; et al.: A Study of the Effects of Exposure on Cleanup Workers at the Chernobyl Nuclear Reactor Accident Using Multiple End Points. *Radiation Research* 148:436-475 (1997).

154 Moyer, Ernest and Bergman, Michael. *Filter Efficiency Degradation in N95 Respirators Caused by Sodium Chloride Aerosol.* NIOSH Certification and Quality Assurance Branch. 5/14/98

155 Personal telephone conversation with Ernest Moyer of the National Institute for Occupational Safety and Health (NIOSH) on 12/21/98.

156 Personal telephone conversation with Larry Olsen of NIOSH on 2/10/99.

157 Stafford, Ronald G. and Ettinger, Harry J. Comparison of Filter Media Against Liquid and Solid Aerosol. *American Industrial Hygiene Association Journal* 32(5):319-326 (1971).

158 Industrial Safety Equipment Association: *Use and Selection Guide for Non-Powered Air Purifying Particulate Respirators.* ISEA publication, Arlington, VA (1996).

APPENDIX A

ARTIFICIAL PERSPIRATION FORMULA

ARTIFICIAL PERSPIRATION FORMULA:

Add the following chemicals to a 1000 ml volumetric flask:

1. Sodium Chloride (J.T. Baker, Phillipsburg, NJ), 3 grams
2. Sodium Sulfate (J.T. Baker, Phillipsburg, NJ), 1 gram
3. Urea (Mallinckrodt Chemical Works, Paris, KY), 2 grams
4. Lactic Acid (J.T. Baker, Phillipsburg, NJ), 2.0 ml
5. Triolein (Sigma Chemical Company, St. Louis, MO), 2.0 grams
6. Tristerin (Sigma Chemical Company, St. Louis, MO), 2.0 grams

Add distilled water to volume and stir overnight at room temperature. Only a portion of the lipids (triolein and tristearin) will dissolve. Filter the undissolved materials from the liquid and store the liquid at 4 ^{o} C to prevent bacterial growth.

Reference: Fisher, A.A.. *Contact Dermatitis 2nd Edition.* Lea and Febiger, Philadelphia, PA. p.27 (1973).

APPENDIX B

RESULTS TABLES

Table B.1 Testing Matrix by Respirator Type and Test Aerosol

N95 Respirators	NaCl	DOP	Al_2O_3	Asphalt	MCF lab	MCF field	Saturation
Gerson 1730	☒						
Gerson 2735S	☒						☒
MSA Affinity Plus	☒		☒	☒	☒	☒	☒
Moldex 2200	☒						
Pro-Tech F200 N95 Filters	☒		☒	☒	☒	☒	
Racal Delta lot A	☒			☒			
Racal Delta lot B	☒			☒			
Racal (mechanical)	☒		☒	☒	☒	☒	☒
Tecnol PFR95	☒			☒			☒
3M 1860 N-95	☒						
3M 8210 N-95	☒		☒		☒	☒	☒
Uvex/Pro-Tech 4010	☒						
Willson Safety N95 Filters	☒						
P100 Respirators							
3M 2091		☒	☒	☒	☒	☒	
3M 7093 (mechanical)		☒					
Pro-Tech G108		☒					

☒=selected for testing

Table B.2 Variability in Upstream Sodium Chloride Readings
Respirator Flow Rate 85 lpm

	Photometer Reading	CNC Reading
Average Upstream Difference	0.0931	-182000
Standard Deviation (σ)	0.161	673728.656
Sample Size	54	54
Paired t test	-1.9877	4.2379
P value	0.0001	0.0520

CMD 0.085 μm, GSD 1.84

Table B.3 Variability in Upstream Sodium Chloride Readings
Respirator Flow Rate 43 lpm

	Photometer Reading	CNC Reading
Average Upstream Difference	0.220	-649000
Standard Deviation (σ)	0.285	869405.093
Sample Size	10	10
Paired t test	2.4381	-2.3589
P value	0.0375	0.0427

CMD 0.085 μm, GSD 1.84

Table B.4 Variability in Upstream DOP Readings
Respirator Flow Rate 43 lpm

	Photometer Reading	CNC Reading
Average Upstream Difference	4.58	1020000
Standard Deviation	17.59154	3590000
Sample number	15	15
Paired t test	1.0079	1.101853
P value	0.3305	0.289108

CMD 0.20μm, GSD 1.60

Table B.5 Face Velocities of N95 Respirators and Filters

Respirator Type	Size	Lot Number	Surface Area (cm2)	Flow Rate (lpm)	Face Velocity (cm/s)
3M 1860	Regular	17031 23 55 9807 Feb97 057	215	85	6.59
3M 8210	Universal	17037 22 7706	220	85	6.44
Gerson 1730	No Size	no lot number	208	85	6.81
Gerson 2735S	Small Fluid Resistant	F2934P006A	176	85	8.05
Moldex 2200 N95	Universal	961112037	226	85	6.27
MSA Affinity Plus	Medium/ Large	1397	196	85	7.23
Pro-Tech F200 N95 Filter	Universal	72701 17	56.7	43	12.64
Racal (mechanical)	Medium	F13/4-23	195	85	7.26
Racal Delta Lot A	Small	E49/1-22	187	85	7.58
Racal Delta Lot B	Medium	E45/3-15	200	85	7.08
Tecnol PFR95	Regular	7A032202	226	85	6.27
Uvex/Pro-Tech 4010	Medium	12496	196	85	7.23
Willson Safety N95 Filters	Universal	7A061	66.5	43	10.78

Table B.6 Average Initial Fit of N95 Respirators Using 2.01 μm Latex Spheres

Sodium Chloride (NIOSH) Method Tests

Initial Fit: % count-measured penetration

Respirator Type	Initial Fit
3M 1860	0.173
3M 8210	0.173
Gerson 1730	0.002
Gerson 2735S	1.669
Moldex 2200	1.251
MSA Affinity Plus	0.026
Pro-Tech F200 Filters	0.015
Racal (mechanical)	0.031
Racal Delta lot A	0.023
Racal Delta lot B	0.012
Tecnol PFR95	<0.001
Uvex/Pro-Tech 4010	0.036
Willson N95 Filters	0.009

N=5 for each respirator type

Table B.7 N95 Respirators Grouped for Comparison to Asphalt Loading CNC-Measured Penetration

Dependent Variable: % penetration (1/2)

Source	Degrees of Freedom	Sums of Squares	Mean Square	F-ratio	P value
Constant	1	5569.42	5569.42	34610.00	≤ 0.0001
mg NaCl	1	1704.27	1704.27	10591.00	≤ 0.0001
respirator type	5	350.382	70.0764	435.47	≤ 0.0001
temperature	1	34.506	34.506	214.43	≤ 0.0001
(mg NaCl)2	1	208.348	208.348	1294.70	≤ 0.0001
mg NaCl* respirator type	5	33.1203	6.62405	41.16	≤ 0.0001
Error	2615	420.805	0.16092		
Total	2628	2751.44			

R 2 =0.847

Table B.8 N95 Respirators Grouped for Comparison to Asphalt Loading Photometer-Measured Penetration

Dependent Variable: log(% penetration+0.11)

Source	Degrees of Freedom	Sums of Squares	Mean Square	F-ratio	P value
Constant	1	474.773	474.773	15862.00	≤ 0.0001
mg NaCl	1	153.334	153.334	5123.00	≤ 0.0001
respirator type	5	53.7563	10.7513	359.21	≤ 0.0001
fit	1	3.48495	3.48495	116.43	≤ 0.0001
(mg NaCl)2	1	15.5669	15.5669	520.10	≤ 0.0001
mg NaCl* respirator type	5	28.4255	5.6851	189.94	≤ 0.0001
Error	2580	77.2211	0.029931		
Total	2593	331.789			

R 2=0.767

Table B.9 N95 Respirators Grouped for Comparison to Aluminum Oxide Dust and Metal Cutting Fluid Mist Loading CNC-Measured Penetration

Dependent Variable: % penetration (3/4)

Source	Degrees of Freedom	Sums of Squares	Mean Square	F-ratio	P value
Constant	1	5402.93	5402.93	9017.70	≤ 0.0001
mg NaCl	1	2590.07	2590.07	4322.90	≤ 0.0001
respirator type	3	424.164	141.388	235.98	≤ 0.0001
temperature	1	191.516	191.516	319.65	≤ 0.0001
(mg NaCl)2	1	551.246	551.246	920.05	≤ 0.0001
(mg NaCl)3	1	148.862	148.862	248.46	≤ 0.0001
mg NaCl* respirator type	3	72.386	24.1287	40.272	≤ 0.0001
Error	1777	1064.69	0.59915		
Total	1787	5042.94			

R 2=0.789

Table B.10 N95 Respirators Grouped for Comparison to Aluminum Oxide Dust and Metal Cutting Fluid Mist Loading Photometer-Measured Penetration

Dependent Variable: (% penetration+0.0001) (1/3)

Source	Degrees of Freedom	Sums of Squares	Mean Square	F-ratio	P value
Constant	1	726.835	726.835	25494.00	≤ 0.0001
mg NaCl	1	100.45	100.45	3523.40	≤ 0.0001
respirator type	3	39.2388	13.0796	458.78	≤ 0.0001
fit	1	4.23826	4.23826	148.66	≤ 0.0001
(mg NaCl)2	1	13.0418	13.0418	457.45	≤ 0.0001
mg NaCl* respirator type	3	20.3569	6.78564	238.01	≤ 0.0001
Error	1770	50.4622	0.02851		
Total	1779	227.788			

R 2=0.778

Table B.11 Face Velocities of P100 Respirator Cartridges and Filters

Respirator Type	Size	Lot Number	Surface Area (cm2)	Flow Rate (lpm)	Face Velocity (cm/s)
3M 2091	Universal	17045/17127	154	43	4.65
3M 7093	Universal	7007	189	43	3.79
Pro-Tech G108	Universal	62511 05	535	43	1.34

Table B.12 3M 2091 Respirator Comparison to Asphalt, Aluminum Oxide Dust, and Metal Cutting Fluid Mist Loading CNC-Measured Penetration

Dependent Variable: (% penetration)(2/5)

Source	Degrees of Freedom	Sums of Squares	Mean Square	F-ratio	P value
Constant	1	0.230075	0.230075	3546.90	≤ 0.0001
mg. DOP loaded	1	0.052356	0.052356	807.13	≤ 0.0001
minutes loaded	1	0.00374	0.00374	57.66	≤ 0.0001
relative humidity	1	0.004265	0.004265	65.74	≤ 0.0001
temperature	1	0.022516	0.022516	347.12	≤ 0.0001
Error	537	0.034834	0.000065		
Total	541	0.117711			

R 2=0.704

Table B.13 3M 2091 Respirator Comparison to Asphalt, Aluminum Oxide Dust, and Metal Cutting Fluid Mist Loading
Photometer-Measured Penetration
Dependent Variable: (% penetration) (4/5)

Source	Degrees of Freedom	Sums of Squares	Mean Square	F-ratio	P value
Constant	1	0.004395	0.004395	2892.6	≤ 0.0001
mg. DOP loaded	1	0.000002	0.000002	1.043	0.3077
relative humidity	1	0.000036	0.000036	23.742	≤ 0.0001
temperature	1	0.000013	0.000013	8.7445	0.0033
minutes loaded	1	0.000055	0.000055	36.258	≤ 0.0001
Error	442	0.000672	0.000002		
Total	446	0.000778			

R 2=0.136

Table B.14 Average Initial Fit of N95 Respirators Using 2.01 μm Latex Spheres
Asphalt Contaminant Tests
Initial Fit: % count-measured penetration

Respirator Type	Initial Fit
MSA Affinity Plus	0.738
Pro-Tech F200	<0.001
Racal (mechanical)	0.073
Racal Delta lot A	0.021
Racal Delta lot B	0.052
Tecnol PFR95	0.136

N= MSA Affinity Plus=8, Pro-Tech F200=8, Racal (mechanical)=16, Racal lot A=8, Racal lot B=12, Tecnol PFR95=8, 3M 2091=8

Table B.15 N95 Respirators Loaded with Asphalt Contaminants
CNC-Measured Penetration
Dependent Variable: 1/(% penetration) (1/3)

Source	Degrees of Freedom	Sums of Squares	Mean Square	F-ratio	P value
Constant	1	33.9222	33.9222	75002	≤ 0.0001
mg. asphalt loaded	1	0.000075	0.000075	0.16557	0.6846
respirator type	5	0.297003	0.059401	131.33	≤ 0.0001
mg. asphalt * respirator type	5	0.012167	0.002433	5.3804	0.0001
Error	164	0.074175	0.000452		
Total	175	0.38342			

R 2=0.806

Table B.16 N95 Respirators Loaded with Asphalt Contaminants
Photometer-Measured Penetration
Dependent Variable: 1/(% penetration) (1/3)

Source	Degrees of Freedom	Sums of Squares	Mean Square	F-ratio	P value
Constant	1	122.79	122.79	17951	≤ 0.0001
mg. asphalt	1	1.40589	1.40589	205.53	≤ 0.0001
respirator type	5	3.54851	0.709701	103.75	≤ 0.0001
(mg. asphalt)2	1	0.083395	0.083395	12.192	0.0006
mg. asphalt * respirator type	5	0.316051	0.06321	9.2408	≤ 0.0001
Error	162	1.10814	0.00684		
Total	174	6.46198			

R 2=0.865

Table B.17 N95 Respirators Loaded with Asphalt Contaminants
Electrostatic Compared to Mechanical N95
CNC-Measured Penetration: 1/(% penetration)(1/3)
Level of 'mg asphalt* respirator type'

Respirator Type	Coefficient	Standard Error	Individual Slope	Z Test	P value
MSA Affinity Plus	-1.14E-04	1.78E-04	-4.02E-04	-0.131	0.4480
Pro-Tech F200	1.13E-03	2.38E-04	8.46E-04	-3.841	0.0001
Racal (mechanical)	-7.85E-05	2.07E-04	-3.66E-04		
Racal Delta lot B	-5.44E-04	4.01E-04	-8.32E-04	-1.033	0.1509
Racal Delta lot A	-9.39E-05	1.40E-04	-3.82E-04	-0.062	0.4754
Tecnol PFR95	-3.03E-04	1.35E-04	-5.91E-04	-0.908	0.1820

Table B.18 N95 Respirators Loaded with Asphalt Contaminants
Electrostatic Compared to Mechanical N95
Photometer-Measured Penetration: 1/(% penetration)(1/3)
Level of 'mg asphalt* respirator type'

Respirator Type	Coefficient	Standard Error	Individual Slope	Z Test	P value
MSA Affinity Plus	2.73E-03	6.99E-04	-5.53E-03	1.95	0.0256
Pro-Tech F200	4.61E-03	1.03E-03	-3.66E-03	3.01	0.0013
Racal (mechanical)	6.11E-04	8.33E-04	-7.65E-03		
Racal Delta lot B	-8.15E-03	1.60E-03	-1.64E-02	-4.87	0.0000
Racal Delta lot A	6.17E-05	6.31E-04	-8.20E-03	-0.53	0.2996
Tecnol PFR95	1.47E-04	6.54E-04	-8.11E-03	-0.44	0.3308

Table B.19 Average Initial Fit of N95 Respirators Using 2.01 μm Latex Spheres
Aluminum Oxide Dust Tests
Initial Fit: % count-measured penetration

Respirator Type	Initial Fit
3M 8210	0.275
MSA Affinity Plus	0.019
Pro-Tech F200	0.007
Racal (mechanical)	0.097

N=5 for each respirator type

Table B.20 Concentration (mg/m3) of Aluminum Oxide Dust by Respirator Flow Rate

	Average Conc. (mg/m3)	Minimum Conc.(mg/m3)	Maximum Conc. (mg/m3)	Standard Deviation
all tests	9.60	4.38	18.50	1.87
flow rate 43 lpm	10.26	6.46	18.50	2.11
flow rate 85 lpm	9.15	4.38	13.74	1.54

Table B.21 Size Distribution of Aluminum Oxide Dust by Respirator Flow Rate

	CMD (μm)	MMD (μm)	GSD
all tests combined			
average (EMBED Equation.2)	1.40±0.54	2.70±0.45	
minimum	4.18	6.04	0.72
maximum	0.74	1.36	0.64
flow rate 43 lpm			
average ($\bar{x}\pm\sigma$)	1.42±0.53	2.70±0.66	
minimum	1.00	1.67	0.64
maximum	4.18	6.04	0.72
flow rate 85 lpm			
average ($\bar{x}\pm\sigma$)	1.39±0.11	2.71±0.22	
minimum	0.74	1.36	0.64
maximum	1.53	2.85	0.66

Size distribution measured with Climet

Table B.22 N95 Respirators Loaded with Aluminum Oxide Dust CNC-Measured Penetration

Dependent Variable: log % penetration

Source	Degrees of Freedom	Sums of Squares	Mean Square	F-ratio	P value
Constant	1	35.1955	35.1955	1614.8	≤ 0.0001
mg Al_2O_3 loaded	1	13.2027	13.2027	605.77	≤ 0.0001
respirator type	3	2.67025	0.890082	40.839	≤ 0.0001
fit	1	0.246346	0.246346	11.303	0.0013
mg Al2 O3 * respirator type	3	0.373323	0.124441	5.7096	0.0015
mg Al2 O3 * fit	1	0.176161	0.176161	8.0826	0.0059
respirator type * fit	3	1.33683	0.445609	20.446	≤ 0.0001
Error	67	1.46026	0.021795		
Total	79	19.4658			

R^2=0.925

Table B.23 N95 Respirators Loaded with Aluminum Oxide Dust Photometer-Measured Penetration

Dependent Variable: log % penetration

Source	Degrees of Freedom	Sums of Squares	Mean Square	F-ratio	P value
Constant	1	3.81073	3.81073	108.11	≤ 0.0001
mg Al2 O3 loaded	1	6.71611	6.71611	190.53	≤ 0.0001
respirator type	3	0.671003	0.223668	6.3453	0.0007
fit	1	0.661912	0.661912	18.778	≤ 0.0001
mg Al2 O3 * respirator type	3	0.50517	0.16839	4.7772	0.0044
respirator type * fit	3	1.56027	0.520089	14.755	≤ 0.0001
Error	68	2.39694	0.035249		
Total	79	12.5114			

R^2=0.808

Table B.24 N95 Respirators Loaded with Aluminum Oxide Dust CNC-Measured Penetration: log (% penetration)

Level of 'mg Al2 O3 * respirator type'

Respirator Type	Coefficient	Standard Error	Individual Slope	Z Test	P value
3M 8210	3.95E-04	3.27E-04	-4.08E-03	-1.35	0.0885
MSA Affinity Plus	-3.35E-04	3.02E-04	-4.80E-03	-3.16	0.0008
Pro-Tech F200	-1.04E-03	4.36E-04	-5.51E-03	-3.88	0.0001
Racal (mechanical)	9.82E-04	2.87E-04	-3.49E-03		

Table B.25 N95 Respirators Loaded with Aluminum Oxide Dust Photometer-Measured Penetration: log (% penetration)

Level of 'mg Al2 O3 * respirator type'

Respirator Type	Coefficient	Standard Error	Individual Slope	Z Test	P value
3M 8210	1.04E-03	3.78E-04	-2.23E-03	0.09	0.4626
MSA Affinity Plus	-2.86E-04	3.76E-04	-3.56E-03	-2.43	0.0075
Pro-Tech F200	-1.74E-03	5.45E-04	-5.01E-03	-4.16	<0.0000
Racal (mechanical)	9.88E-04	3.64E-04	-2.28E-03		

Table B.26 Average Initial Fit of N95 Respirators Using 2.01 μm Latex Spheres

Laboratory-Generated Metal Cutting Fluid Mist

Initial Fit: % count-measured penetration

Respirator Type	Initial Fit
3M 8210	0.126
MSA Affinity Plus	0.002
Pro-Tech F200	0.015
Racal (mechanical)	0.121

N=5 for each respirator type

Table B.27 Concentration (mg/m^3) of Laboratory-Generated Metal Cutting Fluid Mist by Respirator Flow Rate

	Average Conc. (mg/m^3)	Minimum Conc.(mg/m^3)	Maximum Conc. (mg/m^3)	Standard Deviation
all tests	1.73	0.67	3.37	0.44
flow rate 43 lpm	1.77	0.67	3.35	0.53
flow rate 85 lpm	1.71	1.04	3.37	0.38

Table B.28 Size Distribution of Laboratory-Generated Metal Cutting Fluid Mist by Respirator Flow Rate

	CMD (μm)	MMD (μm)	GSD
all tests combined			
average	1.00	1.54	
minimum	0.91	0.42	1.40
maximum	1.16	1.74	1.47
flow rate 43 lpm			
average	1.01	1.52	
minimum	0.91	0.42	1.40
maximum	1.16	1.74	1.47
flow rate 85 lpm			
average	1.00	1.55	
minimum	0.93	1.47	1.40
maximum	1.10	1.64	1.45

Size distribution measured with Climet

Table B.29 N95 Respirators Loaded with Laboratory-Generated Metal Cutting Fluid Mist
CNC-Measured Penetration

Dependent Variable: $1/\%\ penetration^{(1/3)}$

Source	Degrees of Freedom	Sums of Squares	Mean Square	F-ratio	P value
Constant	1	21.4643	21.4643	7650.5	≤ 0.0001
mg MCF loaded	1	0.062089	0.062089	22.13	≤ 0.0001
respirator type	3	0.084924	0.028308	10.09	≤ 0.0001
fit	1	0.021932	0.021932	7.8172	0.0067
mg MCF* respirator type	3	0.001432	0.000477	0.17012	0.9162
respirator type*fit	3	0.045259	0.015086	5.3772	0.0022
Error	68	0.190783	0.002806		
Total	79	0.406418			

R^2=0.531

Table B.30 N95 Respirators Loaded with Laboratory-Generated Metal Cutting Fluid Mist
Photometer-Measured Penetration

Dependent Variable: % penetration

Source	Degrees of Freedom	Sums of Squares	Mean Square	F-ratio	P value
Constant	1	143.476	143.476	1092.6	≤ 0.0001
mg MCF loaded	1	0.625291	0.625291	4.7615	0.0339
respirator type	3	17.9625	5.98752	45.594	≤ 0.0001
fit	1	1.13955	1.13955	8.6776	0.0049
temperature	1	0.46461	0.46461	3.538	0.0659
mg MCF* respirator type	3	0.025235	0.008412	0.06405	0.9786
mg MCF* temperature	1	0.634293	0.634293	4.8301	0.0327
Error	49	6.43475	0.131321		
Total	59	27.2863			

R^2=0.764

Table B.31 N95 Respirators Loaded with Laboratory-Generated Metal Cutting Fluid Mist
CNC-Measured Penetration: 1/% penetration$^{(1/3)}$
Level of 'mg metal cutting fluid * respirator type'

Respirator Type	Coefficient	Standard Error	Individual Slope	Z Test	P value
3M 8210	-2.06E-04	5.75E-04	1.21E-03	-0.011	0.4958
MSA Affinity Plus	2.35E-04	5.73E-04	1.65E-03	-0.543	0.2937
Pro-Tech F200	1.69E-04	8.60E-04	1.59E-03	-0.359	0.3598
Racal (mechanical)	-1.98E-04	5.54E-04	1.22E-03		

Table B.32 N95 Respirators Loaded with Laboratory-Generated Metal Cutting Fluid Mist
Photometer-Measured Penetration: % penetration
Level of 'mg metal cutting fluid * respirator type'

Respirator Type	Coefficient	Standard Error	Individual Slope	Z Test	P value
3M 8210	-1.53E-03	3.89E-03	3.47E-03	-0.723	0.2349
MSA Affinity Plus	-6.03E-03	3.90E-03	-1.03E-03	-1.552	0.0603
Pro-Tech F200	5.17E-03	5.86E-03	1.02E-02	0.400	0.3446
Racal (mechanical)	2.39E-03	3.77E-03	7.39E-03		

Table B.33 Average Initial Fit of N95 Respirators Using 2.01 µm Latex Spheres
Metal Cutting Fluid-Field Generated Tests
Initial Fit: % count-measured penetration

Respirator Type	Initial Fit
3M 8210	0.137
MSA Affinity Plus	0.042
Pro-Tech F200	0.008
Racal (mechanical)	0.073

N=8 for each respirator type

Table B.34 N95 Respirators Loaded with Field-Generated Metal Cutting Fluid Mist
CNC-Measured Penetration
Dependent Variable: log(% penetration)

Source	Degrees of Freedom	Sums of Squares	Mean Square	F-ratio	P value
Constant	1	131.398	131.398	5027.8	≤ 0.0001
mg MCF loaded	1	1.84109	1.84109	70.447	≤ 0.0001
respirator type	3	2.07821	0.692738	26.507	≤ 0.0001
respirator type * mg MCF	3	0.062606	0.020869	0.79852	0.498
Error	87	2.2737	0.026134		
Total	94	6.2556			

R^2=0.636

Table B.35 N95 Respirators Loaded with Field-Generated Metal Cutting Fluid Mist
Photometer-Measured Penetration
Dependent Variable: log(% penetration+0.3)

Source	Degrees of Freedom	Sums of Squares	Mean Square	F-ratio	P value
Constant	1	67.0736	67.0736	2303.3	≤ 0.0001
mg MCF loaded	1	12.0624	12.0624	414.22	≤ 0.0001
respirator type	3	3.49389	1.16463	39.993	≤ 0.0001
(mg MCF loaded)^2	1	1.07963	1.07963	37.074	≤ 0.0001
respirator type * mg MCF	3	0.237818	0.079273	2.7222	0.0493
Error	86	2.50437	0.029121		
Total	94	19.3781			

R^2=0.871

Table B.36 N95 Respirators Loaded with Field-Generated Metal Cutting Fluid Mist
CNC-Measured Penetration: log(% penetration)
Level of 'mg metal cutting fluid * respirator type'

Respirator Type	Coefficient	Standard Error	Individual Slope	Z Test	P value
3M 8210	-9.01E-05	7.44E-05	2.52E-04	-1.519	0.0644
MSA Affinity Plus	-2.43E-05	6.05E-05	3.17E-04	-0.945	0.1723
Pro-Tech F200	5.58E-05	1.09E-04	3.97E-04	-0.023	0.4910
Racal (mechanical)	5.86E-05	6.36E-05	4.00E-04		

Table B.37 N95 Respirators Loaded with Field-Generated Metal Cutting Fluid Mist
Photometer-Measured Penetration: log(% penetration+0.3)
Level of 'mg metal cutting fluid * respirator type'

Respirator Type	Coefficient	Standard Error	Individual Slope	Z Test	P value
3M 8210	-1.36E-04	7.91E-05	1.31E-03	-2.882	0.0020
MSA Affinity Plus	1.00E-04	7.52E-05	1.55E-03	-0.662	0.2541
Pro-Tech F200	-1.33E-04	1.25E-04	1.32E-03	-2.105	0.0176
Racal (mechanical)	1.68E-04	6.96E-05	1.62E-03		

Table B.38 Average Initial Fit of N95 Respirators Using 2.01 μm Latex Spheres
Saturation with Artificial Perspiration Tests
Initial Fit: % count-measured penetration

Respirator Type	Initial Fit
3M 8210	0.231
Gerson 2735S	1.607
MSA Affinity Plus	0.001
Racal (mechanical)	0.099
Tecnol PFR95	<0.001

N=5 for each respirator type

Table B.39 N95 Respirators Saturated with Artificial Perspiration
Average Saturation Duration and Net Weight Changes by Respirator Type

Respirator Type	Saturation Duration (min)	Saturation Weight Gain (g)	Weight Loss from Drying (g)	% Residual Solution *
3M 8210	40.2	17.96	17.61	1.96
Gerson 2735S	40.4	10.27	10.16	1.09
MSA Affinity Plus	36.4	29.10	28.81	1.00
Racal (mechanical)	40.6	11.91	11.75	1.41
Tecnol PFR95	40.0	7.74	7.48	3.36

* Residual artificial perspiration solution remaining on the respirator at the end of the drying cycle
N=5 for each respirator type

Table B.40 N95 Respirators Saturated with Artificial Perspiration
Average and Net Difference in Pressure Drop by Respirator Type

Respirator Type	Initial Pressure Drop (inches water)	Final Pressure Drop (inches water)	% difference
3M 8210	0.45	0.46	1.10
Gerson 2735S	0.47	0.46	-0.65
MSA Affinity Plus	0.51	0.51	-0.39
Racal (mechanical)	0.25	0.25	0.00
Tecnol PFR95	0.25	0.27	7.63

N=5 for each respirator type

Table B.41 N95 Respirators Saturated with Artificial Perspiration
CNC-Measured Penetration: % penetration
Paired t-test Comparing Initial and Final % Penetration

Respirator Type	Initial % Penetration	Final % Penetration	p value
3M 8210	12.035	11.421	0.0353
Gerson 2735S	31.680	31.076	0.3501
MSA Affinity Plus	10.276	9.099	0. 0038
Racal (mechanical)	15.655	15.695	0.8185
Tecnol PFR95	13.310	14.331	0.1230

N=5 for each respirator type

Table B.42 N95 Respirators Saturated with Artificial Perspiration
Photometer-Measured Penetration: % penetration
Paired t-test Comparing Initial and Final % Penetration

Respirator Type	Initial % Penetration	Final % Penetration	p value
3M 8210	1.709	1.684	0.7214
Gerson 2735S	7.173	7.031	0.7365
MSA Affinity Plus	1.159	.0835	0.0004
Racal (mechanical)	1.669	1.842	0.0024
Tecnol PFR95	0.648	.0678	0.4014

N=5 for each respirator type

APPENDIX C

GRAPHS

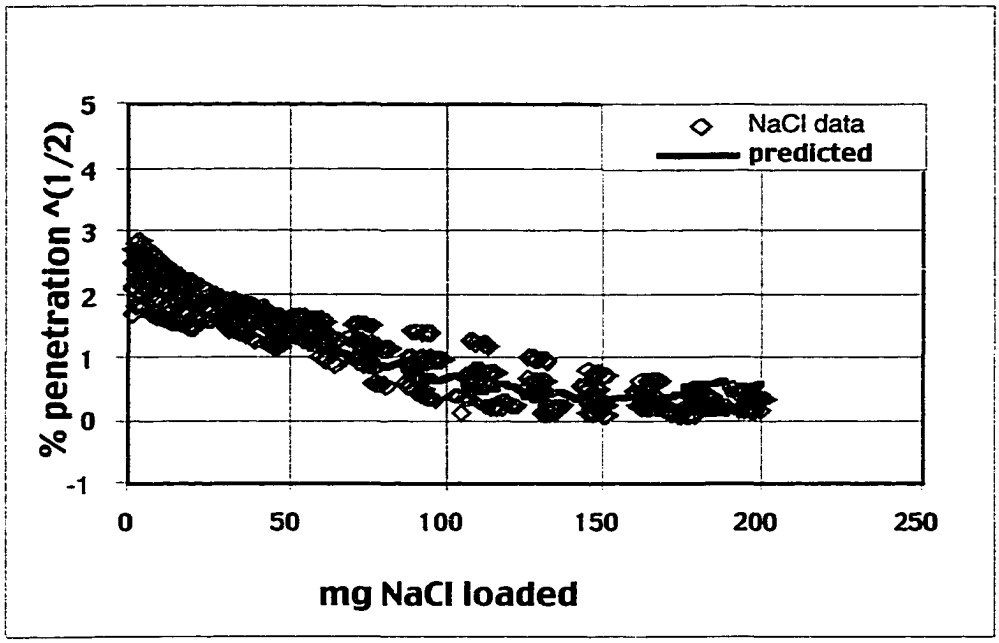

figure C.1 Sodium Chloride Aerosol: Observed and Predicted Penetration MSA Affinity Plus N95 Respirators: Grouped for Loading With Asphalt Contaminants
CNC-Measured Penetration: % penetration $^{(1/2)}$
N=5, fitted CMD= 0.085 μm, fitted GSD=1.84

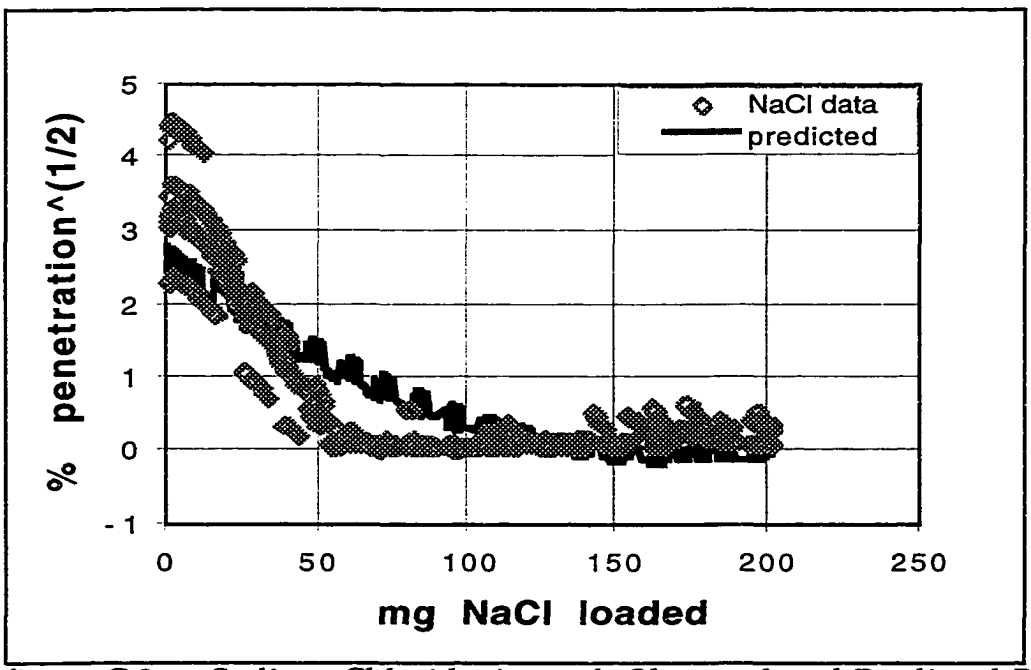

figure C.2 Sodium Chloride Aerosol: Observed and Predicted Penetration Pro-Tech F200 N95 Filter: Grouped for Loading With Asphalt Contaminants
CNC-Measured Penetration: % penetration$^{(1/2)}$
N=5, fitted CMD= 0.085 μm, fitted GSD=1.84

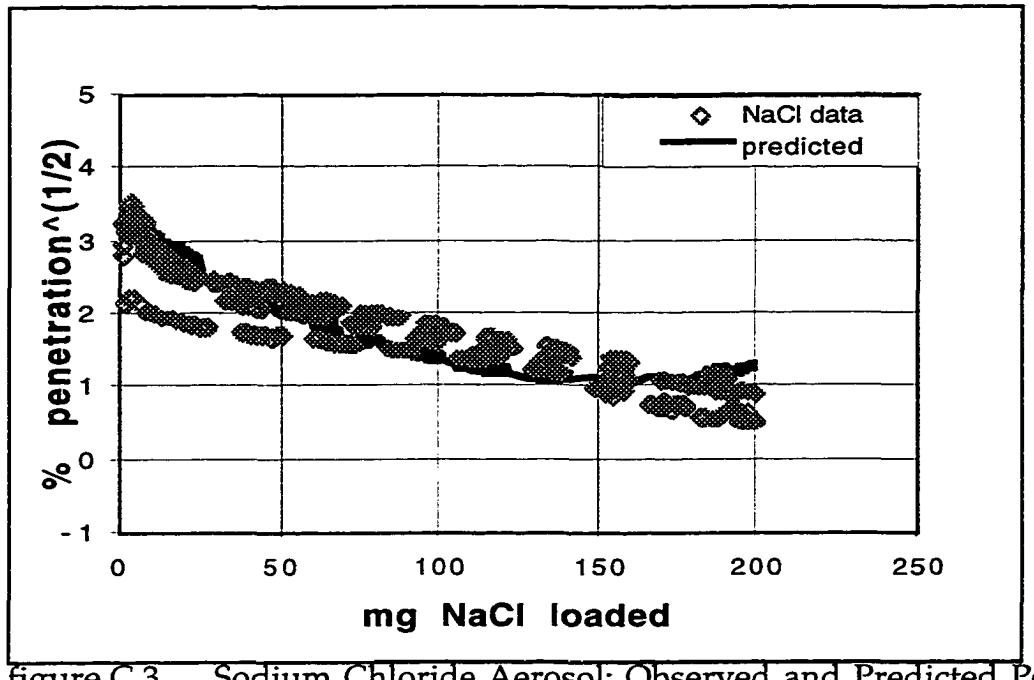

figure C.3 Sodium Chloride Aerosol: Observed and Predicted Penetration Racal (mechanical) N95 Respirators: Grouped for Loading With Asphalt Contaminants
CNC-Measured Penetration: % penetration$^{(1/2)}$
N=5, fitted CMD= 0.085 µm, fitted GSD=1.84

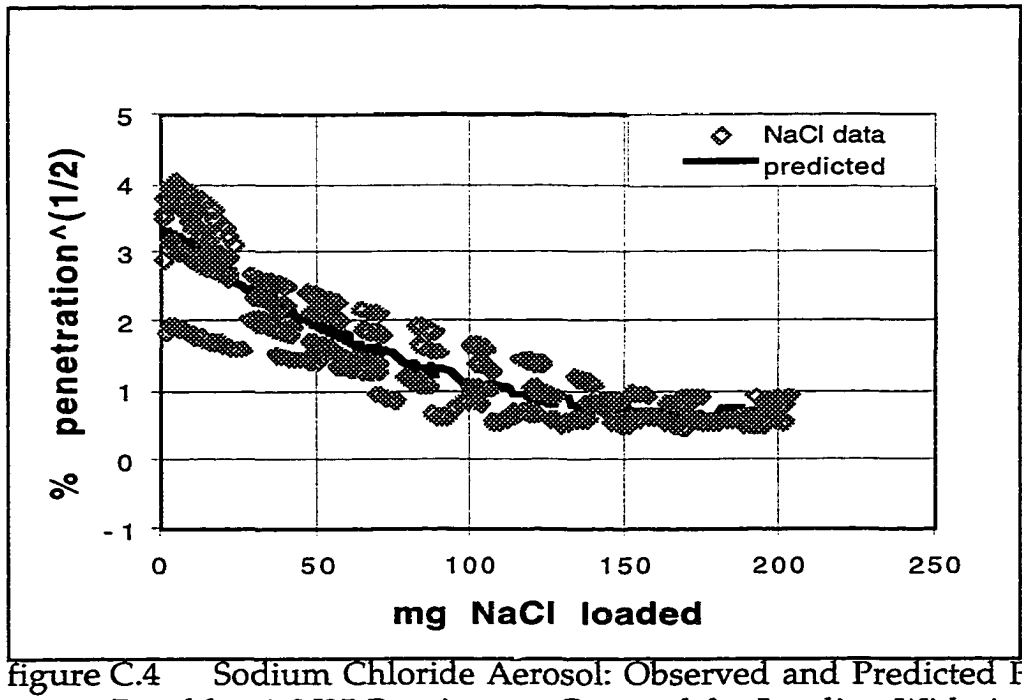

figure C.4 Sodium Chloride Aerosol: Observed and Predicted Penetration Racal lot A N95 Respirators: Grouped for Loading With Asphalt Contaminants
CNC-Measured Penetration: % penetration$^{(1/2)}$
N=5, fitted CMD= 0.085 µm, fitted GSD=1.84

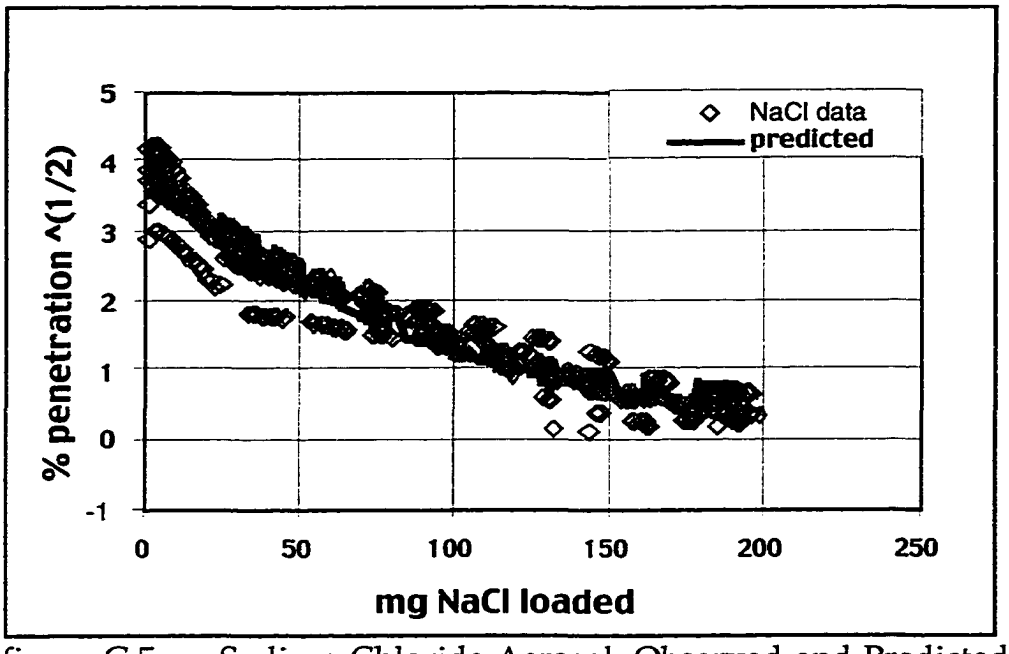

figure C.5 Sodium Chloride Aerosol: Observed and Predicted Penetration Racal lot B N95 Respirators: Grouped for Loading With Asphalt Contaminants
CNC-Measured Penetration: % penetration$^{(1/2)}$
N=5, fitted CMD= 0.085 µm, fitted GSD=1.84

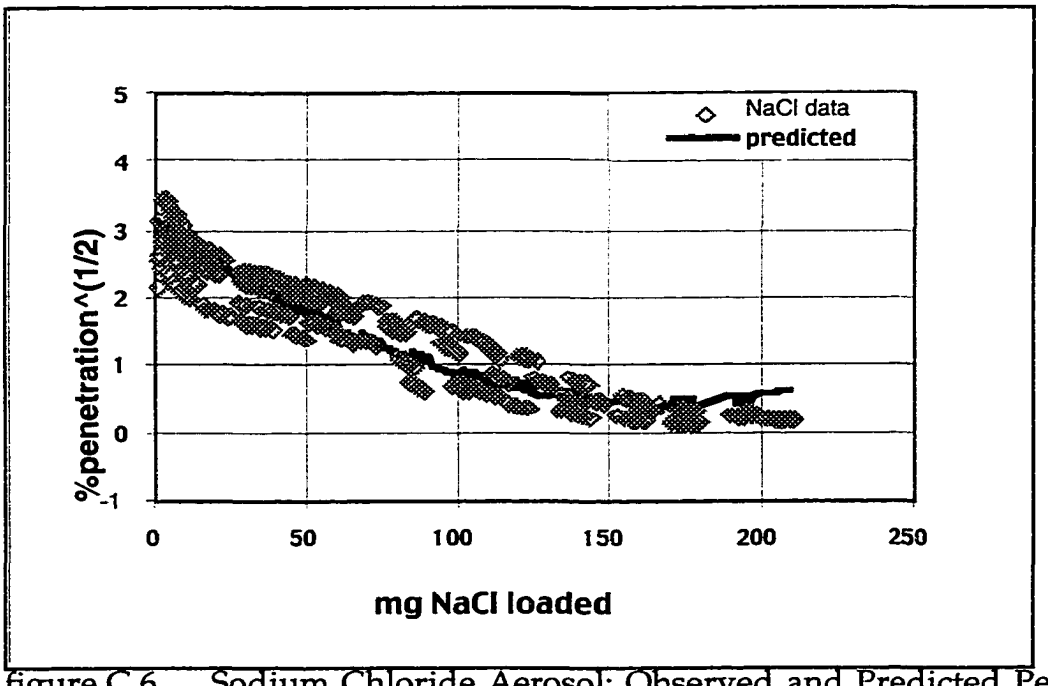

figure C.6 Sodium Chloride Aerosol: Observed and Predicted Penetration Tecnol PFR95 N95 Respirators: Grouped for Loading With Asphalt Contaminants
CNC-Measured Penetration: % penetration$^{(1/2)}$
N=5, fitted CMD= 0.085 µm, fitted GSD=1.84

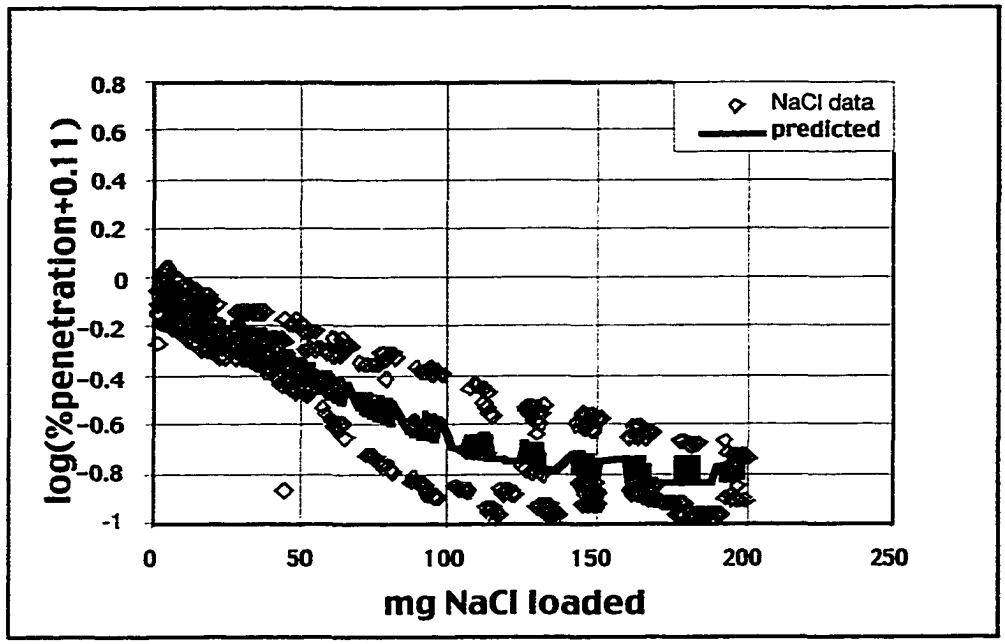

figure C.7 Sodium Chloride Aerosol: Observed and Predicted Penetration MSA Affinity Plus N95 Respirators: Grouped for Loading With Asphalt Contaminants
Photometer-Measured Penetration: log(% penetration+0.11)
N=5, fitted CMD= 0.085 μm, fitted GSD=1.84

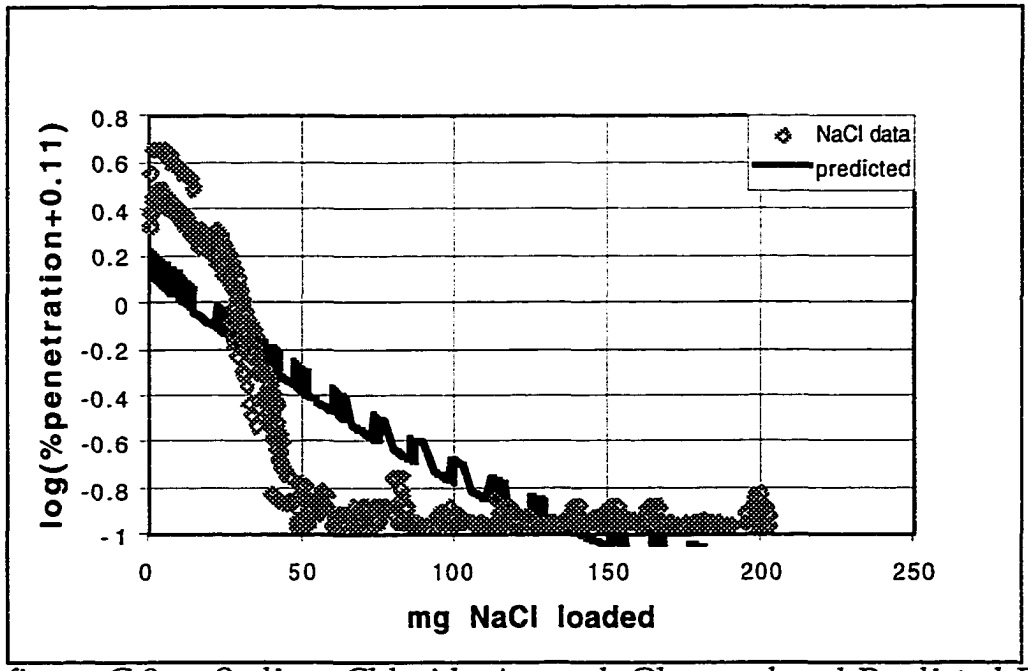

figure C.8 Sodium Chloride Aerosol: Observed and Predicted Penetration Pro-Tech F200 N95 Filters: Grouped for Loading With Asphalt Contaminants
Photometer-Measured Penetration: log(% penetration+0.11)
N=5, fitted CMD= 0.085 μm, fitted GSD=1.84

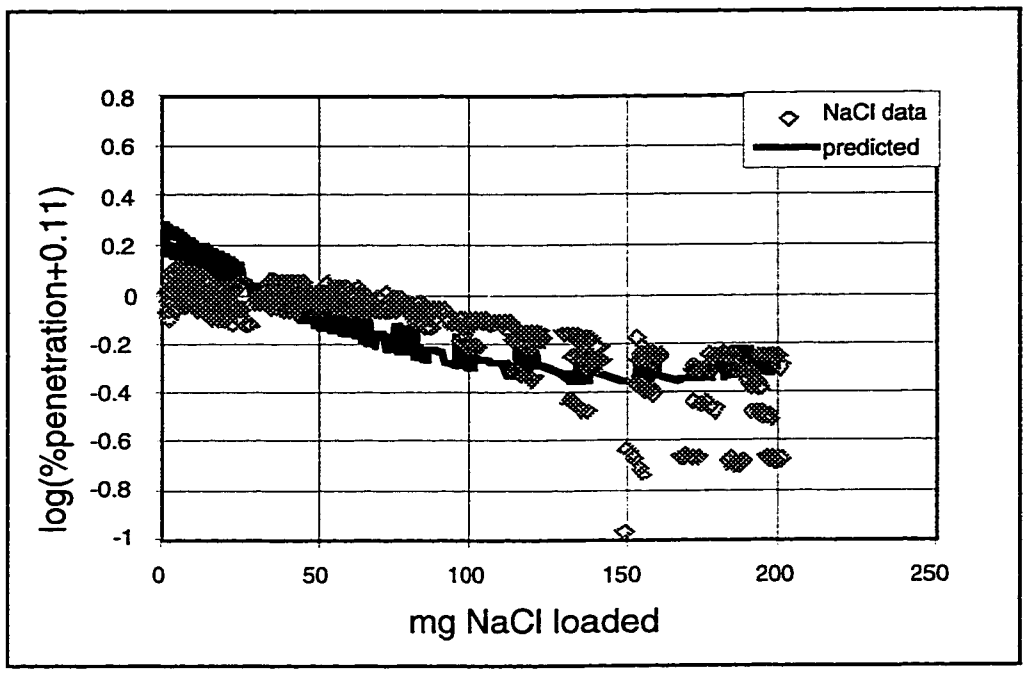

figure C.9 Sodium Chloride Aerosol: Observed and Predicted Penetration Racal (mechanical) N95 Respirators: Grouped for Loading With Asphalt Contaminants
Photometer-Measured Penetration: log(% penetration+0.11)
N=5, fitted CMD= 0.085 µm, fitted GSD=1.84

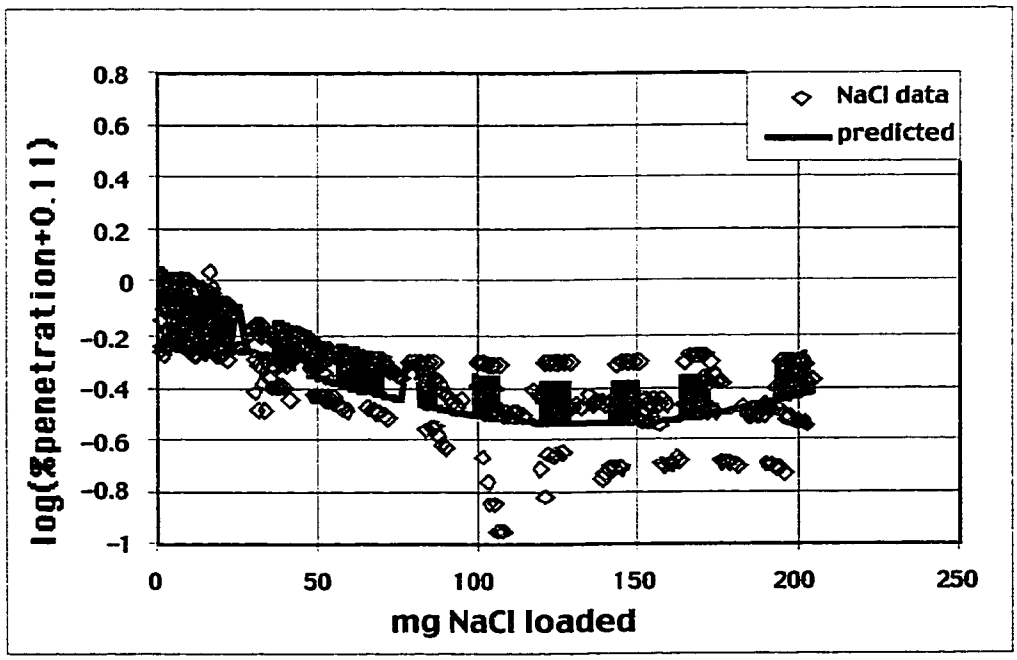

figure C.10 Sodium Chloride Aerosol: Observed and Predicted Penetration Racal lot A N95 Respirators: Grouped for Loading With Asphalt Contaminants
Photometer-Measured Penetration: log(% penetration+0.11)
N=5, fitted CMD= 0.085 µm, fitted GSD=1.84

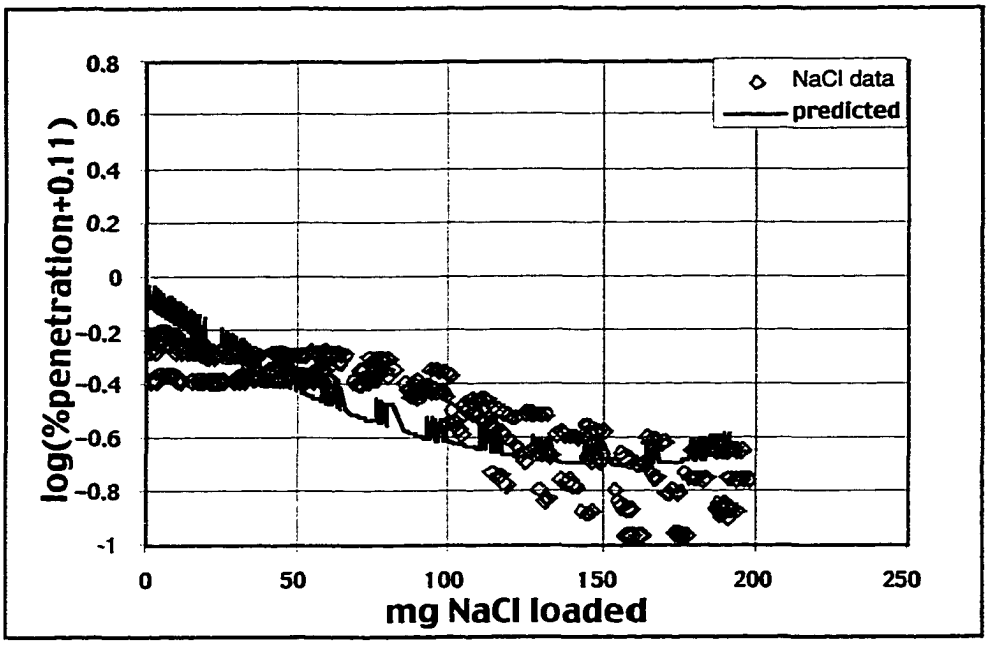

figure C.11 Sodium Chloride Aerosol: Observed and Predicted Penetration Racal lot B N95 Respirators: Grouped for Loading With Asphalt Contaminants
Photometer-Measured Penetration: log(% penetration+0.11)
N=5, fitted CMD= 0.085 µm, fitted GSD=1.84

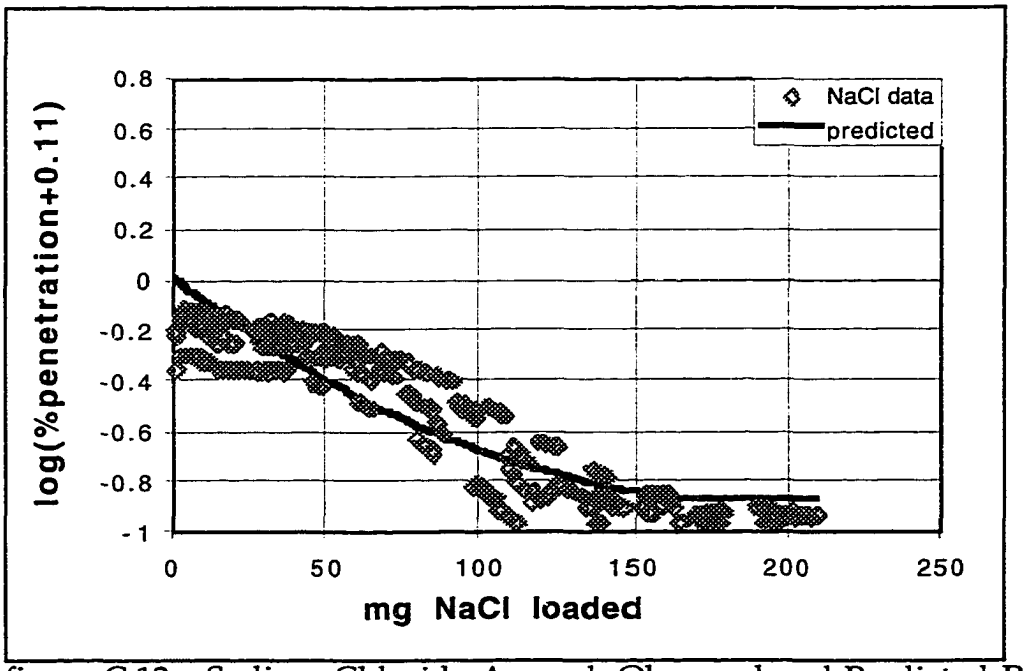

figure C.12 Sodium Chloride Aerosol: Observed and Predicted Penetration Tecnol PFR95 N95 Respirators: Grouped for Loading With Asphalt Contaminants
Photometer-Measured Penetration: log(% penetration+0.11)
N=5, fitted CMD= 0.085 µm, fitted GSD=1.84

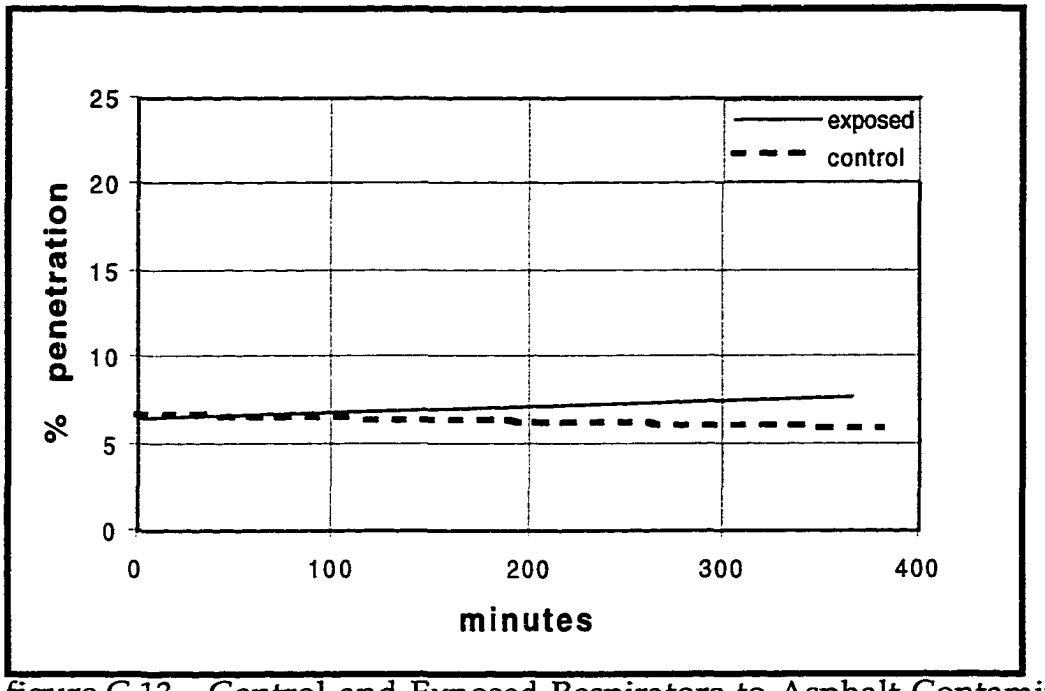

figure C.13 Control and Exposed Respirators to Asphalt Contaminants
MSA Affinity Plus N95 Respirators
CNC-Measured Penetration: % penetration
N exposed=6, N control=2 ,fitted MMAD= 4.36 μm, fitted GSD=1.61

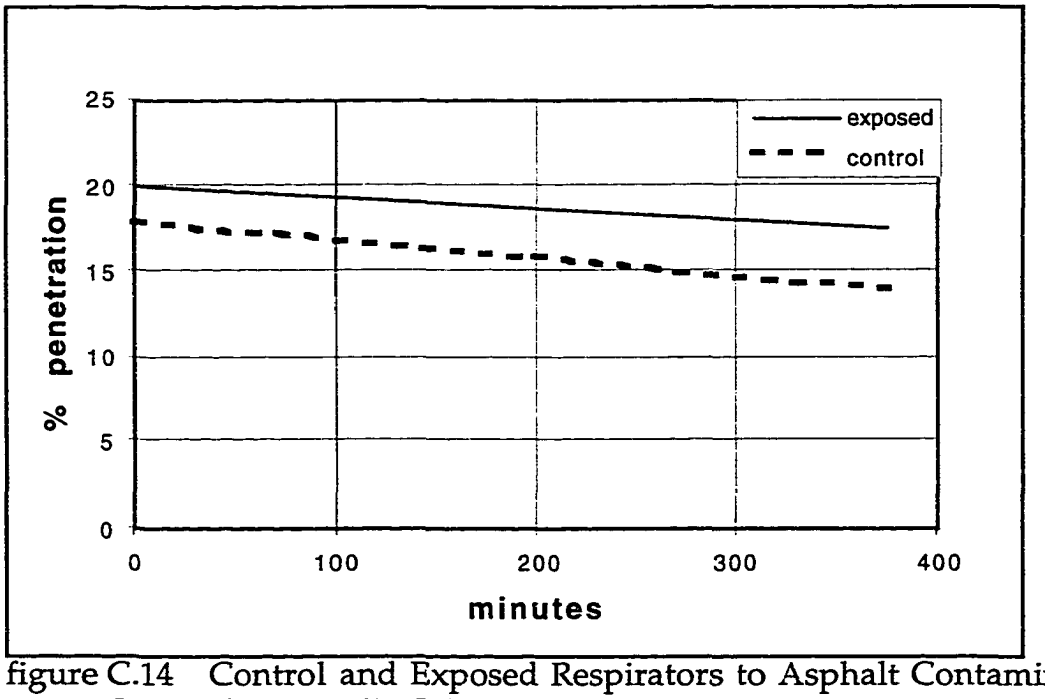

figure C.14 Control and Exposed Respirators to Asphalt Contaminants
Pro-Tech F200 N95 Filters
CNC-Measured Penetration: % penetration
N exposed=6, N control=2 ,fitted MMAD= 4.35 μm, fitted GSD=1.54

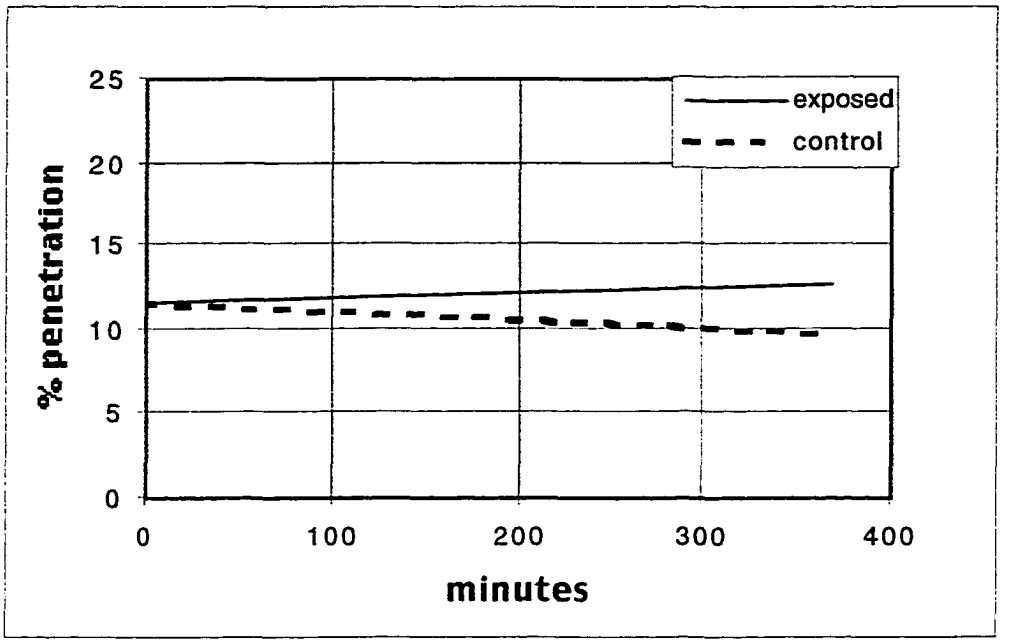

figure C.15 Control and Exposed Respirators to Asphalt Contaminants
Racal (mechanical) N95 Respirators
CNC-Measured Penetration: % penetration
N exposed=12, N control=4 ,fitted MMAD= 5.18 µm, fitted GSD=1.94

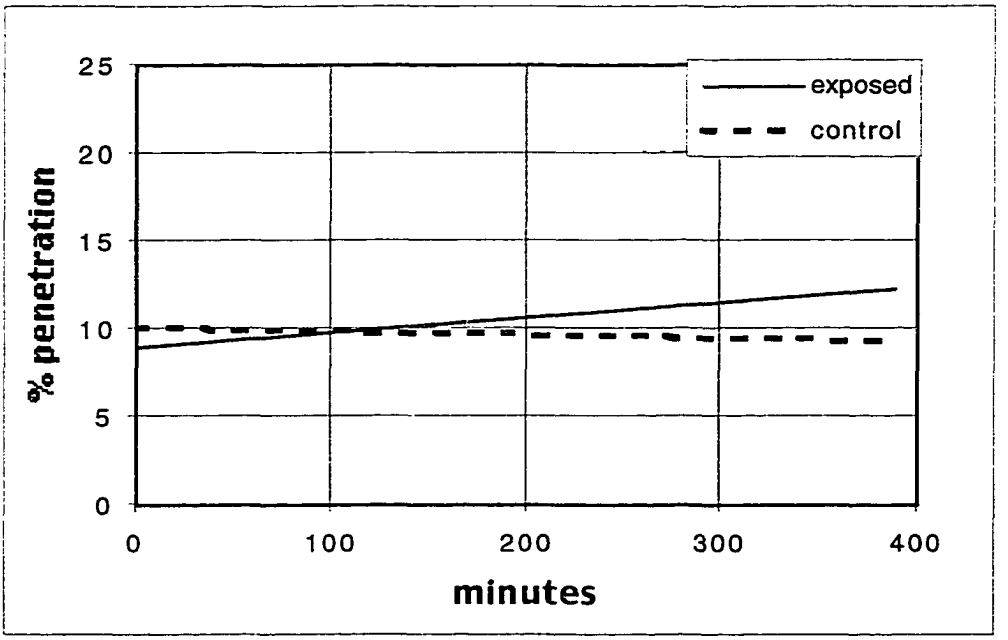

figure C.16 Control and Exposed Respirators to Asphalt Contaminants
Racal Delta lot A N95 Respirators
CNC-Measured Penetration: % penetration
N exposed=6, N control=2 ,fitted MMAD= 4.23 µm, fitted GSD=1.52

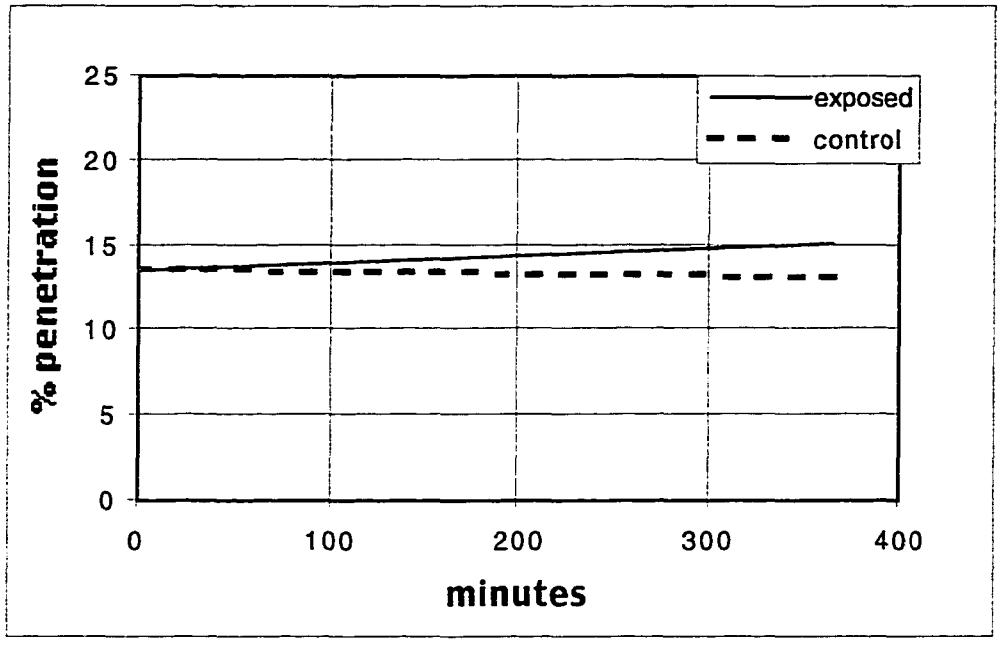

figure C.17 Control and Exposed Respirators to Asphalt Contaminants
Racal Delta lot B N95 Respirators
CNC-Measured Penetration: % penetration
N exposed=9, N control=3 ,fitted MMAD= 3.70 µm, fitted GSD=2.32

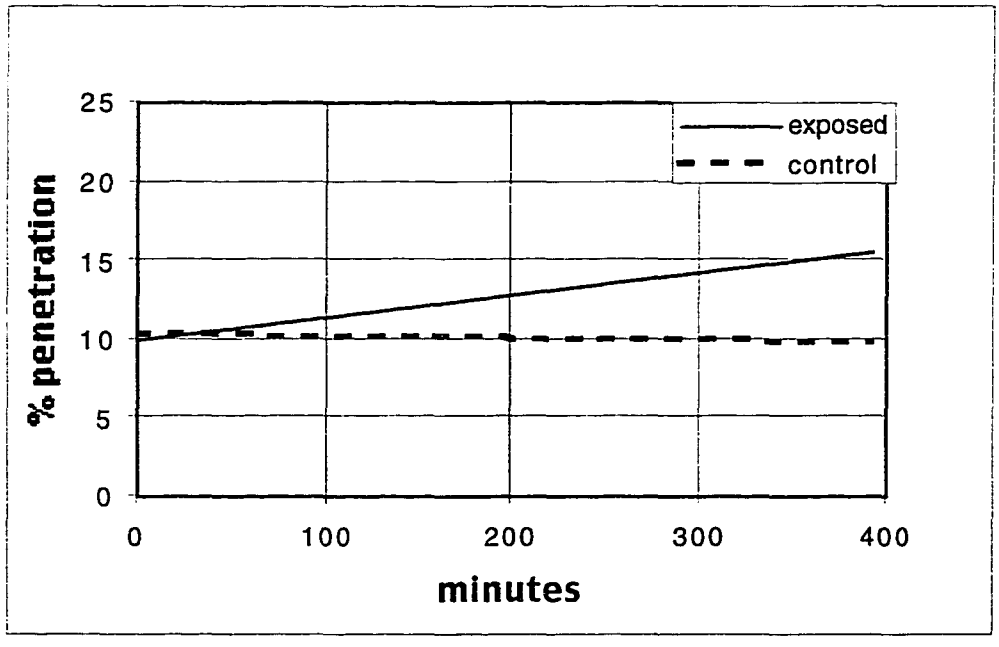

figure C.18 Control and Exposed Respirators to Asphalt Contaminants
Tecnol PFR95 N95 Respirators
CNC-Measured Penetration: % penetration
N exposed=6, N control=2 ,fitted MMAD= 5.01 µm, fitted GSD=1.43

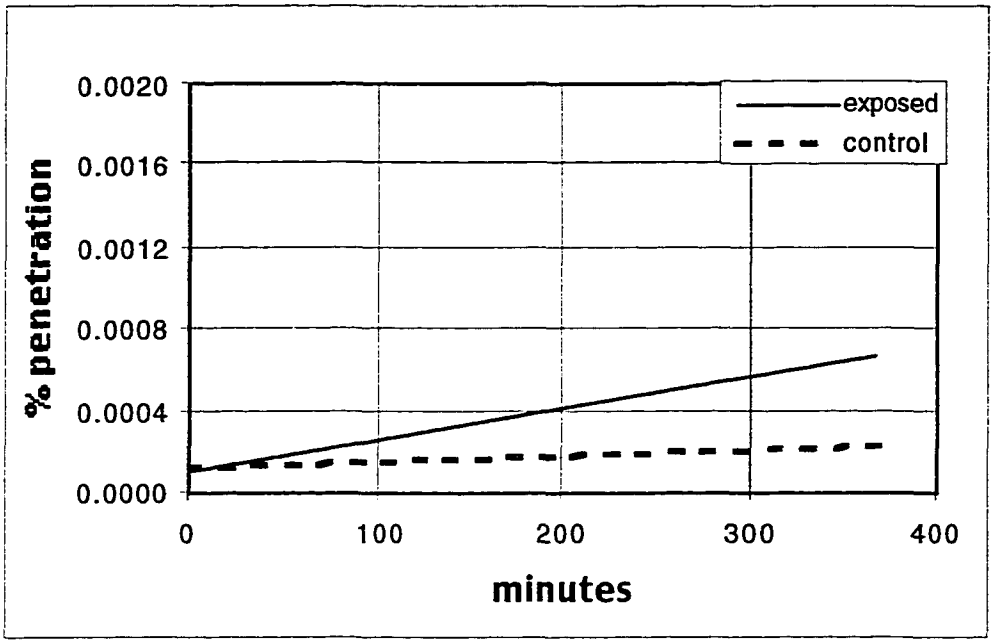

figure C.19 Control and Exposed Respirators to Asphalt Contaminants
3M 2091 P100 Cartridge
CNC-Measured Penetration: % penetration
N exposed=6, N control=2 ,fitted MMAD= 4.66 μm, fitted GSD=1.54

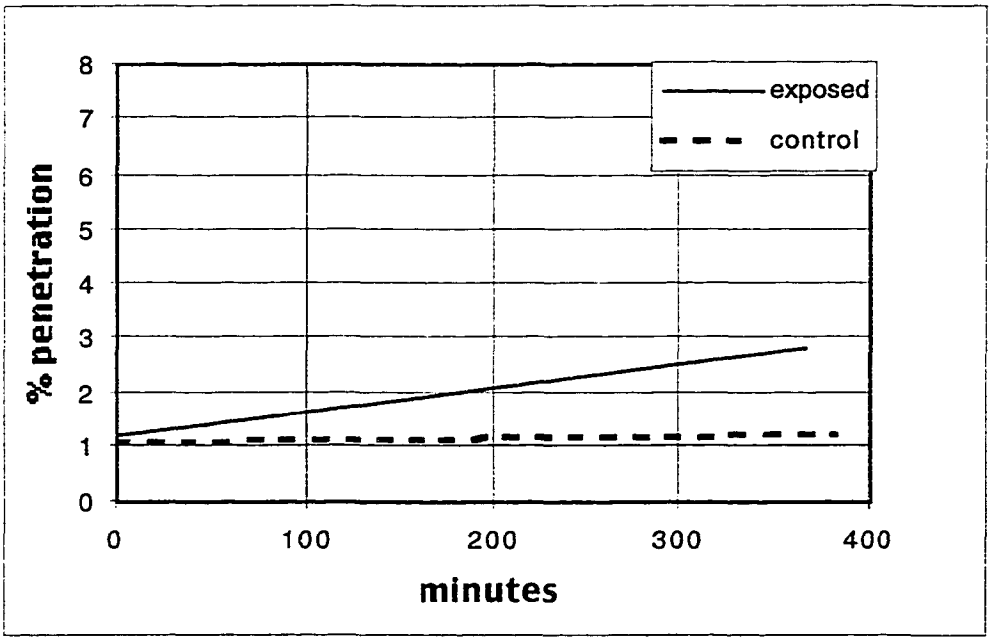

figure C.20 Control and Exposed Respirators to Asphalt Contaminants
MSA Affinity Plus N95 Respirator
Photometer-Measured Penetration: % penetration
N exposed=6,N control=2 ,fitted MMAD= 4.36 μm, fitted GSD=1.61

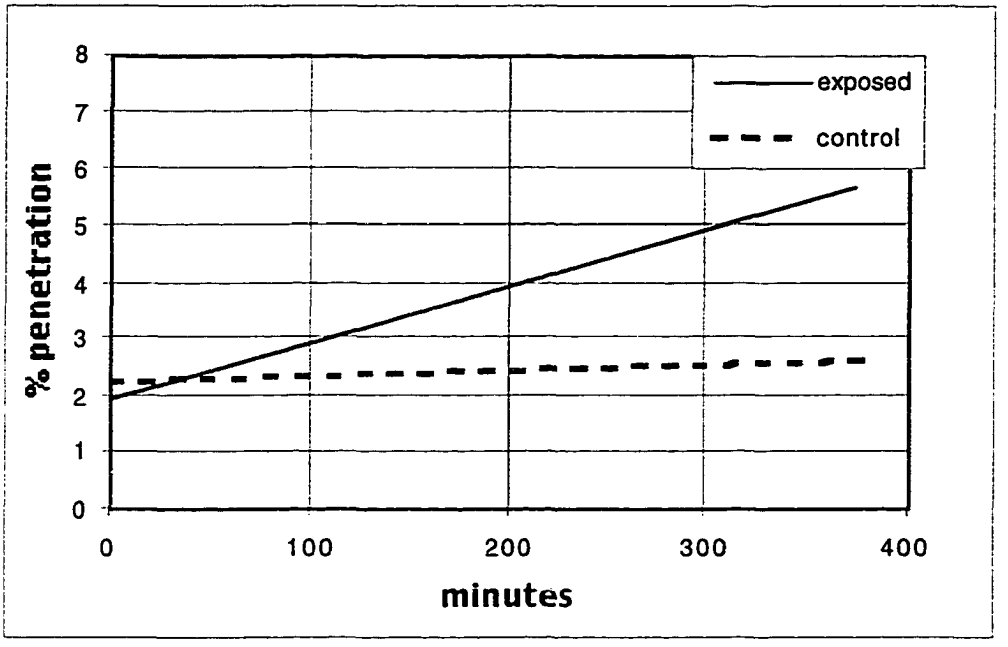

figure C.21 Control and Exposed Respirators to Asphalt Contaminants
Pro-Tech F200 N95 Filters
Photometer-Measured Penetration: % penetration
N exposed=6,N control=2 ,fitted MMAD= 4.35 µm, fitted GSD=1.54

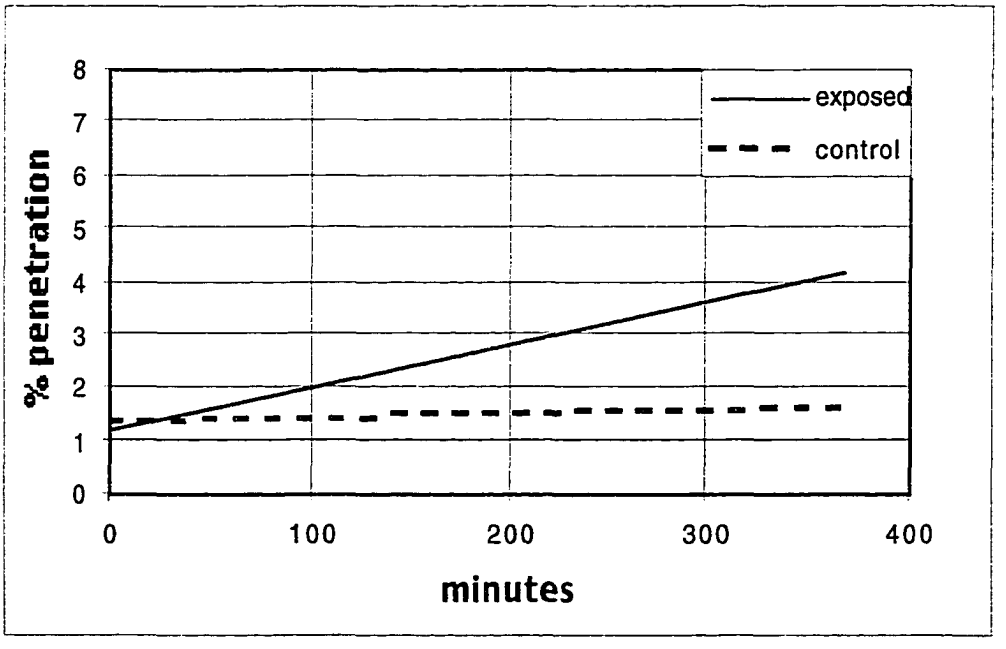

figure C.22 Control and Exposed Respirators to Asphalt Contaminants
Racal (mechanical) N95 Respirators
Photometer-Measured Penetration: % penetration
N exposed=12,N control=4 ,fitted MMAD= 5.18 µm, fitted GSD=1.94

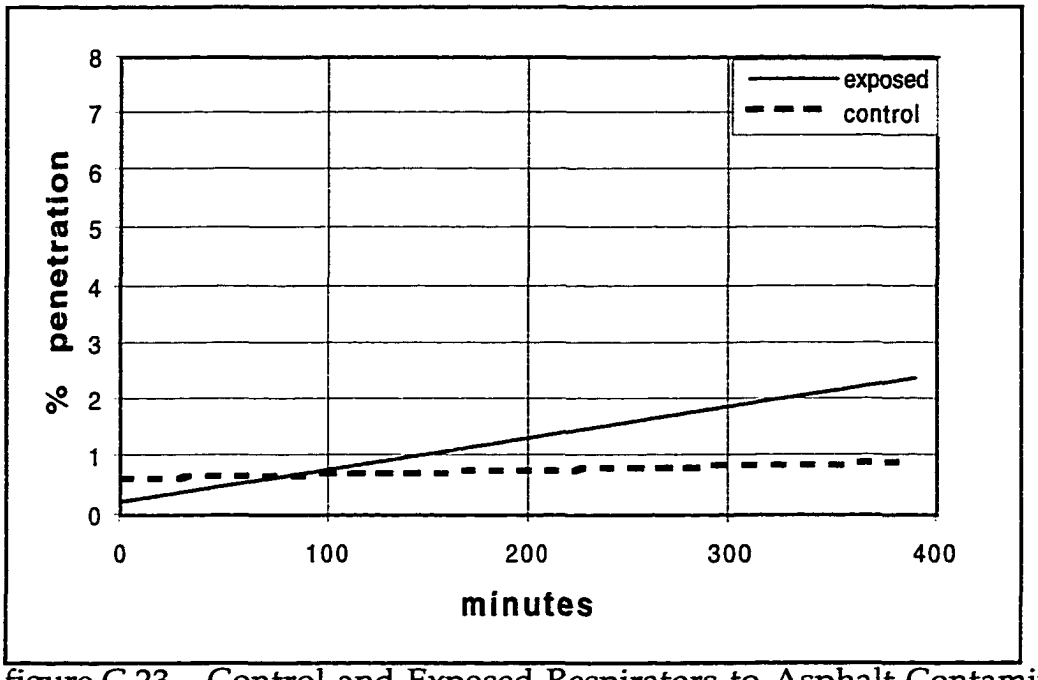

figure C.23 Control and Exposed Respirators to Asphalt Contaminants
Racal Delta lot A N95 Respirators
Photometer-Measured Penetration: % penetration
N exposed=6,N control=2 ,fitted MMAD= 4.23 µm, fitted GSD=1.52

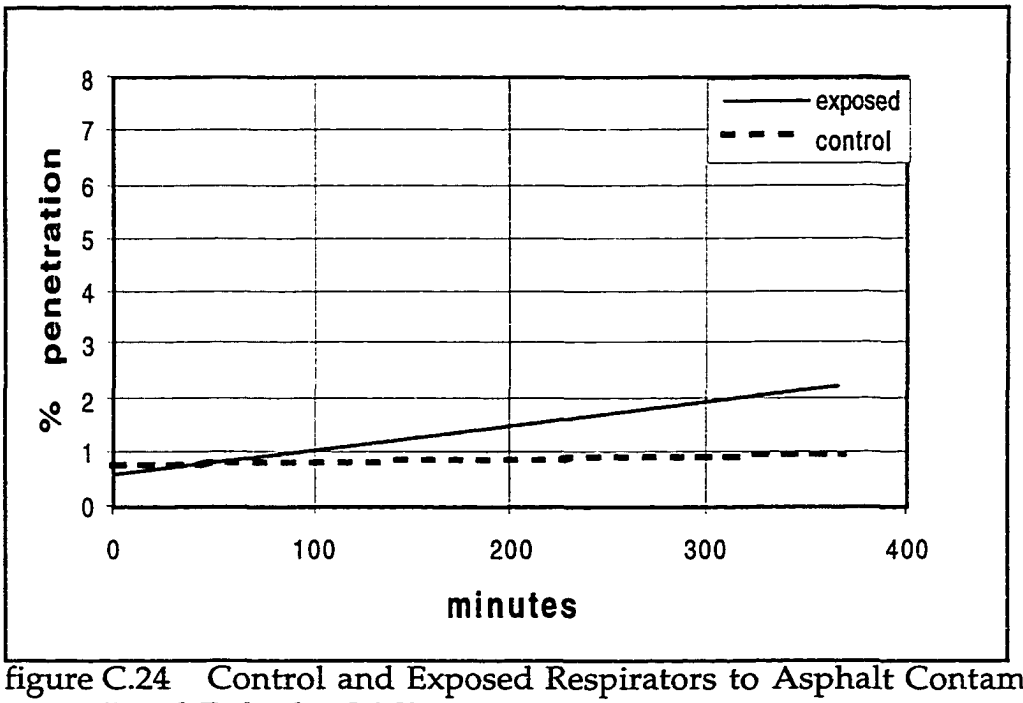

figure C.24 Control and Exposed Respirators to Asphalt Contaminants
Racal Delta lot B N95 Respirators
Photometer-Measured Penetration: % penetration
N exposed=9,N control=3 ,fitted MMAD= 3.70 µm, fitted GSD=2.32

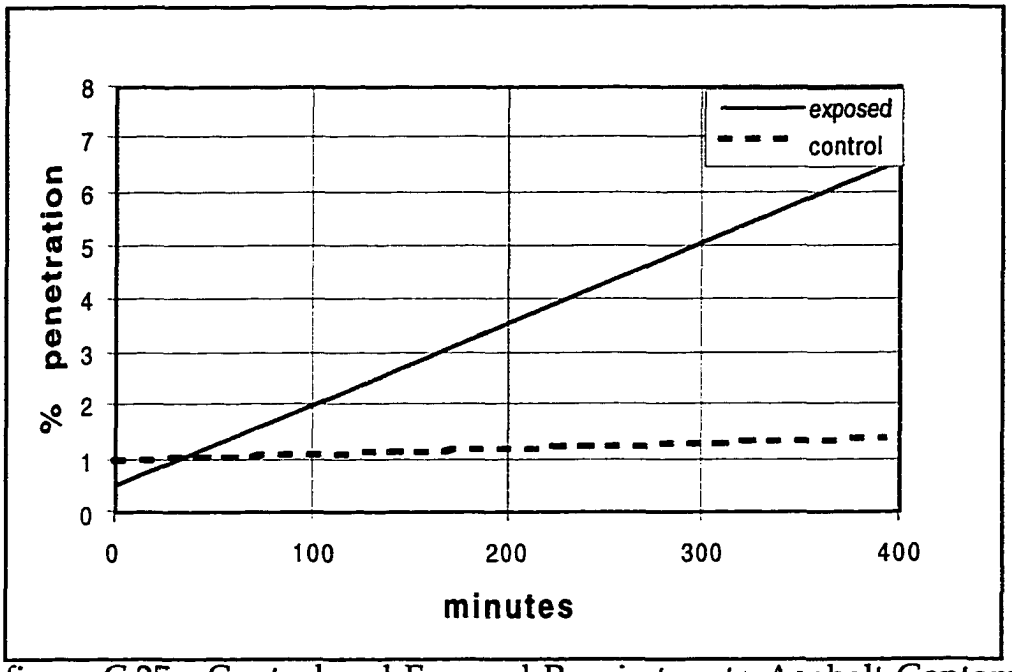

figure C.25 Control and Exposed Respirators to Asphalt Contaminants
Tecnol PFR95 N95 Respirators
Photometer-Measured Penetration: % penetration
N exposed=6,N control=2 ,fitted MMAD= 5.01 µm, fitted GSD=1.43

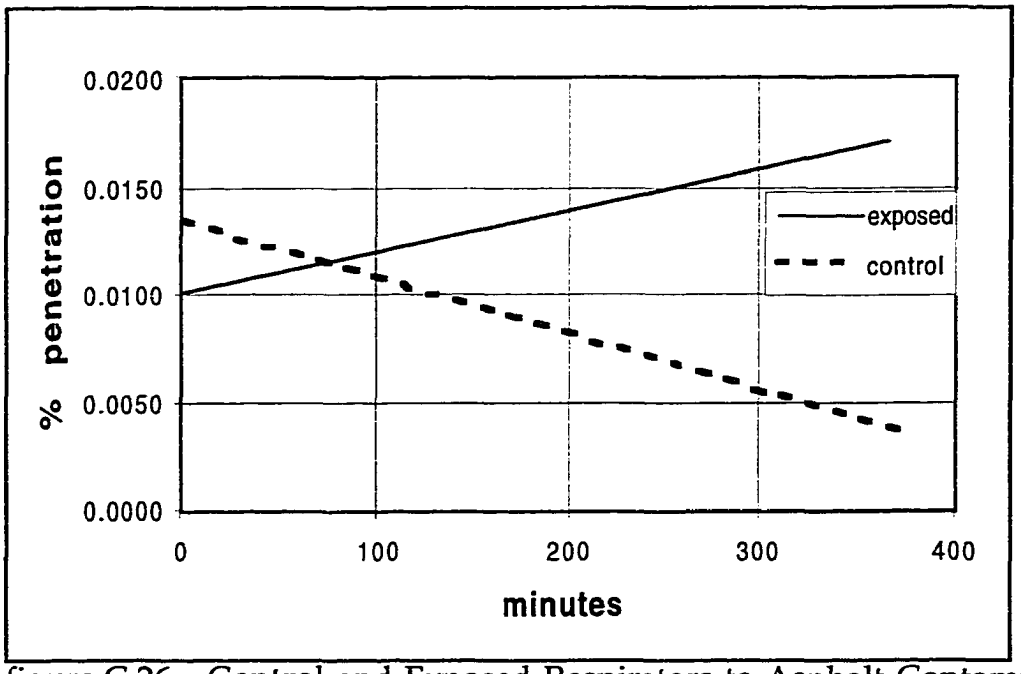

figure C.26 Control and Exposed Respirators to Asphalt Contaminants
3M 2091 P100 Cartridge
Photometer-Measured Penetration: % penetration
N exposed=6,N control=2 ,fitted MMAD= 4.66 µm, fitted GSD=1.54
N=6, fitted CMD= 0.20 µm, fitted GSD=1.60

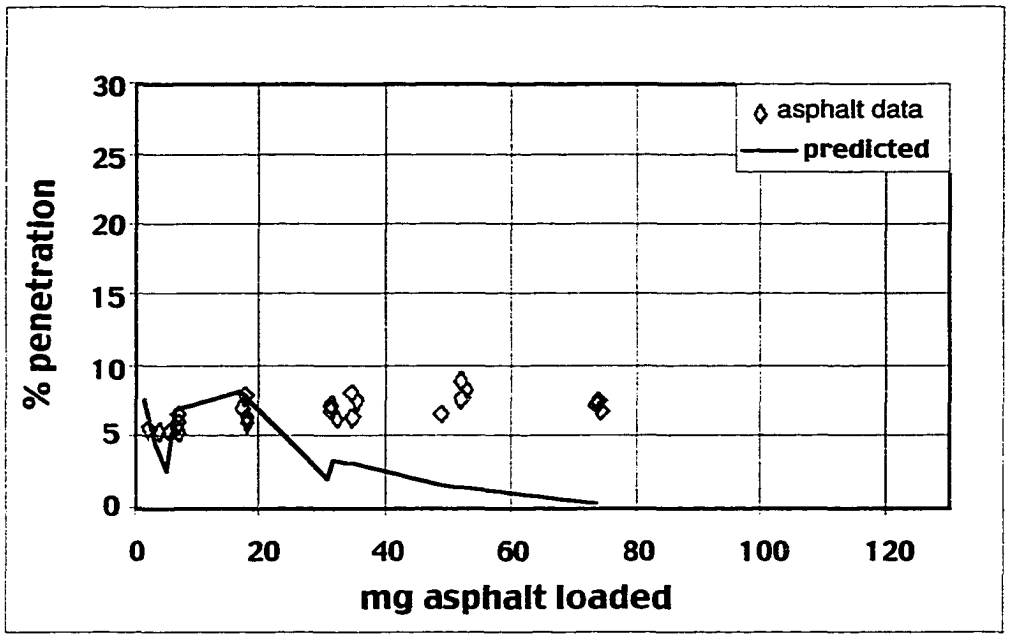

figure C.27 Asphalt Contaminant Loading: Observed and Predicted Penetration
MSA Affinity Plus N95 Respirators
CNC-Measured Penetration: % penetration (backtransformed)
N exposed=6,N control=2 ,fitted MMAD= 4.36 µm, fitted GSD=1.61

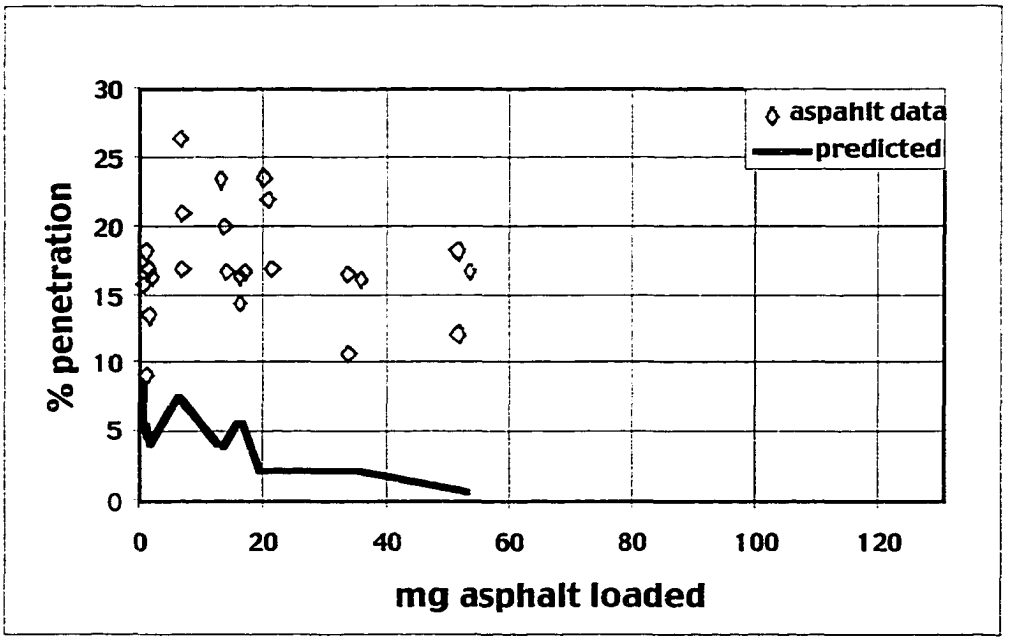

figure C.28 Asphalt Contaminant Loading: Observed and Predicted Penetration
Pro-Tech F200 N95 Filters
CNC-Measured Penetration: % penetration (backtransformed)
N exposed=6,N control=2 ,fitted MMAD= 4.35 µm, fitted GSD=1.54

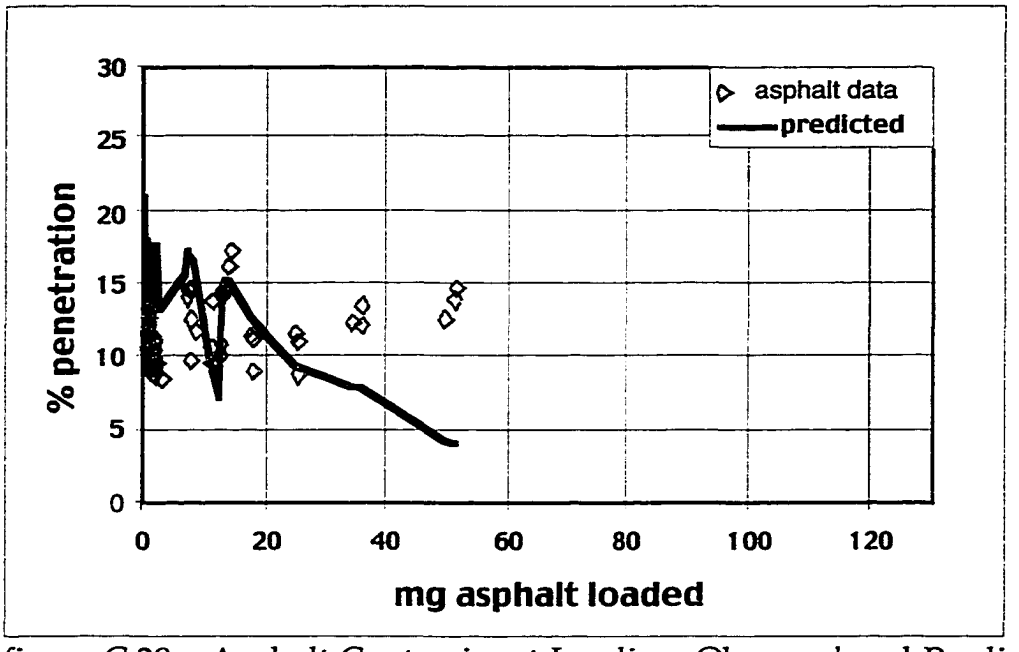

figure C.29 Asphalt Contaminant Loading: Observed and Predicted Penetration
Racal (mechanical) N95 Respirators
CNC-Measured Penetration: % penetration (backtransformed)
N exposed=12,N control=4 ,fitted MMAD= 5.18 µm, fitted GSD=1.94

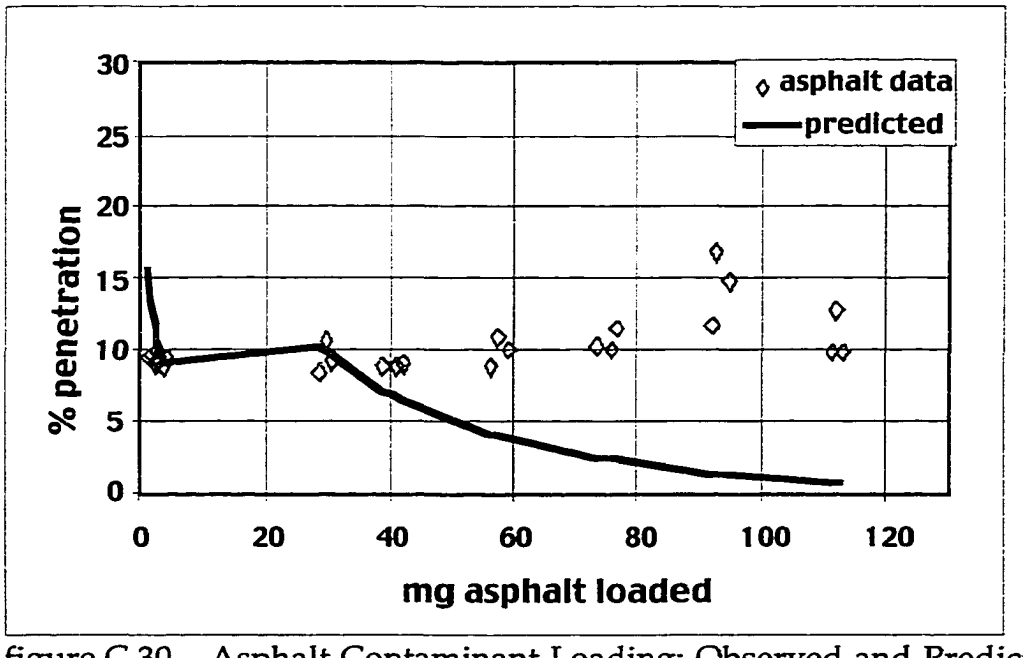

figure C.30 Asphalt Contaminant Loading: Observed and Predicted Penetration
Racal lot A N95 Respirators
CNC-Measured Penetration: % penetration (backtransformed)
N exposed=6,N control=2 ,fitted MMAD= 4.23 µm, fitted GSD=1.52

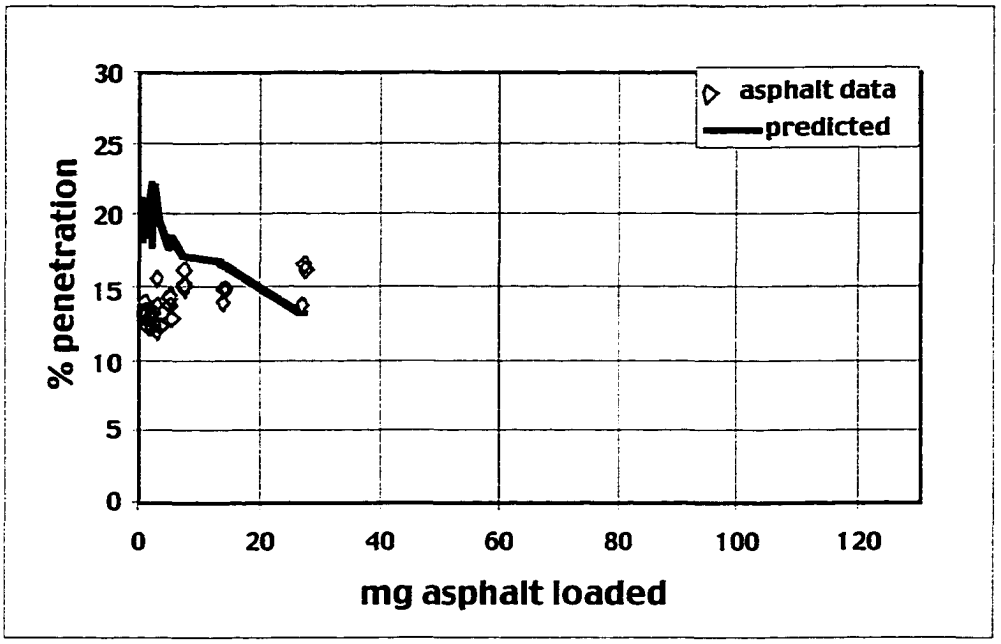

figure C.31 Asphalt Contaminant Loading: Observed and Predicted Penetration
Racal lot B N95 Respirators
CNC-Measured Penetration: % penetration (backtransformed)
N exposed=9,N control=3 ,fitted MMAD= 3.70 µm, fitted GSD=2.32

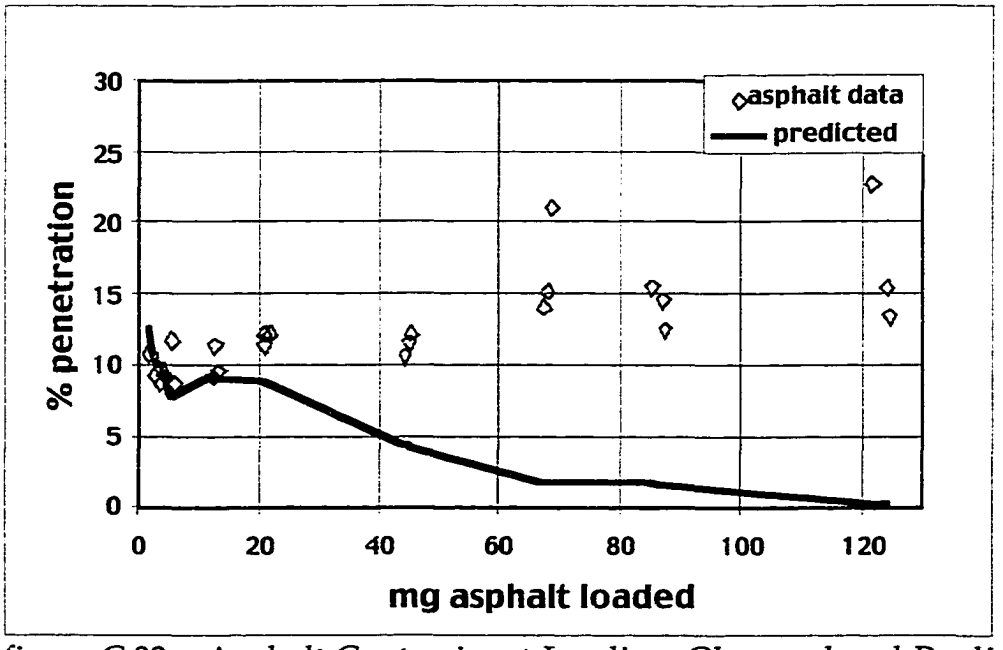

figure C.32 Asphalt Contaminant Loading: Observed and Predicted Penetration
Tecnol PFR95 N95 Respirators
CNC-Measured Penetration: % penetration (backtransformed)
N exposed=6,N control=2 ,fitted MMAD= 5.01 µm, fitted GSD=1.43

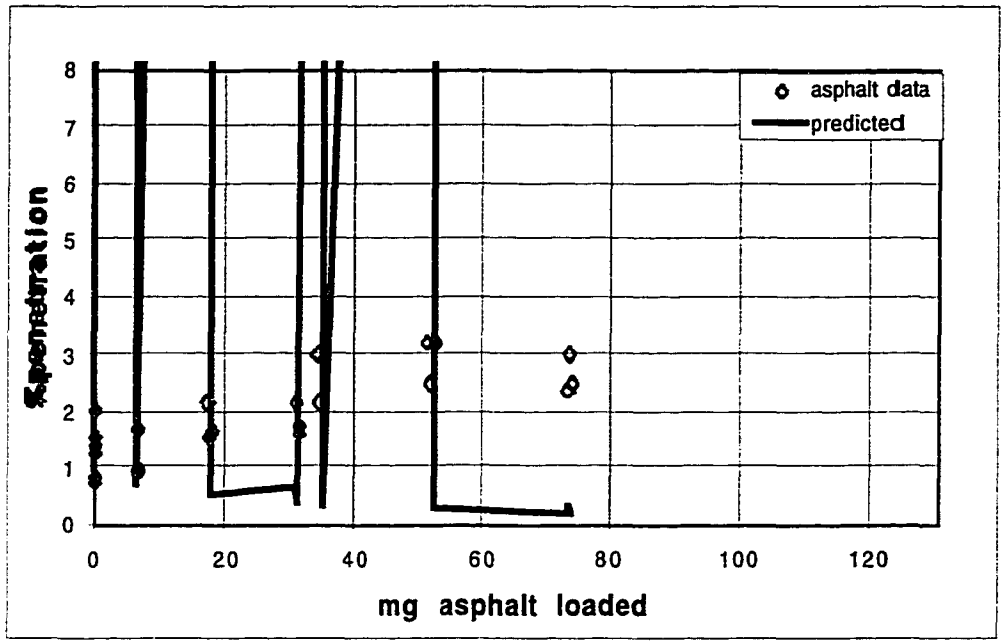

figure C.33 Asphalt Contaminant Loading: Observed and Predicted Penetration
MSA Affinity Plus N95 Respirators
Photometer-Measured Penetration: % penetration (backtransformed)
N exposed=6,N control=2 ,fitted MMAD= 4.36 μm, fitted GSD=1.61

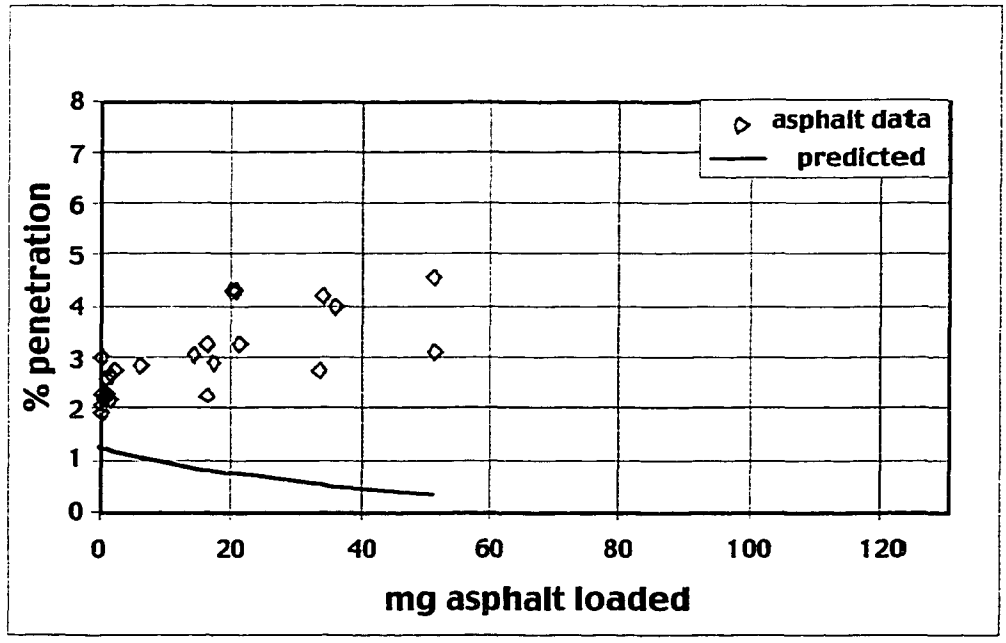

figure C.34 Asphalt Contaminant Loading: Observed and Predicted Penetration
Pro-Tech F200 N95 Filters
Photometer-Measured Penetration: % penetration (backtransformed)
N exposed=6,N control=2 ,fitted MMAD= 4.35 μm, fitted GSD=1.54

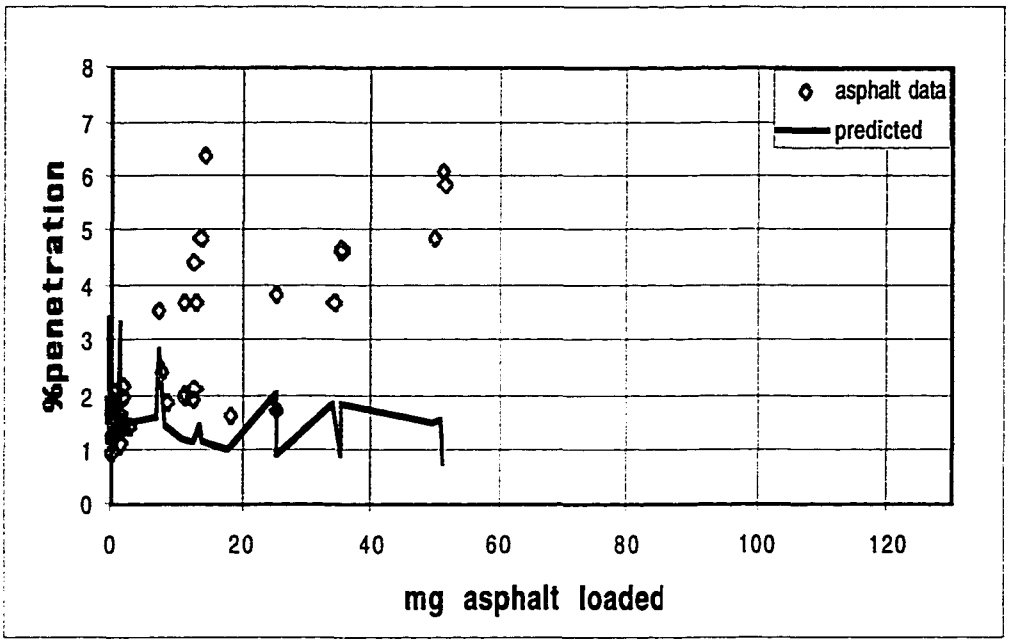

figure C.35 Asphalt Contaminant Loading: Observed and Predicted Penetration
Racal (mechanical) N95 Respirators
Photometer-Measured Penetration: % penetration (backtransformed)
N exposed=12,N control=4 ,fitted MMAD= 5.18 µm, fitted GSD=1.94

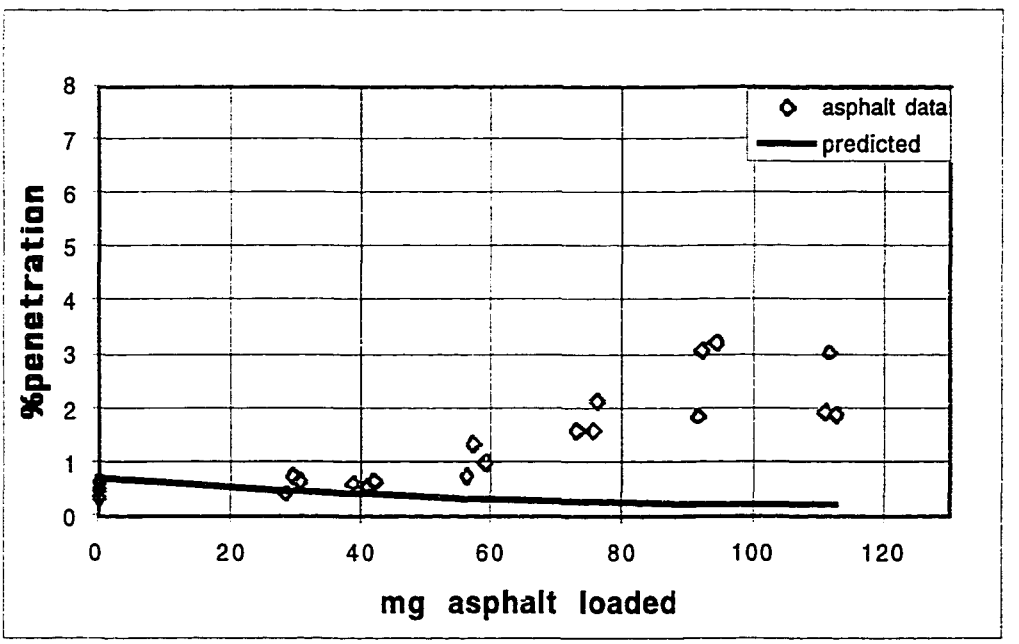

figure C.36 Asphalt Contaminant Loading: Observed and Predicted Penetration
Racal lot A N95 Respirators
Photometer-Measured Penetration: % penetration (backtransformed)
N exposed=6,N control=2 ,fitted MMAD= 4.23 µm, fitted GSD=1.52

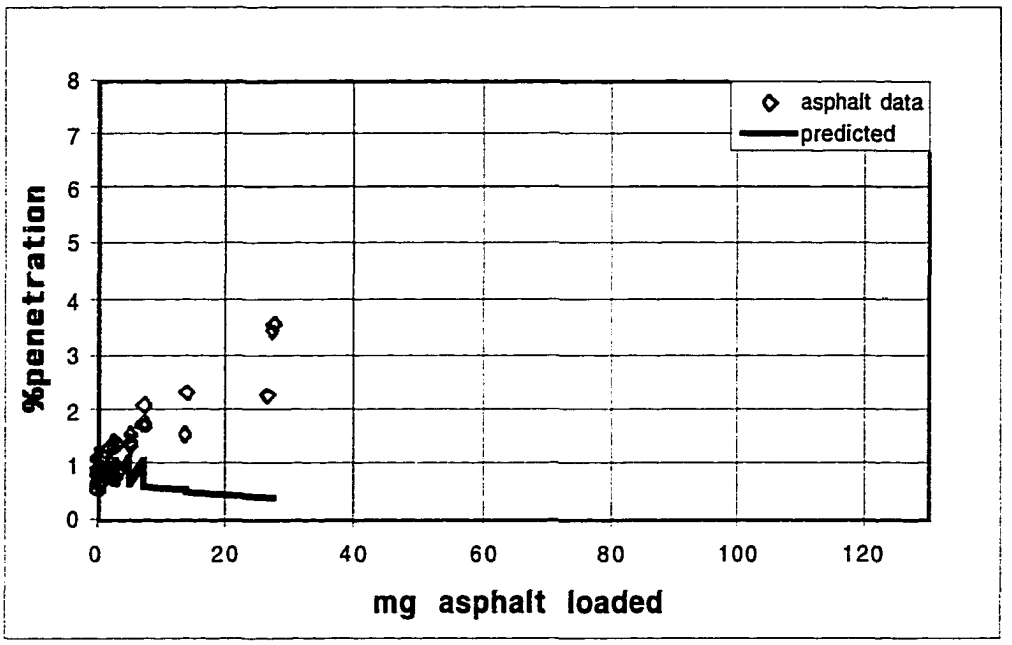

figure C.37 Asphalt Contaminant Loading: Observed and Predicted Penetration
Racal lot B N95 Respirators
Photometer-Measured Penetration: % penetration (backtransformed)
N exposed=9,N control=3 ,fitted MMAD= 3.70 µm, fitted GSD=2.32

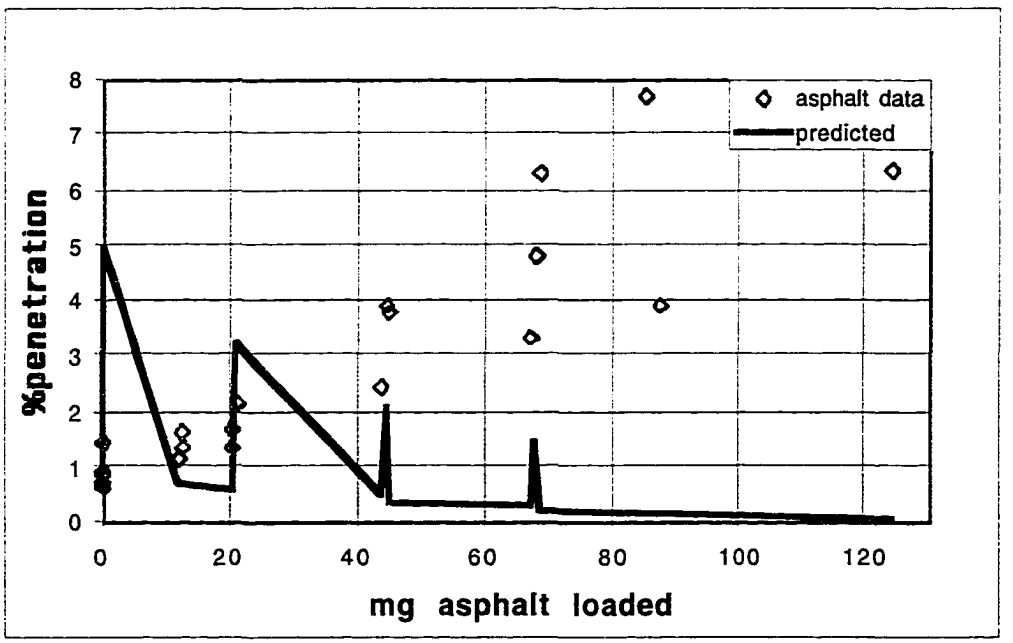

figure C.38 Asphalt Contaminant Loading: Observed and Predicted Penetration
Tecnol PFR95 N95 Respirators
Photometer-Measured Penetration: % penetration (backtransformed)
N exposed=6,N control=2 ,fitted MMAD= 5.01 µm, fitted GSD=1.43

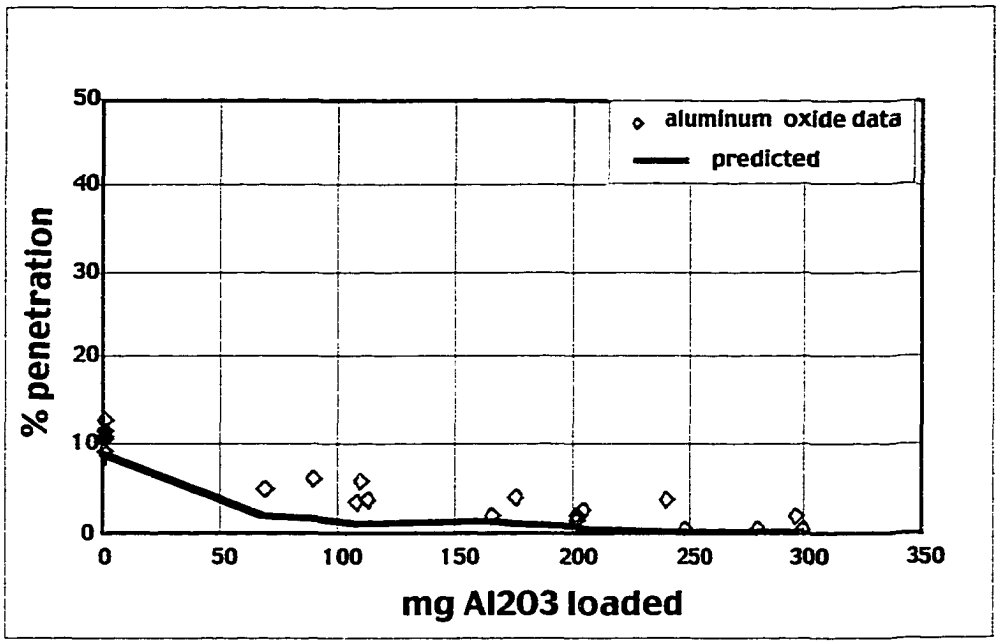

figure C.39 Aluminum Oxide Dust Loading: Observed and Predicted Penetration
3M 8210 N95 Respirators
CNC-Measured Penetration: % penetration (backtransformed)
N=5, fitted MMD= 2.05 μm, fitted GSD=1.41

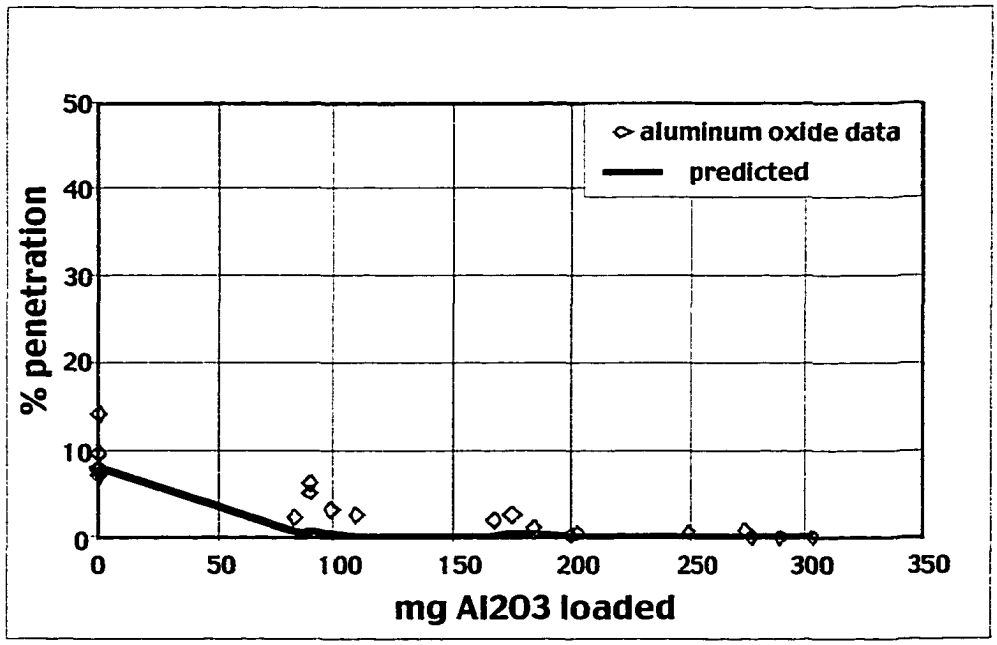

figure C.40 Aluminum Oxide Dust Loading: Observed and Predicted Penetration
MSA Affinity Plus N95 Respirators
CNC-Measured Penetration: % penetration (backtransformed)
N=5, MMD= 2.10 μm, GSD=1.41

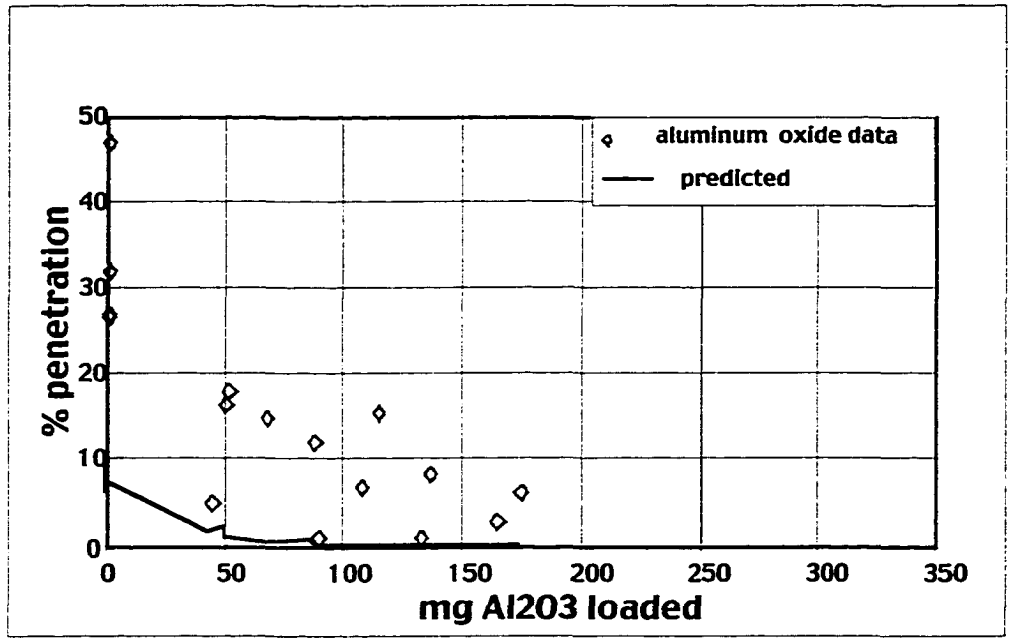

figure C.41 Aluminum Oxide Dust Loading: Observed and Predicted Penetration
Pro-Tech F200 N95 Filters
CNC-Measured Penetration: % penetration (backtransformed)
N=5, MMD= 2.02 μm, GSD=1.41

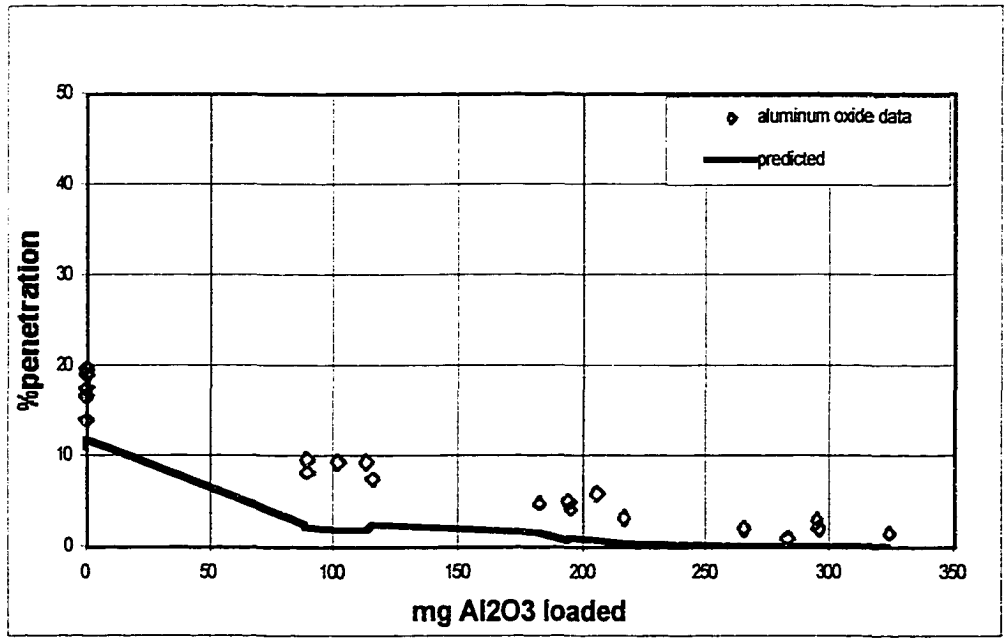

figure C.42 Aluminum Oxide Dust Loading: Observed and Predicted Penetration
Racal (mechanical) N95 Respirators
CNC-Measured Penetration: % penetration (backtransformed)[j]
N=5, MMD= 2.10 μm, GSD=1.41

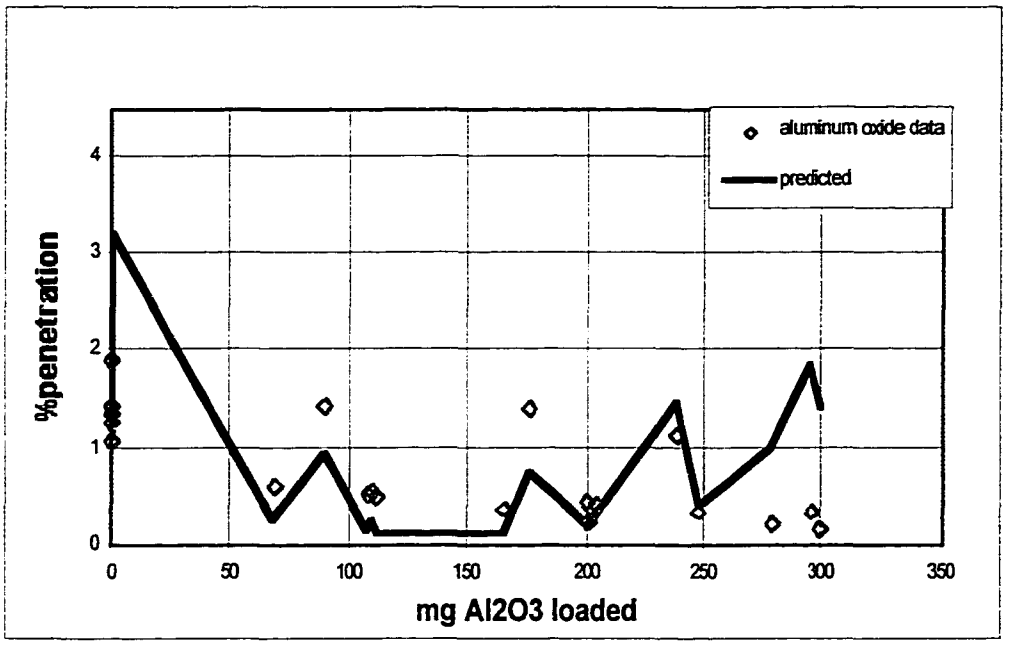

figure C.43 Aluminum Oxide Dust Loading: Observed and Predicted Penetration
3M 8210 N95 Respirators
Photometer-Measured Penetration: % penetration (backtransformed)
N=5, MMD= 2.05 μm, GSD=1.41

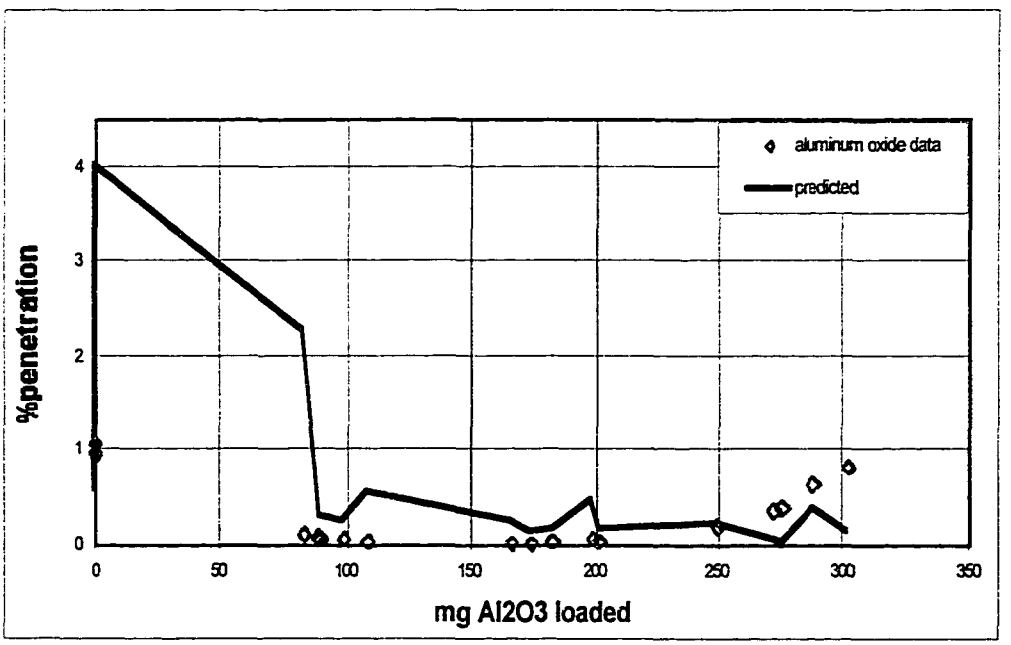

figure C.44 Aluminum Oxide Dust Loading: Observed and Predicted Penetration
MSA Affinity Plus N95 Respirators
Photometer-Measured Penetration: % penetration (backtransformed)
N=5, MMD= 2.10 μm, GSD=1.41

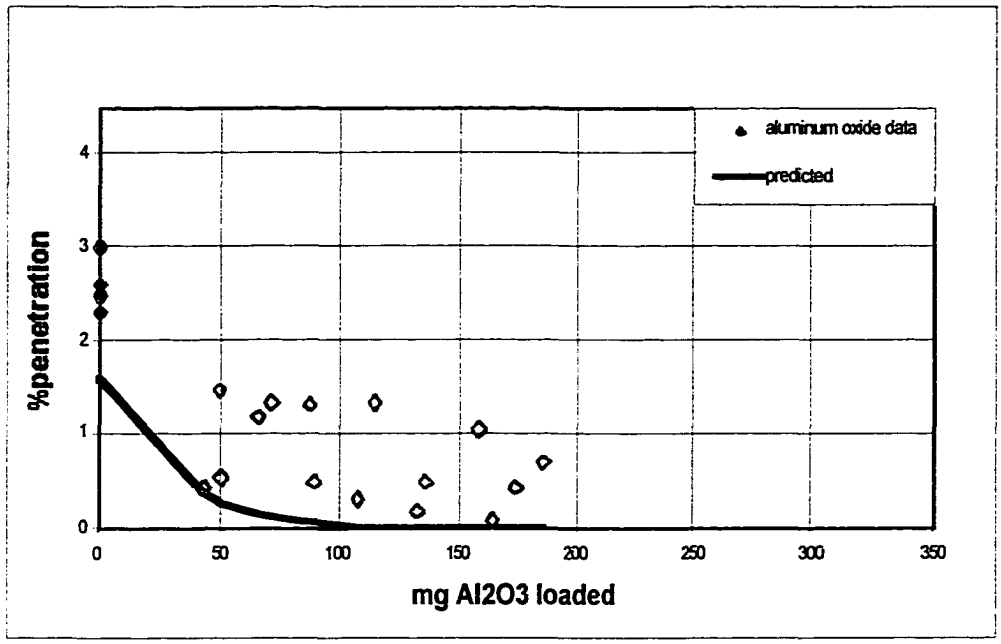

figure C.45 Aluminum Oxide Dust Loading: Observed and Predicted Penetration
Pro-Tech F200 N95 Filters
Photometer-Measured Penetration: % penetration (backtransformed)
N=5, MMD= 2.02 μm, GSD=1.41

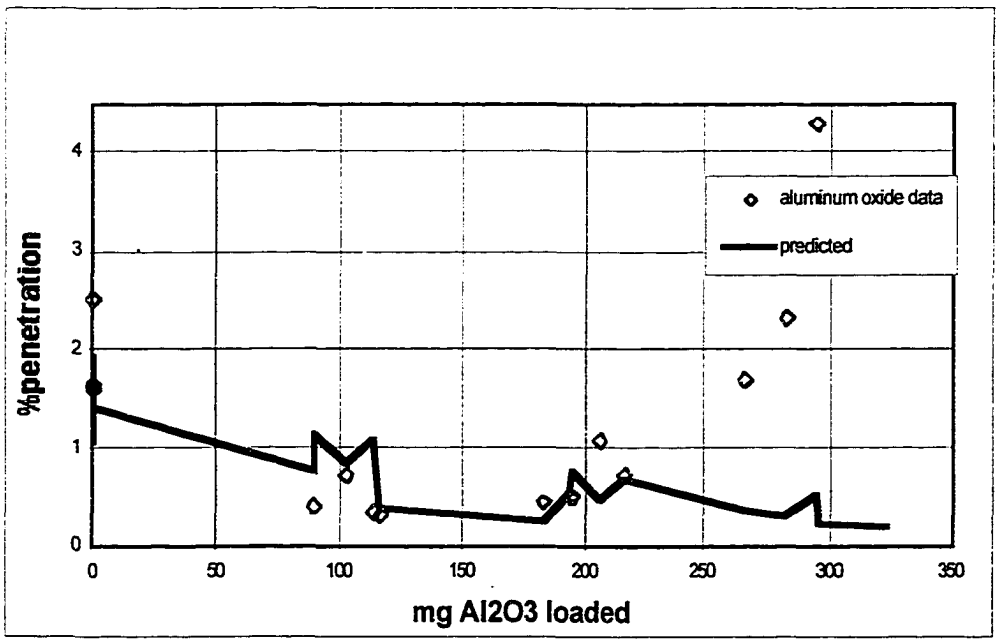

figure C.46 Aluminum Oxide Dust Loading: Observed and Predicted Penetration
Racal(mechanical) N95 Respirators
Photometer-Measured Penetration: % penetration (backtransformed)
N=5, MMD= 2.10 μm, GSD=1.41

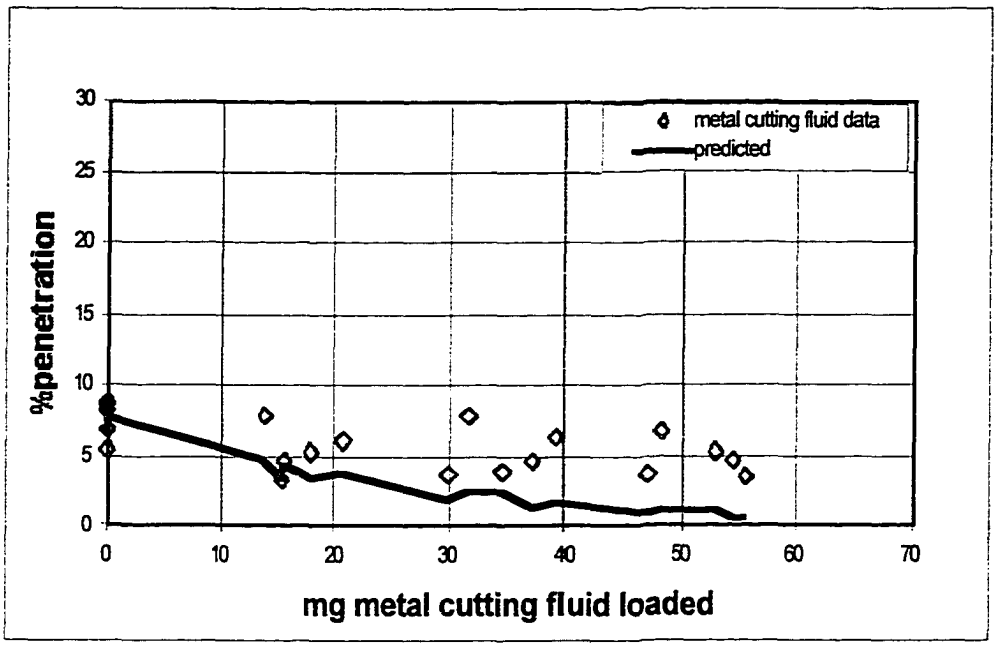

figure C.47 Laboratory-Generated Metal Cutting Fluid Mist: Observed and Predicted Penetration
MSA Affinity Plus N95 Respirators
CNC-Measured Penetration: % penetration (backtransformed)
N=5, MMD= 1.55 μm, GSD=1.43

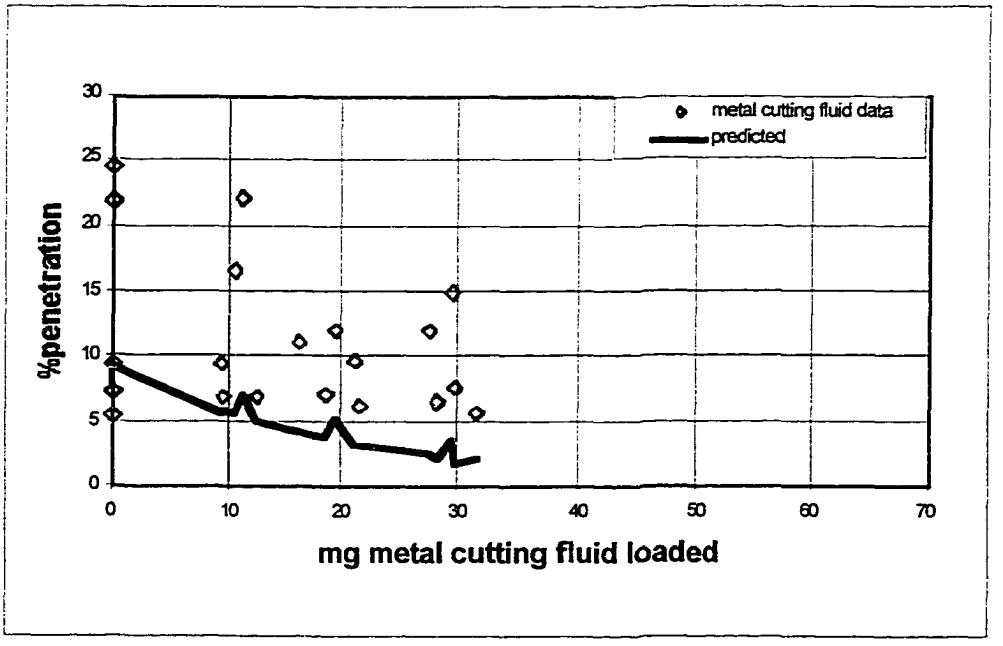

figure C.48 Laboratory-Generated Metal Cutting Fluid Mist: Observed and Predicted Penetration
Pro-Tech F200 N95 Filters
CNC-Measured Penetration: % penetration (backtransformed)
N=5, MMD= 1.49 μm, GSD=1.44

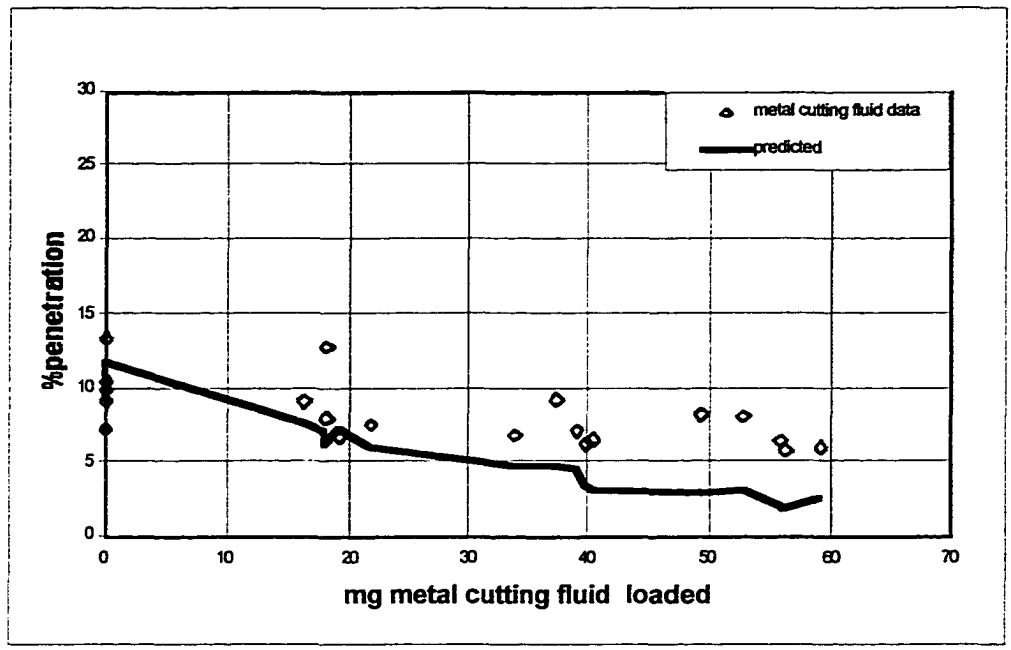

figure C.49 Laboratory-Generated Metal Cutting Fluid Mist: Observed and Predicted Penetration
Racal (mechanical) N95 Respirators
CNC-Measured Penetration: % penetration (backtransformed)
N=5, MMD= 1.55 μm, GSD=1.43

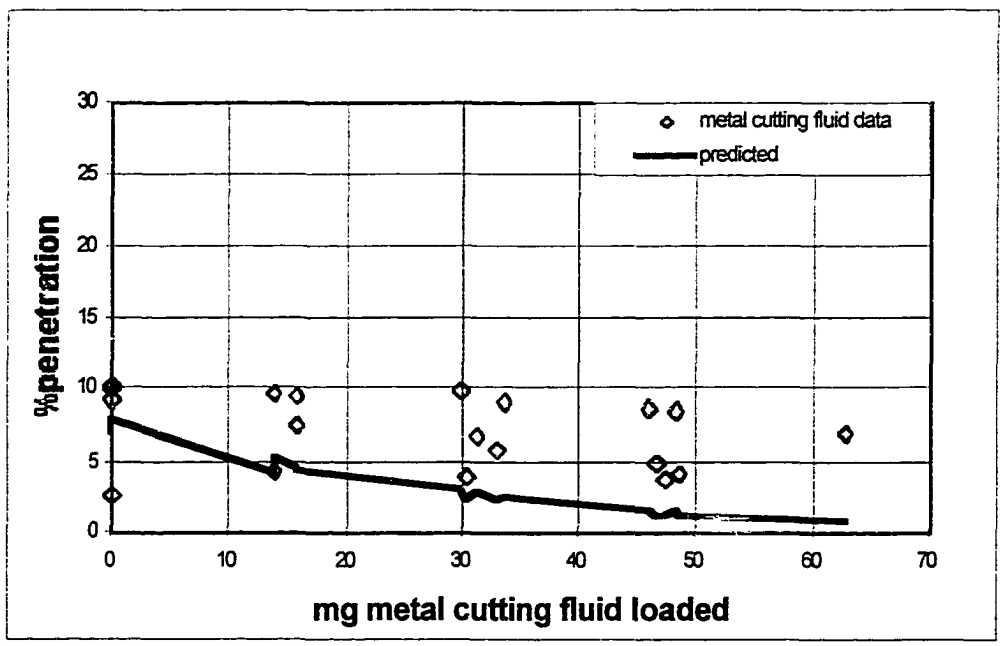

figure C.50 Laboratory-Generated Metal Cutting Fluid Mist: Observed and Predicted Penetration
3M 8210 N95 Respirators
CNC-Measured Penetration: % penetration (backtransformed)
N=5, MMD= 1.54 μm, GSD=1.43

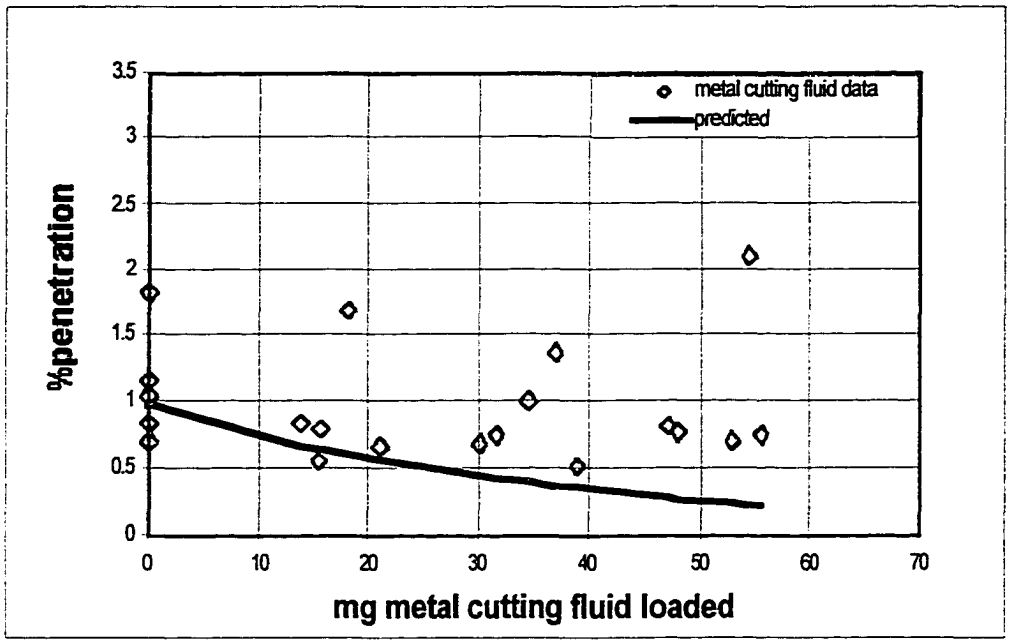

figure C.51 Laboratory-Generated Metal Cutting Fluid Mist: Observed and Predicted Penetration
MSA Affinity Plus N95 Respirators
Photometer-Measured Penetration: % penetration (backtransformed)
N=5, MMD= 1.55 μm, GSD=1.43

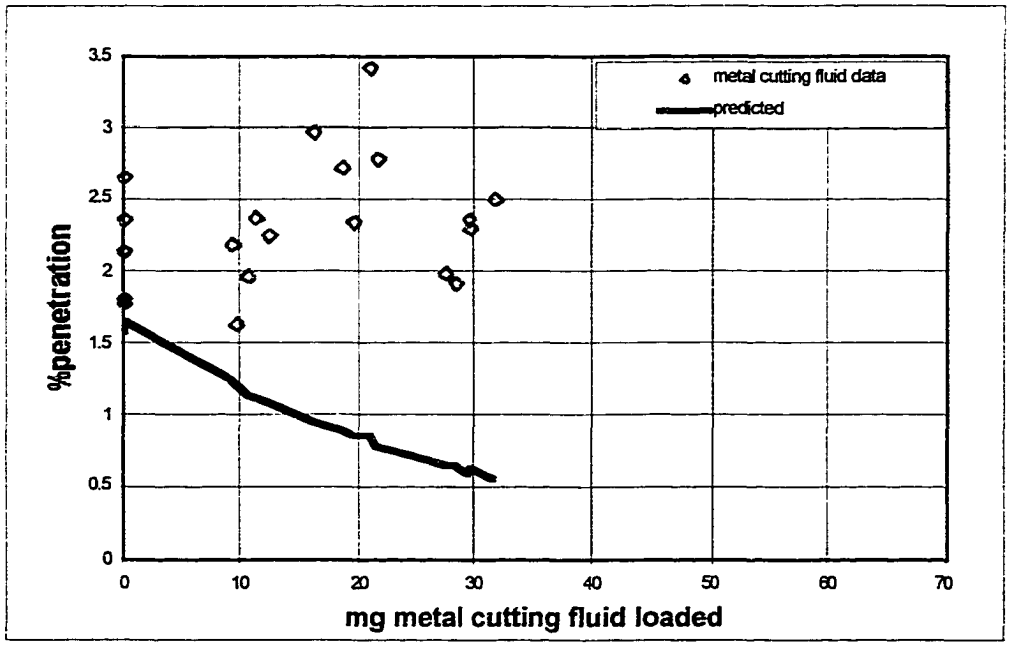

figure C.52 Laboratory-Generated Metal Cutting Fluid Mist: Observed and Predicted Penetration
Pro-Tech F200 Filters
Photometer-Measured Penetration: % penetration (backtransformed)
N=5, MMD= 1.49 μm, GSD=1.44

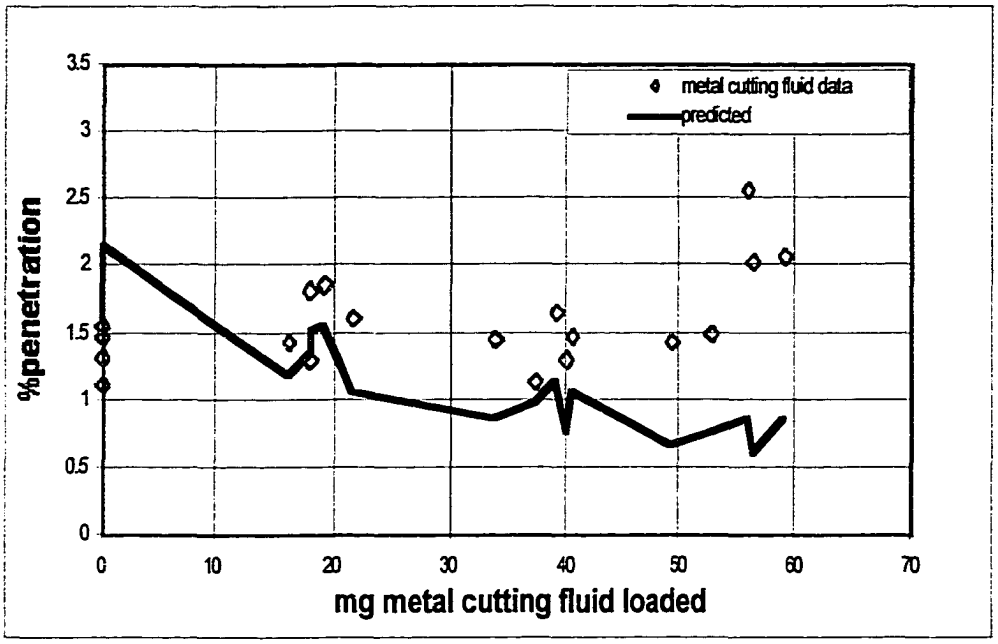

figure C.53 Laboratory-Generated Metal Cutting Fluid Mist: Observed and Predicted Penetration
Racal (mechanical) N95 Respirators
Photometer-Measured Penetration: % penetration (backtransformed)
N=5, MMD= 1.55 μm, GSD=1.43

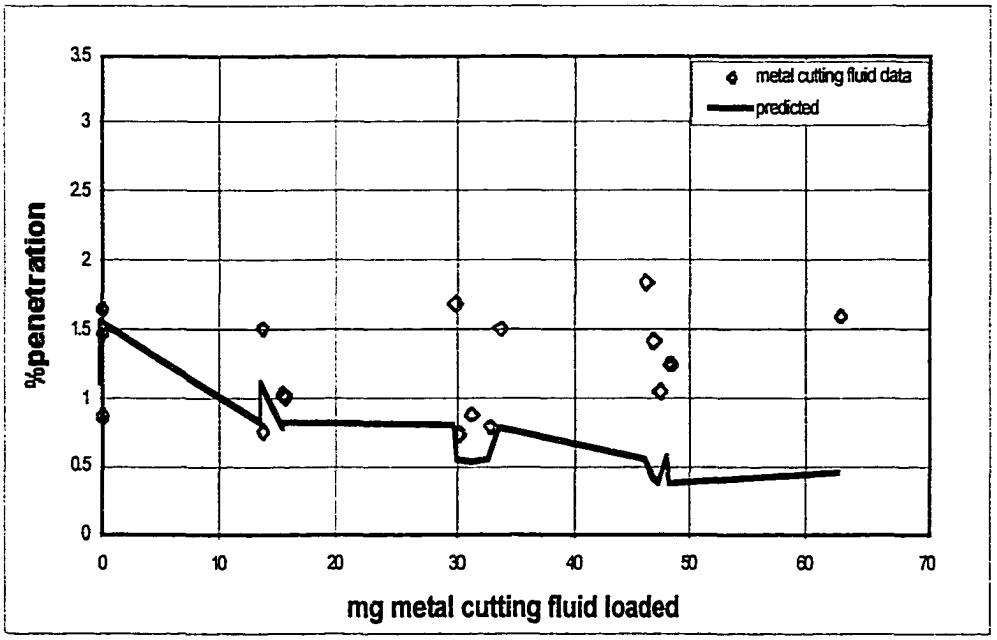

figure C.54 Laboratory-Generated Metal Cutting Fluid Mist: Observed and Predicted Penetration
3M 8210 N95 Respirators
Photometer-Measured Penetration: % penetration (backtransformed)
N=5, MMD= 1.54 μm, GSD=1.43

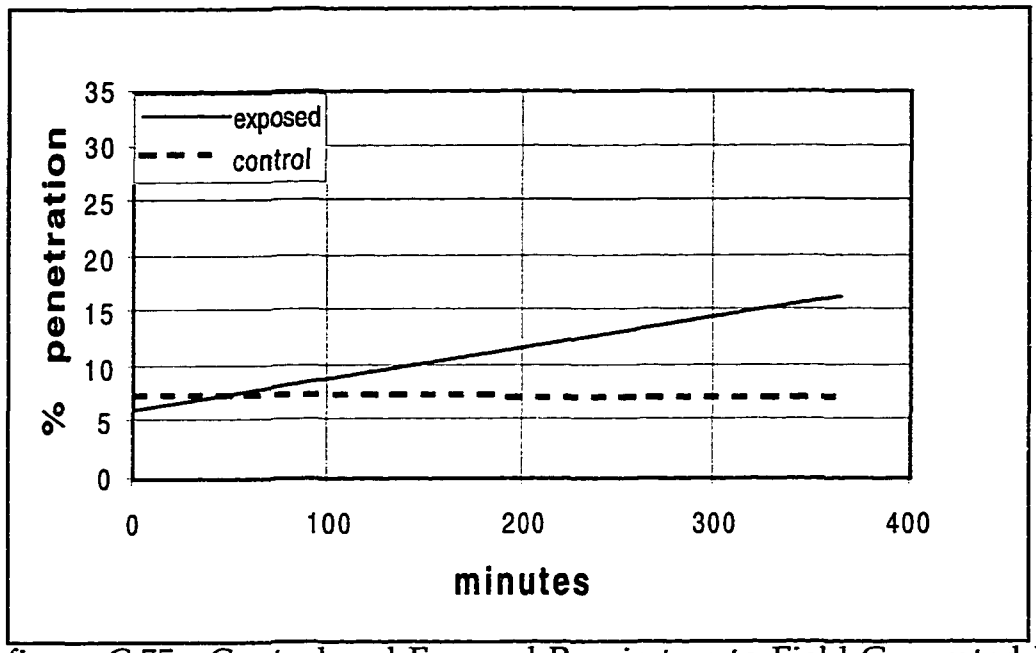

figure C.55 Control and Exposed Respirators to Field-Generated Metal Cutting Fluid Mist
MSA Affinity Plus N95 Respirators
CNC-Measured Penetration: % penetration
N exposed=6,N control=2 ,fitted MMAD= 4.37 μm, fitted GSD=2.03

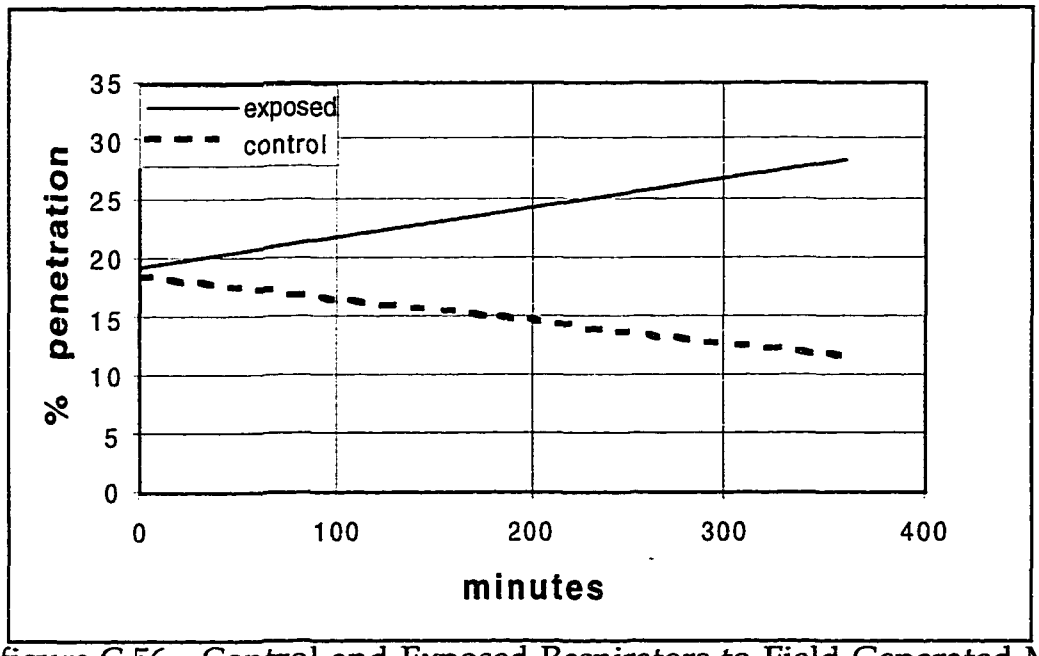

figure C.56 Control and Exposed Respirators to Field-Generated Metal Cutting Fluid Mist
Pro-Tech F200 N95 Filters
CNC-Measured Penetration: % penetration
N exposed=6,N control=2 ,fitted MMAD= 3.56 μm, fitted GSD=2.41

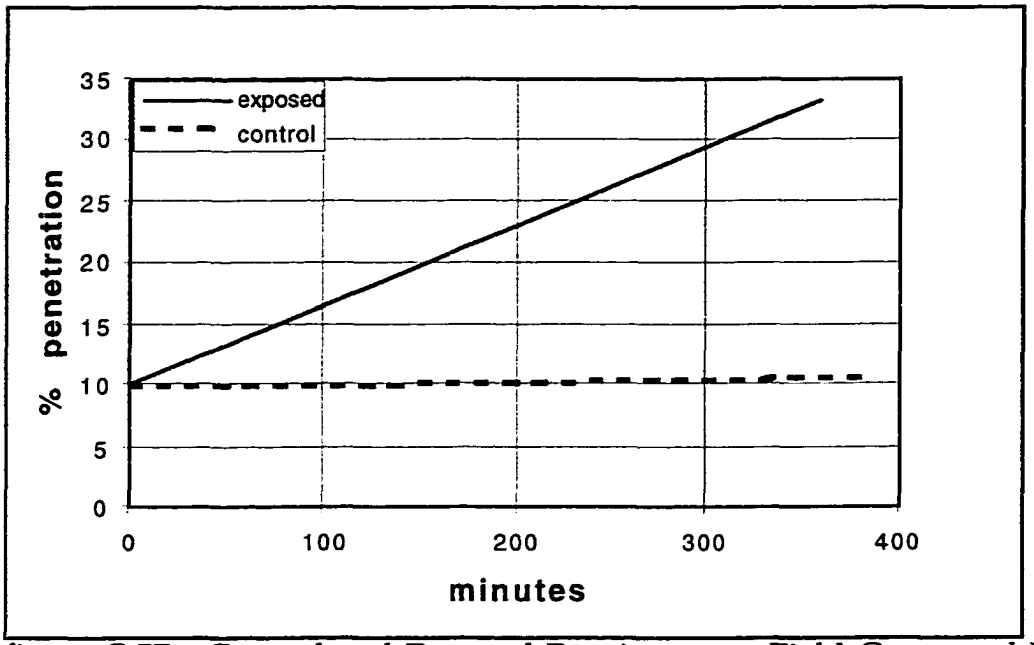

figure C.57 Control and Exposed Respirators to Field-Generated Metal Cutting Fluid Mist
Racal (mechanical) N95 Respirators
CNC-Measured Penetration: % penetration
N exposed=6,N control=2 ,fitted MMAD= 3.54 μm, fitted GSD=2.14

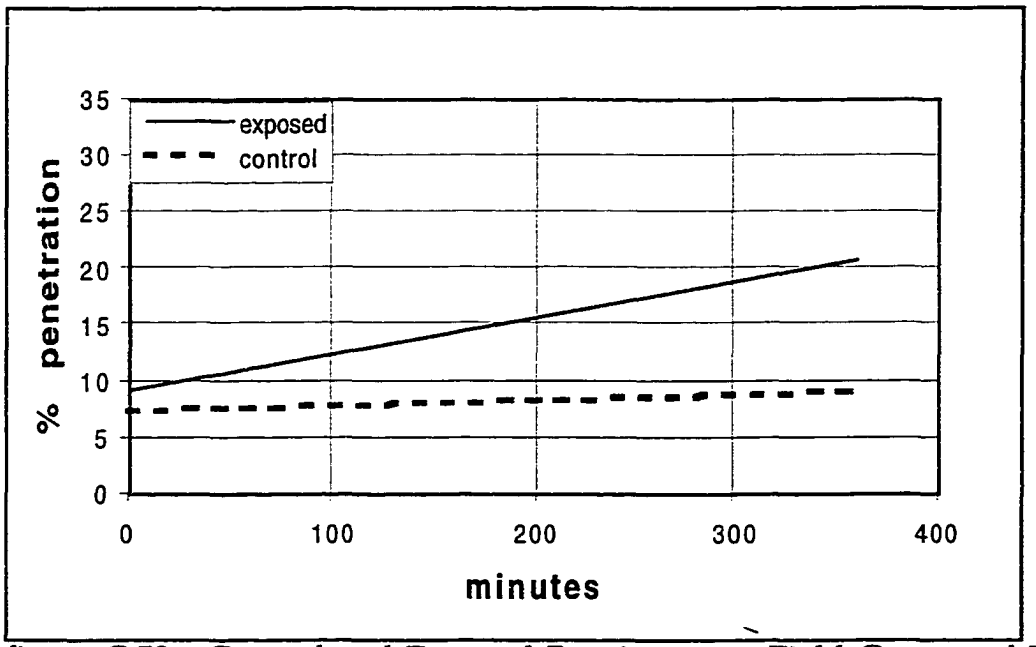

figure C.58 Control and Exposed Respirators to Field-Generated Metal Cutting Fluid Mist
3M 8210 N95 Respirators
CNC-Measured Penetration: % penetration
N exposed=6,N control=2 ,fitted MMAD= 4.47 μm, fitted GSD=1.88

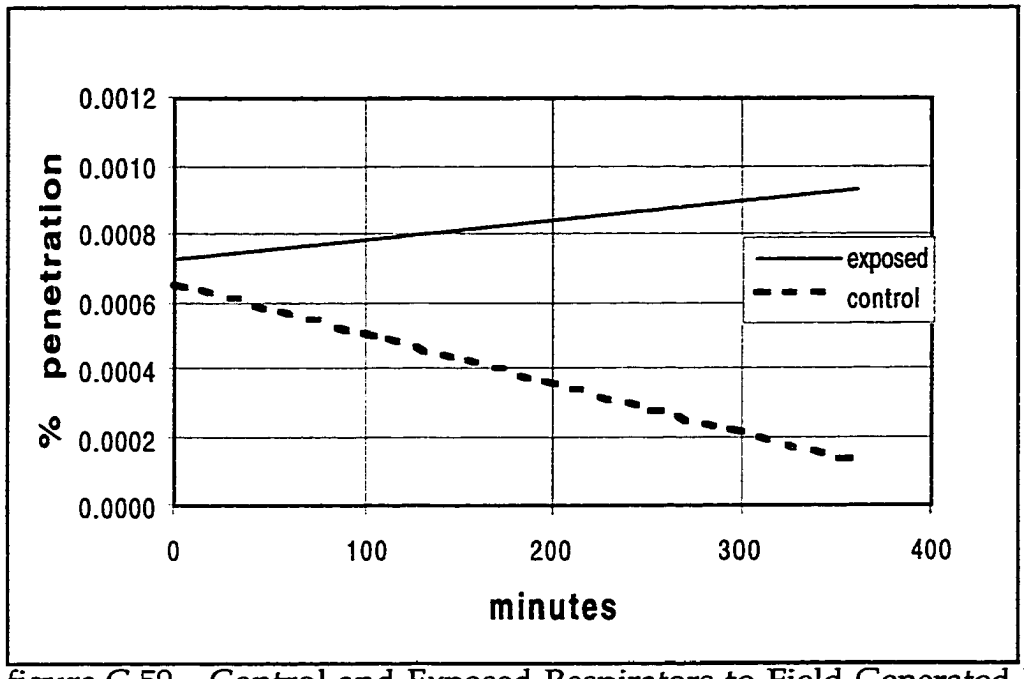

figure C.59 Control and Exposed Respirators to Field-Generated Metal Cutting Fluid Mist
3M 2091 P100 Cartridge
CNC-Measured Penetration: % penetration
N exposed=6,N control=2 ,fitted MMAD= 4.15 µm, fitted GSD=1.84

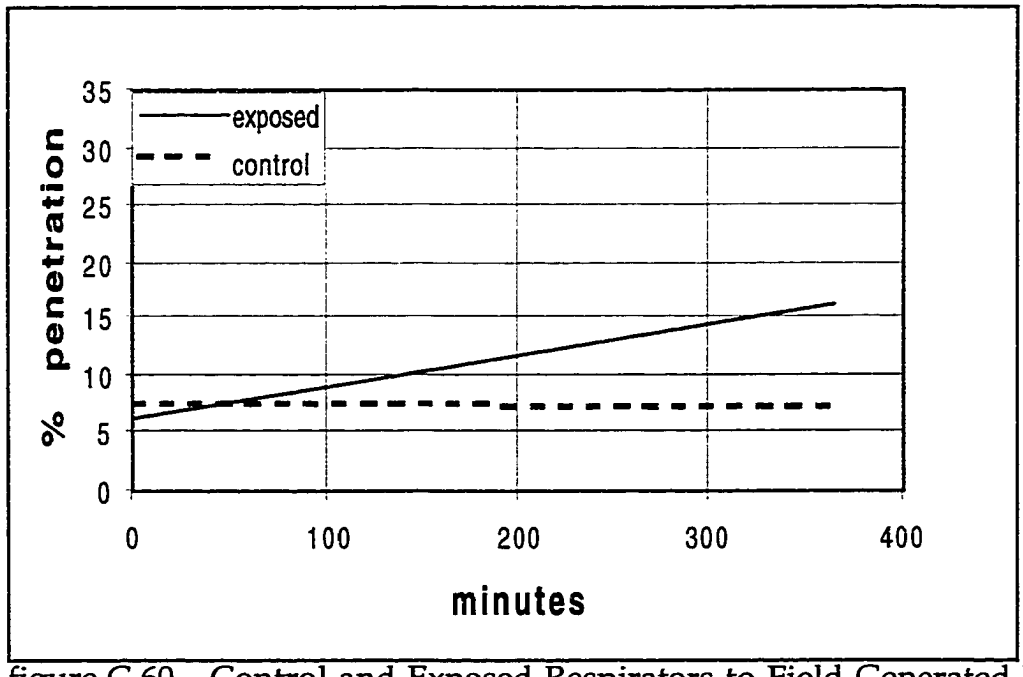

figure C.60 Control and Exposed Respirators to Field-Generated Metal Cutting Fluid Mist
MSA Affinity Plus N95 Respirators
Photometer-Measured Penetration: % penetration
N exposed=6,N control=2 ,fitted MMAD= 4.37 µm, fitted GSD=2.03

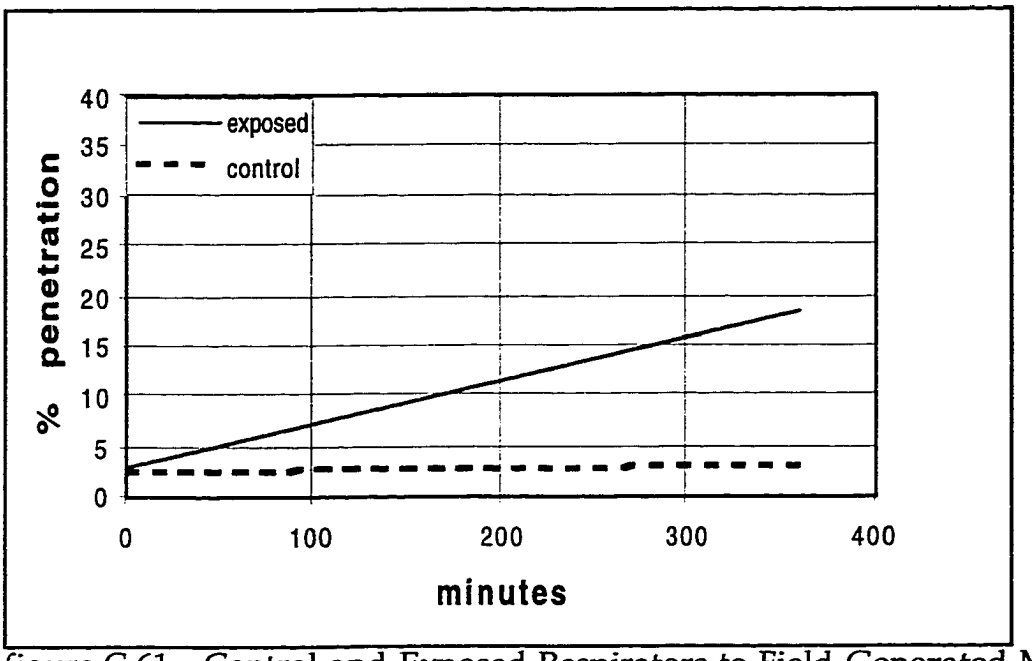

figure C.61 Control and Exposed Respirators to Field-Generated Metal Cutting Fluid Mist
Pro-Tech F200 N95 Filters
Photometer-Measured Penetration: % penetration
N exposed=6,N control=2 ,fitted MMAD= 3.56 μm, fitted GSD=2.41

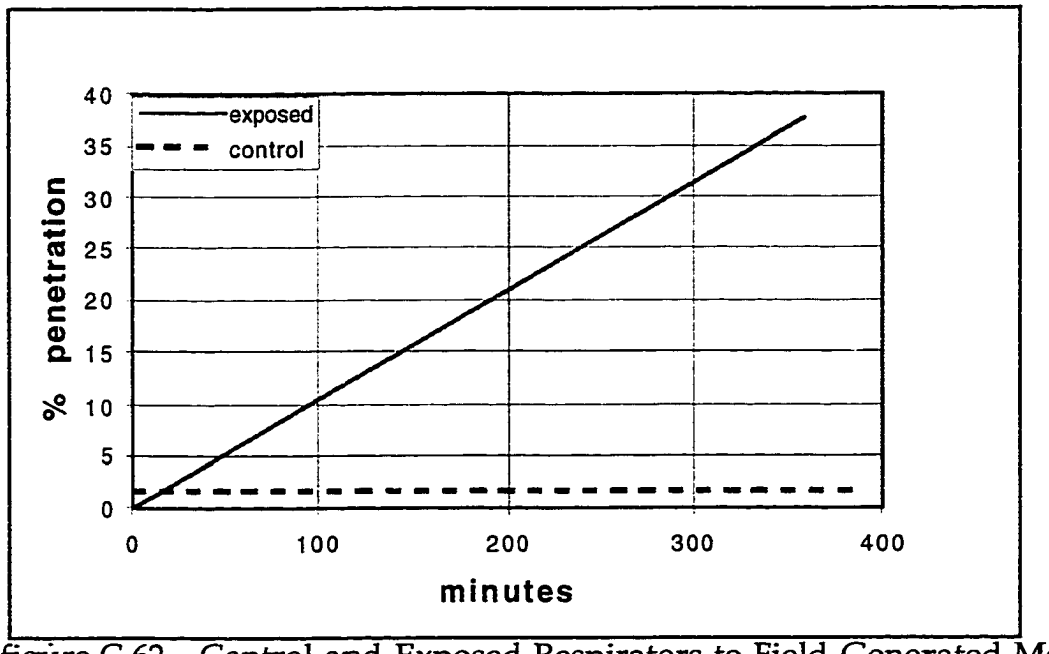

figure C.62 Control and Exposed Respirators to Field-Generated Metal Cutting Fluid Mist
Racal (mechanical) N95 Respirator
Photometer-Measured Penetration: % penetration
N exposed=6,N control=2 ,fitted MMAD= 3.54 μm, fitted GSD=2.14

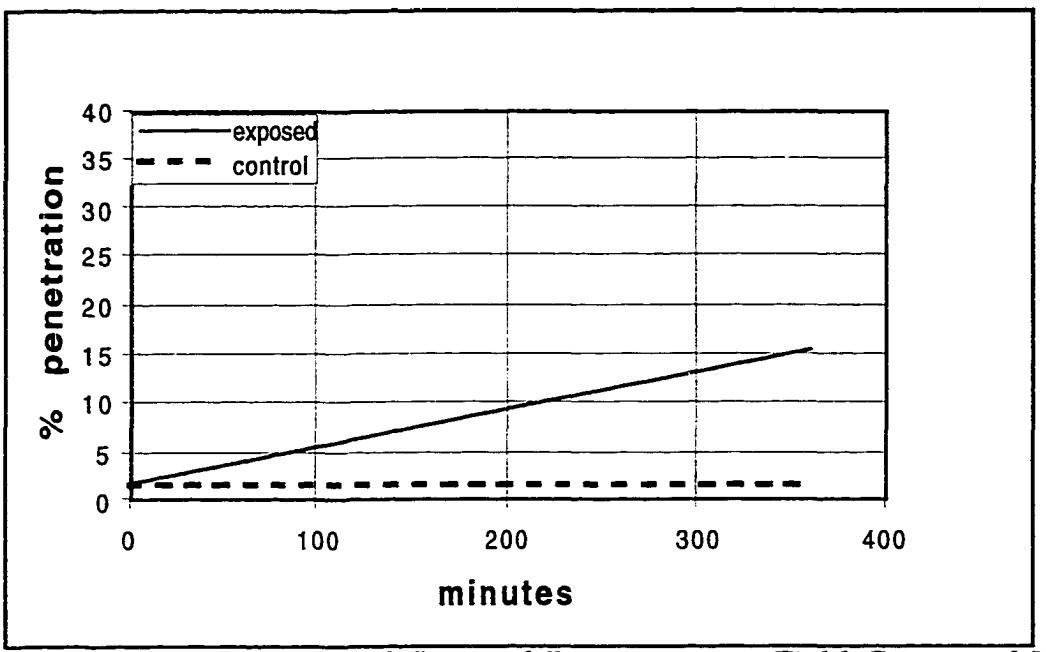

figure C.63 Control and Exposed Respirators to Field-Generated Metal Cutting Fluid Mist
3M 8210 N95 Respirator
Photometer-Measured Penetration: % penetration
N exposed=6,N control=2 ,fitted MMAD= 4.47 μm, fitted GSD=1.88

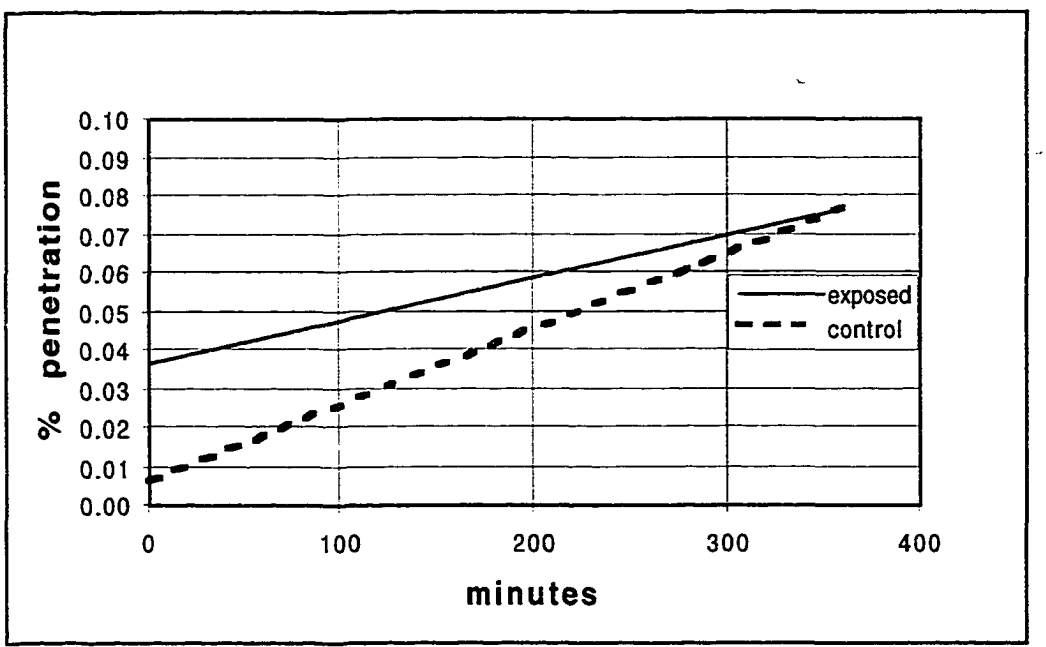

figure C.64 Control and Exposed Respirators to Field-Generated Metal Cutting Fluid Mist
3M 2091 P100 Cartridges
Photometer-Measured Penetration: % penetration
N exposed=6,N control=2 ,fitted MMAD= 4.15 μm, fitted GSD=1.84

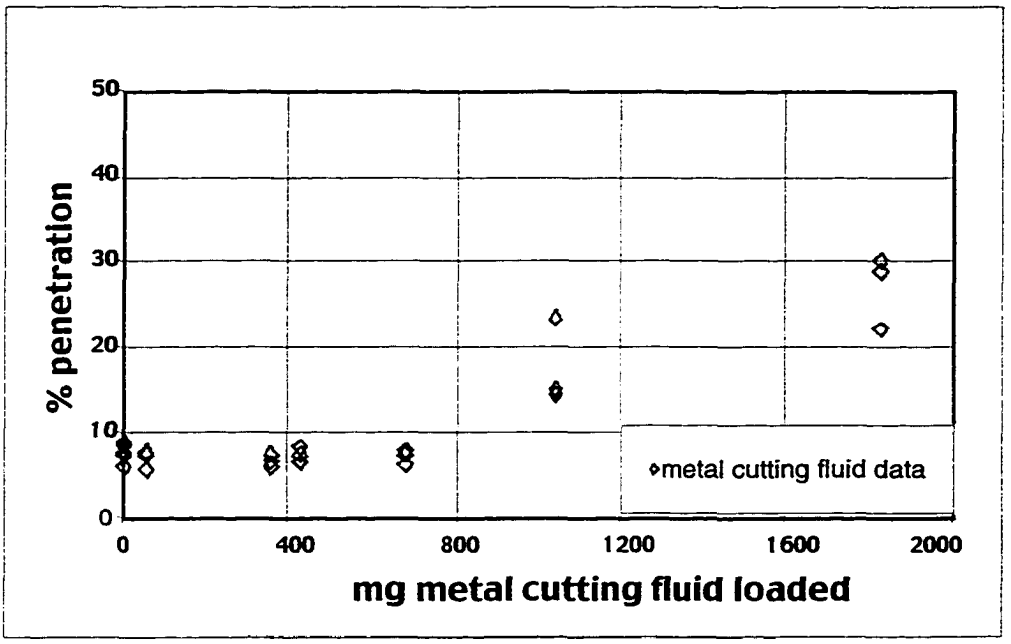

figure C.65 Field Generated-Metal Cutting Fluid Mist: Observed Penetration
MSA Affinity Plus N95 Respirators
CNC-Measured Penetration: % penetration (backtransformed)
N =6, fitted MMAD= 4.37 μm, fitted GSD=2.03

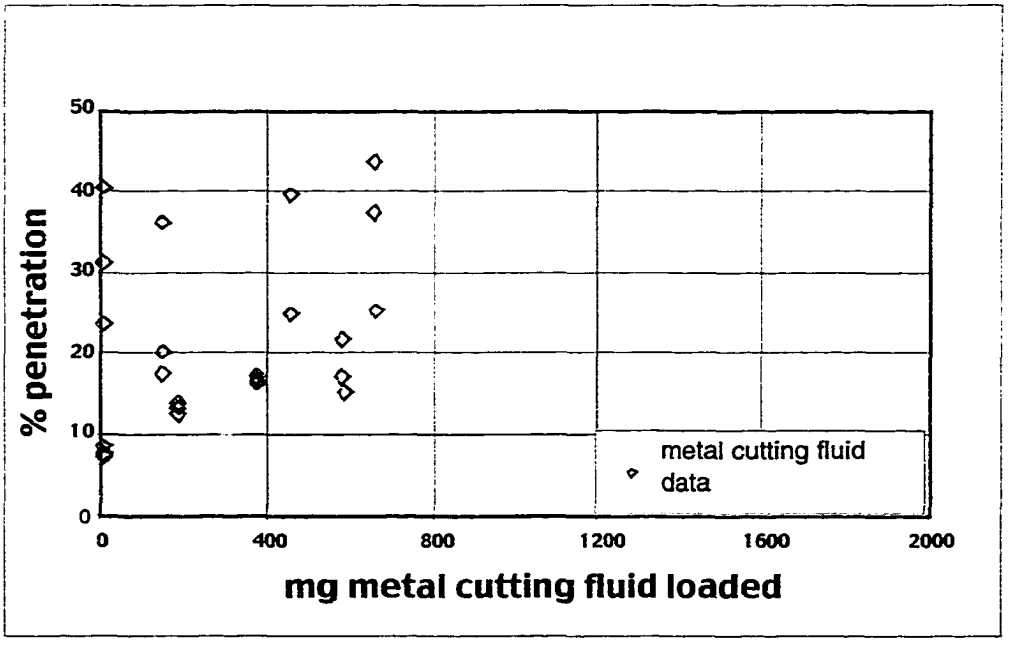

figure C.66 Field Generated-Metal Cutting Fluid Mist: Observed Penetration
Pro-Tech F200 N95 Filters
CNC-Measured Penetration: % penetration (backtransformed)
N =6, fitted MMAD= 3.56 μm, fitted GSD=2.41

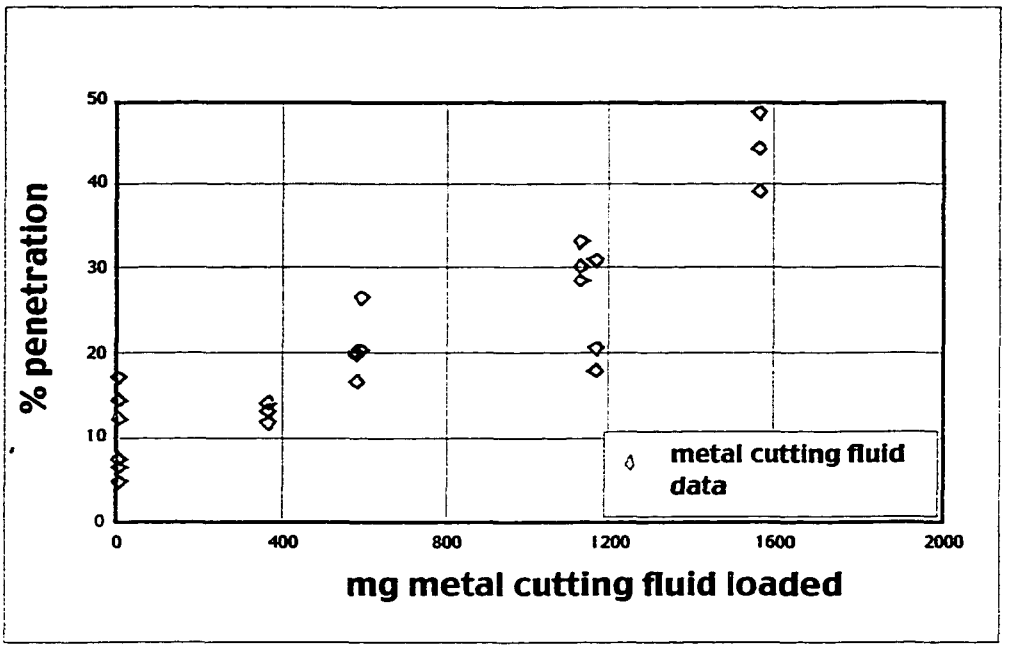

figure C.67 Field Generated-Metal Cutting Fluid Mist: Observed Penetration
Racal (mechanical) N95 Respirators
CNC-Measured Penetration: % penetration (backtransformed)
N =6, fitted MMAD= 3.54 μm, fitted GSD=2.14

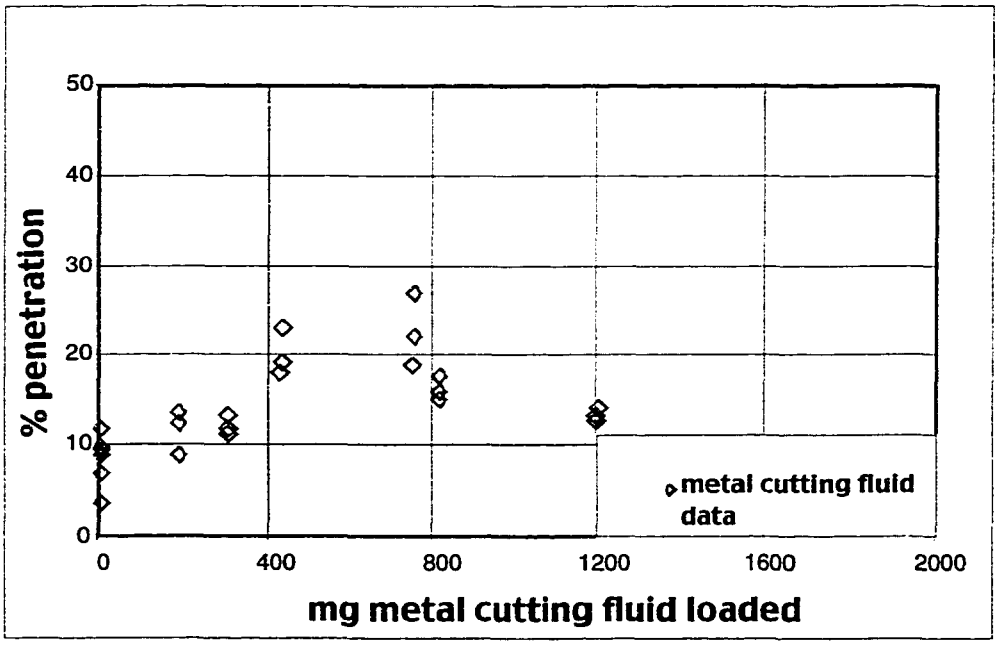

figure C.68 Field Generated-Metal Cutting Fluid Mist: Observed Penetration
3M 8210 N95 Respirators
CNC-Measured Penetration: % penetration (backtransformed)
N =6, fitted MMAD= 4.47 μm, fitted GSD=1.88

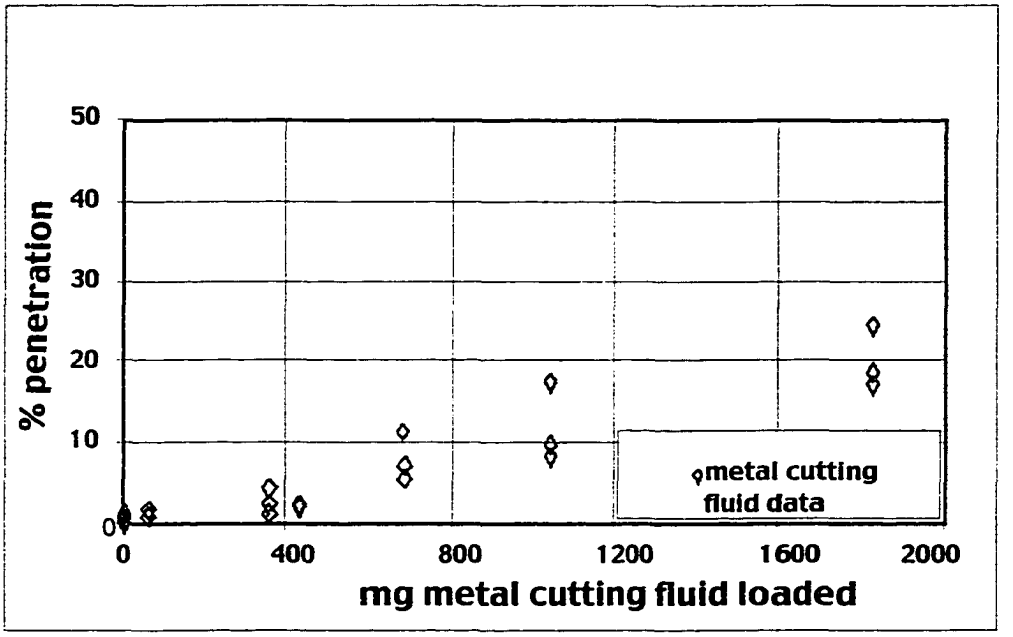

figure C.69 Field Generated-Metal Cutting Fluid Mist: Observed Penetration
MSA Affinity Plus N95 Respirators
Photometer-Measured Penetration: % penetration (backtransformed)
N =6, fitted MMAD= 3.37 μm, fitted GSD=2.03

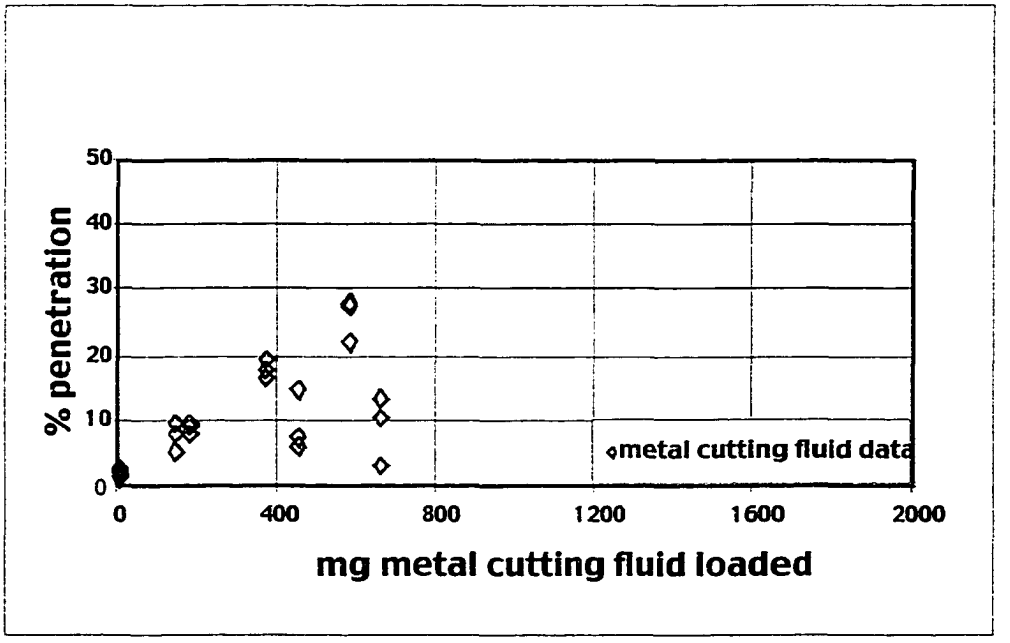

figure C.70 Field Generated-Metal Cutting Fluid Mist: Observed Penetration
Pro-Tech F200 Filters
Photometer-Measured Penetration: % penetration (backtransformed)
N =6, fitted MMAD= 3.56 μm, fitted GSD=2.41

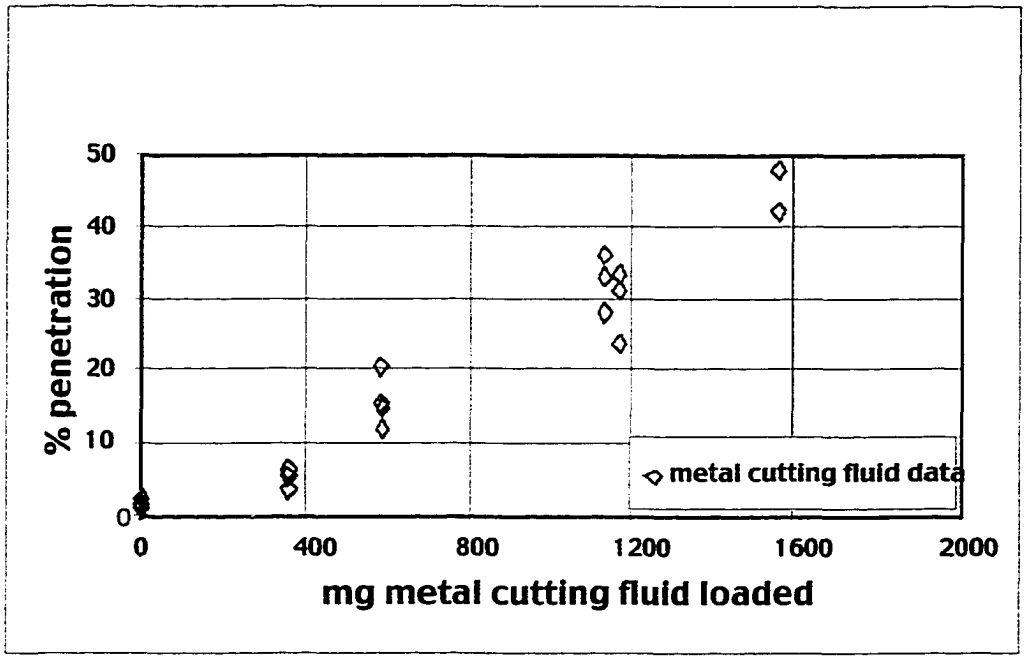

figure C.71 Field Generated-Metal Cutting Fluid Mist: Observed Penetration
Racal Mechanical N95 Respirators
Photometer-Measured Penetration: % penetration (backtransformed)
N =6, fitted MMAD= 3.54 μm, fitted GSD=2.14

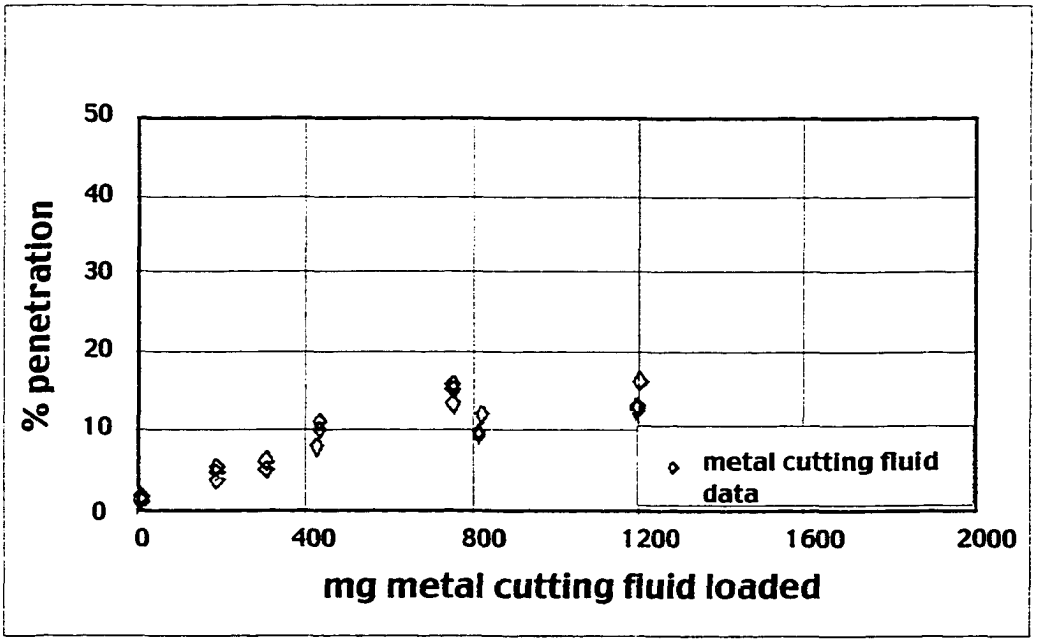

figure C.72 Field Generated-Metal Cutting Fluid Mist: Observed Penetration
3M 8210 N95 Respirators
Photometer-Measured Penetration: % penetration (backtransformed)
N =6, fitted MMAD= 4.47 μm, fitted GSD=1.88

ACRONYMS, SYMBOLS, UNITS, AND TERMS

Acronym	Definition
μ m	micrometer
ACGIH	American Conference of Governmental Industrial Hygienists
Al_2O_3	aluminum oxide
ASTM	American Society for Testing and Materials
cc	cubic centimeter
CFR	Code of Federal Regulation
cm^2	square centimeter
CMD	count median diameter
CNC	Condensation Nucleus Counter
d_d	droplet diameter
d_g	geometric mean diameter
d_i	midpoint diameter of the *i*th group
DMA	Differential Mobility Analyzer
DOP	dioctyl phthalate
d_s	size of final aerosol particle
exp	Inverse natural log
F_v	volume fraction of solid material
g	gram

Acronym	Definition
GSD	geometric standard deviation
HEPA	high-efficiency particulate air (filter)
L	liter
ln	natural log
lpm	liters per minute
MCF	metal cutting fluid
mCi	millicurie
mg/m^3	milligrams per cubic meter
min	minute
MMD	mass median diameter
MSA	Mine Safety Appliance
N	total number
NaCl	sodium chloride
n_i	number of particles in the *i*th group
NIOSH	National Institute for Occupational Safety and Health
OSHA	Occupational Safety and Health Administration
PTFE	polytetrafluroethylene
REL	Recommended Exposure Limit
scfh	standard cubic feet per hour
TLV	Threshold Limit Value
TSI	Thermo-Systems Inc.
σ	standard deviation